SYNTHESIS OF A NEW CLASS OF LINEAR AND CROSS-LINKED POLYZWITTERION-ANIONS AND THEIR APPLICATIONS AS CORROSION INHIBITORS AND ADSORBENTS

BY

SHAMSUDDEEN ABDULLAHI HALADU

A Dissertation Presented to the

DEANSHIP OF GRADUATE STUDIES

KING FAHD UNIVERSITY OF PETROLEUM & MINERALS

DHAHRAN, SAUDI ARABIA

In Partial Fulfillment of the

Requirements for the Degree of

DOCTOR OF PHILOSOPHY

In

CHEMISTRY

APRIL 2014

KING FAHD UNIVERSITY OF PETROLEUM & MINERALS

DHAHRAN- 31261, SAUDI ARABIA

DEANSHIP OF GRADUATE STUDIES

This thesis, written by **SHAMSUDDEEN ABDULLAHI HALADU** under the direction of his thesis advisor and approved by his thesis committee, has been presented and accepted by the Dean of Graduate Studies, in partial fulfillment of the requirements for the degree of **DOCTOR OF PHILOSOPHY IN CHEMISTRY.**

Sk. Asrof Ali

Dr. Shaikh Asrof Ali
(Advisor)

Dr. Abdullah J. Al-Hamdan
Department Chairman

Dr. Anvarhusein A. Isab
(Member)

Dr. Salam A. Zummo
Dean of Graduate Studies

Dr. Mohammed Wazeer
(Member)

12/6/14

Date

Dr. Ibnelwaleed Ali Hussein
(Member)

Dr. Hasan Al-Muallem
(Member)

Dedicated to my Mother

ACKNOWLEDGMENTS

All praise is to Allah for giving me the opportunity to accomplish this research. I have neither power nor ability except with Allah. His peace and blessings be upon his messenger Muhammad, his family members, his companions and those who will follow him in righteousness to the Day of Judgment.

I am expressing my sincere appreciation to my parents for their prayers and support. The efforts of my brothers and sisters who supported me are highly appreciated. I also thank my family for their support during my studies.

My special thanks go to my helpful advisor, Dr. Shaikh Asrof Ali for his enormous assistance, time dedication and encouragement.

I would like to express my sincere gratitude to my thesis committee members Dr. Mohammed Wazeer, Dr. Anvarhusein A. Isab, Dr. Ibnelwaleed Ali Hussein and Dr. Hasan Al-Muallem for their contributions.

I would like to thank my friends and colleagues especially, Mr. Mansur Bala, Dr. Othman Al- Hamouz, Mr. Zakariyya Abdulkareem, Dr. Izzat Kazi, Mr. Mouhyeddin Al Haffar for their support on the course of my studies.

I do thank King Abdulaziz City for Science and Technology (KACST). The whole of this thesis was supported by KACST through the Science & Technology Unit at King Fahd University of Petroleum & Minerals (KFUPM) through project No. 11-ADV2132-04 as part of the National Science, Technology and Innovation Plan.

TABLE OF CONTENTS

LIST OF SCHEMES

LIST OF TABLES

LIST OF FIGURES

ABSTRACT

Full Name : Shamsuddeen Abdullahi Haladu

Thesis Title : [Synthesis of a New Class of Linear and Cross-linked Polyzwitterion-anions and Their Applications as Corrosion Inhibitors and Adsorbents]

Major Field : [Chemistry]

Date of Degree : [April 2014]

A class of new specialty quaternary diallylammonium salt monomers, each containing a pair among the three functionalities: propylphosphonate, methylcarboxylate, and propylsulfonate, has been synthesized using Butler's cyclopolymerization protocol. The zwitterionic monomer, *N*-carboethoxymethyl-3-(*N*,*N*-diallylamino)propanesulfonate (**I**) was cyclopolymerized using tert-butyl hydroperoxide and cyclocopolymerized with sulfur dioxide using azobisobutyronitrile to afford the corresponding polyzwitterions (PZ) (**Ia**) and (**Ib**) respectively. Acid hydrolysis of the PZs gave pH-responsive polyzwitterionic acid (PZA) (**IIa**) and (**IIb**) that generated poly(eletrolyte-zwitterion) (PEZ) (**IIIa**) and (**IIIb**) on treatment with sodium hydroxide. The solubility, viscosity behaviors, and solution properties of the polymers were determined. The PZ (**Ia**) was soluble in water while PZ (**Ib**) was water insoluble. The apparent basicity constants of the carboxyl groups in both PEZs have been determined. The PEZs possess dual type of structural character common to both conventional anionic polyelectrolytes and polyzwitterions, and its aqueous solution behavior is found to be similar to that observed for a typical alternating anionic-zwitterionic copolymer. The monomer 3-[diallyl{3-(diethoxyphosphoryl)propyl}ammonio]propane-1-sulfonate (**IV**), upon cyclopolymerization, generated polyzwitterion (**Va**) and afforded another polyzwitterion (**Vb**), poly(**V**-*alt*-SO_2), with sulfurdioxide. The effects of charge types and densities on the interesting solubility and viscosity behaviors were studied by treating the pH-responsive polyzwitterionic acids (PZAs) (**VIa**) and (**VIb**) derived from the hydrolysis of (**Va**) and (**Vb**), with different equivalents of NaOH to generate polyzwitterion/anion (± −) (PZAN) (**VIIa**) and (**VIIb**) and polyzwitterion/dianion (± =) (PZDAN) (**VIIIa**) and (**VIIIb**). The apparent protonation constants of the PZDANs and PZANs as well as the

corresponding monomeric units have been determined using potentiometric titrations. The symmetrically substituted cationic monomer bis[3-(diethoxyphosphoryl)propyl]diallylammonium chloride (**IX**) was cyclopolymerized in the presence of ammonium persulfate to give cationic polyelectrolyte (CPE) (**X**). The hydrolysis of the ester in (CPE) gave a pH-responsive cationic polyacid (CPA) (**XI**). The CPA under pH-induced transformation was converted into a water-insoluble polyzwitterion acid **(±)** (PZA) (**XII**) or water-soluble polyzwitterion/anion **(± −)** (PZAN) (**XIIa**) or polyzwitterion/dianion **(± =)** (PZDAN) (**XIIb**) or polyzwitterion/trianion **(± ≡)** (PZTAN) (**XIIc**), all having identical degree of polymerization. The solubility and viscosity behaviors of the polymers have been investigated in some detail. The apparent protonation constants of the anioinic centers in (**XIIc**) and the corresponding monomer have been determined. Evaluation of antiscaling properties of the PZAs, (**VIa**), (**VIb**) and (**XI**), using supersaturated solution of $CaSO_4$ revealed ≈100%, ≈100% and 98% scale inhibition efficiency at a meager concentration of 20, 20 and 10 ppm for 45 h, 13 h and 71 h, respectively, at 40 °C. The PZAs have the potential to be used effectively as antiscalants in reverse osmosis plants. Novel cross-linked polyzwitterion/anions (CPZAs) have been synthesized; they were derived from the NaOH treatment of the cross-linked polyzwitterionic acids (CPZAs) obtained by the polymerization of the acid hydrolyzed monomer (**I**) with a cross-linker, 1,1,4,4-tetraallylpiperazinium dichloride, in the presence and absence of sulfur dioxide. The resins were found to be effective in the removal of toxic Sr^{2+}, Cu^{2+} and Cd^{2+} at low concentrations (200 -1000 ppb range). The adsorption isotherms, kinetic and thermodynamic parameters of the adsorption process have been determined. Some of the monomers and polymers have been evaluated as corrosion inhibitors of mild steel at 200 ppm by gravimetric and electrochemical methods. The inhibitor molecules imparted an inhibition efficiency of greater than 90%.

ملخص الرسالة

الاسم الكامـــل: شـمـس الديـن عبد الله هلادو

عنوان الرسالة: إصطناع صنف جديد من البوليمرات الخطية و الشبكية ثنائية الشحنة وتطبيقاتها كمثبطات للتآكل و كمواد ممتزّة

التخصـــــص: الكيميـــــــاء

تاريخ الدرجة العلمية: أبريل 2014

تم تصنيع فئة جديدة من المنوميرات الحاوية على ملح رباعي من ثنائي أليل الأمونيوم، وكل واحدة منها تحتوي على زوج من المحموعات الوظيفية الثلاثة التالية: فوسفونات البروبيل، و كربوكسيلات المثيل، و سلفونات البروبيل، وذلك باستخدام برتوكول بوتلر (Butler) في البلمرة الحلقية.

تمت عملية البلمرة الحلقية للمونومير ثنائي الشحنة N-carboethoxymethyl-3-(N,N-diallylamino)propanesulfonate (I) باستخدام رباعي بيوتل هيدروبيروكسيد (TBHP)، كما تمت البلمرة الحلقية المشتركة مع ثاني أكسيد الكبريت بوجود (azoisobutyronitrile) لإعطاء البوليمرات الحلقية المطابقة لـ (Ia) و (Ib).

أعطت عملية التميؤ الحمضي للبوليمرات ثنائية الشحنة بوليمرات حامضية ثنائية الشحنة مستجيبة للأس الهيدروجيني (**IIa**) و (**IIb**) و التي بدورها أعطت بوليمر ثنائي الشحنة-ألكتروليتي (**IIIa**) و (**IIIb**) وذلك بمعالجتها بمحلول هيدروكسيد الصوديوم.

تم تحديد الخصائص الفيزيائية لمحاليل البوليمرات كاللزوجة و الإنحلالية. و قد وجد أن البوليمر (**Ia**) انحل بالماء بينما البوليمر (**Ib**) لم ينحل. كما تم تحديد ثابت التفكك القاعدي الظاهري لمجموعة الكربوكسيل في كل البوليمرات ثنائية الشحنة.

أظهرت البوليمرات ثنائية الشحنة نوعاً من الطابع الهيكلي المزدوج و الشائع في كل من البوليمرات الألكتروليتية سالبة الشحنة و البوليمرات ثنائية الشحنة، و وجد أن سلوك محاليلها المائية مشابه لسلوك محاليل البوليمرات المشتركة المتعاقبة ثنائية الشحنة.

أنتجت البلمرة الحلقية للمونومير 3-[diallyl{3-((diethoxyphosphoryl)propyl}ammonio]propane-1-sulfonate (**IV**) البوليمر ثنائي الشحنة

(**Va**) ، كما أنتجت بوليمير آخر ثنائي الشحنة (**Vb**) (poly(**V**-*alt*-SO_2)) بالتفاعل مع ثاني أكسيد الكبريت.

تمت دراسة آثار أنواع الشحنة و كثافتها على الإنحلالية واللزوجة وذلك بدراسة تأثير مفاعلة كميات مختلفة من هيدروكسيد الصوديوم مع البوليمرات الحامضية ثنائية الشحنة المستجيبة للأس الهيدروجيني (**VIa**) و(**VIb**) المشتقة من تميؤ (**Va**) و(**Vb**)، و التي تنتج عن ذلك بوليميرات ثنائية الشحنة / أحادية الشحنة السالبة (± -) (PZAN) (**VIIa**) و(**VIIb**) وبوليمرات ثنائية الشحنة / ثنائية الشحنة السالبة (± =) (PZDAN) (**VIIIa**) و (**VIIIb**).

تم تحديد الثوابت الظاهرية لإضافة أيون هيدروجين موجب لـ (PZDANs) و(PZANs)، وايضا للمونوميرات المناظرة لهم باستخدام المعايرة الجهدية. كما تم اجراء بلمرة حلقية للمونومير الموجب الشحنة ذي المجموعات المتناظرة (bis[3-(diethoxyphosphoryl)propyl]diallylammonium chloride) (**IX**) بوجود فوق كبريتات الأمونيوم لإعطاء بوليمير ألكتروليتي موجب الشحنة (CPE) (**X**). و قد أعطت عملية التميؤ لمجموعة الأستر في (CPE) بوليمر حامضي ذي استجابة للأس الهيدروجيني (CPA) (**XI**).

تم تحويل البوليمر (CPA) عن طريق تغيير الأس الهيدروجيني إلى بوليمر ثنائي الشحنة حمضي لا ينحل في الماء (±) (PZA) (**XII**)، أو إلى بوليمر ثنائي الشحنة / أحادي الشحنة السالبة (± −) (PZAN) (**XIIa**) ينحل في الماء، أو إلى بوليمير ثنائي الشحنة/ثنائي الشحنة السالبة (± =) (PZDAN) (**XIIb**) ينحل في الماء، أو إلى بوليمير ثنائي الشحنة/ ثلاثي الشحنة السالبة (± ≡) (PZTAN) (**XIIc**) ينحل في الماء، وجميعهم لهم درجة متماثلة من البلمرة. كما تمت دراسة سلوكيات اللزوجة والانحلالية لهذه البوليمرات مع بشيء من التفصيل. و تم تحديد الثوابت الظاهرية لإضافة أيون هيدروجين موجب للمراكز ذات الشحنة السالبة في البوليمر (**XIIc**) وكذلك للمونمير المقابل له.

قيمت خصائص منع التكلس في عمليات التناضح العكسي لِـ (PZAs) في البوليمرات ثنائية الشحنة (**VIa**) و(**VIb**) و(**XI**) باستخدام محلول فوق مشبع من كبريتات الكالسيوم ≈ 100% و أظهرت النتائج كفاءة تثبيط ≈100% و 98% بنطاق تراكيز 20 و20 و10 جزء بالمليون لمدة 45 ساعة و 13 ساعة و71 ساعة، على التوالي عند درجة حرارة 40 درجة مئوية.

و لذا فإن البوليمرات (PZAs) قابلة لأن تستخدم بشكل فعال في محطات التناضح العكسي. كما تم تصنيع بوليمرات جديدة شبكية ثنائية الشحنة / سالبة الشحنة (CPZAs) و قد تم اشتقاقها عن طريق

المعالجة بهيدروكسيد الصوديوم للبوليمرات الحامضية ثنائية الشحنة / سالبة الشحنة المتشابكة (CPZAs) و التي تم الحصول عليها عن طريق بلمرة المونومير المنحل حامضياً **(I)** مع الرابط الشبكي ,1,1,4,4-tetraallylpiperazinium dichloride في وجود أو غياب ثاني أكسيد الكبريت.

تم اكتشاف أن الراتنجات فعالة في إزالة الأيونات السامة Sr^{2+} و Cu^{2+} وCd^{2+} بتراكيز منخفضة (200-1000 جزء من البليون). و تم تحديد خصائص أيزوثيرم الامتزاز، و ثوابت الحركية و الحركية الحرارية لعملية الامتزاز. كما تم تقييم بعض المونوميرات و البوليمرات كمثبطات لتآكل الفولاذ الطري عند تركيز 200 جزء بالمليون باستخدام وسائل الجاذبية والكهروكيميائية. و قد أظهرت هذه المثبطات كفاءة تقدر بنسبة أكبر من 90%.

CHAPTER 1

Introduction

1.1 Ionic polymers by cyclopolymerization

The discovery[1,2] of cyclopolymerization of *N,N*-diallyl quaternary ammonium salts **1** and subsequently, their copolymerization with sulfur dioxide[3] led to the synthesis of an array of water-soluble cationic polyelectrolytes (CPE) **2** and **3** of tremendous scientific and technological interest (Scheme 1.1). The resulting polymer-architecture having five–membered cyclic units embedded in the backbone has been recognized as the eighth major structural type of synthetic polymers.[4] Butler's exciting discovery has had a dramatic impact on commercial production of the cyclopolymers **2** (Scheme 1.1)[5]; over 33 million pounds of poly(diallyldimethylammonium chloride) [**2**, R^1=R^2=Me] alone are sold annually for water treatment and another 2 million pounds are used for personal care formulation.

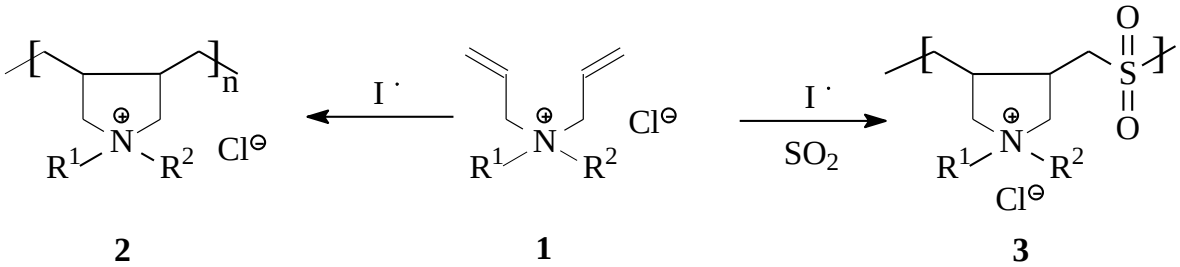

2 **1** **3**

Scheme 1.1 Cyclopolymerization of *N,N*-diallyl quaternary ammonium salts.

The polymerization reaction of a zwitterionic monomer ($M^{\pm}$) having charges of both algebraic signs in the same molecular framework leads to polyzwitterions[6-9] (Scheme 1.2); however, the presence of both M^{+} and M^{-} in the same polymer chain constitutes a polyampholyte with or without charge symmetry.[10] While biopolymers like proteins or DNA mediate life processes, commercial polyampholytes and polyzwitterions, which seem to mimic biopolymers, have offered many new applications. The polyzwitterions derived from acrylamide and acrylate based zwitterionic monomers have been widely used in industries dealing with textiles, medical products, charge dispersing agents, colloids, and related materials.[11]

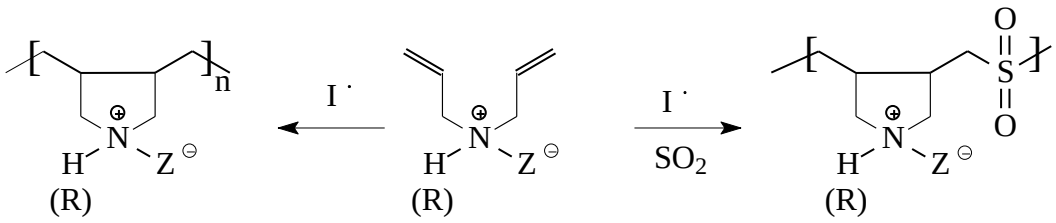

5 **4** **6**

Scheme 1.2 Cyclopolymerization of zwitterionic monomer.

Butler's cyclopolymerization reaction of zwitterionic diallylammonium monomers **4** or their copolymerizations with sulfur dioxide has been an attractive method for the synthesis of polyzwitterions **5** and **6** (Scheme 1.2).[12-17] Polyampholytes and polyzwitterions, unlike polyelectrolytes, exhibit 'anti-polyelectrolyte behavior'[17-20] i.e. enhancement in viscosity and solubility in the presence of added electrolytes (e.g. NaCl)

due to the neutralization of the ionically cross-linked network in a collapsed coil conformation of the polymers (Figure 1.1).

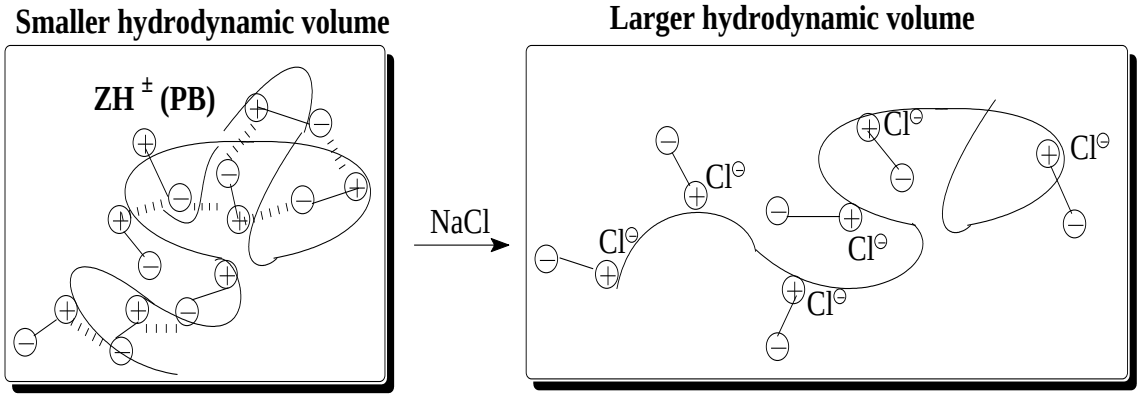

Figure 1.1 Antipolyelectrolyte behavior of polyzwitterions. Dashed lines (|||||||) indicate interchain attraction

1.2 Corrosion problems in Oil and Gas industries

Corrosion is a costly problem. In any industrialized nation, its cost is greater than the financial cost of the floods, earthquakes, and severe natural disasters combined. About 40% of our steel production goes to replace steel lost due to corrosion. In addition, corrosion can lead to serious accidents, explosions and environmental damage. However, the cost of corrosion can be drastically reduced by properly available technology. Corrosive acid solutions are widely used in oil industry, the most important field of application being acid pickling, industrial acid cleaning, acid descaling etc. Crude oil itself is actively corrosive towards iron and steel. It is obvious that an environment containing acid gases (H_2S, CO_2), moisture and dissolved salts, when operated at high

temperature has a potential of corroding metal pipelines. Corrosion inhibitors are extensively used in oil and gas industries to arrest corrosion.

The enormity of the corrosion problem is due to the fact that all metals tend to revert back to one of the thermodynamically more stable forms in which they are originally found in the nature. To protect metals from corrosion, a number of methods are being used; namely, cathodic protection, anodic protection, galvanization, organic coatings, inorganic coatings, ceramic/glass lining and addition of inhibitors. Inhibitors are mixed in a small quantity to the corrosive environment (often liquid and sometimes vapor) to reduce the rate of corrosion. They are preferred in situation where the corrosive medium is being recycled, *e.g.*, water in cooling towers, acid solutions for acid pickling, acid cleaning, cooling system of automobiles and other equipment.

Petroleum industry contains a wide variety of corrosive environment. Crude oil itself is actively corrosive towards iron and steel. Treatment chemicals are used in all facets of the natural gas industry from well development through transmission and storage of natural gas. It is obvious that an environment containing acid gases (H_2S, CO_2), moisture and dissolved salts, when operated at high temperature has a potential of initiating electrochemical reaction when metal cathode and anodes are present. As natural gas wells are developed, chemicals are applied during drilling, fracturing, completion, and often throughout years of service. If one considers that all facets of the natural gas industries are subsets of a much larger systems, there is a large and diverse group of chemicals products are added to the system.[21]

The life of pipeline tubing can be extended with the use of organic corrosion inhibitors. The mechanisms through which the corrosion inhibitors function have been ascribed to adsorption processes on the anodic or cathodic sites on the steel surfaces. The adsorption/polymerization processes will create a protective film on the steel surface reducing the corrosion through acid/steel reaction. The essential requirements for a good protective film are

1) Polar groups with high affinity to the metal surface
2) Long chain hydrocarbon tails, attached to the polar groups and hydrophobic in character.
3) Polymeric compound formed in secondary reaction between the adsorbed inhibitor molecules.

It is difficult to combine the above requirements in a single component. Hence, commercial corrosion inhibitors are usually composed of a number of surface-active compounds. It has been reported that the effective formulations used in the corrosion inhibition of oil field steel are mixtures of *N*-containing compounds, acetylenic compounds, surfactants, and aldehydes.[22] Imidazoline-based inhibitors are well known to have a high inhibiting ability in acidic media; hence they are widely used to minimize CO_2 induced corrosion by oil and gas industries.[23] Quaternary amine salt and imidazoline derivatives have been used in drilling fluids containing high concentration of H_2S to protect corrosion of drill pipe during drilling.[24] Development of a structure activity relationship for oil-field corrosion inhibitors (anionic RCO_2^-; cationic R_4N^+ etc.) in carbonated brine media has been reported.[25]

A review on the behavior of aggressive agents as corrosion inhibitors in gas and oil production has been published.[26] The article also reviewed the guidelines for determining the conditions where protective films will be generated under production conditions. A mechanism for carbon dioxide corrosion in oxygen-free aqueous oil and gas field media was proposed.[27] The CO_2 corrosion is by far the most prevalent form of attack encountered in upstream operations. The present mechanistic understanding and practical implications of CO_2 corrosion of C and low-alloy steels in hydrocarbon production were reviewed.[28] The corrosion mechanisms of CO_2 and H_2S on steels in oil and gas fields' development have been studied.[29]

It is known that polymers are adsorbed stronger than their monomer analogs[30-33] hence it is expected that polymers will be better inhibitors for mild steel corrosion than the corresponding monomers.

1.3 Sorbents for the removal of toxic metal ions

Cross-linked polymeric materials containing chelating functional groups of amine, carboxylate, phosphonate, etc, motifs have attracted considerable attention in the separation and removal of toxic metals. Functional group having aminomethylphosphonate motifs have shown extraordinary chelating properties in the removal of toxic metals from aqueous solutions.[34,35] Pollution caused by toxic metal ions has been found to have a large negative impact on the environment. Metal ions like Pb^{2+}, Zn^{2+}, Cu^{2+} and Cd^{2+} metal ions cause various diseases and disorders; for example, copper poisoning can cause liver and kidney damage, irritation of the respiratory system,

whereas cadmium can cause nervous system damage, bone damage as well as other serious illness.[36-41]

According to World Health Organization (WHO) standards, the maximum allowable concentration of copper in drinking water is 0.2 mg/L[42], while it is 0.2 and less than 2 ppm for agriculture irrigation and ponds fish farming, respectively.[43] In order to protect humans and the environment, it is of utmost importance to remove copper ions from environments. For Cd, the drinking water guideline value recommended by WHO is 0.003 mg Cd/L.[44] It is difficult for chemical precipitation methodologies to treat economically low concentration (less than 5 mg/L) of cadmium. Ion exchange and reverse osmosis have been effective in achieving the metal concentration limits but have high operation and maintenance costs.[45]

Radioactive wastes containing a variety of radionuclides severely pollute the environment. Fission product like strontium ^{89}Sr and ^{90}Sr with half-lives of 51 days and 29 years, respectively[46], can contaminate underlying layers of soil and groundwater.[47,48] Strontium's resemblance to calcium enables its easy incorporation into bone and by virtue of being a very strong β-emitter, it leads to the development of bone sarcoma and leukemia.[46,49,50] It is thus quite necessary to remove Sr, one of the most hazardous elements, from wastewater. Adsorption with solid adsorbents like polyacrylonitrile/zeolite composite[51], bentonite[52], zeolites and clays have been studied for the removal of Sr^{2+} ions[53,54], and the adsorption capacity is found to be somewhat low. Derivatives of crown ethers[55,56], cross-linked polymers containing carboxyl motifs[57,58] including gels based on carboxylated polysaccharide derivatives[59] were also used to adsorb Sr^{2+} ions.

Polyzwitterions synthesized from *N*-vinyl imidazole have been used as sorbents for the removal of Sr^{2+}. The polysulfobetaines (polyzwitterions) carrying charges of both algebraic signs on the same repeating unit are good candidate for the water technologies on accounts of its dual role in removing the cationic or anionic effluent and they also can impart anti-microbial properties.[60] Recently, the researchers have focused on the syntheses of zwitterionic cross-linked inorganic/organic hybrid materials for the removal of toxic heavy metal ions *via* electrostatic effects.[36,61,62]

The literature presented above describes many sorbent materials to remove larger concentration of strontium ions; however, it remains challenging to develop new materials for removing strontium ions at ppb-levels.

1.4 Objectives

The aim of this proposed research is to synthesize a series of pH-responsive polymers via cyclopolymerization of a new class of specialty diallylammonium monomers. The aim of this research is two-fold: (i) synthesis of an interesting new class of ionic polymers, and (ii) their applications in corrosion inhibition and metals adsorption. The proposed work is thus of both academic and industrial interests. The presence of multiple cationic and anionic sites within a polymer chain is anticipated to undergo strong adsorption on the metal surface (to prevent corrosion) and chelate harmful metal ions.

To achieve this, the proposed study will have the following objectives:

To have academic significance:

1. To synthesize a new diallyl quaternary ammonium (DQA) monomer containing carboxylate and sulfonate pendants and its polymerization (Scheme 1.3).

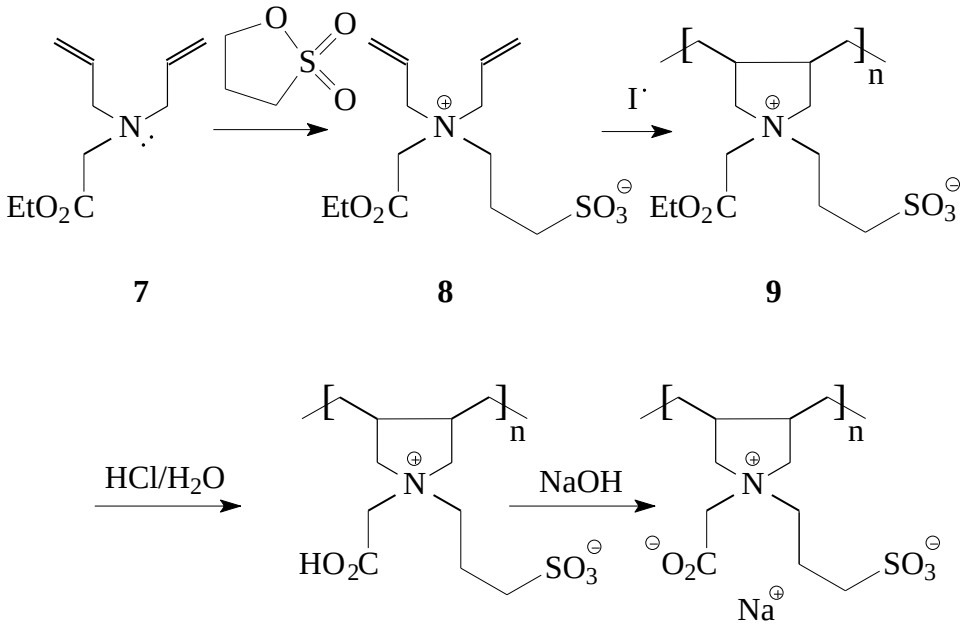

7 **8** **9**

10 **11**

Scheme 1.3

2. To synthesize a new DQA monomer containing phosphonate and sulfonate pendants and its polymerization (Scheme 1.4).

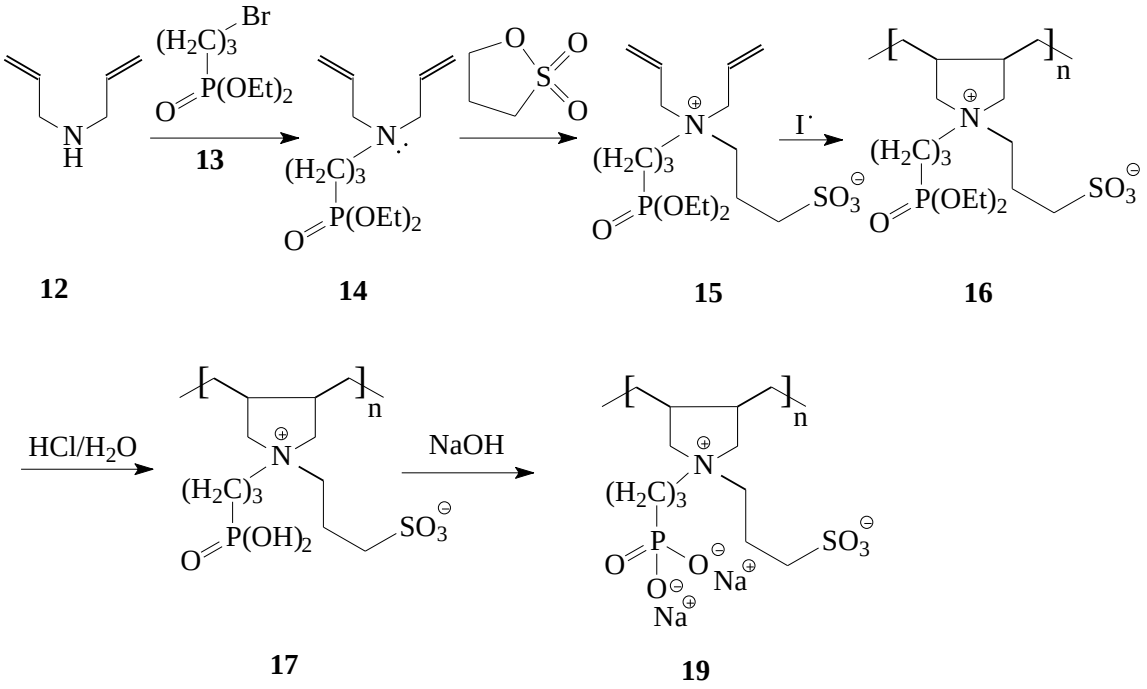

Scheme 1.4

3. To synthesize a new DQA monomer containing phosphonate and carboxylate pendants and its polymerization (Scheme 1.5).

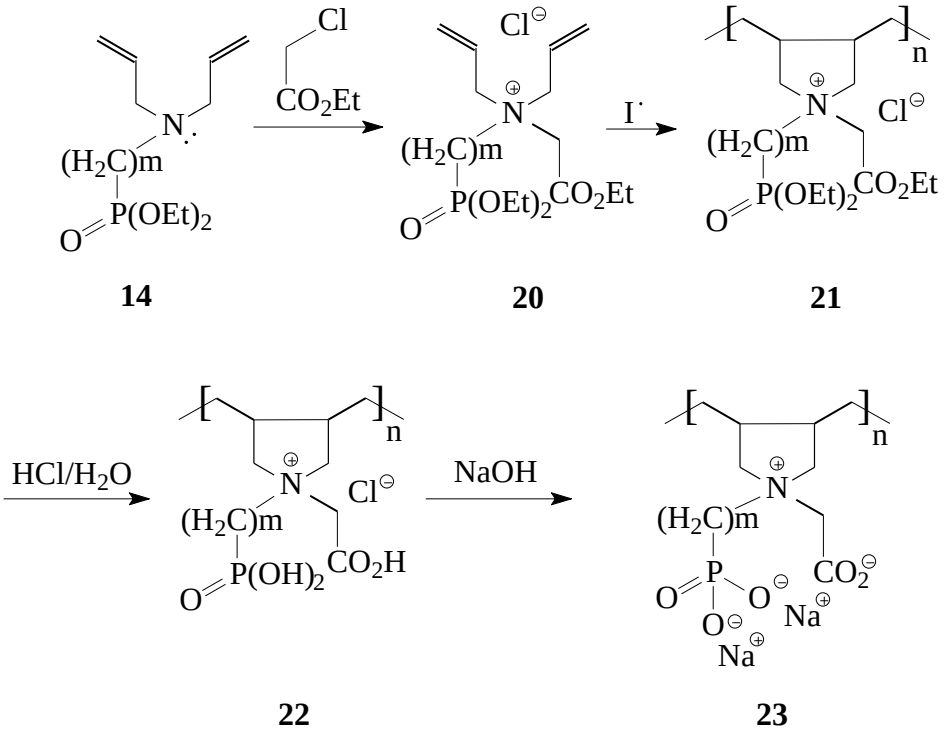

14 **20** **21**

22 **23**

Scheme 1.5

4. The resulting polymers (Schemes 1.3-1.5) would be interconverted to polyzwitterions, polyelectrolytes, polyzwitterion/anion (Figure 1.2, Schemes 1.3-1.5). The solution behavior of the resulting polymers will be studied in detail.

5. To synthesize novel cross-linked resins containing phophonate, sulfonate, and carboxylate pendants (Scheme 1.6).

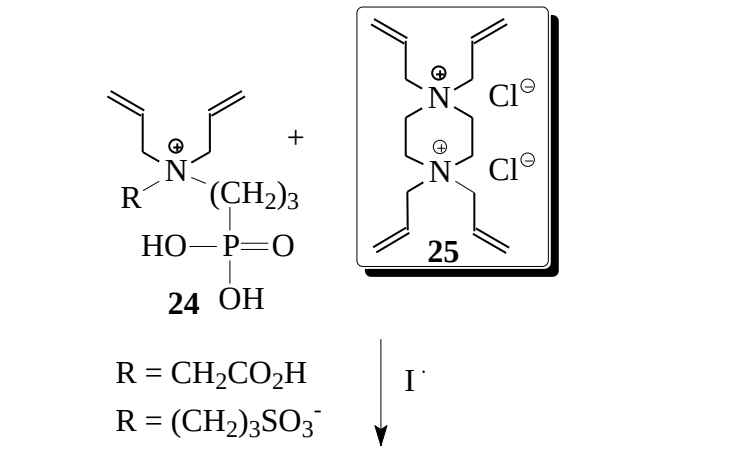

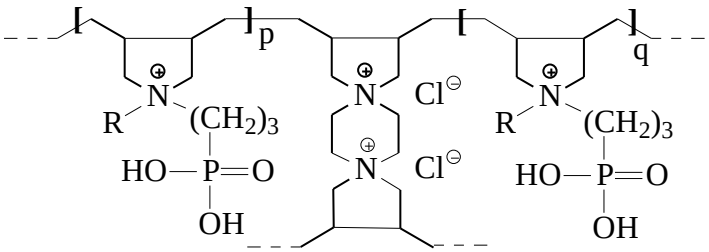

26

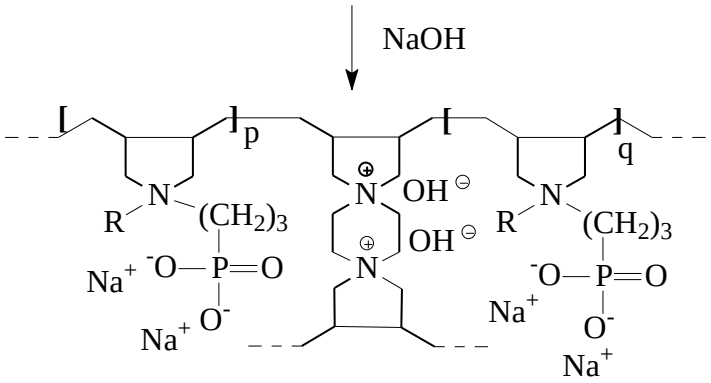

27

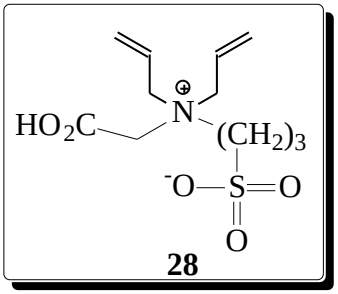

28

Scheme 1.6

To have industrial significance:

6. Preliminary evaluation (screening) of the synthesized monomers and polymers as corrosion inhibitors.

7. Evaluation of the cross-linked resins as adsorbents for the removal of heavy metal ions like Sr^{2+}, Pb^{2+} and Cu^{2+} ions from aqueous solutions.

Note that the project involves the synthesis of a large number of new monomers and polymers. The polymers will be judiciously selected to carry out the preliminary study of corrosion inhibition properties and adsorbent behavior towards toxic metal ions removal.

1.5 Present state of the problem

Extraordinary chelating properties of compounds containing aminomethylphosphonic acid groups have attracted considerable attention to synthesize low molecular-weight chelating agents containing these functional groups that should be able to form polymer-heavy metal ion complexes from waste water.[63-65]

In pursuit of tailoring pH-responsive polymers, this work describes herein the synthesis of new monomers **8, 15, 20, 24** and **28**. To the best of our knowledge, cyclopolymers would represent the first examples of this class of ionic polymers having quenched nitrogen valency along with attachment of a combination of carboxylate, sulfonate and phophonate motifs. The synthesis of a series of new pH-responsive polymers would pave the way to study cationic polyelectrolyte-to-polyzwitterionic-to- polyzwitterionic/anionic transitions involving polymers having identical degree of polymerization. The linear polymers of this type will be tested for the first time as inhibitors of corrosion in oil and gas industries.

In this work, a series of novel cross-linked polymers containing ammonium-phosphonate, -carboxylate and sulfonate motifs will be synthesized and tested for their efficiency as adsorbents for the removal of heavy metal ions like Sr(II), Pb(II) and Cu(II) ions from aqueous solutions.

1.6 General description of the objectives and the work plan

1.6.1 Synthesis of monomers and their cyclopolymerizations

The monomers required for the cyclopolymerization will be synthesized and will be subjected to undergo homocyclopolymerization or cocyclopolymerization with SO_2 as presented in Schemes 1.3-1.5. The monomers will be designed in such a way that would permit the interconversion of the pH-responsive polymers as outlined in Figure 1.2.

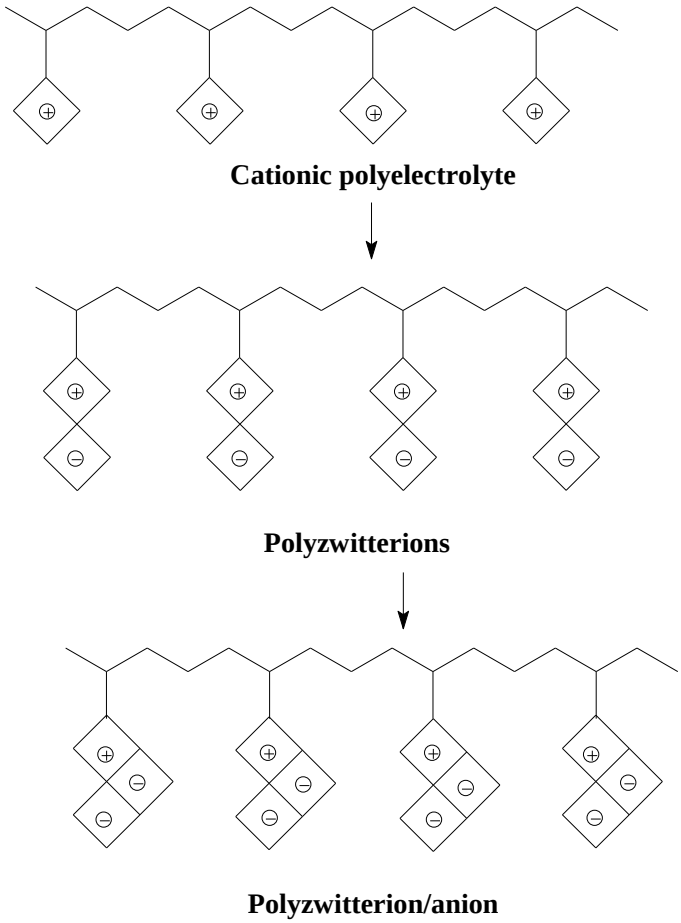

Figure 1.2 Illustration of some ionic polymers.

A new zwitterionic monomer **8** will be prepared by reacting **7** with 1,3-propanesultone.[66] The polyzwitterions **9** would then be converted to pH-responsive zwitterionic/anionic polymer **10** as outlined in Scheme 1.3. The synthesis of these interesting polymer having carboxylate and sulfonate functionalities (with chelating properties) will be a new contribution to the literature of water-soluble polymers.

Another new zwitterionic monomer **15** with phosphonate and sulfonate functionalities will be prepared as outlined in Scheme 1.4. The bromophosphonate **13** will be prepared as described.[67,68] The polyzwitterion **16** would then be converted to pH-responsive

zwitterionic/dianionic polymer **19** as outlined in Scheme 1.4. The synthesis of this interesting polymer having phosphonate and sulfonate functionalities (with chelating properties) will be a new contribution to the literature of polymers.

A new cationic monomer **20** with phosphonate and carboxylate functionalities will be prepared as outlined in Scheme 1.5. CPE **21** would then be converted to pH-responsive zwitterionic/dianionic polymer **23** as outlined in Scheme 1.5. The synthesis of the interesting polymer having phosphonate and carboxylate functionalities (with chelating properties) will be a new contribution to the literature of polymer science.

1.6.2 Synthesis of cross-linked resins

To the best of our knowledge, the following synthesis of the resins would represent the first examples of cross-linked polymers (containing aminophosphonate, sulfonate or carboxyl motifs) by the cyclopolymerization protocol involving monomers having quenched nitrogen valency. The cross-linker **25** will be prepared as described.[69] The monomers **24** and **28** (Scheme 1.6) will be prepared by acidic hydrolysis of the monomers **8, 15** and **20**.

1.6.3 Testing of the Inhibitors to arrest CO_2 Corrosion

The newly developed corrosion inhibitors are organic in nature and are tailored to provide protection to steel in corrosive environment of petroleum industry. All synthesized inhibitors will be tested at ambient conditions in 3% NaCl solution, saturated with CO_2. Before the beginning of testing at atmospheric pressure, the solution will be saturated by passing CO_2 for 15 minutes. During the experiment, the passage of the gases

at a slow rate would maintain the saturation. Corrosion tests will comprise of Tafel extrapolation and linear polarization.

The linear polarization technique is chosen in this study to minimize the level of polarization which in turn will minimize the changes in the surface characteristics. Standard coupons will be exposed to the test solutions for a fixed period of time before the polarization data are recorded. The experiments will be done in a standard corrosion cell as described in ASTM G 59-97. The cell which will contain the test coupon as working electrode, a graphite rod as counter electrode and Ag/AgCl electrode as reference electrode, will be connected to a potentiostat. In this work we will use an existing Model 283 potentiostat and commercial software, both from E G & G PARC. Linear polarization data will be acquired in the test solutions after a predetermined exposure. The data will be used to calculate the values of polarization resistance (R_p), which will be used to calculate corrosion current using Stern and Geary equation:

$$i_{corr} = \frac{\beta_a \beta_c}{2.3(\beta_a + \beta_c) R_p}$$

where β_a and β_c are Tafel constants.

The corrosion rate can be determined in mills per year (mpy) using:

$$CR = 0.129 \frac{a * i}{n * D}$$

where,

CR = corrosion rate in mpy

a = atomic weight of the metal

n = number of electrons in the reduction of the metal ions.

D = density of the metal in g/cm^3.

i = corrosion current density $\mu A/cm^2$.

Finally, the corrosion inhibition efficiencies of each solution can be determined by:

$$\text{Corrosion Inhibition Effeciency} = \frac{CR_{blank} - CR_{inhibitor}}{CR_{blank}} x100 .$$

1.6.4 Evaluation of toxic metal ion removal efficiency

Toxic metal removal efficiency will be tested using known protocol in the literature.[36-39, 70]

CHAPTER 2

Cyclopolymerization protocol for the synthesis of a new poly(electrolyte-zwitterion) containing quaternary nitrogen, carboxylate, and sulfonate functionalities

Taken from Shamsuddeen A. Haladu and Shaikh A. Ali, Cyclopolymerization protocol for the synthesis of a new poly(electrolyte-zwitterion) containing quaternary nitrogen, carboxylate, and sulfonate functionalities, *European Polymer Journal* 49 (2013) 1591–1600.

Abstract

A new zwitterionic monomer, *N*-carboethoxymethyl-3-(*N*,*N*-diallylamino)propanesulfonate, on cyclopolymerization in aqueous solution using tert-butyl hydroperoxide, afforded a polyzwitterion (PZ) which on acidic hydrolysis of the ester groups led to the corresponding polyzwitterionic acid (PZA). The pH-responsive PZA on treatment with sodium hydroxide gave a new poly(eletrolyte-zwitterion) (PEZ) in excellent yield. The solution properties of the salt-tolerant PZ, PZA and PEZ were studied in some detail. Unlike common polyzwitterions, PZ and PZA were found to be soluble in salt-free as well as salt-added water. The apparent basicity constants of the carboxyl group in PEZ have been determined in salt-free water and 0.1 M NaCl. The poly(electrolyte-zwitterion) (PEZ), as the name implies, possesses dual type of structural character common to both conventional anionic polyelectrolytes and polyzwitterions, and its aqueous solution behavior is found to be similar to that observed for a typical alternating anionic–zwitterionic copolymer.

2.1 Introduction

Cyclopolymerization[5] of *N,N*-diallyl quaternary ammonium salts as well as their cocyclopolymerization with sulfur dioxide[71] and[72] has led to the synthesis of numerous water-soluble cationic polyelectrolytes (PEs) (e.g., **1**, **2**) of significant scientific and technological interest[6-8], (Scheme 2.1). Cationic polyelectrolyte, poly(diallyldimethylammonium chloride) **1**, alone has over 1000 patents and publications. The cyclopolymerization process has also provided entries into polybetaines [also known as polyzwitterions (PZs)] (e.g., **3–7**) having charges of both algebraic signs in the same repeating units. [6,7,9,12,14,17,67] Commercial polyampholytes (having repeating units of cationic and anionic charges with or without charge symmetry) and PZs, whose structure and behavior seem to mimic biopolymers, have offered many new applications in medicine, biotechnology, hydrometallurgy and oil industry.[6,7,9] Contrary to the PEs, PZs demonstrate anti-polyelectrolyte behavior, i.e. their viscosity and solubility are enhanced upon addition of electrolytes (e.g. NaCl) owing to the neutralization of the ionically cross-linked network in a collapsed coil conformation of the polymers.[17-20] The monomers of diallylamine salts $(H_2C = CH–CH_2)_2NH^+–Y^-$ containing zwitterionic motifs have generated entries into ionic polymers (e.g., **3**,**7**) that have demonstrated interesting pH-responsive solution behavior.[66,73,74]

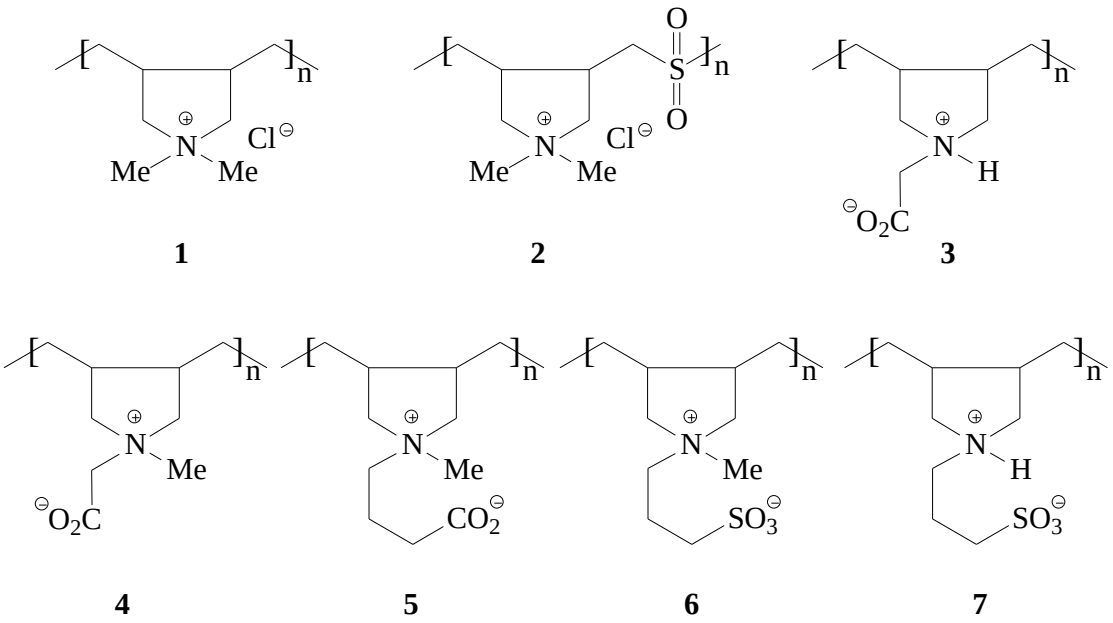

Scheme 2.1 Ionic polymers *via* Butler's cyclopolymerization process.

In pursuit of tailoring stimuli-responsive polymers, we embarked on the synthesis of a specialty monomer **11** which would lead to an interesting new polymer **14**, a poly(electrolyte-zwitterion) (PEZ), having zwitterionic and anionic motifs in the same repeating unit (Scheme 2.2). The investigation of the solution properties of PEZ **14,** whose repeat units are triply charged, is of considerable interest as few experimental data are currently available on well-defined systems such as the one reported here. The cyclopolymerization has so far documented two such PEZs in the literature.[16, 75] In both the cases, the anionic motifs in the corresponding monomer **8** were either sulfonate ($x = y = 3$)[75] or carboxylate ($x = 5, y = 1$).[16] To the best of our knowledge, cyclocopolymer **14** would represent the first example of this class of PEZ having different anionic motifs (carboxylate and sulfonate) in the same repeating unit. While a strongly acidic SO_3H motif ensures its complete ionization to anionic motif SO_3^- in dilute

aqueous solution, the weak nature of the CO_2H group will allow us to fine-tune its anionic/neutral character by adjusting the pH. The synthesis of the new pH-responsive polymers would thus provide an opportunity to study polyzwitterionic (**12 or 13**) – to – poly(zwitterionic/anionic) (**14**) transition involving polymers having identical degree of polymerization. It would be interesting to find out whether anionic or zwitterionic interactions prevail in PEZ **14**.

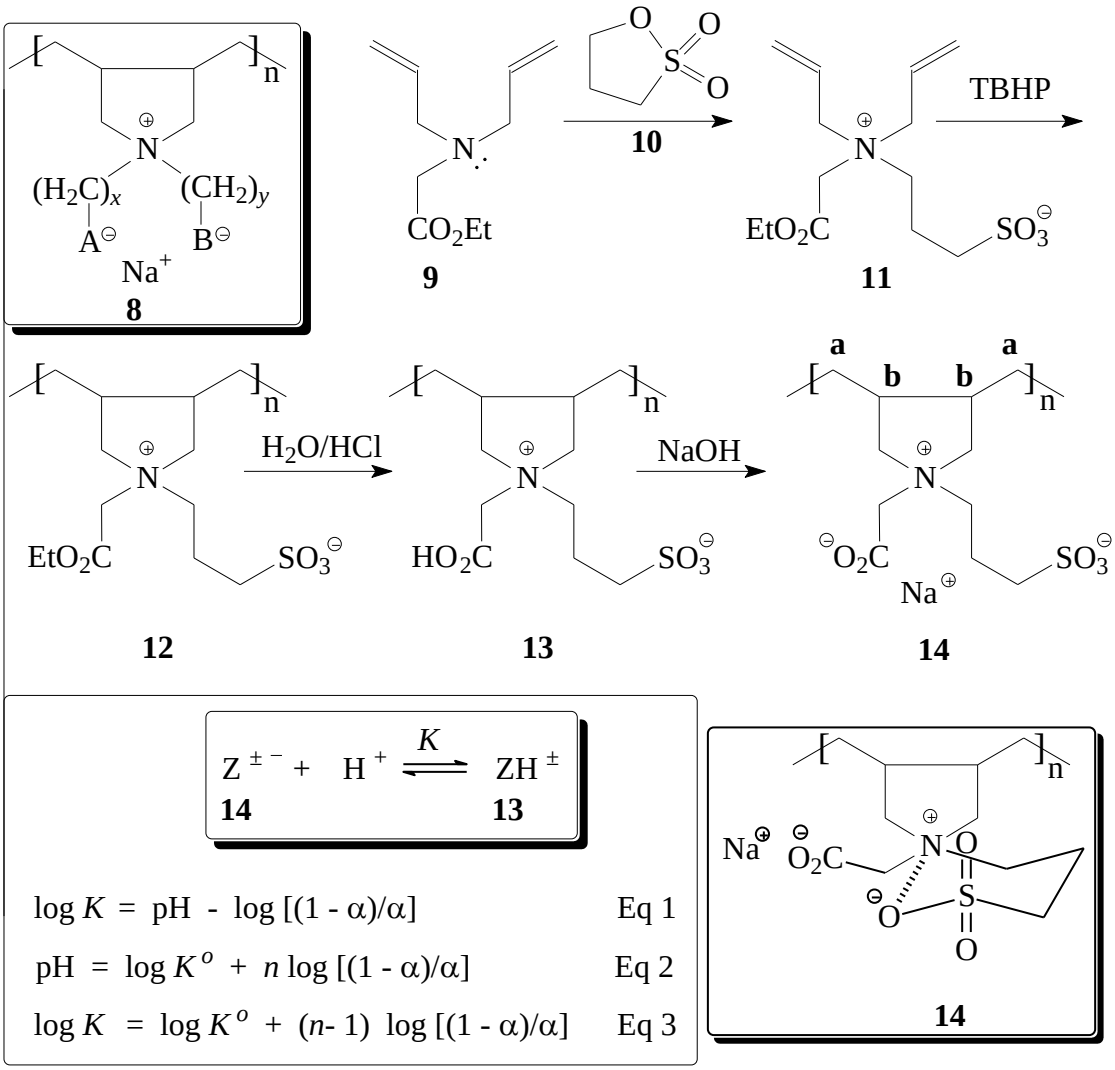

Scheme 2.2 Synthesis of a polyzwitterion and its conversion to poly(electrolyte-zwitterion).

2.2 Experimental

2.2.1 Physical methods

Elemental analysis was carried out on a Perkin Elmer Elemental Analyzer Series II Model 2400. IR spectra were recorded on a Perkin Elmer 16F PC FTIR spectrometer. The ^{13}C and ^{1}H NMR spectra of the polymers have been measured in D_2O (using HOD signal at 4.65 and dioxane ^{13}C peak at δ67.4 as internal standards) on a JEOL LA 500 MHz spectrometer. Viscosity measurements have been made by Ubbelohde viscometer (having viscometer constant of 0.005718 cSt/s at all temperatures) using CO_2-free water under N_2 in order to prevent CO_2 absorption that may affect the viscosity data. For the potentiometric titrations, the pH of the solutions was recorded using a Corning pH Meter 220. Molecular weights of some of the synthesized polymers were determined by the GPC measurement performed on an Agilent 1200 series apparatus equipped with a Refractive Index (RI) detector and PL aquagel-OH MIXED column using polyethylene oxide/glycol as a standard and water as eluent at a flow rate of 1.0 mL/min at 25 °C.

2.2.2 Materials

Ammonium persulfate (APS), tert-butyl hydroperoxide (TBHP), and 3-propanesultone **10** from Fluka AG (Buchs, Switzerland) were used as received. For dialysis, a Spectra/Por membrane with a molecular weight cut-off (MWCO) value of 6000–8000 was procured from Spectrum Laboratories, Inc. All glasswares were cleaned with deionized water.

2.2.3 N-carboethoxymethyl-3-(N,N-diallylamino)propanesulfonate (11)

A solution of *N*,*N*-diallyl-*N*-carboethoxymethylamine[76] **9** (24.4 g, 0.133 mol) and 1,3-propanesultone **10** (16.3 g, 0.133 mol) in acetonitrile (130 cm^3) was stirred under N_2 at 72 °C for 72 h. The reaction mixture was homogeneous but solidified as it cooled to room temperature. After removal of the solvent by a gentle stream of N_2 at 60 °C, the solid salt of zwitterionic monomer **11** was recrystallized from methanol/acetone/diethyl ether mixture as white crystals (33.4 g, 82%). Mp 162–163 °C (closed capillary); (Found: C, 50.9; H, 7.7; N, 4.5; S, 10.4%. $C_{13}H_{23}NO_5S$ requires C, 51.13; H, 7.59; N, 4.59; S, 10.50%); ν_{max} (KBr): 3415, 2984, 1740, 1639, 1468, 1410, 1217, 1042, 961, 733 and 606 cm^{-1}; δ_H (D_2O) 1.28 (3H, t, *J* 7.05 Hz), 2.24 (2H, quint, *J*7.05 Hz), 2.92 (2H, t, *J* 6.7 Hz), 3.65 (2H, apparent t, *J* 7.95 Hz), 4.31–4.17 (8H, m), 5.75 (4H, m), 6.02 (2H, m), (HOD: 4.65); δ_C (D_2O) 14.08, 18.65, 48.09, 57.20, 58.87, 63.21 (2C), 64.46, 124.38 (2C), 130.79 (2C), 166.05 (dioxane: 67.40 ppm). The peak assignments of the signals in the ^1H NMR and ^{13}C NMR spectra are displayed in Figure 2.1 and Figure 2.2, respectively.

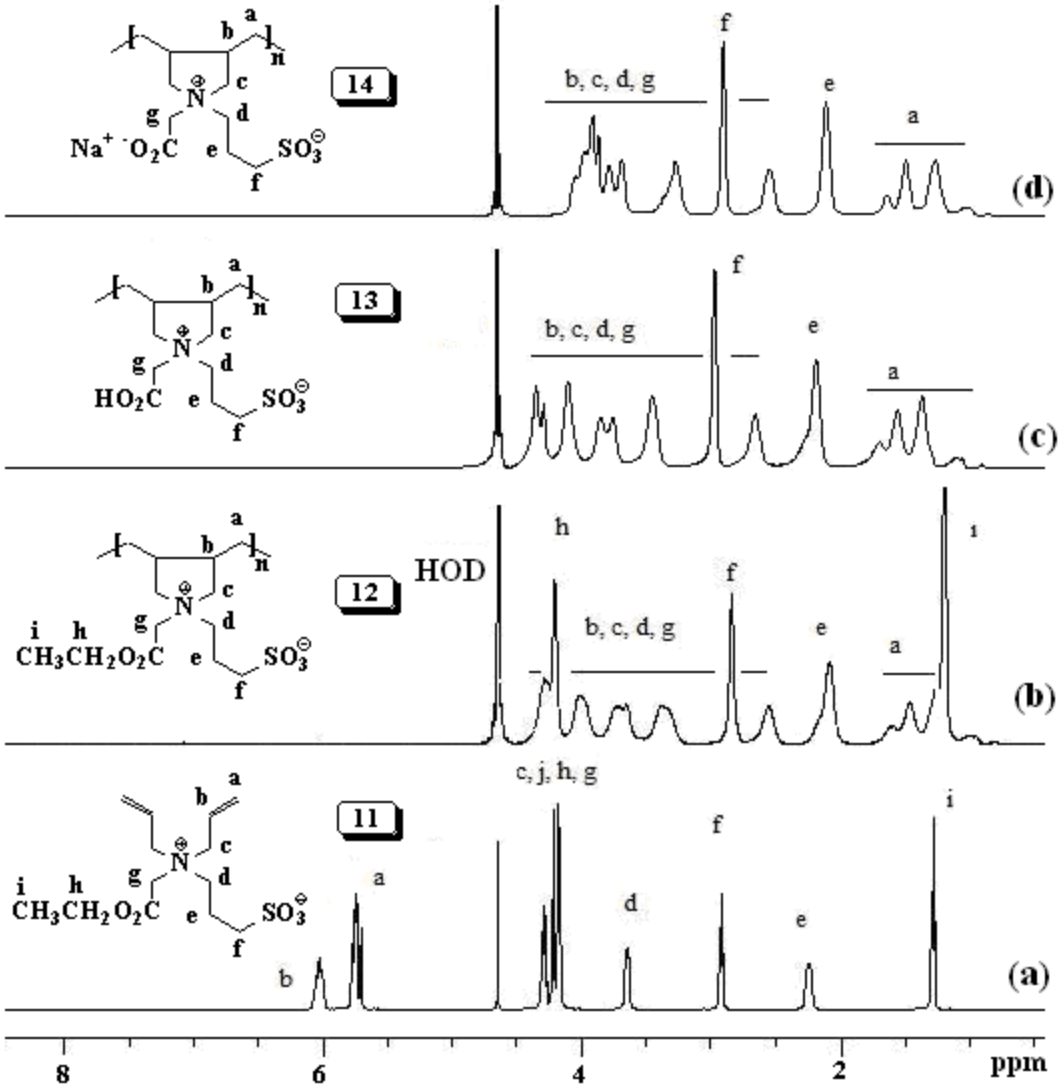

FIGURE 1

Figure 2.1 ^{1}H NMR spectrum of (a) **11**, (b) **12**, (c) **13** and (d) **14** in D_2O.

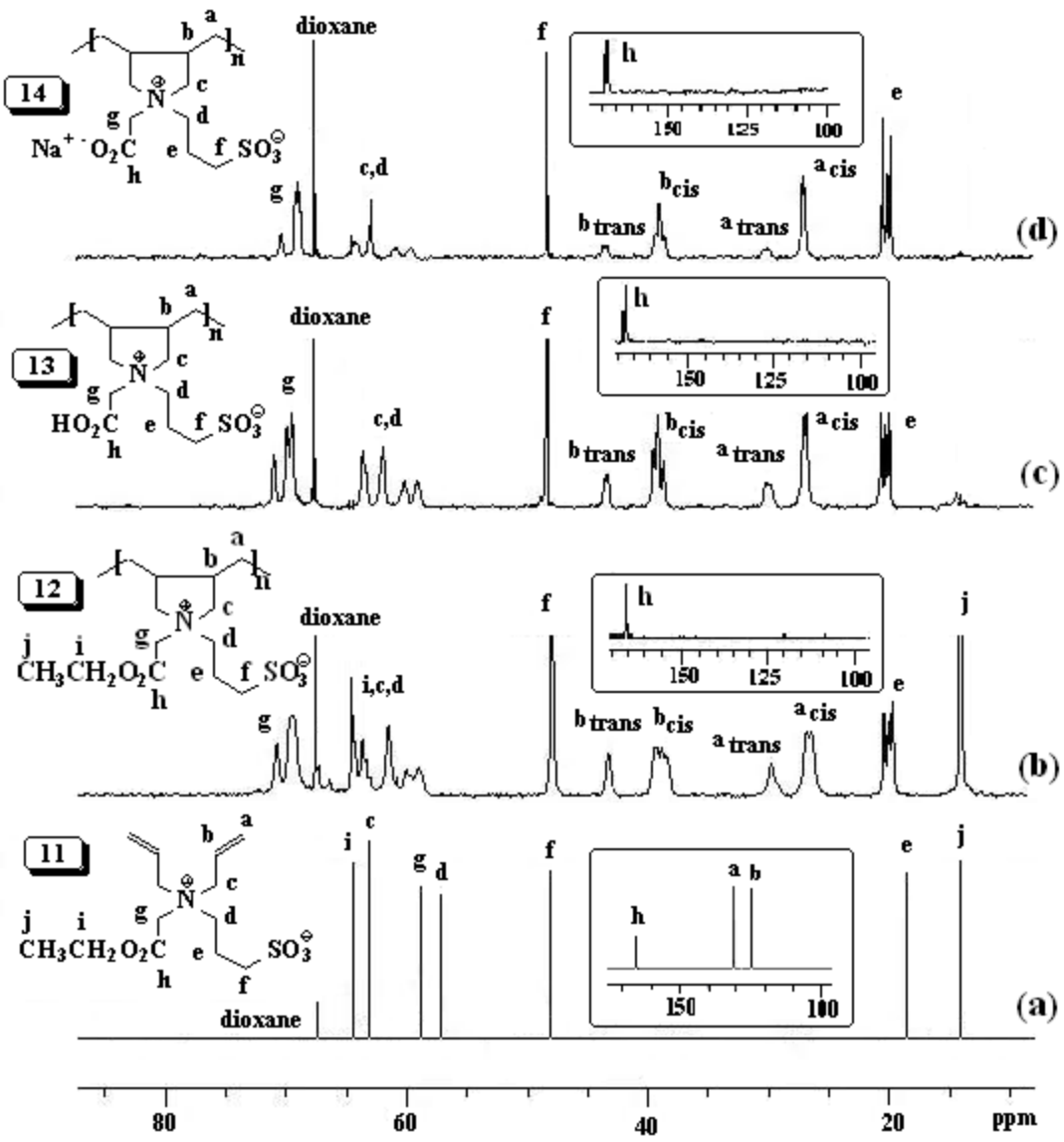

FIGURE 2

Figure 2.2 ^{13}C NMR spectrum of (a) **11**, (b) **12**, (c) **13** and (d) **14** in D_2O.

2.2.4 General procedure for the cyclopolymerization of 11

All the polymerizations were carried out under the conditions presented in Table 2.1 using 10 mmol of monomer in each entry. However, the experiment under entry seven was repeated on a larger scale. A solution of monomer **11** (6.1 g, 20 mmol) and

1 M NaCl (2 cm^3) in a 10-cm^3 round-bottom flask was purged with N_2, and after adding the desired quantity of TBHP (80 mg), the mixture was stirred in the closed flask at 90 °C for 48 h. The reaction mixture was cooled and dialyzed against deionized water for 48 h for the removal of the unreacted monomer and NaCl (confirmed with an $AgNO_3$ test). The polymer solution was then freeze-dried to obtain PZ **12** as a white polymer (4.45 g, 73%). The onset of thermal decomposition (Closed capillary): the color changed to dark brown at 290 °C and decomposed at 315 °C. (Found: C, 50.8; H, 7.8; N, 4.5; S, 10.2%. $C_{13}H_{23}NO_5S$ requires C, 51.13; H, 7.59; N, 4.59; S, 10.50%); ν_{max} (KBr) 3608, 3501, 2988, 2942, 1742, 1640, 1457, 1411, 1218, 1042, 907, 733, 601 cm^{-1}. ^1H NMR and ^{13}C NMR spectra are displayed in Figure 2.1 and Figure 2.2 respectively.

Table 2.1 Cyclopolymerization of monomer **11**.

Entry No.	Initiator[a] (mg)	NaCl (M)	Temp. (^oC)	Time (h)	Yield[b] (%)	$[\eta]^c$ (dL g^{-1})	$\overline{M}_w$	(PDI)[d]
1	TBHP (20)	3.00	80	48	38 (44)	0.0700	–	–
2	TBHP (20)	1.50	80	48	49 (56)	0.0658	–	–
3	TBHP (20)	0.750	80	48	49 (51)	0.0736	–	–
4	TBHP (40)	0.750	90	24	68 (83)	0.0773	49.1×10^3	2.46
5	TBHP (40)	0	90	24	21 (29)	0.0746	_	_
6	APS (150)	0.750	90	4	54 (60)	0.0695	_	_
7	TBHP (80)	1.00	90	24	73 (85)	0.0789	51.0×10^3	2.43

[a]Polymerization reactions were carried out in aqueous solution of monomer **11** (10 mmol) (75 w/w% monomer) in the presence of ammonium persulfate (APS) or tert- butyl hydroperoxide (TBHP). Polynmerization under entry 7 was carried out on a larger scale of 20 mmol.
[b]Isolated yields; the yields determined by ^{1}H NMR analyses of the crude reaction mixture are written in parentheses.
[c]Viscosity of 1-0.25 % polymer solution in 0.1 M NaCl at 30^{o}C was measured with Ubbelohde Viscometer (K=0.005718).
[d]Polydispersity index.

2.2.5 Acidic hydrolysis of PZ 12 to PZA 13

A solution of PZ **12** (3.0 g, 9.8 mmol) (derived from entry 7, Table 2.1) in 6 M HCl (60 mL) was heated in a closed vessel at 53 °C for 48 h. The homogeneous mixture was cooled to room temperature and dialyzed against deionized water (to remove HCl) for 24 h. During dialysis, the clear polymer solution became turbid after 1 h and again transparent after 5 h. The resulting solution was freeze dried to obtain PZA **13** as a white solid (2.5 g, 92%). PZA **13** was found to be water-soluble at 2% w/w at 20 °C. However, at a 10% w/w, it was found to be soluble at 60 °C while insoluble at 20 °C. The onset of

thermal decomposition (closed capillary): the color changed to dark brown at 270 °C and changed to black at 310 °C. (Found: C, 47.4; H, 7.2; N, 4.8; S, 11.3%. $C_{11}H_{19}NO_5S$ requires C, 47.64; H, 6.91; N, 5.05; S, 11.56%); ν_{max} (KBr) 3450 (br), 2942, 2872, 2635, 2539, 1737, 1643, 1457, 1213, 1039, 898, and 733 cm^{-1}. The ^{1}H and ^{13}C NMR spectra are displayed in Figure 2.1 and Figure 2.2, respectively.

2.2.6 Transformation of PZA 13 to PEZ 14

A mixture of **13** (derived from entry 7, Table 2.1) (0.730 g, 2.63 mmol) and NaOH (0.12 g, 3 mmol) in 2 cm^3water was stirred until the polymer dissolved (ca. 5 min). The resultant polymer PEZ **14** was precipitated in methanol. After filtration and washing with excess methanol, the polymer was dried under vacuum at 55 °C to constant weight (0.68 g, 86%). The resulting polymer was found to be extremely hygroscopic. The onset of thermal decomposition (closed capillary): the color changed to brown at 335 °C and changed to black at 350 °C. (Found: C, 43.8; H, 6.2; N, 4.5; S, 10.5%. $C_{11}H_{18}NNaO_5S$ requires C, 44.14; H, 6.06; N, 4.68; S, 10.71%); ν_{max} (KBr): 3447, 3023, 2941, 2859, 1628, 1460, 1408, 1337, 1204, 1045, 909, 732 cm^{-1}. The ^{1}H and ^{13}C NMR spectra are displayed in Figure 2.1 and Figure 2.2, respectively.

2.2.7 Solubility measurements

A 2% (w/w) mixture of PZ **12** or PEZ **14** in a solvent was heated to 70 °C for 1 h and then cooled to 23 °C. The results of the solubility are shown in Table 2.2.

Table 2.2 Solubility[a,b] of PZ **12**, PZA **13**, and PEZ **14**.

Solvent	ε	PZ **12**	PZA **13**	PEZ **14**
Formamide	111	+	+	+
Water[c]	78.4	+	+	+
Formic acid	58.5	+	+	+
DMSO	47.0	−	±	+
Ethylene glycol	37.3	±	−	−
DMF	37.0	−	±	−
Methanol	32.3	−	±	−
Triethylene glycol	23.7	−	−	−
Acetic acid	6.15	−	−	−

[a]2% (w/w) of polymer-water mixture (solution) was made after heating the mixture at 70 °C for 1 h and then cooling to 23 °C.
[b] '+' indicates soluble, '-' indicates insoluble, and '±' indicates partially soluble.
[c]10% (w/w) of PZA **13** was insoluble in water

2.2.8 Potentiometric titrations

The potentiometric titrations were carried out as described elsewhere using a solution of certain mmol (Table 2.3) of PZ **13** in 200 cm^3 of salt-free water or 0.1 M NaCl.[67,71] The Log *K* of the carboxyl group is calculated at each pH value by the Henderson–Hasselbalch Eq. (1) where α is the ratio $[ZH^{\pm}]_{eq}/[Z]_o$. For the titration with NaOH, the $[Z]_o$ is the initial concentration of repeating units in PZ **13**, and $[ZH^{\pm}]_{eq}$ is the concentration of the protonated species at the equilibrium given by $[ZH^{\pm}]_{eq} = [Z]_o - C_{OH^-} - [H^+] + [OH^-]$, where C_{OH^-} is the concentration of the added NaOH; $[H^+]$ and $[OH^-]$ at equilibrium were calculated from the pH value.[77,78] The polyelectrolytes having apparent basicity constants could be described by the Eq. (2) (Scheme 2.2) where

log K^o = pH at $\alpha = 0.5$ and $n = 1$ in the case of sharp basicity constants. The linear regression fit of pH *vs*. log [(1-α)/α)] gave log K^o and '*n*' as the intercept and slope, respectively. In titration using HCl in 0.1 M NaCl, titration was carried out in the presence of 1.5–2.5 cm^3 of 0.1036 N NaOH to attain the required values of the α. In this case $[ZH^{\pm}]_{eq} = [Z]_o + C_{H+} - C_{OH^-} - [H^+] + [OH^-]$, where C_{H+} is the concentration of the added HCl. Simultaneous protonation of the two basic sites (CO_2^- and SO_3^-) is least likely since the basicity constant for the SO_3^- group (log *K*: ~−2.1)[79] is less than that of the CO_2^- group by at least five orders of magnitude. Note that basicity constant log *K* of RSO_3^- (or any base) is the pK_a of its conjugate acid RSO_3H.

2.3 Results and discussions

2.3.1 Synthesis and physical characterization of the polymers

Tertiary amine **9** upon treatment with propane sultone **10** afforded zwitterionic monomer **11** in very good yield (82%) (Scheme 2.2). Monomer **11** underwent cyclopolymerization in the presence of initiator TBHP (or APS) to give polyzwitterion (PZ) **12** in moderate to good yields. The results of the polymerization under various conditions are given in Table 2.1. As evident from Table 2.1, maximum yield and intrinsic viscosity [η] of the polymer was obtained with an initiator concentration of 4 mg/mmol monomer in a 1 M NaCl solution at 90 ^oC (entry 7). It is interesting to note that the presence of a salt (NaCl) has a considerable beneficial influence on the polymer yields (*cf*. entry 4 *vs*. 5). In the polymerization of a zwitterionic monomer like **11**, the coiled zwitterionic macroradical is expanded in the presence of NaCl thereby allowing easier access to the monomer molecules so as to continue with the propagation.

The PZ (±) **12** was hydrolyzed in 6 M HCl to give PZA (±) **13**, which on treatment with NaOH afforded PEZ (− ±) **14**, so named as a result of having both anionic electrolyte as well as zwitterionic motifs in the same repeating unit. Polymers **12–14** were observed to be stable up to around 300 ^{o}C. All the polymers were found to be soluble in water (2% w/w) as well as in most of the protic solvents having higher dielectric constants (Table 2.1). While a 10% w/w (aqueous) PZA **13** formed a heterogeneous mixture at 23 ^{o}C, complete solubility was attained above 45 ^{o}C.

PZs are in general expected to be insoluble in water. However, their solubility in water is not unusual; a considerable number of polycarbobetaines (PCB) having pK_a values of around 2.0, and polysulfobetaines (PSB) (pK_a = −2.1)[79] are reported to be soluble in salt-free water.[14,80-82] The polycarbobetaines **3**[80], **4**[81] and **5**[83] having carboxyl pK_a of >2 are reported to be water-soluble, while the polysulfobetaines **6**[84] and **7**[66] are found to be insoluble in water but soluble in the presence of added salt (NaCl) which screens the zwitterionic charges from displaying zwitterionic interactions. The negative charges on the carbobetaines having higher carboxyl pK_a values are expected to be less dispersed, hence more hydrated[14,80,81] and as such tend to exhibit weaker Coulombic interactions with the cationic charges on the nitrogens[82] thus imparting solubility in salt-free water. In a recent article, simulation results show that the negative charges in carboxybetaines interact with water molecules stronger than the sulofobetaines.[85] Thus while carbobetaine **3**[80] (carboxyl pK_a > 2) is soluble in water, a critical NaCl concentration of 0.670 M is required to promote solubility of sulfobetaine **7**[66] (sulfonyl pK_a = −2.1).[79] Note that both PZ **12** and PSB **6** have quaternary nitrogens, yet the former is water-soluble while the latter is water-insoluble. Steric factor[17,86] thus seems to play a

dominant part in dictating the solubility behavior; the sterically crowded cationic charges in PZ **12**, owing to the presence of the bulkier CH_2CO_2Et group (*vs*. Me group in **6**), are unable to move closer to the sulfonates to manifest effective intra- or intermolecular Coulombic interactions, thereby leading to its solubility in water. Also note that CH_2CO_2Et group in **12** being more polar than Me group in **6** is expected to impart greater solubility in the former polymer. The anionic–zwitterionic **14** is readily soluble in salt-free water; its sulfonyl moiety is expected to be involved in zwitterionic interactions as depicted in Scheme 2.2 leaving out the carboxyl moiety to impart anionic character and solubility.

2.3.2 Infrared and NMR spectra

The IR spectrum of **11–14** indicates the presence of sulfonate group by its typical characteristic bands around ~1218 cm^{-1} and ~1042 cm^{-1}. Absorptions at 1742 cm^{-1} and 1737 cm^{-1} were assigned to C=O stretch of COOEt and COOH of **11** and **13,** respectively, while the symmetric and anti-symmetric stretching of COO^- in **14** appeared at 1408 cm^{-1} and 1628 cm^{-1}. The absorption peaks of COO^- are in agreement with those observed for simple amino acids.[87] The ^1H and ^{13}C NMR spectra of monomer **11** and polymers **12–14** are shown in Figure 2.1 and Figure 2.2, respectively. The absence of any residual alkene proton or carbon signal in the polymer spectra suggested that the formation of the polymer chains happened by termination *via* the chain transfer and/or coupling process.[88] The absence of methyl protons and carbon peaks of the ester group (OCH_2CH_3) in the spectra of **13** and **14** indicates its complete removal by hydrolysis. The assignments of the ^{13}C peaks are based on earlier works.[14,89,90] Integration of the relevant peaks in the ^{13}C NMR spectrum yielded a 75/25 *cis-trans* ratio

of the ring substituents at $C_{b,b}$ (Scheme 2.2) and is similar to that observed for polymers derived from quaternary ammonium salts.[7,91]

2.3.3 Viscosity measurements

Viscosity data for the polymers **12-14,** having identical degree of polymerization, were evaluated by the Huggins equation: $\eta_{sp}/C = [\eta] + k\,[\eta]^2 C$. Figures 2.3a and b display the viscosity behavior of the polymers (entry 7, Table 2.1) in salt-free water and 0.1 M NaCl, respectively. In salt-free water, the viscosity plots for PZA (±)**13** and PEZ (− ±)**14** are typical of polyelectrolytes i.e. concave upwards; whereas, the plot for (±) PZ **12** is linear, similar to that observed for a normal uncharged polymer (Figure 2.3a). The presence of an extra negative charge per repeating unit in anionic-zwitterionic (− ±) PEZ **14** makes its viscosity behavior typical of anionic polyelectrolytes. The anionic motifs in PEZ **14** thus dominate the viscosity behavior. The weakly acidic CO_2H group in zwitterionic (±) **13** undergoes dissociation in aqueous solution to anionic-zwitterionic (− ±) motifs in **14** (i.e. [(..$N^{\pm}$…CO_2H (**13**) ⇌ ..$N^{\pm}$… CO_2^- (**14**)]), and since the extent of dissociation increases with dilution, the reduced viscosity increases with decreasing concentration of PZA **13**. Based on the carboxyl pK_a value of 3.33 in (±) PZA **13** in salt-free water (*vide infra*), its percent dissociation in 1, 0.5, 0.25 and 0.125 g/dL solutions has been calculated to be 11, 15, 20 and 27, respectively. Note that polymer (− ±) **14** has higher viscosity values than (±) **13** as a result of the polymer chains of the former experiencing increased repulsions among the completely dissociated CO_2^- anions.

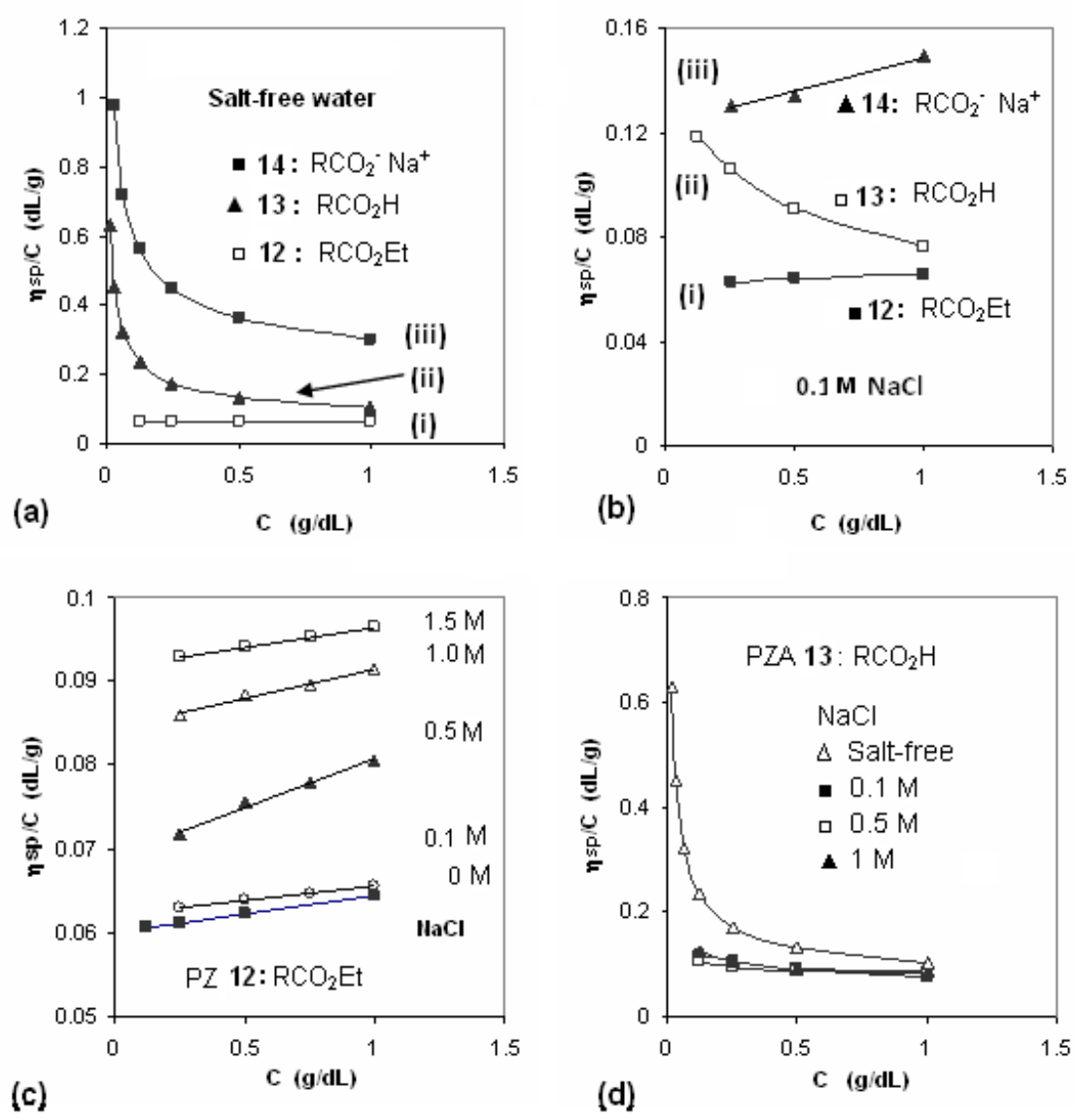

Figure 2.3 Using an Ubbelohde Viscometer at 30 ^{o}C: The viscosity behavior of: (**a**) PZ **12,** PZA **13,** and PEZ **14** (from or derived from entry 7, Table 2.1) in salt-free water and **(b)** 0.1 M NaCl. Variation of viscosity of: (**c**) PZ **12** (from entry 7, Table 2.1) and (d) PZA **13** (derived from entry 7, Table 2.1) with salt (NaCl) concentration.

In the presence of added salt (0.1 N) the viscosity plots for PZ (±) **12** and PEZ (−±) **14** remain linear as expected of any polyelectrolyte (Figure 2.3b). The progressive dissociation of the CO_2H groups in (±) PZA **13**, however keeps the curve concave

upwards. Based on the carboxyl pK_a value of 2.95 in 0.1 M NaCl (*vide infra*), its percent dissociation in 1, 0.5, 0.25 and 0.125 g/dL solutions has been determined to be 16, 22, 30 and 39, respectively. Polymer **14**, as expected, has higher viscosity values than **13** as a result of the CO_2^- groups of the former being in the almost complete dissociated form.

The dependency of viscosity of (±) PZ **12** and (±) PZA **13** in aqueous solution containing various concentration of NaCl are shown in Figure 2.3c and d, respectively. An increase in the intrinsic viscosity with increasing NaCl concentration explains the antipolyelectrolyte behavior of PZ **12**. The viscosity values of (±) PZA **13**, on the other hand, decrease with the increase in the salt concentration from salt-free to 0.1 M NaCl, and thereafter remain almost similar with further increase in the salt concentration to 0.5 and 1 M NaCl. The carboxyl pK_a in PZA **13** is 3.33 and 2.95 in salt-free and 0.1 M NaCl, respectively; as such the percent dissociation of CO_2H groups is expected to increase with the increase in the ionic strength of the medium. The increased CO_2H dissociation is thus expected to increase the viscosity values as a result of the increased repulsion among the CO_2^- anions. The strong binding ability of the cationic nitrogens by Cl^- is also expected to increasingly expose the CO_2^- and SO_3^- to experience strong repulsions since the Na^+ ion with its fairly large hydration shell cannot effectively shield the anions.[18] Yet the viscosity values decrease with the increase in NaCl concentration; the exposed anionic carboxylate and sulfonate pendents in a sea of Na^+ ions are thus shielded considerably so as to minimize repulsions among them and thus decrease the viscosity values (Figure 2.3d).

The solution behavior of polyampholytes with or without charge symmetry has been described mathematically[20,92-94] in terms of:

$$v^* = -\frac{\pi(fI_B)^2}{\kappa_S} + \frac{4\pi I_B \Delta f^2}{\kappa_S^2} \qquad (4)$$

where I_B is the Bjerrum length, f is the total fraction of charged monomers, Δf is the charge imbalance, and κ_S is the Debye–Huckel screening parameter. Since the $\Delta f = 0$ for the electroneutral (±) PZ **12**, the screening of the Coulombic repulsive interactions among excess charges, described by the second term of Eq. (4), vanishes; the solution behavior must then be described by the first term describing the screening of the attractive polyampholytic interactions. The negative electrostatic excluded volume indicates contraction to a collapsed polymer chain. For (±) PZA **13** and (− ±) PEZ **14,** $\Delta f \neq 0$; the charge imbalance is maximum for the PEZ, while it depends on the extent of dissociation in the case of the PZA. In either case, the size of the polymer chain depends on the relative importance of the first and second terms of Eq. (4). For PEZ **14** having the maximum value of Δf, the second term in Eq. (4) dominates, and the resultant positive electrostatic excluded volume led to the expansion of the polymer chains. The increased percent dissociation of CO_2H in PZA **13** associated with the decrease in polymer concentration increases the progressive importance of the second term (Eq. (4)). This is indeed corroborated by the observed increase of the viscosity values with decrease in the polymer concentration (Figure 2.3d). As the salt (NaCl) concentration increases (from 0 to 0.1 N), the magnitude of the first and second term increases and decreases, respectively. As a result, the contraction of the polymer chain occurs. At higher concentrations of salt (0.5 M or more), the electrostatic contribution to the polymer size

becomes insignificant as a result of minimized importance of both terms in eq 4 (Figures 2.3d, 2.4a).

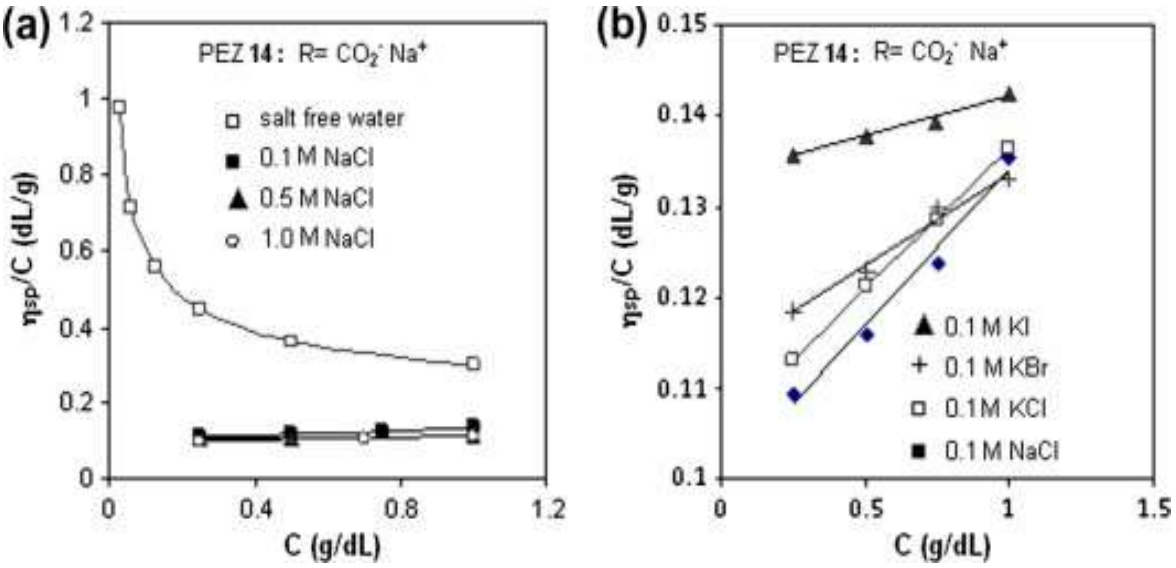

Figure 2.4 Viscosity behavior of PEZ **14** (**a**) with salt (NaCl) concentration and (**b**) with 0.1 M concentration of various salts using an Ubbelohde Viscometer at 30 ^{o}C.

The dependency of viscosity of PEZ (− ±) **14** in aqueous solution containing various concentration of NaCl are shown in Figure 2.4a. Note that the viscosity values remain similar in 0.1, 0.5 and 1 M NaCl. The increased salt concentration thus has an equal and opposite influence on the anionic (−) and zwitterionic (±) motifs; the presence of NaCl helps the anionic portions to coil up and the zwitterionic portions to expand. It is worth mentioning that PEZ **14** is salt-tolerant in the sense that its viscosity is quite independent of the salt concentration.

The intrinsic viscosity [η] of (− ±) PEZ **14** in 0.1 M NaCl, KCl, KBr, KI at 30 °C was determined to be 0.0997, 0.105, 0.113, and 0.133 dL/g, respectively. The intrinsic viscosity is thus found to decrease in the order KCl > NaCl (for common anions) and KI > KBr > KCl (for common cations) (Figure 2.4b). It is known that while the intrinsic

viscosity of cationic polyelectrolytes[91] decreases in 0.1 N aqueous salt solution in the order KCl > KBr > KI, the order is reversed for polybetaines or polyampholytes.[15,18,66,80] The observed salt effect thus reflects the zwitterionic motifs' dominance in dictating the viscosity behavior of PEZ **14** since the viscosity of anionic polyelectrolytes is expected to be independent of the effect of anions (like Cl^- and Br^-). This is expected since the more polarizable (soft) iodide anion is particularly effective in neutralizing the cationic charges on the polymer backbone thereby forcing the expansion of the macromolecule so as to minimize repulsion among the more exposed negatives charges on the pendents.[95] The interesting aqueous solution behavior of PEZ **14** is found to be similar to that observed for an alternating anionic–zwitterionic copolymer derived from monomers **15** and **16** (Scheme 2.3).[96] The current PEZ **14** may also be described as an alternate anionic–zwitterionic polymer as depicted in Scheme 2.3.

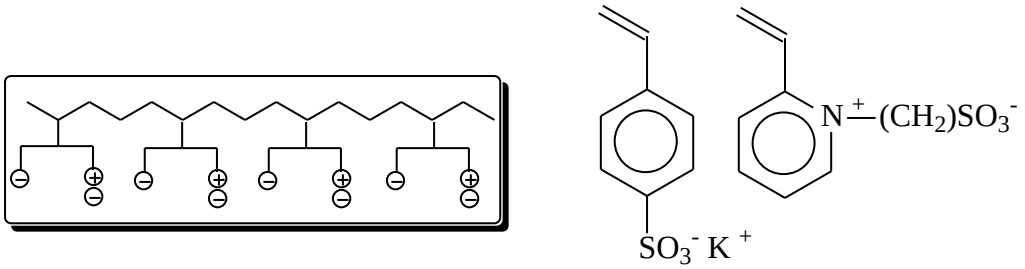

14 **15** **16**

Scheme 3.

Scheme 2.3 Monomers for the formation of an alternating poly(electrolyte-zwitterion).

2.3.4 Basicity constants

The basicity constant log *K* for the protonation of the CO_2^- of PEZ **14** is of "apparent"[97] nature (Scheme 2.2) as demonstrated in Figure 2.5, which reveals a change in log *K* with

the degree of protonation (α) in going from one end to the other end of the titration. The *n* values of 2.52 and 1.30 in salt-free water and 0.1 M NaCl, respectively, reflect a stronger polyelectrolyte effect in the former medium (Table 2.3). The *n* values of >1 indicate the decrease in the basicity of CO_2^- anions with the increase in α owing to a progressive decrease in the electrostatic field force that encourages protonation as a result of changing the overall negative charge density in (− ±) PEZ **14** to electroneutral (±) PZA **13**. It is worth mentioning that the *n* value for the protonation of basic CO_2^-, which is in the α-position with respect to the positive nitrogens as in **3** and **4**, is found to be less than 1.[80,81] With the increase in the degree of protonation (α), the number of zwitterionic and cationic motifs in **3** or **4** decreases and increases, respectively. The uncoiling of a tightly compact zwitterionic conformation, thus allow the protons to have easier access to the CO_2^- anions. The *n* values of <1 in **3** and **4** thereby ascertain the increase of basicity constant with the increase in α.

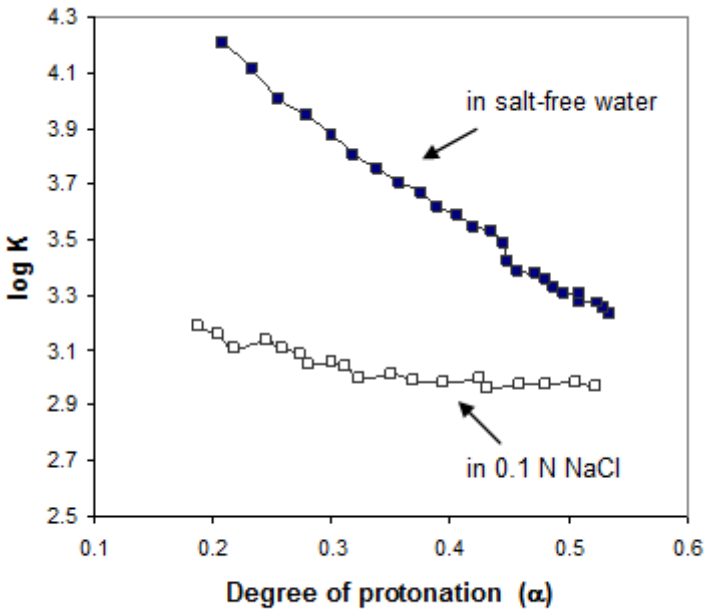

Figure 2.5 Plot for the apparent log K versus degree of protonation (α) for PZA **13** in salt-free water and 0.1 M NaCl.

Table 2.3 Experimental Details for the Protonation of the Polymers PZA **13** ($ZH^{\pm}$) at 23 ^{o}C in Salt-Free Water and 0.1 M NaCl.

run	$ZH^{\pm}$ (mmol)	C_T [a] (mol dm^{-3})	α−range	pH−range	Points[b]	Log K^{o} [c]	N [c]	R^2, [d]
Polymer in Salt-Free water								
1	0.3570 ($ZH^{\pm}$)	- 0.1036	0.53−0.21	3.17− 4.79	25	3.31	2.53	0.9983
2	0.2881 ($ZH^{\pm}$)	- 0.1036	0.55−0.23	3.19−4.68	22	3.37	2.55	0.9969
3	0.2268 ($ZH^{\pm}$)	- 0.1036	0.53−0.21	3.27−4.76	20	3.32	2.49	0.9960
	Average					3.33 (3)	2.52 (3)	
Log K [e] = 3.33 + 1.52 log [(1-α)/α] For the reaction: $Z^{\pm -} + H^{+} \rightleftharpoons ZH^{\pm}$								
Polymer in 0.1 M NaCl								
1	0.3195 [f] ($ZH^{\pm}$)	0.09930	0.16−0.59	3.88−2.75	24	2.91	1.25	0.9935
2	0.2578 [f] ($ZH^{\pm}$)	0.09930	0.18−0.52	3.89−2.98	21	2.98	1.35	0.9942
3	0.2034 [f] ($ZH^{\pm}$)	0.09930	0.19−0.52	3.82−2.93	19	2.95	1.31	0.9912
	Average					2.95 (4)	1.30 (5)	
Log K [e] = 2.95 + 0.30 log [(1-α)/α] For the reaction: $Z^{\pm -} + H^{+} \rightleftharpoons ZH^{\pm}$								

[a]Titrant concentration (negative and positive values indicate titrations with NaOH and HCl, respectively).
[b]Number of data points from titration curve. [c]Values in the parentheses are standard deviations in the last digit.
[d]R = Correlation coefficient. [e]log K = log K^{o} + (n – 1) log [(1 - α)/α]. [f]titration was carried out in the presence of 1.5-2.5 cm^3 of 0.1036 M added NaOH to attain the required values of the α.

The neutralization process, which transforms the anionic motifs in (− ±) PEZ **14** to zwitterionic motifs in (±) PZA **13**, may be described by the viscometric transformation of Figure 2.3a(iii) to (ii) in salt-free water and Figure 2.3b(iii) to (ii) in 0.1 M NaCl. The former revealing a bigger change in viscosity values than the later transformation. Since PEZ **14** in salt-free water (Figure 2.3a-iii) is the most expanded hence more hydrated, the greater number of water molecules are released as a result of each protonation in salt-free water than in 0.1 M NaCl thereby leading to an entropy-driven[98] higher basicity constant and *n* in the former medium (Table 2.3). The basicity constant (log K^{o}) of the carboxyl group was found to be 3.33 and 2.95 in salt-free water and 0.1 M NaCl, respectively. Note that carboxyl basicity constant (log K^{o}) in PEZ **14** is the pK_a value for the corresponding conjugate acid PZA **13**.

2.4 Conclusions

Zwitterionic monomer **11** was synthesized by a simple reaction. The work described in this paper represents the use of cyclopolymerization technique to provide the first synthetic example of a poly(electrolyte-zwitterion) **14** having carboxylate and sulfonate pendants. The apparent basicity constants of the carboxyl group in **14** have been determined. The study describes a simple way to convert a polyzwitterion to a poly(electrolyte-zwitterion) and hence gives an opportunity for the direct comparison of the solution properties of these ionic polymers having the same degree of polymerization. The solution behavior of PEZ **14** has been found to be similar to a typical alternate anionic–zwitterionic polymer. Currently, work is underway in our laboratory to synthesize cross-linked resins *via* cyclopolymerization of **11** and suitable cross-linkers so

as to study the adsorption efficacy of the resulting resin containing the anionic–zwitterionic functionalities.

CHAPTER 3

Cyclopolymerization Protocol for the Synthesis of a Poly(zwitterion-alt-sulfur dioxide) to Investigate the Polyzwitterion-to-Poly(anion-zwitterion) Transition

Taken from Shaikh A. Ali and Shamsuddeen A. Haladu, Cyclopolymerization Protocol for the Synthesis of a Poly(zwitterion-alt-sulfur dioxide) to Investigate the Polyzwitterion-to-Poly(anion-zwitterion) Transition, *Journal of Applied Polymer Science*, 129: 1394–1404, 2013

Abstract

The zwitterionic monomer, 3-(*N*,*N*-diallyl,*N*-carboethoxymethylammonio)propanesulfonate, on cocyclopolymerization with sulfur dioxide in DMSO using azobisobutyronitrile as the initiator afforded the polyzwitterion (PZ) copolymer in excellent yields. The PZ on acidic hydrolysis of the ester groups led to the corresponding polyzwitterionic acid (PZA). The pH-responsive PZA on treatment with sodium hydroxide gave the new poly(eletrolyte-zwitterion) (PEZ). The solubility, viscosity behaviors, and solution properties of the salt-tolerant PZ, PZA and PEZ were studied in detail. Like common PZs, PZ was found to be insoluble in salt-free but soluble in salt-added water. The apparent basicity constants of the carboxyl group in PEZ have been determined. As the name implies, the PEZ possesses dual type of structural feature common to both conventional anionic polyelectrolytes and PZs, and its aqueous solution behavior is found to be similar to that observed for a typical alternating anionic-zwitterionic copolymer.

3.1 Introduction

Butler's cyclopolymerization[5-9] as well as cocyclopolymerization of *N*,*N*-diallyl quaternary ammonium and amine salts with sulfur dioxide[71,72,99,100] led to the synthesis of a range of water-soluble cationic polyelectrolytes having quenched and unquenched nitrogen valances, respectively. The cyclopolymers containing the five-membered rings embedded into the polymer backbone are considered to have the eighth major structural feature of synthetic high polymers. These polymers are of significant scientific and technological interest; poly(diallyldimethylammonium chloride) alone has over 1000 patents and publications. Quaternary ammonium polyelectrolytes find manifold application in industrial processes and daily life. The technical applications based on Coulombic attraction between the positively charged macromolecules and negatively charged macro-ions, surfactants, etc., have resulted in different materials including membranes, modified surfaces, coated particles, etc.[8,101,102]

The cyclopolymerization protocol involving zwitterionic diallylammonium monomers has been an interesting avenue for the synthesis of polyzwitterions (PZs) (having charges of both algebraic signs in the same repeating units).[12,17] The unquenched valency of nitrogens in diallylamine salts containing sulfonate and hydrolyzable ester functionalities as pendents led to the synthesis of a variety of pH-responsive poly sulfo-, carbo-, and polyphosphobetaines (i.e., PZs).[6,7,9] The pH-induced changes in the charge types and their densities in a cyclopolymer backbone have been shown to change a cationic polyelectrolyte to a PZ or a polyampholyte having repeating units containing cationic and anionic charges with or without charge symmetry.[10]

A polysulfobetaine (PSB) having weakly basic sulfonate group remains zwitterionic over a wide range of pH, while a polycarbobetaine (PCB), because of the weak acid nature of the carboxylic acid group, can be rendered cationic by lowering the pH of the aqueous medium.[7] The pH-responsive PSBs and PCBs having unquenched nitrogens can also be changed to polyanions by neutralization of the ammonio proton.[71,72,99,100] The synthesis of copolyzwitterions incorporating 25 mol % carboxybetaine and 75 mol % sulfobetaine and its interesting pH-dependent solution properties have been reported.[73] Nearly monodisperse PZs have been synthesized by group transfer polymerization (GTP) of 2-(dimethylamino)ethyl methacrylate (DMAEMA) followed by quantitatively betainization using 1,3-propanesultone.[103] Well-defined sulfobetaine-based statistical copolymers of DMAEMA with *n*-butyl methacrylate were synthesized via GTP followed by betainization.[104]

PZs have collapsed or globular conformations in salt-free solutions due to the intragroup, intra- and interchain electrostatic dipole–dipole attractions among the dipolar motifs. They exhibit "antipolyelectrolyte" effect which is globule-to-coil transitions in the salt-added solutions owing to the neutralization of the ionically crosslinked network in a collapsed coil conformation of the polymers.[6,17,20,105] The PZs containing the permanent dipole can thus be tailored for enhancement in solubility and viscosity in the presence of added salt owing to the shielding of the Coulombic (dipole–dipole) attractions.[18-20,106,107] The high dipole moment of PZs renders the properties of excellent polar host matrix in which only target ions can migrate.[108,109] The stoichiometric blends of some PZs with alkali metal salts have produced excellent matrices having high ionic conductivity.[110] The pH-responsive PZs, whose structure and behavior seem to mimic

biopolymers, have been utilized for the development of anticarcinogenic drugs in combination with fullerenes[111] and improvement of the biocompatibility of various medical[112] and nanotechnology tools.[113] The unique "antipolyelectrolyte" behavior makes PZs attractive candidates for application in enhanced oil recovery, drag reduction, personal care products, cosmetics, and pharmaceuticals.[114-116] Numerous applications also include their uses as fungicides, fire-resistant polymers, lubricating oil additives, emulsifying agents, and bioadherent coatings.[9,117-119] The PZs have been utilized for efficient separations of biomolecules[7] and to develop procedures for DNA assay.[120] They have also drawn attention in the field of ion exchange; their abilities to chelate toxic trace metals (Hg, Cd, Cu, and Ni) have been exploited in wastewater treatment.[6,115] PZs are also used as drilling-mud additives[121] and for the separation of water and oil from water-in-oil emulsions.[122]

In pursuit of pH-responsive polymers, we have recently reported[123] the synthesis and homocyclocopolymerization of a specialty monomer **4** (Scheme 3.1). We describe herein the cocyclocopolymerization of **4** with SO_2 that would lead to a polymer **7** having zwitterionic and anionic motifs in the same repeating unit. The cyclopolymerization protocol has so far documented two such (electrolyte-zwitterion)/SO_2 copolymers in the literature; in both cases the anionic motifs in monomer **1** were either sulfonate ($x = y = 3$)[75] or carboxylate ($x = 5$, $y = 1$).[16] The current work involves monomer **4**/SO_2 copolymerization that would lead to poly(electrolyte-zwitterion) (PEZ **7**) (Scheme 3.1).[16,75] To the best of our knowledge, polymer **7**, obtained via the cyclopolymerization protocol, would represent the first example of this class of PEZ having different anionic motifs (carboxylate and sulfonate) in the same repeating unit as

well as a SO_2 spacer in the polymer backbone. The synthesis of the new pH-responsive polymers would provide an opportunity to study PZ **5** to PEZ **7** transition involving polymers having identical degree of polymerization. The effects of backbone stiffening SO_2 spacer on the solution properties of these polymers will be measured and compared with those of the corresponding homocyclopolymer.[123]

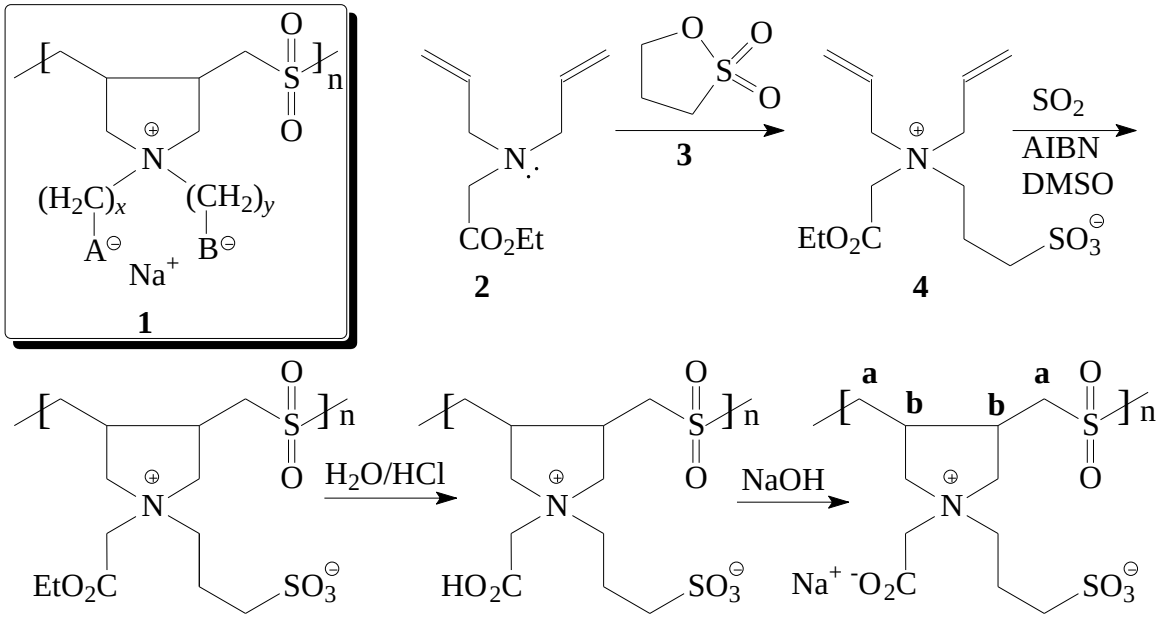

$$Z^{\pm -} + H^{+} \underset{}{\overset{K}{\rightleftharpoons}} ZH^{\pm}$$

7 **6**

$$\log K = pH - \log[(1-\alpha)/\alpha] \quad \text{Eq 1}$$

$$pH = \log K^{o} + n \log[(1-\alpha)/\alpha] \quad \text{Eq 2}$$

$$\log K = \log K^{o} + (n-1) \log[(1-\alpha)/\alpha] \quad \text{Eq 3}$$

Scheme 3.1 Cyclopolymerization protocol for the synthesis of polyzwitterion and polyanion-zwitterion.

3.2 Experimental

3.2.1 Physical Methods

Elemental analysis was carried out on a Perkin Elmer Elemental Analyzer Series II Model 2400. IR spectra were recorded on a Perkin Elmer 16F PC FTIR spectrometer. The ^{13}C and ^{1}H NMR spectra of the polymers have been measured in D_2O (using HOD signal at 4.65 and dioxane ^{13}C peak at δ67.4 as internal standards) on a JEOL LA 500 MHz spectrometer. Viscosity measurements have been made by Ubbelohde viscometer (having viscometer constant of 0.005718 cSt/s at all temperatures) using CO_2-free water under N_2 in order to prevent CO_2 absorption that may affect the viscosity data. For the potentiometric titrations, the pH of the solutions was recorded using a Corning pH Meter 220. Molecular weights of some of the synthesized polymers were determined by gel permeation chromatography (GPC) analysis using Viscotek GPCmax VE 2001. The system was calibrated with nine polyethylene oxide monodispersed standards at 30°C using two Viscotek columns G5000 and G6000 in series.

3.2.2 Materials

2,2′-Azobisobutyronitrile (AIBN) from Fluka AG (Buchs, Switzerland) was purified by crystallization from a chloroform–ethanol mixture. Dimethylsulfoxide (DMSO) was dried over calcium hydride overnight and then distilled under reduced pressure at a boiling point of 64–65°C (4 mmHg). For dialysis, a Spectra/Por membrane with a molecular weight cut-off (MWCO) value of 6000–8000 was purchased from Spectrum Laboratories, Rancho Dominguez, CA. All glassware were cleaned with deionized water. Zwitterionic monomer **4** was prepared in 82% yield by heating an equimolar mixture of *N*,*N*-diallyl-*N*-carboethoxymethylamine (**2**)[76] and 1,3-propanesulfone (**3**) in

acetonitrile (130 cm^3 for 0.13 mol amine) at 72°C for 72 h. M.p. (methanol/acetone/diethyl ether) 162–163°C.

3.2.3 General Procedure for the Copolymerization of the Monomer 4 with SO_2 and Physical Characterization of PZ 5

All the polymerizations were carried out under the conditions described in Table 3.1. In a typical experiment (entry 4), SO_2 (20 mmol) was absorbed in a solution of monomer **4** (20 mmol) in DMSO (5.8 g). The required amount of the initiator (AIBN) (60 mg) was then added under N_2 and the closed flask was stirred using magnetic stir-bar at 60°C for 24 h. Within 2 h, the magnetic bar stopped stirring, and the initial reaction mixture became a solid mass of white polymer. At the end of the elapsed time, the hard polymeric mass was crushed to powder, soaked in methanol, filtered, and washed with liberal excess of hot (50°C) methanol to ensure the complete removal of the unreacted monomer (as indicated by ^{1}H NMR). Copolymer **5** was then dried under vacuum at 60°C to a constant weight. The onset of thermal decomposition (closed capillary): the color changed to brown at 255°C and turned to black at 270°C. (Found: C, 42.0; H, 6.5; N, 3.7; S, 16.9%. $C_{13}H_{23}NO_7S_2$ requires C, 42.26; H, 6.27; N, 3.79; S, 17.36%); ν_{max} (KBr): 3755, 3441, 2983, 1744, 1646, 1471, 1417, 1311, 1216, 1127, 1037, 909, 860, 729, 602 cm^{-1}. ^{1}H and ^{13}C NMR spectra of PZ **5** are displayed in Figures 3.1 and 3.2.

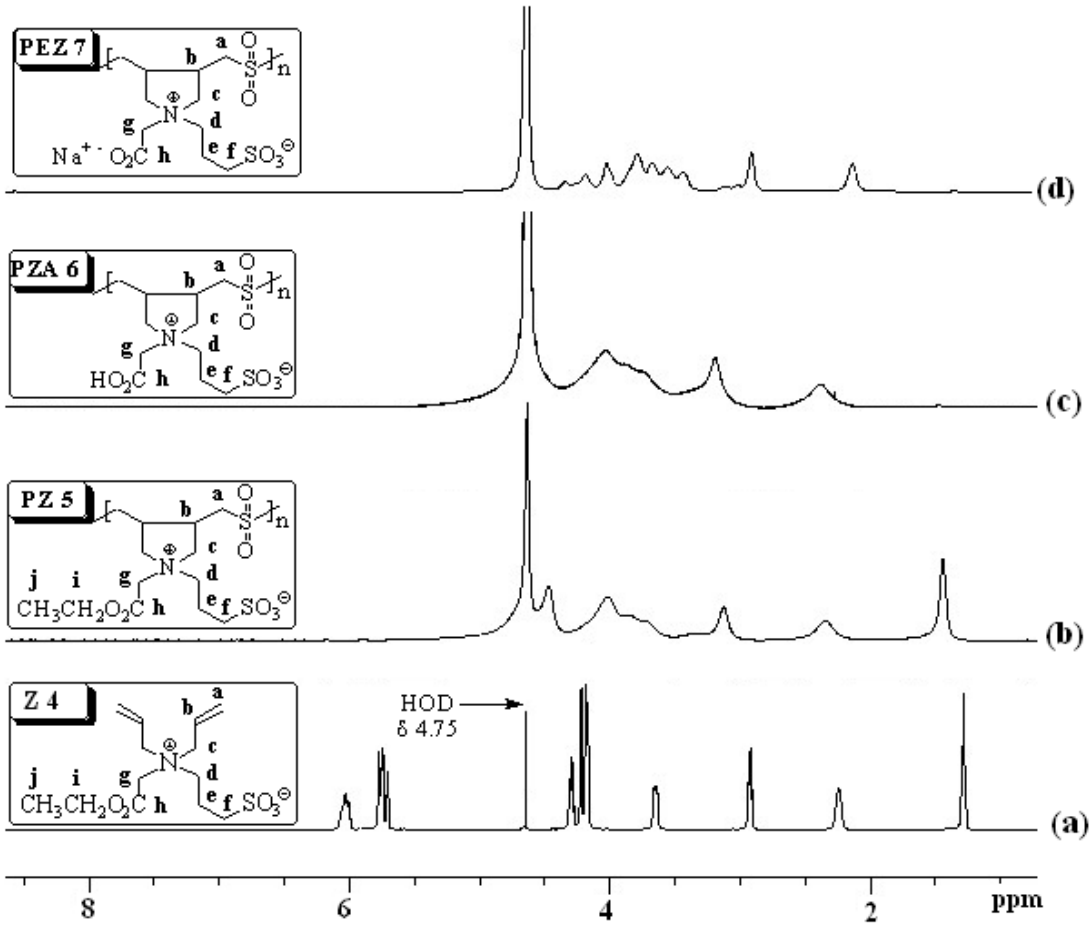

Figure 3.1 ^{1}H NMR spectrum of (a) **4** in D_2O, (b) **5** in (D_2O+ NaCl), (c) **6** (D_2O+ NaCl) and (d) **7** in D_2O.

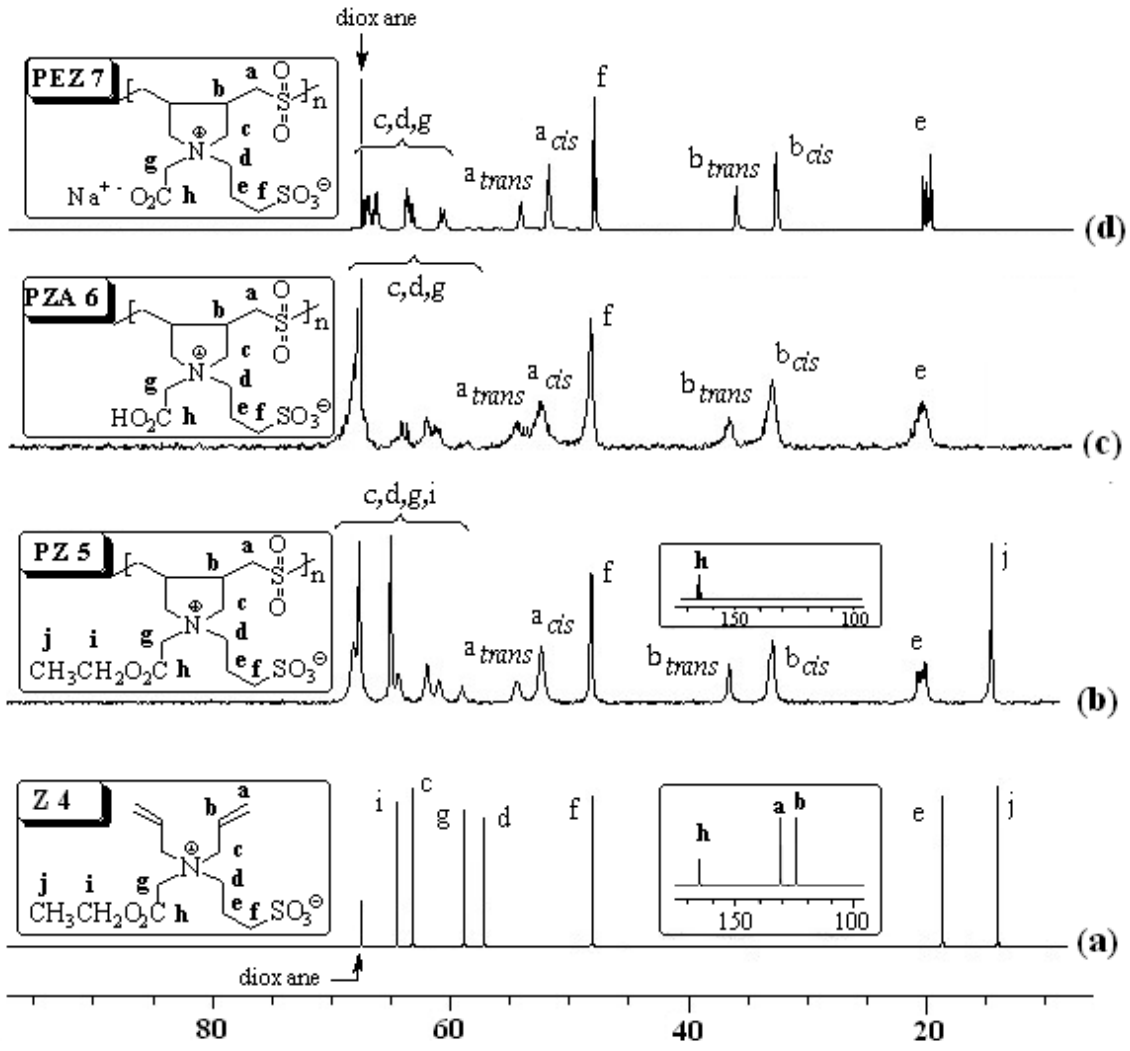

Figure 3.2 ^{13}C NMR spectrum of a) **4** in D_2O, (b) **5** in (D_2O+ NaCl), (c) **6** (D_2O+ NaCl) and (d) **7** in D_2O.

Table 3.1 Copolymerization of Monomer **4** with Sulfur dioxide

Entry No.	Monomer (mmol)	DMSO (g)	Initiator[a] (mg)	Yield (%)	$[\eta]^b$ (dL g^{-1})	$\overline{M}_w$	(PDI)[d]
1	10	2.3	30	82	0.164	–	–
2	10	3.6	30	95	0.186	–	–
3	10	5.8	30	85	0.140	1.01×10^5	2.34
4	20	5.8	60	90	0.188	1.33×10^5	2.47

Polymerization reactions were carried out in DMSO using equimolar mixture of monomer **4** and SO_2 at 60^oC for 24 h.
[a]Azobisisobutyronitrile.
[b]Viscosity of 1-0.25 % polymer solution in 0.5 N NaCl at 30^oC was measured with Ubbelohde Viscometer (K=0.005718).
[c]Polydispersity index

For the determination of molecular weights, the polymer PZ **5** was analyzed using an aqueous solution of 0.5*N* NaCl as the eluant. Refractive index and viscometer detectors were used to detect polymers. The molecular weight ($\overline{M}_w$) and PDI of some of the polymers are given in Table 3.1.

3.2.4 Acid Hydrolysis of PZ 5 to Poly(zwitterion acid) 6 with Aqueous HCl

PZ **5** (3.0 g, 8.12 mmol) (entry 4, Table 3.1) was hydrolyzed in a 6*M* HCl (60 mL) at 53°C for 48 h. The homogeneous mixture was cooled to room temperature and dialyzed against deionized water (to remove HCl) for 24 h. During dialysis, precipitation of the polymer occurred immediately and its amount increased with time. The resulting mixture

containing the solid was freeze dried to obtain poly(zwitterion acid) (PZA **6**) as a white solid (2.36 g, 92%). The polymer was found to be insoluble in water but soluble in the presence of HCl. The onset of thermal decomposition (closed capillary): the color changed to dark brown at 275°C and to black at 285°C; (Found: C, 38.4; H, 5.8; N, 3.9; S, 18.5%. $C_{11}H_{19}NO_7S_2$ requires C, 38.70; H, 5.61; N, 4.10; S, 18.78%); v_{max} (KBr): 3620, 3451, 2973, 2930, 2372, 1741, 1643, 1461, 1423, 1310, 1213, 1129, 1034, 700, 729, 578 cm^{-1}. The ^{1}H and ^{13}C NMR spectra of PZA **6** are displayed in Figures 3.1 and 3.2.

3.2.5 Basification of PZA 6 to PEZ 7

To a sample of **6** (derived from entry 4, Table 3.1) (0.688 g, 2.02 mmol) was added NaOH (0.163 g, 4.1 mmol) in 2.5 cm^3 deionized water. After stirring for 5 min, PEZ **7** was precipitated in methanol. Filtration and washing with excess methanol gave the white polymer **7** which was dried under vacuum at 55°C to a constant weight (0.68 g, 93%). The onset of thermal decomposition (closed capillary): the color changed to brown at 280°C and black at 305°C. (Found: C, 36.1; H, 5.2; N, 3.7; S, 17.4%. $C_{11}H_{18}NNaO_7S_2$ requires C, 36.36; H, 4.99; N, 3.85; S, 17.65%); v_{max} (KBr): 3446, 3031, 2970, 2921, 1628, 1460, 1405, 1304, 1204, 1131, 1044, 913, 731 cm^{-1}. The ^{1}H and ^{13}C NMR spectra of PEZ **7** are displayed in Figures 3.1 and 3.2.

3.2.6 Solubility Measurements and Cloud Point Titration in Aqueous Salt Solutions

A 1% (wt/wt) mixture of PZ **5**, PZA **6**, and PEZ **7** in a solvent was heated to 70°C for 1 h and then cooled to 23°C. The results of the solubility are shown in Table 3.2.

Table 3.2 Solubility[a,b] of PZ **5**, PZA **6**, and PEZ **7**

Solvent	ε	PZ **5**	PZA **6**	PEZ **7**
Formamide	111	+	±	+
Water	78.4	−	−	+
Formic acid	58.5	+	−	−
DMSO	47.0	−	−	−
Ethylene glycol	37.3	−	−	−
DMF	37.0	−	−	−
Methanol	32.3	−	−	−
Triethylene glycol	23.7	−	−	−
Acetic acid	6.15	−	−	−

[a] 2% (w/w) of polymer-water mixture (solution) was made after heating the mixture at 70 °C for 1 h and then cooling to 23 °C.

[b] '+' indicates soluble, '−' indicates insoluble, and '±' indicates partially soluble.

The critical (minimum) salt concentration (CSC) required to promote water solubility of PZ **5** (entry 4, Table 3.1) at 23°C was measured by titration of a 1% wt/wt polymer solution at sufficiently high salt concentration with deionized water. The accuracy of the CSC values, obtained by visual determination of the first cloud point, was approximately ±2%. The CSC values are reported in Table 3.3.

Table 3.3 Critical Salt Concentration for Aqueous Solutions of PZ **5** at 23 °C

Salt	CSC (M)
LiCl	0.32
NaCl	0.29
KCl	0.31
KBr	0.047
KI	0.0060
NH_4Cl	0.32
$CaCl_2$	0.25
HCl	0.38

3.2.7 Potentiometric Titrations

The potentiometric titrations were carried out as described elsewhere using a solution of certain mmol (Table 3.4) of PZA **6** in 200 cm^3 of salt-free water or 0.1*N* NaCl.[71] The log *K* of the carboxyl group is calculated at each pH value by the Henderson–Hasselbalch eq. (2) (Scheme 3.1) where degree of protonation α is the ratio $[ZH^{\pm}]_{eq}/[Z]_o$, $[Z]_o$ is the initial concentration of repeating units in PZA **6**, and $[ZH^{\pm}]_{eq}$ is the concentration of the protonated species at the equilibrium. The titration with HCl was carried out in the presence of 1.5–2.5 cm^3 of 0.1036 *N* NaOH to attain the required values of the α. In this case, $[ZH^{\pm}]_{eq} = [Z]_o + C_{H+} - C_{OH^-} - [H^+] + [OH^-]$, where C_{H+} and C_{OH^-} are the

concentration of the added HCl and NaOH, respectively; [H^+] and [OH^-] at equilibrium were calculated from the pH value.[77,78] The polyelectrolytes having apparent basicity constants could be described by the eq. (3) (Scheme 3.1) where log $K°$ = pH at $\alpha = 0.5$ and $n = 1$ in the case of sharp basicity constants. The linear regression fit of pH vs. log $[(1 - \alpha)/\alpha)]$ gave log $K°$ and "n" as the intercept and slope, respectively. Simultaneous protonation of the two basic sites (CO_2^- and SO_3^-) is least likely since the basicity constant for the SO_3^- group (log K: ~ -2.1) is less than that of the CO_2^- (log K: $\sim +3$) group by almost five orders of magnitude.

Table 3.4 Experimental Details for the Protonation of the Polymers PZA 6 ($ZH^{\pm}$) at **23** ^{o}C in Salt-Free Water and 0.1 N NaCl.

run	$ZH^{\pm}$ (mmol)	C_T [a] (mol dm^{-3})	α−range	pH−range	Points[b]	Log K^{o} [c]	n [c]	R^2, [d]
Polymer in Salt-Free water [e]								
1	0.3536	0.09930	0.17−0.60	4.98−3.04	24	3.43	2.19	0.9988
2	0.2910	0.09930	0.17−0.53	5.01−3.27	22	3.46	2.24	0.9959
3	0.2352	0.09930	0.14−0.53	5.23−3.28	20	3.38	2.29	0.9960
Average						3.42 (4)	2.24 (5)	
Log K [f] = 3.42 + 1.24 log [(1-α)/α] For the reaction: $Z^{\pm -}$ + H^{+} ⇌ $ZH^{\pm}$								
Polymer in 0.1 N NaCl [e]								
1	0.2847	0.09930	0.20−0.51	3.74−2.95	23	2.95	1.21	0.9887
3	0.2302	0.09930	0.15−0.50	3.81−2.91	20	2.90	1.20	0.9962
2	0.1878	0.09930	0.14−0.52	4.11−3.05	22	3.08	1.27	0.9958
Average						2.98 (9)	1.23 (4)	
Log K [f] = 2.98 + 0.23 log [(1-α)/α] For the reaction: $Z^{\pm -}$ + H^{+} ⇌ $ZH^{\pm}$								

[a]Concentration of titrant HCl [b]Number of data points from titration curve. [c]Values in the parentheses are standard deviations in the last digit. [d]R = Correlation coefficient. [e]titration was carried out in the presence of 2.0-3.0 cm^3 of 0.1031 N added NaOH to attain the required values of the α. [f]$\log K_i = \log K^{o} + (n-1) \log [(1-\alpha)/\alpha]$.

3.3 RESULTS AND DISCUSSIONS

3.3.1 Synthesis of the Copolymers

Zwitterionic monomer **4**/SO_2 underwent cocyclopolymerization in the presence of initiator AIBN to give PZ **5** in excellent yields. The results of the polymerization under various conditions are given in Table 3.1. As evident from the table, changing the amount of solvent DMSO does not have any appreciable effects on the yield or intrinsic viscosity [η] of PZ **5**. (±) PZ **5** upon hydrolysis in 6*M* HCl afforded (±) PZA **6** which on treatment with equivalent amount of NaOH gave (− ±) PEZ **7**, so named as a result of having both anionic electrolytes as well as zwitterionic motifs in the same repeating unit. Polymers **5–7** were observed to be stable up to around 260°C.

3.3.2 Infrared and NMR Spectra

The IR spectrum of **5–7** indicates the presence of sulfonate group by its strong characteristic bands at ∼1200 $cm^{-1}$and ∼1040 cm^{-1}. The two strong bands at ∼1300 cm^{-1} and ∼1130 cm^{-1} were assigned to the asymmetric and symmetric vibrations of SO_2 unit. Absorption at ∼1740 cm^{-1} was attributed to C=O stretch of COOEt and COOH of **5** and **6**. The symmetric and anti-symmetric stretching of COO^- in **7** appeared at 1405 cm^{-1} and 1628 cm^{-1}, respectively.

The ^1H and ^{13}C NMR spectra of monomer **4** and polymers **5–7** are shown in Figures 3.1 and 3.2, respectively. The alkene and carbonyl carbons of **4** and **5** are shown in the insets of Figure 3.2 (a,b). The carbonyl carbon of **6** and **7** appeared at 167.68 and 169.58, respectively [not shown in Figure 3.2 (c,d)]. The absence of any residual alkene proton or carbon signal in the spectra of **5–7** indicated the chain transfer process for the termination

reaction involving the macroradical abstracting the labile allylic hydrogen of the monomer.[88,124,125] The absence of the signals for the methyl protons and carbon of $OCH_2\underline{CH_3}$ at ~δ1.4 [Figure 3.1 (c)] and δ14.5 [Figure 3.2 (c)], respectively, ascertained the complete hydrolysis of the ester functionality in **5** giving **6**. Integration of the relevant peaks in the ^{13}C NMR spectrum yielded a 75/25 *cis–trans* ratio of the ring substituents at $C_{b,b}$ (Scheme 3.1) and is similar to that observed for polymers derived from quartenary ammonium salts.[7,14,91]

3.3.3 Solubility in Protic and Nonprotic Solvents

All three polymers are found to be insoluble in majority of the protic as well as nonprotic solvents of very high dielectric constants (ε) (Table 3.2). However, the polymers are soluble or partially soluble in formamide having a very high dielectric constant of 111. Polymers (±) **5** and (±) **6** are insoluble in salt-free water as expected of PZs while the anionic/zwittreionic polymer (− ±) **7** is water-soluble thereby ascertaining its electrolytic nature.

3.3.4 Polymer Structure versus Solution Properties

Polybetaines (i.e., PZs) are in general expected to be insoluble in salt-free water, but a considerable number of PCBs and PSBs were reported to be water-soluble.[51–54] A number of PCBs (**8**,[80] **10**[81]) and PSBs (**12**,[66] **14**,[84] **15**[123]) as well as their copolymers with SO_2 (**5**, **9**,[80] **11**,[15] **13**[126]) are listed in Scheme 3.2. The PCBs **8** and **10** having carboxyl pK_a of > 2 are reported to be water-soluble, while the corresponding SO_2-copolymers **9** and **11** are insoluble in water. Among the listed PSBs (**5**, **12–15**), all are reported to be insoluble in water except **15**. The difference in the solubility behavior between **14** and **15** has been rationalized in terms of steric factor[17,86,123]; more crowded

surroundings around the charges in **15** owing to the presence of bulkier CH_2CO_2Et group (vs. Me group **14**) do not encourage effective intra- or intermolecular Coulombic interactions.[123] The reported solubility data thus reveals that the presence of SO_2 and SO_3^- leads to stronger zwitterionic interactions and insolubility (Scheme 3.2). In a recent article, simulation results show that the negative charges in carboxybetaines interact with water molecules stronger than the sulofobetaines.[85] The respective carboxyl and sulfonyl pK_a values of >2 and −2.1 ascertain that the negative charges on the carboxyl moiety are expected to be less dispersed, hence more hydrated[14,80,81] and as such tend to exhibit weaker Coulombic interactions with the cationic charges on nitrogens[82] thus imparting solubility in salt-free water. The sulfobetaine moiety on the other hand, having more dispersed charges and thus being less hydrated, is able to exert stronger zwitterionic interactions. While a critical NaCl concentration of 0.67 *M* is required to shield the zwitterionic interactions and induce solubility of sulfobetaine **12**,[66] a much higher concentration of 1.5 *M* NaCl is required to disrupt zwitterionic interactions and promote solubility of PSB **13**[126] having SO_2 moieties on the polymer backbone (Scheme 3.2). The influence of SO_2 units is manifested by the difference of two orders of magnitude in the pK_a values of PSBs **12** and **13** (Scheme 3.2). The presence of electron-withdrawing SO_2 units is expected to disperse the positive charges on nitrogens thus making them less hydrated thereby augmenting the Coulombic interactions with the sulfonate groups. The dipole moment of sulfobetaine moiety (in triethylammoniopropanesulfonate)[127] and carbobetaine (in alanine)[128] has been reported to be 23.0 D and 15.9 D, respectively. The chain collapse may thus be attributed to the greater dipole–dipole intramolecular interactions between the sulfobetaine moieties.

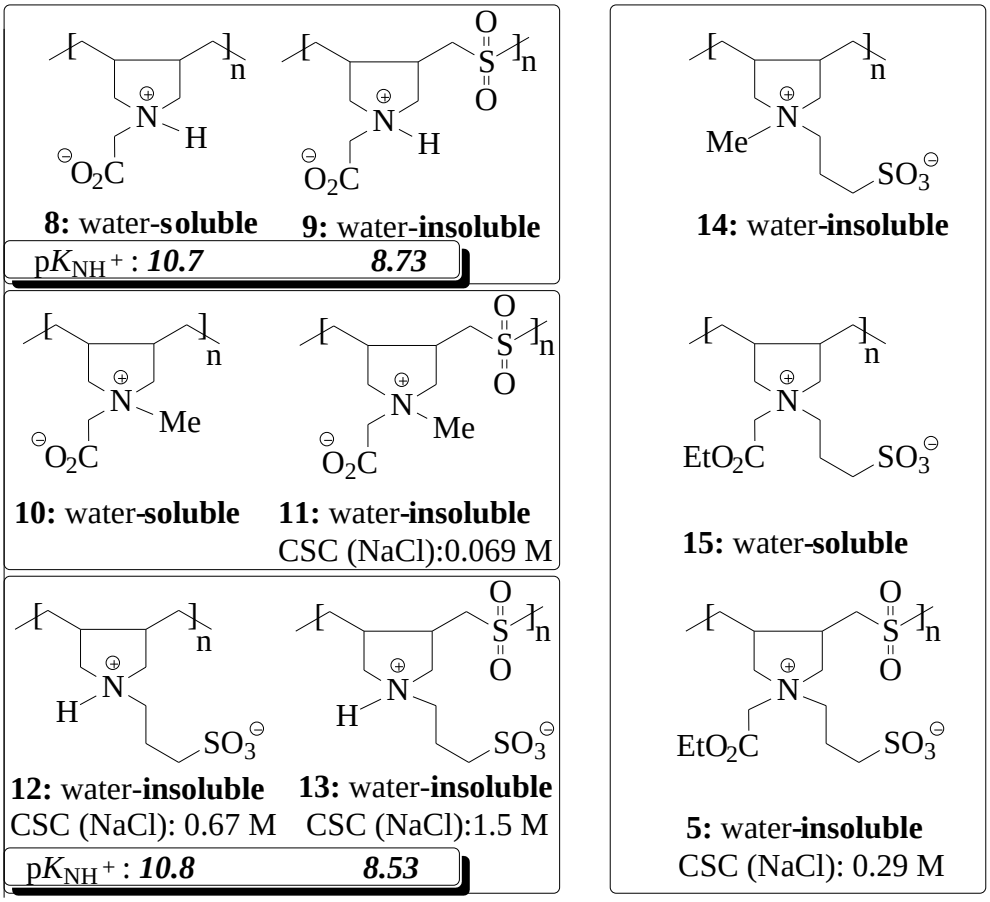

Scheme 3.2 Solubility behavior, pK_{NH^+}, and CSC of several polyzwitterions.

3.3.5 Critical Salt Concentrations

As discussed above, the presence of SO_2 is responsible for the stronger zwitterionic interactions in PZ **5** which is insoluble in salt-free water while the corresponding homopolymer **15** is water-soluble. The PZ **5** is found to be soluble in aqueous solutions of HCl and in the presence of variety of salts including divalent Ca^{2+} which is known to precipitate polyelectrolytes. For various salts, the critical minimum CSCs required to promote water solubility of PZ **5** at 23°C are shown in Table 3.3. For a common anion,

Cl^-, the cations do not show any appreciable effect on the solubility power; this is expected since the fairly large hydration shell of the cations due to their large charge/radius ratio cannot approach close enough to neutralize the highly dispersed charge on the sulfonate group.[18] The anions, on the other hand, are known to play a more dominant role in deciding the solubility behavior by effectively shielding the cationic charges on the nitrogens; for a common cation, K^+, the sequence of increasing solubilizing power was found to be:

$$Cl^- < Br^- << I^-$$

The concentration of KCl required to promote water solubility was found to be 6.6 and 52 times more than that of KBr and KI, respectively. The increased solubilizing power of KI is attributed to the most polarizable (soft) iodide anion's ability to effectively neutralize the ionic crosslinks. Note that the CSC (NaCl) required for promoting solubility of PZ **5** and **13** were found to be 0.29 and 1.5*M*, respectively; the considerable difference is attributed to the less crowded cationic charges in the later (Scheme 3.2).

PZA **6** is found to be insoluble in salt-free water; a 1 wt % mixture remained insoluble at 23°C even after stirring overnight. However, it was soluble while stirring in the presence of 0.025*N* NaCl. It is worth mentioning that the CSC of PZA **6** cannot be determined since dilution of its solution in 0.025*N* NaCl with salt-free water did not produce any turbidity while the turbidity returned by adding a few drops of 6*M* HCl. The interesting solubility behavior of PZA **6** may be attributed to the presence of zwitterionic moiety and the undissociated CO_2H in the solid state. Once the polymer is dissolved in the presence of the added salt (NaCl), dissociation of the carboxyl groups introduces the anionic

motifs and keeps it in the solution state as the (±) PZA **6** moves towards (− ±) PEZ **7** (i.e., [(..$N^{\pm}$…CO_2H (**6**) ⇋..$N^{\pm}$… CO_2^- (**7**) + H^+]). Dilution with salt-free water further increases the CO_2H dissociation and solubility. The addition of HCl, however, shifts the equilibrium from soluble (− ±) PEZ **7** toward insoluble (±) PZA **6**.

The sulfonyl moiety in PEZ **7** is expected to be involved in zwitterionic interactions as depicted in Scheme 3.3 leaving out the carboxyl moiety to impart anionic character and solubility.

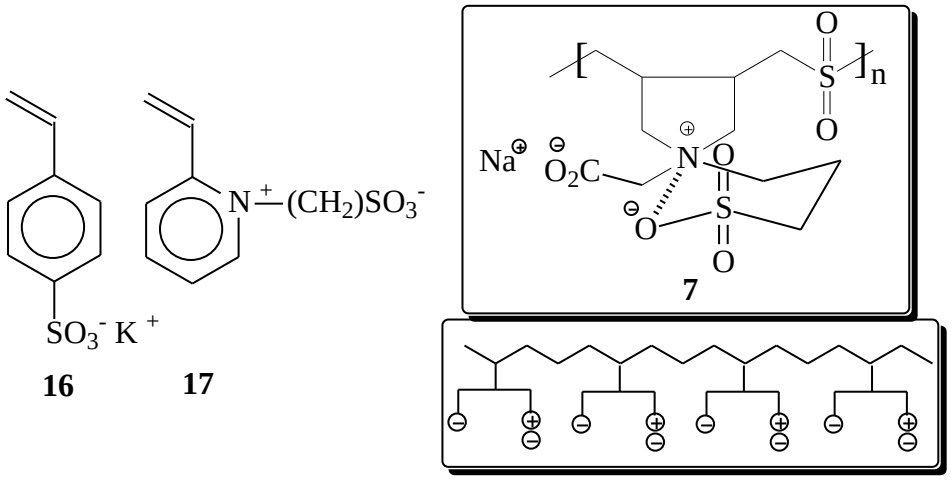

Scheme 3.3 Conformation of an (anion-zwitterion) motif.

3.3.6 Viscosity Measurements

Viscosity data for the polymers **5–7**, having almost identical degree of polymerization, were evaluated by the Huggins equation: $\eta_{sp}/C = [\eta] + k [\eta]^2 C$. The dependency of viscosity of (±) PZ **5**, (±) PZA **6**, and (− ±) PEZ **7** in aqueous solution containing various concentration of NaCl are shown in Figure 3.3 (a–c), respectively. An increase in the intrinsic viscosity with increasing NaCl concentration explains theantipolyelectrolyte

behavior of PZ **5** [Figure 3.3 (a)]. The increasing dissociation of the CO_2H groups in (±) PZA **6** with dilution keeps the viscosity curve concave upwards [Figure 3.3 (b)]. Based on the carboxyl pK_a value of 2.98 in 0.1*N* NaCl (*vide infra*), its percent dissociation in 1, 0.5, 0.25, and 0.125 g/dL solutions has been calculated to be 17, 23, 31, and 41, respectively. Therefore, increasing introduction of CO_2^- anionic motifs would expand the polymer backbone hence increase the viscosity values with dilution.

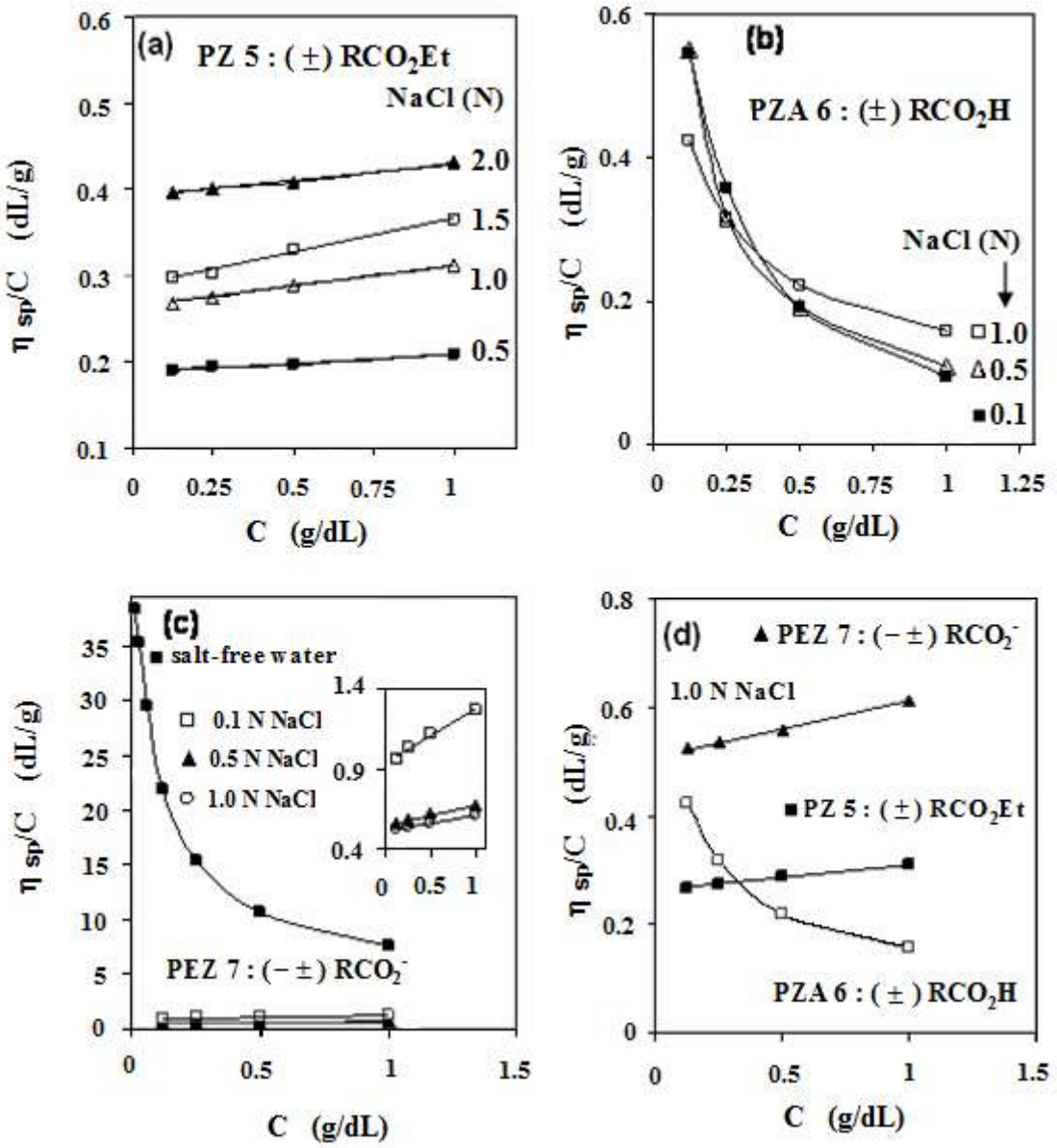

Figure 3.3 Using an Ubbelohde Viscometer at 30 ^{o}C: Variation of viscosity of: (**a**) PZ **5** (from entry 4, Table 3.1), (**b**) PZA **6** (derived from entry 4, Table 3.1), and (**c**) PEZ **7** (derived from entry 4, Table 3.1) with salt (NaCl) concentration. The viscosity behavior of: (d) PZ **5**, PZA **6**, and PEZ **7** (from or derived from entry 4, Table 3.1) in 1.0 N NaCl.

Note that the viscosity values of (±) PZA **6** remain almost similar with further increase in the salt concentration to 0.5*N* and 1*N* NaCl [Figure 3.3 (b)]. The carboxyl pK_a in

PZA **6** has been determined to be 3.42 and 2.98 in salt-free and 0.1*N* NaCl, respectively (*vide infra*); percent dissociation of CO_2H groups is thus expected to increase with the increase in the ionic strength of the medium. The near constancy of the viscosity values with the salt concentrations may be attributed to the opposite effect of increasing dissociation to CO_2^- and increased shielding of the charges on the viscosity values; while the dissociation increases the viscosity, shielding decreases it.

Figure 3.3 (c) displays the viscosity behavior of PEZ (− ±) **7** in salt-free water and various concentrations of NaCl. In salt-free water, the viscosity plot is typical of a polyelectrolyte, i.e. concave upwards. The presence of an extra negative charge per repeating unit in anionic-zwitterionic (− ±) PEZ **7** makes its viscosity behavior as typical of an anionic polyelectrolyte. The viscosity behavior of PZ **5**, PZA **6**, and PEZ**7** having identical degree of polymerization are compared in Figure 3.3 (d) in 1.0*N* NaCl. Polymer (− ±) **7** having completely dissociated CO_2^- anions has higher viscosity values than that of (±) **6** having partially dissociated CO_2H groups. Note that under extreme dilution the viscosity values of both the polymers are expected to be identical.

The dependency of viscosity of PZA (±) **6** in aqueous solution containing various concentration of NaOH in 0.1*N* NaCl is shown in Figure 3.4 (a). The viscosity increases with increasing amount of NaOH which gradually transforms (±) PZA **6** to (− ±) PEZ **7**.

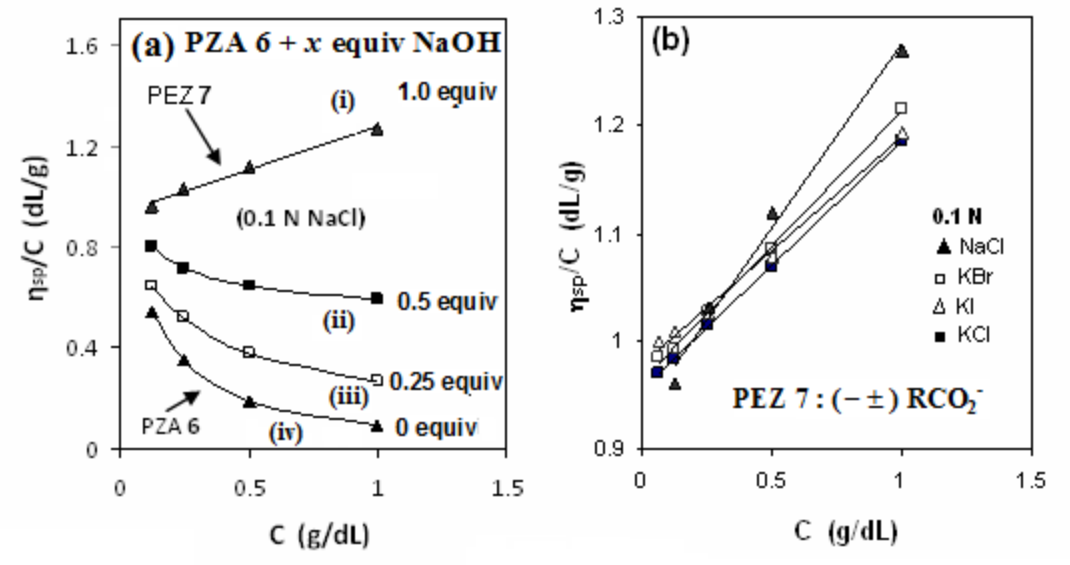

Figure 3.4 Using an Ubbelohde Viscometer at 30 °C: Variation of viscosity of: (**a**) PZA **6** (derived from entry 4, Table 3.1) with NaOH concentration and (**b**) PEZ **7** (derived from entry 4, Table 3.1) with various 0.1 N Salts.

The intrinsic viscosity [η] of (− ±) PEZ **7** in 0.1*N* NaCl, KCl, KBr, KI at 30°C was determined to be 0.935, 0.956, 0.965, and 0.980 dL/g, respectively [Figure 3.4 (b)]. It is known that the intrinsic viscosity of polybetaines or polyampholytes in 0.1*N* aqueous salt solution decreases in the order KI > KBr >KCl.[15,18,66,80] However, the presence of salt has an equal and opposite influence on the anionic (−) and zwitterionic (±) motifs; it helps the anionic portion to coil up and the zwitterionic part to expand. Since the viscosity of anionic polyelectrolytes is mostly independent of the effect of anions (like Cl^-, Br^-, etc.), more polarizable (soft) iodide anion is expected to effectively neutralize the cationic charges thereby forcing the expansion of the macromolecule so as to minimize repulsion among the more exposed negatives charges CO_2^- and SO_3^- .[95] However, this is found not to be the case; the salt effect on intrinsic viscosity is found

to be minimal as a result of shielding of the anionic motifs as well in a sea of cations [Figure 3.4 (b)]. The aqueous solution behavior of PEZ **7** is found to be similar to that observed for an alternating anionic-zwitterionic copolymer derived from monomers **16** and **17** (Scheme 3.3).[96] The current PEZ **7** may also be described as an alternate anionic-zwitterionic polymer as depicted in the Scheme.

The solution behavior of polyampholytes with or without charge symmetry has been described mathematically[20,92-94] in terms of:

$$v^* = -\frac{\pi(fI_B)^2}{\kappa_S} + \frac{4\pi I_B \Delta f^2}{\kappa_S^2} \qquad (4)$$

where v^* is the electrostatic excluded volume, I_B is the Bjerrum length, f is the total fraction of charged monomers, Δf is the charge imbalance, and κ_S is the Debye–Huckel screening parameter. The screening of the attractive polyampholytic and Coulombic repulsive interactions are described by the first and second term of eq. (4), respectively. Solution behavior of the electroneutral (±) PZ **5** must then be described by the screening of the attractive polyampholytic interactions only since the second term of eq. (4) becomes zero as a result of $\Delta f = 0$. The negative electrostatic excluded volume indicates contraction to a collapsed polymer chain. In the presence of added salt NaCl, the elctroneutrality of (±) PZ **5** cannot be maintained since the cationic nitrogens are more effectively screened by Cl^- ions, while Na^+ with its larger hydration shell cannot shield the SO_3^- to the same extent.[18] As a result, PZ **5** will acquire an overall anionic charge thus helping expansion of the polymer coil by making v^* less negative than in the absence of NaCl.

For (±) PZA **6** and (− ±) PEZ **7**, $\Delta f \neq 0$; the charge imbalance is maximum for the PEZ ($\Delta f = 0.33$), while it depends on the extent of dissociation in the case of the PZA. Since the percent dissociation of CO_2H (i.e., $RCO_2H \leftrightharpoons RCO_2^- + H^+$) in 0.1*N* NaCl for 1, 0.5, 0.25, and 0.125 g/dL solutions of PZA **6** has been determined to be 17, 23, 31, and 41, respectively, the corresponding Δf values are calculated as 0.078, 0.10, 0.13, and 0.17. The increasing importance of the second term in eq. (4) with decreasing polymer concentration thus leads to the expansion of polymer coil. This correlates directly with the viscosity data in Figure 3.3 (b) i.e., the increase of viscosity values with the decrease in polymer concentration. The polymer has a higher ampholytic character at a concentration of 1 g/dL than at 0.125 g/dL. Indeed, this is corroborated by the experimental observation; a closer look at Figure 3.3 (b) reveals that the viscosity value increases with the increase in NaCl concentration at the higher end of the polymer concentration (i.e., 1 g/dL), while it decreases at the lower end (i.e., 0.125 g/dL). At the higher end, there is an overall expansion; the expansion due to screening of the ampholytic motifs is greater than the contraction due to screening of the anionic motifs.

At the higher concentrations of salt (0.5*N* or more), the viscosity values of (− ±) PEZ **7** remain constant as a result of the near completion of screening of both the ampholytic and anionic motifs [Figure 3.3 (d): inset)]; the electrostatic contribution to the polymer size becomes insignificant as a result of minimized importance of both terms in eq. (4) as a result of complete shielding of all electrostatic effects.

3.3.7 Basicity Constants

An *n* values of >1 ascertain the decrease of basicity constant (*K*) with the degree of protonation (α) of the CO_2^- in PEZ **7** thus reflecting the "apparent"[97] nature of *K* (Figure

3.5, Scheme 3.1, Table 3.4). The *n* values of 2.24 and 1.27 in salt-free water and 0.1*N* NaCl, respectively, reflect a stronger polyelectrolyte effect in the former medium (Table 3.4). After each protonation, the anionic/zwitterionic motif (− ±) in PEZ **7** is progressively transformed to electroneutral motif (±) in PZA **6**; the decrease in the overall negative charge density per each repeating unit in partially protonated (− ±) PEZ **7** thus leads to a progressive decrease in the electrostatic field force that encourages protonation. It is worth mentioning that the *n* value for the protonation of basic CO_2^-, which is in the α-position with respect to the positive nitrogens as in **8** and **10**, is found to be < 1.[112,113] The *n* value of < 1 in **8** or **10** is diagonostic of a tightly compact zwitterionic (±) conformation which uncoils during protonation (leading to cationic motifs) thereby allowing the protons to have easier access to the CO_2^- anions with the increase in the α.[129] To our knowledge, this is the second example in which the log *K* of the CO_2^- in an α-position with respect to the positive nitrogens in an anionic/zwitetrionic motif has been determined and found to be >1.

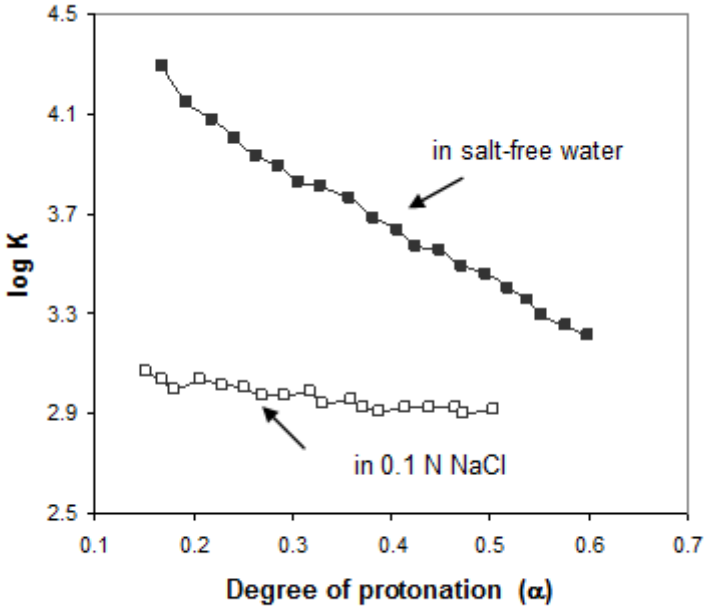

Figure 3.5 Plot for the apparent log *K* versus degree of protonation (α) for PZA **6** in salt-free water and 0.1 N NaCl.

The neutralization process, which transforms the anionic motifs in (− ±) PEZ **7** to zwitterionic motifs in (±) PZA **6**, may be described by the viscometric transformation of Figure 3.4 (a) (i) to 4(a) (iv) in 0.1*N* NaCl. Even though the corresponding transformation of (− ±) PEZ **7** from salt-free water [Figure 3.3 (c)] to (±) PZA **6** in salt-free-water cannot be achieved owing to the insolubility of the later, it can be assumed that the magnitude of the viscosity change would be much larger than in 0.1*N* NaCl. Since PEZ **7** in salt-free water [Figure 3.3 (c)] is the most expanded hence more hydrated, the greater number of water molecules are released as a result of each protonation in salt-free water than in 0.1*N* NaCl thereby leading to an entropy-driven[98] higher basicity constant and *n* in the former medium (Table 3.3). The basicity constant (log *K*°) of the carboxyl group was found to be 3.42 and 2.98 in salt-free water and 0.1*N* NaCl, respectively. Note that the

carboxyl basicity constant (log $K°$) in PEZ **7** is the pK_a value for the corresponding conjugate acid PZA **6**.

3.4 CONCLUSIONS

Zwitterionic monomer **4**, synthesized by a simple reaction, underwent cocyclopolymerization with sulfur dioxide to provide the first synthetic example of a poly (electrolyte-zwitterion)-*alt*-SO_2 **7** having carboxylate and sulfonate pendants. The presence of SO_2 in the polymer backbone has been shown to have a profound effect on the solution properties of the polymer. The apparent basicity constants of the carboxyl group in **7** have been determined. The study describes a simple way to convert a PZ to a PEZ and hence gives an opportunity for the direct comparison of the solution properties of these ionic polymers having the same degree of polymerization. The solution behavior of PEZ **7** has been found to be similar to a typical alternate anionic-zwitterionic polymer.

Only a few PEZs **7**, including the one presented in this work, have been documented so far in the literature. This new class of materials awaits potential applications in various fields to exploit the properties of the unique structural motifs (anionic and zwitterionic). The current challenge in the field of polymers is the construction of stimuli responsive advanced materials that have high added-value applications in drug delivery systems, separation materials, sensors, catalysts, etc. The PEZs' effectiveness in various such applications has to be tested. Currently, work is underway in our laboratory to synthesize crosslinked resins via cyclopolymerization of **4** and suitable crosslinkers so as to study the adsorption efficacies of the resulting resin that can be transformed to crosslinked polymer containing the anionic-zwitterionic functionalities.

CHAPTER 4

A pH-Responsive Cyclopolymer Having Phospho- and Sulfopropyl Pendents in the Same Repeating Unit: Synthesis, Characterization and its Application as an Antiscalant

Taken from Shamsuddeen A. Haladu, Shaikh A. Ali A, A pH-Responsive Cyclopolymer Having Phospho- and Sulfopropyl Pendents in the Same Repeating Unit: Synthesis, Characterization and its Application as an Antiscalant, *Journal of Polymer Science Part A: Polymer Chemistry* 2013, 51, 5130–5142.

Abstract

A new zwitterionic monomer 3-[diallyl{3-(diethoxyphosphoryl)propyl}ammonio]propane-1-sulfonate has been synthesized and cyclopolymerized to give the corresponding polyzwitterion (±) (PZ) bearing both phosphonate and sulfonate functionalities on each repeating unit. Phosphonate ester hydrolysis in PZ gave a pH-responsive dibasic polyzwitterionic acid (±) (PZA) bearing —PO_3H_2 units. The PZA under pH-induced transformation was converted into polyzwitterion/anion (± −) (PZAN) and polyzwitterion/dianion (± =) (PZDAN) having respective —PO_3H^- and —PO_3^{2-} units. The polymers′ interesting solubility and viscosity behaviors have been investigated in detail. The apparent protonation constants in salt-free water and 0.1 M NaCl of the —PO_3^{2-} in (± =) (PZDAN) and —PO_3H^- in (± −) (PZAN) as well as in their corresponding monomeric units have been determined. Evaluation of antiscaling properties of the PZA using supersaturated solution of $CaSO_4$ revealed ≈100% scale inhibition efficiency at a meager concentration of 20 ppm for a duration of

45 h at 40 °C. The PZA has the potential to be used effectively as an antiscalant in reverse osmosis plant.

4.1 INTRODUCTION

Butler's cocyclopolymerization protocol[5-8] involving *N,N*-diallyl quaternary ammonium salts generated a plethora of industrially significant water-soluble cationic polyelectrolytes. Use of ammonio monomers [$(CH_2{=}CH{-}CH_2)_2NH^+R\text{-}Y^-$] having unquenched nitrogen valency and pendent (R) bearing carboxylate, phosphonate, or sulfonate functionalities (Y^-) have provided entries into polymers which can participate in pH-induced equilibrations involving cationic (+), anionic (−), zwitterionic (±), and ampholytic (+ −) centers in the polymer chains.[10,66,80,130] Bio-mimicking polyampholytes and polyzwitterions have also offered many new applications[6,7] in biotechnology, medicine, oil industry, and hydrometallurgy.

Cationic or anionic polyelectrolytes demonstrate polyelectrolyte behavior, that is, their viscosity is diminished upon addition of electrolytes (e.g., NaCl), while PZs evince antipolyelectrolyte behavior of enhanced viscosity and solubility as a result of globule-to-coil transition. The transition is an outcome of salt-induced disruption of intragroup, intrachain, and interchain ionic crosslinks.[6,17-20]

We report herein the synthesis of a specialty zwitterionic monomer **4** and its corresponding cyclopolymer (±) **5** where the phosphonate ester functionality would offer latitude for chemical transformation to a polyzwitterionic acid (PZA) (±) **6**, poly(zwitterions/anion) (PZAN) (± −)**7**, and poly(zwitterions/dianion) (PZDAN) **8** (± =) (Scheme 4.1). The polymers **5–8** having different charges on the polymer backbone but

identical degree of polymerization would permit a reasonable comparison and correlation of their solution properties with the charge types and their densities on the polymer backbone. Very few cyclopolymers based on monomer type **1** bearing sulfonate and carboxylate groups have so far been documented in the literature.[16,75,123] To our knowledge, cyclocopolymer **8** would represent the first example of a cyclopolymer having phosphonate and sulfonate functionalities in the same repeating unit. The tribasic repeating unit having three different pK_a values would permit the change of the charge type by adjusting the pH.

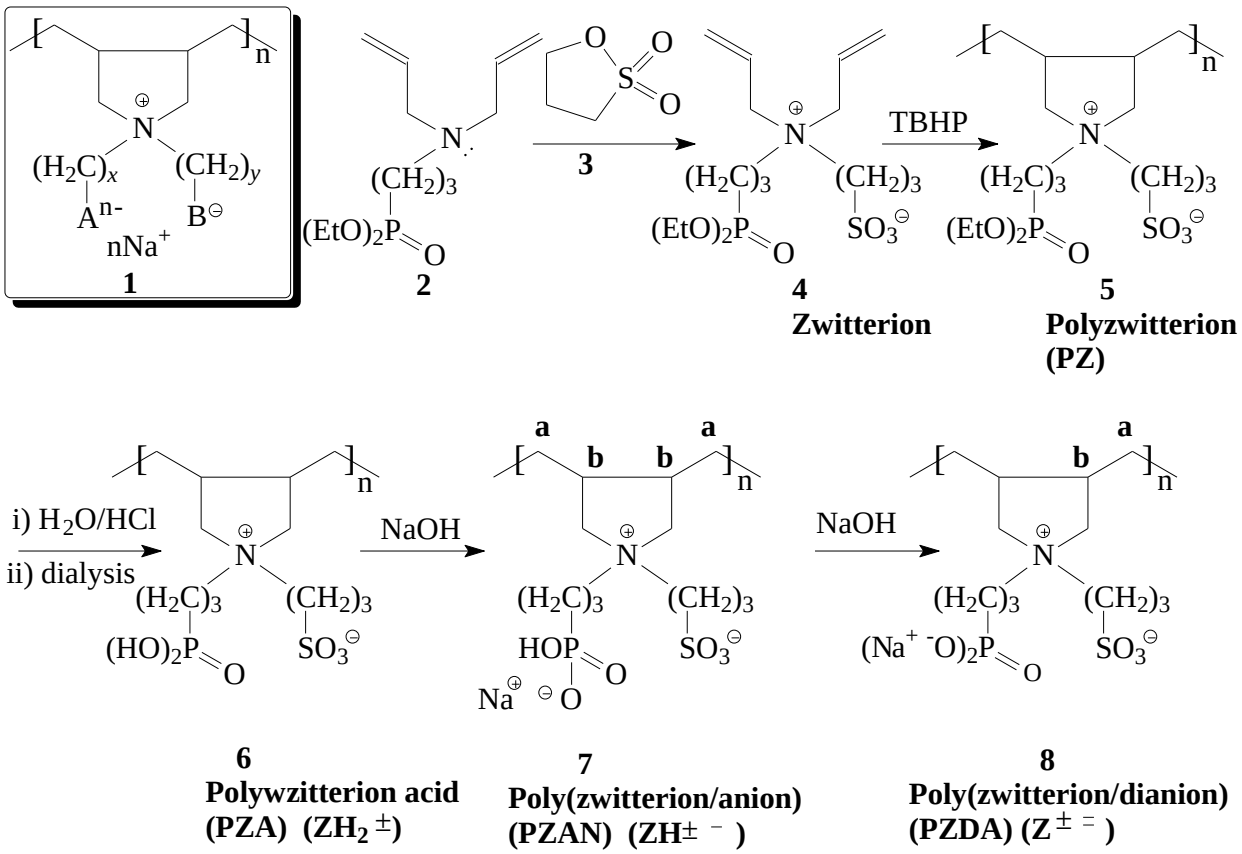

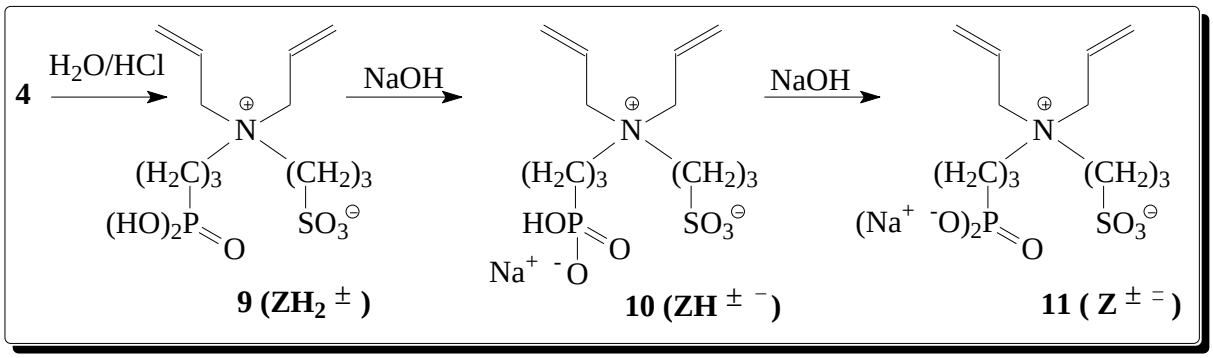

$$Z^{\pm =} + H^{+} \underset{}{\overset{K_1}{\rightleftharpoons}} ZH^{\pm -}$$

8 (or 11) **7 (or 10)**

$$ZH^{\pm -} + H^{+} \overset{K_2}{\rightleftharpoons} ZH_2^{\pm}$$

7 (or 10) **6 (or 9)**

$$\log K_i = \text{pH} - \log[(1-\alpha)/\alpha] \quad \text{Eq 1}$$

$$\text{pH} = \log K_i^{o} + n \log[(1-\alpha)/\alpha] \quad \text{Eq 2}$$

$$\log K_i = \log K_i^{o} + (n-1) \log[(1-\alpha)/\alpha] \quad \text{Eq 3}$$

Scheme 4.1 **Cyclopolymers *via* Butler's cyclopolymerization protocol.**

We intend to study the antiscalant properties of the polymer **6**. Antiscalants are chemical substances that inhibit the formation of scales which is a nuisance in the operation of desalination plants.[131] Calcium sulfate and calcium carbonate are primary contributors to scale formation. Scale deposits, which are generated and extended mainly by means of crystal growth, can be inhibited by modification of its growth and dispersion of the scale forming minerals. Various polyelectrolytes, which are usually added to saline water in substoichiometric amounts, are adsorbed onto the surfaces of the crystals so as to inhibit further crystal growth. A mixture of 90:10 copolymer of acrylic acid/$(CH_2{=}CH{-}CH_2)_2N^+(Me)CH_2CH_2SO_3^-$ and 2-phosphono butane 1,2,4-tricarboxylic acid (PBTA) has been reported[132] to perform better scale inhibition than poly(acrylic acid) (PAA) alone or a mixture of PAA and PBTA. The results thus indicated the beneficial effect of the presence of sulfobetaine structure ($R_3N^+CH_2CH_2SO_3^-$) in the polymer for superior performance. With the above discussion in mind, we anticipate an exciting outcome of the use of polymer **8** (having phosphonate as well as sulfonate motifs) as a novel antiscalant in inhibiting the formation of calcium sulfate scale.

4.2 EXPERIMENTAL

4.2.1 Physical Methods

A Perkin Elmer Elemental Analyzer Series II Model 2400 instrument and a Perkin Elmer 16F PC FTIR spectrometer were used to carry out elemental analysis and record IR spectra, respectively. The ^{13}C, ^{1}H, and ^{31}P NMR spectra have been measured in D_2O on a JEOL LA 500 MHz spectrometer. The ^{1}H HOD signal at δ 4.65 and ^{13}C peak of dioxane

at δ 67.4 were used as internal standards.[7] ^{1}P was referenced with 85% H_3PO_4 in dimethyl sulfoxide. Ubbelohde viscometer was used to carry out viscosity measurements under N_2 to avoid prevent CO_2 absorption. A Sartorius pH Meter PB 11 was utilized for potentiometric titrations. The temperature (25–800 °C) for the TGA, carried out in a thermal analyzer (STA 449F3), was increased at a rate of 15 °C min^{-1} using air (flowing rate of 100 mL min^{-1}). An Agilent 1200 series instrument having a RI detector and PL aquagel-OH MIXED column (8 µm, 300 × 7.5 mm) helped to determine the molecular weights. The MW range for the column used is 100–10,000,000 g mol^{-1} as written in the certificate with the column. The GPC measurements were performed using injection volume of 20 µL of an aqueous solution of the polymer (0.5 wt %) with water flowing at a rate of 1.0 mL/min at 25 °C and three different standards of polyethylene oxide/glycol.

4.2.2 Materials

Tertiary butylhydroperoxide (TBHP) (70 w/w % in water), 1,3-propanesultone, NaOH (>98%), NaCl (>99.5) from Fluka AG (Buchs, Switzerland) were used as received. All the solvents used were of HPLC grade. A spectra/Por membrane (MWCO of 6000–8000 from Spectrum Laboratories) was used for dialysis. Diethyl 3-(diallylamino)propylphosphonate was prepared as described.[67]

4.2.3 Synthesis of Monomer

3-[Diallyl{3-(diethoxyphosphoryl)propyl}ammonio]propane-1-sulfonate (4)

Under N_2 at 70 °C, a solution of diethyl 3-(diallylamino)propylphosphonate (**2)** (15.0 g, 54.5 mmol) and **3** (7.0 g, 57.3 mmol) in acetonitrile (30 cm^3) was stirred for 60 h. The residue, after removal of acetonitrile, was crystallized from acetone (30 cm^3) in the presence of a small amount of methanol to give white crystals of **4** (19.5 g, 90%).

Mp 140–142 °C (closed capillary); (Found: C, 47.9; H, 8.4; N, 3.4; S, 7.8%. $C_{16}H_{32}NO_6PS$ requires C, 48.35; H, 8.11; N, 3.52; S, 8.07%);ν_{max} (KBr): 3402, 2985, 2940, 1644, 1479, 1428, 1394, 1213, 1042, 967, 875, 786, 733, and 605 cm^{-1}; δ_H (D_2O) 1.22 (6H, t, $J = 7$ Hz), 1.86 (2H, m), 1.96 (2H, m), 2.11 (2H, m), 2.84 (2H, t, $J = 7.5$ Hz), 3.23 (2H, apparent t, $J = 10$ Hz), 3.31 (2H, apparent t, $J = 10$ Hz), 3.85 (4H, d, $J = 7$ Hz), 4.04 (4H, m), 5.64 (4H, m), 5.89 (2H, m), (HOD: 4.65); δ_C (D_2O) 15.83 (s, PCH_2CH_2), 16.47 (d, 2C, Me, ^3J (PC) 4.1 Hz), 18.29 (s, SCH_2CH_2), 21.45 (d, PCH_2, ^1J (PC) 143 Hz), 47.97 (s, $SCH_2CH_2CH_2$), 57.26 (s, $SCH_2CH_2CH_2$), 58.32 (d, PCH2CH2CH_2, ^3J (PC) 16.4 Hz), 61.72 (2C, $=CH-CH_2$, s), 64.38 (d, 2C, OCH_2CH_3, ^2J (PC) 6.2 Hz), 124.40 (2C, s, $CH_2=CH$), 129.80 (2C, s, $CH_2=CH$) (dioxane: 67.40 ppm); δ_P (202 MHz, D_2O): 31.01(s). DEPT 135 NMR analysis was carried out to assign the ^{13}C signals.

4.2.4 Cyclopolymerization of 4

A solution of monomer **4** (7.94 g, 20 mmol), 1 M NaCl (2.64 g), and TBHP (60 mg) under N_2 was stirred in a closed 25-cm^3 round-bottom flask at 90 °C for 24 h (Table 4.1, entry 3). Dialysis (24 h) of the resultant polymer against deionized water followed by freeze-drying afforded PZ **5** as a white polymer. Thermal decomposition: the color became dark brown at 270 °C and decomposition happened at 320 °C.

Table 4.1 Cyclopolymerization[a] of Monomer **4**

Entry No.	Monomer (mmol)	Initiator (mg)	NaCl (M)	Yield (%)	$[\eta]^b$ (dL g^{-1})	$\overline{M}_w$ (g mol^{-1})	$(PDI)^c$
1	10	TBHP (40)	1.00	80	0.0741	3.53×10^4	2.1
2	10	TBHP (40)	0	trace	-		
3	20	TBHP (60)	1.00	76	0.0969	4.37×10^4	2.3

[a] Carried out using 75 w/w% monomer **4** (10 mmol) solution in the presence of tert- butyl hydroperoxide (TBHP) at 90 °C for 24 h.
[b] Viscosity of 1-0.125 % polymer solution in 0.1 M NaCl was measured with Ubbelohde Viscometer (K=0.005718) at 30°C.
[c] Polydispersity index.

(Found: C, 48.0; H, 8.3; N, 3.4; S, 7.7%. $C_{16}H_{32}NO_6PS$ requires C, 48.35; H, 8.11; N, 3.52; S, 8.07%); $\nu_{max.}$(KBr) 3407, 2985, 2941, 1650, 1463, 1395, 1370, 1214, 1044, 969, 789, 734, and 604 cm^{-1}. δ_P (202 MHz, D_2O): 31.13.

4.2.5 Conversion of PZ 5 to PZA 6

A solution of PZ **5** (3.0 g, 7.5 mmol) (derived from entry 3, Table 4.1) in water (18 mL) and concentrated HCl (24 mL) was heated in a flask at 90–95 °C for 24 h or until the ester hydrolysis was complete. During dialysis (24 h) of the homogeneous hydrolyzed mixture against water, insoluble polymer started to precipitate out within 1 h but redissolved after 3 h. The solution of the polymer was freeze-dried to obtain PZA **6** as a white solid (2.5 g, 98%). Thermal decomposition: dark brown at 300 °C and black at 325 °C.

(Found: C, 41.9; H, 7.3; N, 4.0; S, 9.1%. $C_{12}H_{24}NO_6PS$ requires C, 42.22; H, 7.09; N, 4.10; S, 9.39%); ν_{max} (KBr) 3449 (br), 2942, 1653, 1465, 1417, 1216, 1043, 984, 938, 786, 732, and 610 cm^{-1}. δ_P (202 MHz, D_2O): 25.35.

4.2.6 Acid Hydrolysis of 4 to Zwitterion Acid ZA 9

A solution of **4** (2.7 g, 6.8 mmol) in water (5.5 mL) and concentrated HCl (4.8 mL) was heated in a flask at 95 °C for 48 h. Removal of the solvent followed by dissolution of the residual liquid in methanol and precipitation into acetone gave ZA **9** as a white solid (dried under reduced pressure at 50 °C) (2.1 g, 91%).

Mp. 75–80 °C. (Found: C, 41.8; H, 7.3; N, 3.9; S, 9.1%. $C_{12}H_{24}NO_6PS$ requires C, 42.22; H, 7.09; N, 4.10; S, 9.39%); ν_{max} (KBr) 3600–2500 (very broad), 1699, 1642, 1477, 1430, 1373, 1221 (br), 1163, 1041, 1001, 952, 870, 784, 732, 602, and 526 cm^{-1}. δ_H (D_2O) 1.55 (2H, dt, J = 18.4 and 7.6 Hz), 1.77 (2H, m), 1.93 (2H, m), 2.11 (2H, m), 2.66 (2H, t, J = 7 Hz), 3.04 (2H, m), 3.10 (2H, m), 3.66 (4H, d, J = 7 Hz), 5.44 (4H, m), 5.73 (2H, m), (HOD: 4.65); δ_C (D_2O) 16.28 (s, PCH_2CH_2), 18.26 (s, SCH_2CH_2), 23.68 (d, PCH_2, ^1J (PC) 138 Hz), 47.99 (s, $SCH_2CH_2CH_2$), 57.30 (s, $SCH_2CH_2CH_2$), 58.65 (d, $PCH_2CH_2CH_2$, ^3J (PC) 18.6 Hz), 61.74 (2C, $=CH-CH_2$, s), 124.43 (2C, s, $CH_2=CH$), 129.73 (2C, s, $CH_2=CH$) (dioxane: 67.40 ppm); δ_P (202 MHz, D_2O): 28.02 (m). DEPT 135 NMR analysis was carried out to assign the ^{13}C signals.

4.2.7 Conversion of ZA 9 to Zwitterion/Dianion (ZDAN) 11

A mixture of ZA **9** (1.45 g g, 4.25 mmol) in methanol (2 mL) and NaOH (0.51 g, 12.7 mmol) in methanol (4 mL) was stirred at 23 °C for 2 min. The removal of the solvent followed by trituration of the residue with acetone/ether mixture afforded **11** as a white

solid (1.4 g, 85%). Because of the extremely hygroscopic nature of the salt, its elemental analysis was not performed.

Mp. Did not melt; brown at 300 °C and black at 330 °C. ν_{max} (KBr) broad adsorption in the range 3600–2600, 1644, 1477, 1418, 1364, 1215, 1049, 976, 862, 735, and 606 cm^{-1}. δ_H (D_2O) 1.28 (2H, m), 1.83 (2H, m), 1.93 (2H, m), 2.13 (2H, m), 2.86 (2H, m), 3.19 (2H, m), 3.29 (2H, m), 3.83 (4H, d, $J = 7$ Hz), 5.63 (4H, m), 5.93 (2H, m), (HOD: 4.65); δ_C (D_2O) 17.83 (d, PCH_2CH_2, ^2J (PC) 15.0 Hz), 26.04 (d, PCH_2, ^1J(PC) 210 Hz), 28.62 (s, SCH_2CH_2), 47.71 (s, $SCH_2CH_2CH_2$), 56.82 (s, $SCH_2CH_2CH_2$), 59.90 (d, $PCH_2CH_2CH_2$, ^3J (PC) 33.4 Hz), 61.13 (2C, $=CH-CH_2$, s), 124.36 (2C, s, $CH_2=CH$), 129.10 (2C, s, $CH_2=CH$) (dioxane: 67.40 ppm); δ_P (202 MHz, D_2O): 17.41. DEPT 135 NMR analysis was carried out to assign the ^{13}C signals.

4.2.8 Solubility Measurements

PZ **5** or PZA **6** (2 w/w % mixture) in a solvent was stirred at 70 °C (1 h) and then brought back to 23 °C. The solubility behaviors are given in Table 4.2.

Table 4.2 Solubility[a] of PZ **5** and PZA **6**

Solvent	ε	PZ **5**	PZA **6**
Formamide	111	+	+
Water	78.4	+	+
Formic acid	58.5	+	+
DMSO	47.0	−	+
Ethylene glycol	37.3	−	+
DMF	37.0	−	−
Methanol	32.3	−	+
Triethylene glycol	23.7	−	+
Acetic acid	6.15	−	+

[a] '+' indicates soluble and '−' indicates insoluble.

4.2.9 Solubility Measurements in Salt-free Water and in the Presence of HCl

A 5 w/w % PZA **6** remained insoluble in salt-free water while at 2 w/w % th**e** mixture became homogeneous. A solution of PZA **6** (32 mg, 0.0937 mmol) in 0.730 M HCl (3.40 mL) was titrated with water until cloudiness. The first appearance of the cloud required addition of water (4.00 mL). The calculation at this point revealed that the polymer (0.013 M) is insoluble in the presence of 0.335 M HCl. Continued addition of water (13.4 mL) leads to disappearance of the cloudy mixture to a colorless solution. That was translated into the solubility of the polymer (0.00450 M) in 0.119 M HCl.

4.2.10 Potentiometric Titrations

Protonation constants (K_1 and K_2) of polymer **8** [$ZH_2^{\pm -}$] and its corresponding monomer unit **11** [$ZH_2^{\pm -}$] were determined by potentiometric titrations which were carried out in an atmosphere of N_2 in CO_2-free water as described elsewhere[67,80] using a solution (Tables 4.3 and 4.4) of PZA **6** [$ZH_2^{\pm}$] or monomer form **11** [$ZH_2^{\pm -}$] in 200 cm^3 of salt-free water or 0.1 N NaCl . The Log K_1 and Log K_2 of the respective —PO_3^{2-} (in **8** or **11**) and —PO_3H^- (in **7** or **10**) were calculated at each pH value by the Henderson-Hasselbalch eq 2 (Scheme 4.1) where the degree of protonation (α) is the ratios [$ZH^{\pm -}$]$_{eq}$/[Z]$_o$ and [$ZH_2^{\pm}$]$_{eq}$/[Z]$_o$, respectively. The [$ZH^{\pm -}$]$_{eq}$ and [$ZH_2^{\pm}$]$_{eq}$represent the respective equilibrium concentrations of the first (**7**) and second (**6**) protonated species whereas [Z]$_o$ describes the initial concentration of repeating units.

For the determination of the second step protonation constant (log K_2) of —PO_3H^- (i.e., [$ZH^{\pm -}$]) using the titration of polymer **6** [$ZH_2^{\pm}$] with NaOH, [Z]$_o$ and [$ZH_2^{\pm}$]$_{eq}$ are related by $[ZH_2^{\pm}]_{eq} = [Z]_o - C_{OH^-} - [H^+] + [OH^-]$, where C_{OH^-} represent the added NaOH concentration. The equilibrium [H^+] and [OH^-] values were calculated from the pH value.[77,78,129] The first step protonation constant (log K_1) involving —PO_3^{2-}(i.e., [$Z^{\pm -}$]) was determined using volume of the titrant after deducting the equivalent volume from the total volume. In this case, α represents the ratio [$ZH^{\pm -}$]$_{eq}$/[Z]$_o$ whereby [$ZH^{\pm -}$]$_{eq}$ equals $[Z]_o - C_{OH^-} - [H^+] + [OH^-]$. For the titration of **11** [$Z^{\pm -}$] with HCl, the protonated species' concentration is given by: $[ZH_{i=1,2}]_{eq} = C_{H^+} - [H^+] + [OH^-]$.[67,80]

Equation 3 (Scheme 4.1) describes the apparent basicity constants of —PO_3^{2-} where $\log K^o = \text{pH}$ at $\alpha = 0.5$ and $n = 1$ in the case of sharp basicity constants. The "*n*" and log K^o as the respective slope and intercept were determined from the linear regression fit

of pH versus log [$(1-\alpha)/\alpha$)] [Figure 4.1 a)]. Protonation at the same time of the three basic sites: —$PO_3^{=}$ (log $K_1 \approx +8$), —PO_3H^{-} (log K_2: $\approx +3$) and —SO_3^{-}(log K_3: ≈ -2.1)[78] is not likely due to differences of their basicity constants by about 5 orders of magnitude (*vide infra*). Note that basicity constant log K of any base B is the pK_a of its conjugate acid BH^+.

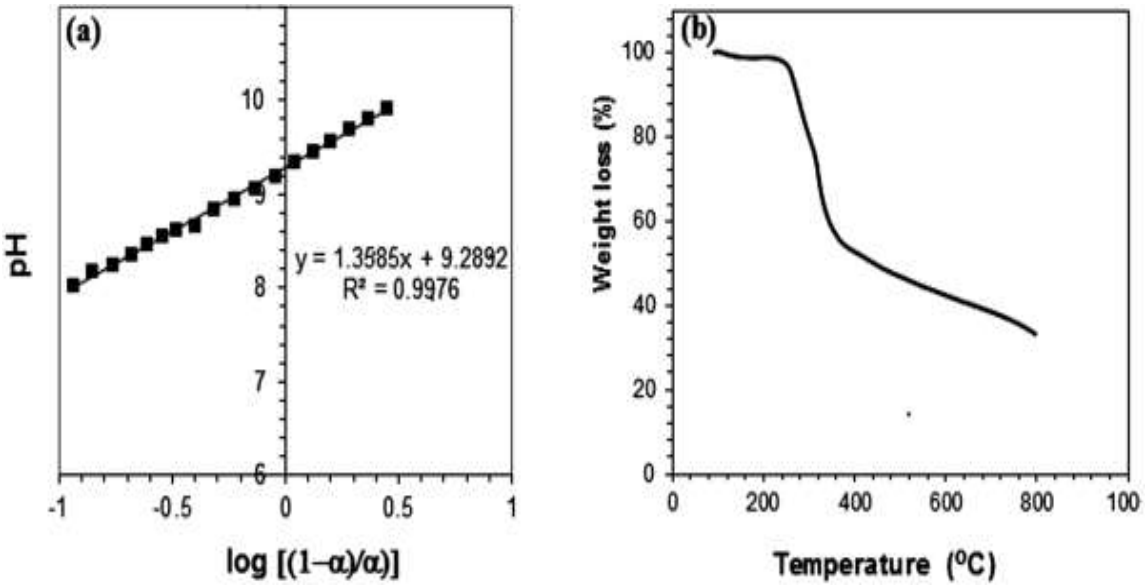

Figure 4.1 (**a**) Titration curve for the transformation of (± =) PZDAN **8** to (± −) PZAN **7** (entry 2, polymer 6 in salt-free water, Table 4.3); (**b**) TGA curve of PZ **5**.

4.2.11 Evaluation of Antiscalant Behavior

A typical analysis[133] of brackish water and reject brine (i.e., concentrated brine, denoted as 1 CB, at 70% recovery) from a reverse osmosis (RO) plant revealed the concentration of Ca^{2+} as 281.2 and 866.7 ppm, respectively; while the corresponding concentration of SO_4^{2-} to be 611 and 2100 ppm.

The evaluation of the newly developed scale inhibitor PZA **6** was performed in a solution containing Ca^{2+} and SO_4^{2-} by 3 times the concentration in the 1 CB. The 3 CB solutions

containing 3 × 866.7 mg L^{-1}, that is, 2600 mg L^{-1} in Ca^{2+} and 3 × 2100 mg L^{-1}, that is, 6300 mg L^{-1} in SO_4^{2-} would be supersaturated as confirmed from solubility data of $CaSO_4$. Solutions containing Ca^{2+} and SO_4^{2-} ions equals to six times the concentrated brine (1 CB) were prepared by dissolving the calculated amount of $CaCl_2$ and Na_2SO_4, respectively, in deionized water. To a solution of 6 CB calcium chloride (60 mL) containing PZA **6** (40 ppm) in a round bottom flask at 40 ± 1 °C stirred at 300 rpm using a magnetic stir-bar, a preheated (40 °C) solution of 6 CB sodium sulfate (60 mL) was added quickly. Conductivity measurements of the resultant solution containing 20 ppm of PZA **6** were made at an interval of every 10 min initially to quantify the effectiveness of newly developed antiscalant PZA **6**. The precipitation of $CaSO_4$ is indicated by a drop in conductivity. Visual inspection was carefully done to see any turbidity arising from precipitation.

4.3 RESULTS AND DISCUSSION

4.3.1 Synthesis and Characterization of the Ionic Polymers

Zwitterion monomer **4**, obtained in excellent yield by reacting tertiary amine **2** with propane sultone **3**, underwent cyclopolymerization to afford polyzwitterion (PZ) **5** in very good yields (Scheme 4.1). The results, given in Table 4.1, revealed that the polymer under entry 3 using 3 mg initiator/mmol monomer has higher intrinsic viscosity [η] than that obtained with an initiator concentration of 4 mg $mmol^{-1}$ monomer in a 1 M NaCl solution at 90 °C (entry 1). Note that the presence of salt (NaCl) is a requirement to obtain the polymer; in its absence only a trace amount of the polymer could be obtained (entry 2). The interesting beneficial influence of NaCl on the polymer yields could be attributed to the expansion of the collapsed coil zwitterionic macroradical. The presence

of salt disrupts the zwitterionic interactions thereby forcing out the cocooned radical-head so as to have easier access to the monomer molecules for further propagation in an expanded semicoil.

The PZ (±) **5** was hydrolyzed in 5.6 M HCl to give PZA (±) **6**, which on neutralization with 1 and 2 equiv. of NaOH is expected to generate PZAN (± −) **7** and PZDAN (± =) **8**. Likewise, zwitterion monomer **4** was hydrolyzed to zwitterion acid (ZA) **9**, which on neutralization with NaOH afforded the zwitterion/dianion (ZDAN) **11**.

PZ **5** was observed to be stable up to around 225 °C as shown in the thermogravimetric analysis (TGA) curve [Figure 4.1 (b)]. The first steep weight loss of 40% in the temperature range 225–360 °C range was attributed to the loss of sulfopropyl moiety, while the second gradual loss of 25% in the 360–800 °C range was due to decomposition of the phosphonate ester functionality and the release of H_2O, NO_x, and CO_2 gases.[134] The remaining mass of 35% is attributed to P_2O_5.[134]

Monomer **4** was extremely hygroscopic and insoluble in acetone but soluble in methanol or water. While PZA (±) **6** was soluble in almost all the tested solvents, PZ (±) **5** was soluble only in the protic solvents of higher dielectric constants (Table 4.2). Even though PZs are usually insoluble in salt-free water,[66,84] the water-solubility of the current polymers is not unusual since a considerable number of polycarbobetaines and polysulfobetaines (PSB) has been documented to be soluble in salt-free water.[14,80-82, 123] Water-insoluble PZs have been shown to be water-soluble with the assistance of NaCl which screens the zwitterionic charges from displaying zwitterionic interactions. Steric factor[17,86,123] around the crowded cationic charges in PZ **5** and **6**, makes it difficult for

the sulfonate group to move closer to impart effective zwitterionic interactions, thereby making them water-soluble.

Interestingly, it was observed during the dialysis of PZA **6** in 5.6 M HCl that precipitation of the polymer happened within 1 h and its dissolution after 3 h. On further investigation, it was revealed that a 5-wt % PZA **6** forms a heterogeneous mixture in salt-free water, while became soluble when diluted to 2 wt %. The heterogeneous mixture became soluble in the presence of 0.1 M NaCl. Based on the pK_a value of —PO_3H_2 in (±) **6** as 3.26, it is calculated that it will be dissociated to (± −) **7** to the extent of 6 and 9 mol % in 5 and 2 wt % solution, respectively, in salt-free water. Greater dissociation thus makes the polymer soluble in the latter medium of 2-wt % solution. The higher solubility in the presence of NaCl could be attributed to its ability to break up the zwitteionic interactions[6,17-20] in (±) **6** and its greater dissociation to (± −) **7**; for a pK_a value of —PO_3H_2 in (±) **6** as 2.83 in 0.1 M NaCl, the extent of dissociation becomes 10 and 15 mol % in respective 5 and 2 wt % solutions.

A solution of PZA **6** (32 mg, 0.0937 mmol) in 0.730 M HCl (3.40 mL) was titrated with water until it became cloudy. The first appearance of the cloud required the addition of water (4.00 mL). That means the polymer (0.013 M) is insoluble in the presence of 0.335 M HCl. Continued addition of water (13.4 mL) leads to disappearance of the cloudy mixture to a colorless solution. That translates into the solubility of the polymer (0.00450 M) in 0.119 M HCl. The above results as well as the observation during dialysis can be rationalized in terms of the equilibria presented in Scheme 4.2. Undissociated PZA **6** by virtue of being zwitterionic is insoluble in neutral water, however in the presence of concentrated HCl during the initial stage of dialysis, it is converted to some extent into

the soluble cationic polyelectrolyte (CPE) **12** which upon extended dialysis was transformed to a water-insoluble undissociated PZA **6** with the depletion of HCl. Continued dialysis in the absence of HCl encourages the participation of PZA **6** in the equilibrium to give PZAN **14** whose water solubility is dictated by the anionic portion of the zwitterion/anion motifs. Note that increased dilution will lead to greater solubility as the degree of dissociation of a weak acid is increased with decreasing concentration.

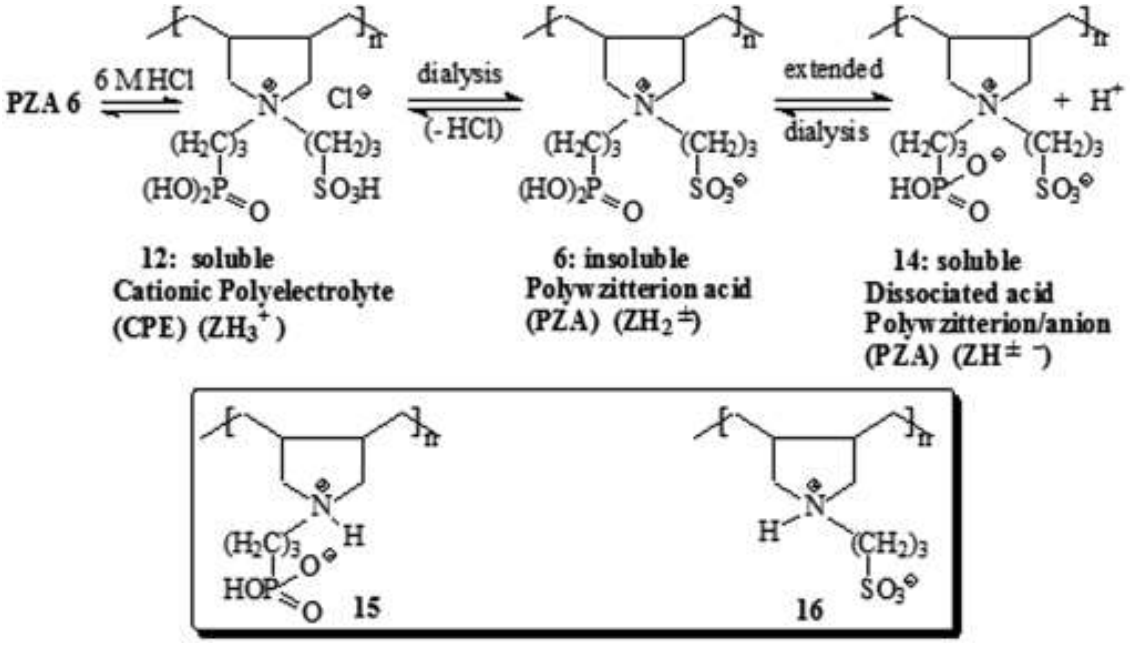

Scheme 4.2 PZA **6** under pH-induced equilibration.

4.3.2 IR and NMR Spectra

The IR absorptions around ~1215 and ~1045 cm^{-1} indicate the presence of sulfonate and phosphonate groups in the monomers and polymers. Figure 4.1 and 4.2 show the ^{1}H and ^{13}C NMR spectra of **4**, **5**, **6**, and **9**, respectively. The DEPT 135 NMR analysis supported the assignments of the ^{13}C signals. The termination via chain transfer and/or coupling process[88,124] is ascertained by the complete disappearance of any alkene proton

or carbon signals in the polymer spectra. The absence of the ester group (OCH_2CH_3) signals in the spectra of **5** and **9** indicates its complete removal by hydrolysis. The integration of the ^{13}C peaks revealed a 75/25 *cis-trans* ratio of the ring substituents at $C_{b,b}$ similar to the earlier findings[7,89-91] (Scheme 4.1).[7,91] ^{31}P NMR signal for monomer Z **4**, ZA **9,** ZDAN **11**, PZ **5**, and PZA **6** appeared at δ31.01, 28.02, 17.41, 31.13, and 25.35 ppm, respectively. The upfield shift of P signal in ZDAN **11** is attributed to the presence of negatively charged oxygens, which increase the electron density around P.

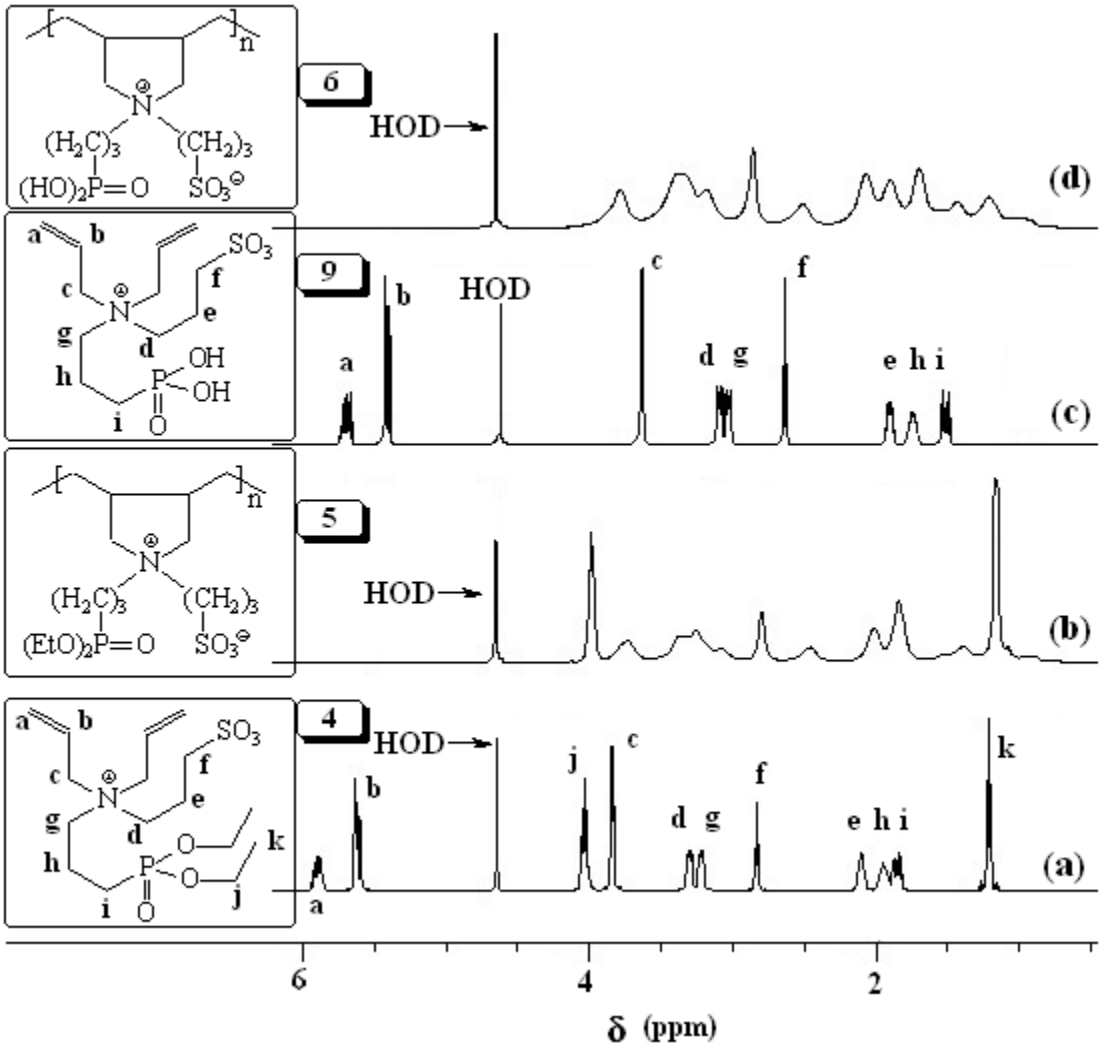

Figure 4.2 ^{1}H NMR spectra of **(**a**) 4, (**b**) 5, (**c**) 9** and **(**d**) 6** (+NaCl) in D_2O.

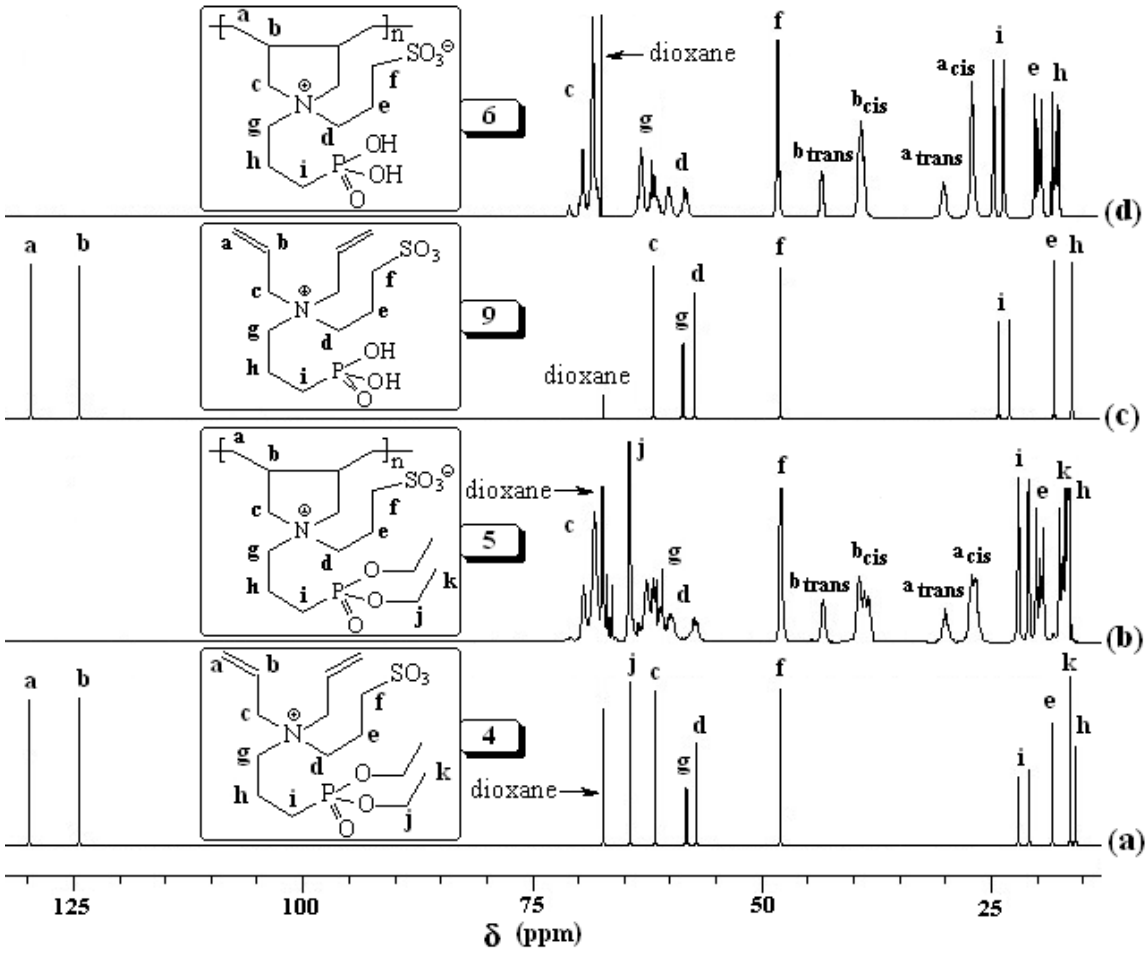

Figure 4.3 [13] NMR spectra of **(**a**) 4, (**b**) 5, (**c**) 9** and **(**d**) 6** (+NaCl) in D_2O.

4.3.3 Viscosity Measurements

Figure 4.4 (a,b) displays the viscosity plots, as examined by the Huggins equation: $\eta_{sp}/C = [\eta] + k\,[\eta]^2\,C$, for the polymers **5–8** having identical number of repeating units. The intrinsic viscosity [η] of PZ **5** in 0.1 M NaCl, 0.5 M NaCl, and salt-free water, was measured to be 0.0700, 0.0968, and 0.104 dL g^{-1}, respectively [Figure 4.4 (b-iii–v)]. With increasing NaCl concentration, an increase in the intrinsic viscosity ascertains the antipolyelectrolyte behavior of PZ (±) **5**. The Cl^- ions are more effective in

shielding or neutralizing the positive nitrogens than the shielding of SO_3^- by Na^+ ions, which with their large hydration shells cannot reach close enough to shield the anionic charges. In the presence of NaCl, this unequal shielding disturbs the electroneutrality of PZ (±) **5** in favor of a polymer chain having repeating units with overall negative charges, the repulsions among which lead to its expansion and increase in the [η]s.[18,95]

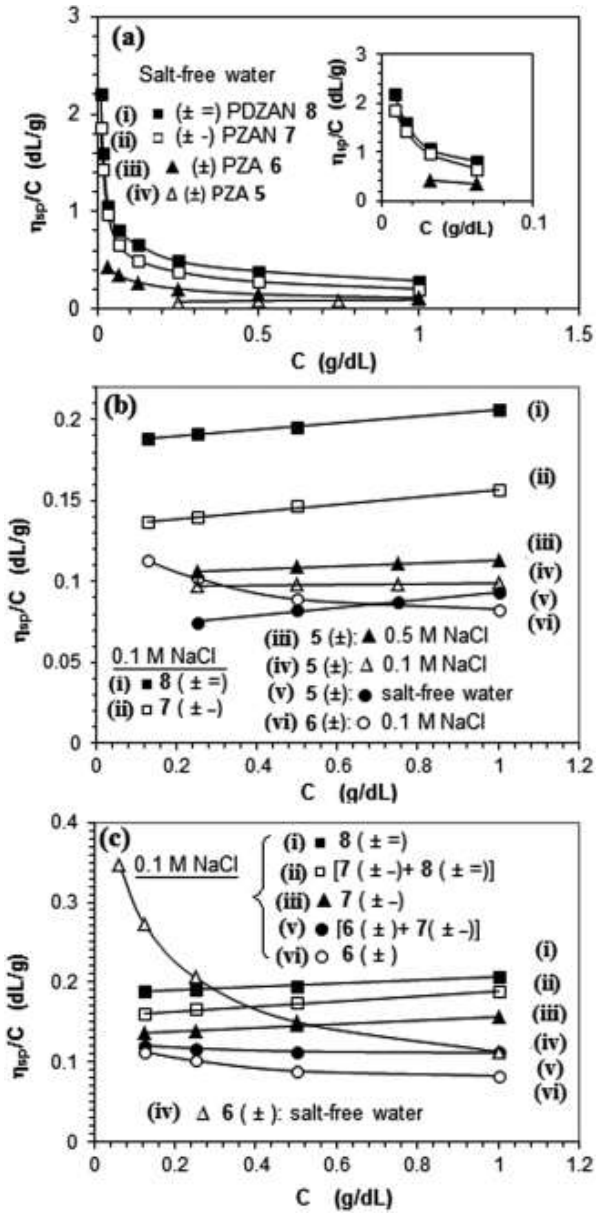

Figure 4.4 Using an Ubbelohde Viscometer at 30 ^{o}C, the viscosity behavior: (**a**) in salt-free water of: (i) ■ (± =) PZDAN **8**, (ii) □ (± −) PZAN **7**, (iii) ▲ (±) PZA **6** and (iv) Δ (±) PZ **5**. [Inset describes the viscosity plots of **6-8** in the higher dilution range]; (**b**) in 0.1 M NaCl of: (**i**) ■ (±=) PZDAN **8**, (**ii**) □ (±-) PZAN **7**, (±) PZ **5** in **(iii**) ▲ 0.5 M NaCl, (**iv**) Δ 0.1 M NaCl, (**v**) ● in salt-free water and (**vi**) ○ (±) PZA 6 in 0.1 M NaCl; (**c**) in 0.1 M NaCl of: (**i**) ■ (±=) PZDAN 8, (**ii**) □ 1:1 (± −) PZAN **7**/(± =) PZDAN **8**; (**iii**) ▲(± −) PZAN 7 (**iv**) Δ (±) PZA **6** in salt-free water, (**v**) ● 1:1 (±) PZA **6**/(± −) PZAN **7** in 0.1 M NaCl and (**vi**) ○ (±) PZA **6** in 0.1 M NaCl. (All polymers are derived from entry 3, Table 4.1).

The viscosity values of (±) **5**, (±) **6,** (± −) **7**, and (± =) **8** both in salt-free water and 0.1 M NaCl (in dilute solution range) were found to be increasing in the order: **5**<**6**<**7**<**8 [**Figure 4.4 (a,b)]. All the polymers have the common trait of a zwitterionic motif whereas **7** and **8** have in addition anionic and dianionic functionalities. The highest viscosity values of (± =) PZDAN **8** is attributed to the increased repulsion among the anionic charges leading to the expansion of the polymer backbone [Figure 4.4 (a-i,b-i)]. Note that the viscosity plot of (±) **6**, unlike (±) **5**, is typical of polyelectrolytes, that is, concave upward in salt-free water [Figure 4.4 (c-iv)]. But the plot also remains concave upwards in 0.1 M NaCl [Figure 4.4 (c-vi)] while a typical polyelectrolyte is expected to have a linear plot. The discrepancy is attributed to the dissociation of the —PO_3H_2(pK_a: 2.83) in (±) **6** to polymer having the backbone of (±) **6**/(± −) **14** (Scheme 4.2). With decreasing polymer concentration, an increasing incorporation of anionic fraction —PO_3H^- in the polymer backbone of (±) **6**/(± −) **14** leads to an increase in the repulsion among negative charges, the hydrodynamic volume of the polymer chain and viscosity values. Based on the pK_a value of 2.83 in 0.1 M NaCl, the extent of dissociation of —PO_3H_2 in 1, 0.5, 0.25, and 0.125 g dL^{-1} solutions has been determined to be 20, 27, 36, and 46 mol %, respectively. Note that the concave upwards [Figure 4.4 (a-ii)] and linear [Figure 4.4 (b-ii)] viscosity plots of (± −) **7** in respective salt-free water and 0.1 M NaCl ascertain its typical polyelectrolyte nature; the weak acidity of —PO_3H^- (pK_a: 8.2) in (± −) **7** leads to an insignificant level of dissociation to (± =) **8**: the percent dissociation remains 0.05–0.13 in the concentration range 1–0.125 g dL^{-1}.

Inspection of Figure 4.4 (c-iv,vi) reveals that the polyelectrolyte effect of (±) PZA **6** is more pronounced in salt-free water than in 0.1 M NaCl even though the pK_a (—PO_3H_2)

value of 3.26 in salt-free water is higher than that of 2.83 in 0.1 M NaCl. The percent dissociation of —$PO_3H_2$of (±) PZA **6** to —PO_3H^- of (± −) **14** in 1, 0.5, 0.25, and 0.125 g dL^{-1} solutions in salt-free water is calculated to be 13, 18, 24, and 32 mol %, respectively, which are less than its percent dissociations in 0.1 M NaCl. Increased dissociation in 0.1 M NaCl and repulsion among the anions is expected to increase the viscosity values. However, the lower viscosity values in 0.1 M NaCl [cf. Figure 4.4 (c-iv and c-vi)] is attributed to the contraction of the polymer chain of (±) **6**/(± −) **14** by shielding of the —PO_3H^- anions by Na^+ ions (polyelectrolyte effect). The contraction of the negative part more than offsets the expansion of the zwitterionic portion as a consequence of more effective shielding of the positive nitrogens by Cl^- ions than the shielding of SO_3^- by Na^+ ions resulting in an overall net negative charge on the zwitterionic portion (antipolyelectrolyte effect).[18,95]

Conversion of (±) PZA **6** by addition of 0.5, 1.0, 1.5, and 2 equiv. of NaOH to 1:1 (±) **6**/(± −) **7,** (± −) **7,** 1:1 (± −) **7**/(± =) **8,** and (± =) **8**, respectively, results in the increase in viscosity value as a result of increasing concentration of the anionic portions [Figure 4.4 (c)]. The anionic motifs thus dominate the viscosity behavior.

Equation 4 has been developed[20,92-94] to interpret the solution behavior of charge symmetric or asymmetric polyampholytes. The solution behavior of the current polymers can also be described mathematically in terms of:

$$v^* = -\frac{\pi(fI_B)^2}{\kappa_S} + \frac{4\pi I_B \Delta f^2}{\kappa_S^2} \qquad (4)$$

where f is the total fraction of charged repeating units, Δf is the charge imbalance, I_B is the Bjerrum length, and κ_S is the Debye-Huckel screening parameter. The first and second term in eq 4 describe the shielding of the attractive polyampholytic and Coulombic repulsive interactions, interactions, respectively. The negative or positive electrostatic excluded volume (v*) indicates contraction to a coiled polymer chain or its expansion to a semicoil, respectively. For the electroneutral (±) PZA **5**, the second term vanishes as a result of $\Delta f = 0$, the solution behavior is then described by the first term describing the screening of the attractive polyampholytic interactions that results in a negative excluded volume. However, in the presence of NaCl the electroneutral zwitterionic moiety gains an overall negative charge and thus for $\Delta f \neq 0$, contribution of the second term in eq 4 makes the v* less negative thereby leading to the expansion of the polymer chain and increase in the viscosity values as revealed in Figure 4.4 (b-iii–v).

For (±) PZA **6** in equilibrium with its dissociated form (± −) **14**, (PZAN) (± −) **7**, and (PZDAN) (± =) **8**, $\Delta f \neq 0$; the charge imbalance is maximum for (± =) **8**. The increasing contribution or even dominance of the second term in eq (1), results in higher (more positive or less negative) excluded volume and viscosity. The relative importance of the first and second terms of eq (1) thus dictates the solution behavior. As the salt (NaCl) concentration increases (from 0 to 0.1 N), the magnitude of the first and second term increases and decreases, respectively. The anionic (−) and zwitterionic (±) motifs experience opposite influence in the presence of salt; NaCl helps the anionic portions to coil up (Δf becomes less as a result of shielding) and the zwitterionic portions to expand (Δf becomes more as a result of more effective shielding of positive nitrogens by Cl^- ions than that of $–O^-$ by Na^+ ions). The increased percent dissociation of —PO_3H_2 in PZA **6**

associated with the decrease in polymer concentration increases the progressive importance of the second term as a result of increase in the values of the charge imbalance (eq (1)). This is indeed corroborated by the observed increase in the viscosity values with decreasing polymer concentrations especially in salt-free water and less so in 0.1 N NaCl [Figure 4.4 (c-iv vs. c-vi)]. The less pronounced increment in the viscosity values in the later medium could be attributed to the lower values of Δf in salt-added solutions as a result of more effective contraction of the anionic part than the expansion of the zwitterionic fraction so as to make $\Delta f_{0.1\ M\ NaCl} < \Delta f_{salt\text{-}free}$. The second term (eq (1)) which controls the expansion factor thus becomes less important in 0.1 N NaCl. It is interesting to note that both the viscosity plots for (± −) **7** and (± =) **8**, concave upwards in salt-free water and linear in 0.1 N NaCl [Figure 4.4 (a,b)], are typical of polyelectrolytes; the decrease in viscosity in the later medium is a consequence of $\Delta f_{0.1\ M\ NaCl} < \Delta f_{salt\text{-}free}$ as discussed above. Note that (± −) **7** may be considered as an alternating anionic-zwitterionic polymer since its behavior is akin to that of an alternating anionic-zwitterionic copolymer derived from *p*-vinylbenzene sulfonate and *o*-vinyl-*N*-(3-sulfopropy)pyridine.[96]

4.3.4 Basicity Constants

Unlike the monomer, the polymer's basicity constant of a repeating unit depends on the charges on the neighboring repeating units. Both the basicity constant $\log K_1$ and $\log K_2$ for the respective protonation of the —PO_3^{2-} (in **8**) and —PO_3H^- (in **7**) in salt-free water and 0.1 M NaCl are of "apparent"[97] nature (Scheme 4.1) as demonstrated in Figure 4.5 (a,b), which reveals a decrease in $\log K$ with the increase in degree of protonation (α). A decrease in the basicity of —PO_3^{2-} (owing to gradual change of (± =)

motifs to (± −) with the increase in α is a direct consequence of a decrease in the electrostatic field force that encourages protonation.

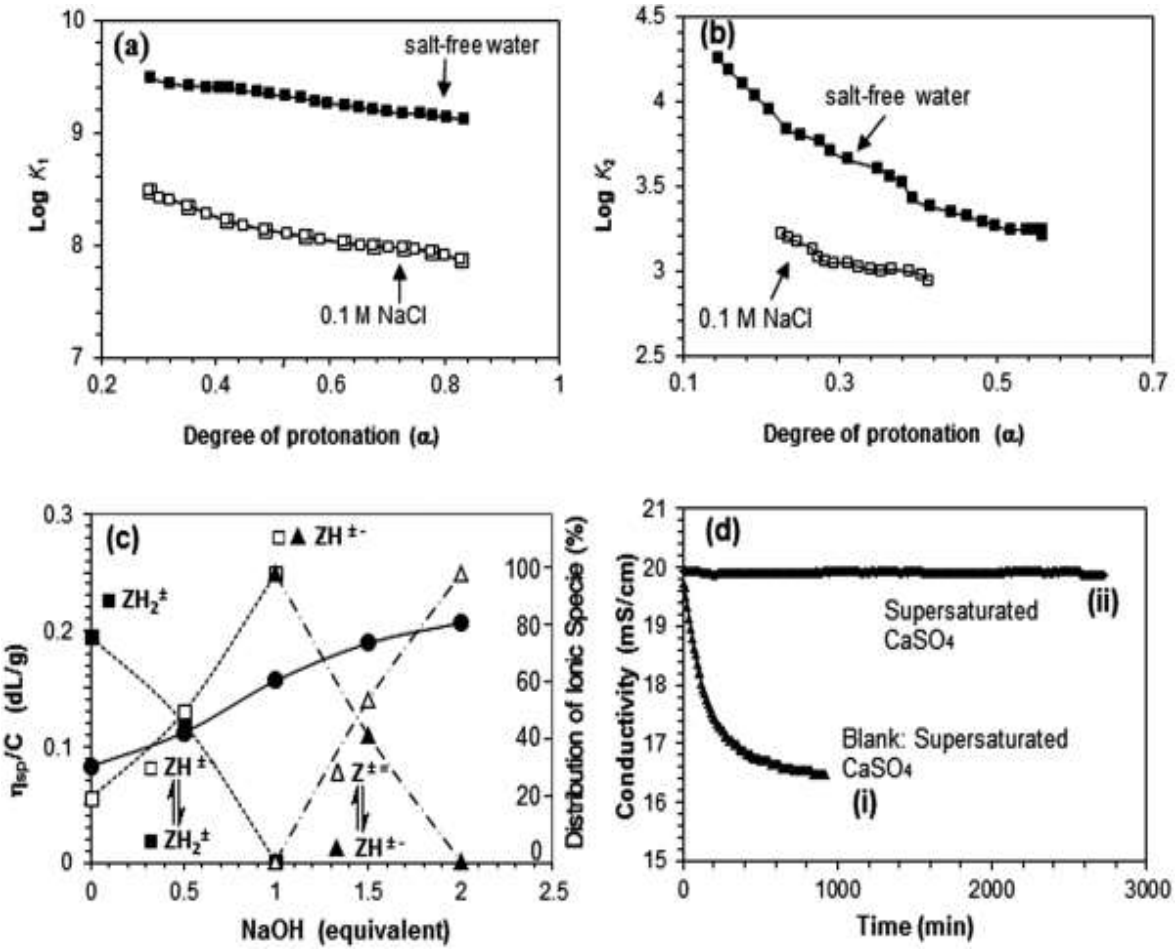

Figure 4.5 Plot for the apparent **(a**) log K_1 versus degree of protonation (α) (entry 3, Table 4.3); (**b**) log K_2 versus α for PZA **6** in salt-free water and 0.1 M NaCl (entry 3, Table 4.4); (**c**) Reduced viscosity (α_{sp}/C) at 30°C of a 0.0293 M (i.e. 1 g/dL) solution of polymer PZA **6** ($ZH_2^{\pm}$) in 0.1 N NaCl (•) versus equivalent of added NaOH at 23°C. Distribution curves (dashed lines) of the various ionized species [■ **6** ($ZH_2^{\pm}$), □▲ **7** ($ZH^{\pm -}$), Δ **8** ($Z^{\pm =}$)] calculated using eq 2 and pH of the solutions in 0.1 M NaCl at 23°C; (**d**) Precipitation behavior of a supersaturated solution of $CaSO_4$ in the presence (20 ppm) and absence of PZA **6**.

Note that the higher values of log K_i in salt-free water than in 0.1 M NaCl may be attributed to the beneficial entropy effects[98] associated with the release of a greater

number of hydrated water molecules from the repeating unit during protonation in the former medium (Table 4.3 and 4.4). The rationale given is supported by higher viscosity values in salt-free water in which the polymer backbone is more extended and as such more hydrated than in 0.1 NaCl. A closer look at the viscosity plots in the dilute solution range 0.03125–0.0625 g dL^{-1} reveals the greater changes of viscosity values in going from **8** to **7** to **6** during protonation in salt-free water [Figure 4.4 (a), inset] compared to 0.1 M NaCl [Figure 4.4 (b)]. A similar concentration range was used for the determination of basicity constants. Thereby, during protonation, the polymer backbone undergoes higher degree of contraction hence release of greater number of hydrated water molecules in salt-free water. The highest *n* value of 2.16, that is, the highest polyelectrolyte index is associated with the transformation of (± −) **7** having excess negative charge to electroneutral (±) **6** in salt-free water (Table 4.4). The transformation experiences the greater change in viscosity values in the salt-free medium than in 0.1 M NaCl [cf. Figure 4.4 (a), inset vs. Figure 4.4 (b)]. In the former medium, the progressive change of **7–6** is associated with a semicoil-to-globule transformation in which the anionic charge-heads are cocooned in the globule and are not easily accessible for protonation. However, this is not the case in 0.1 M NaCl in which the **7–6** transformation is associated with a lesser change in viscosity values in the dilute solutions [cf. Figure 4.4 (b-ii and b-vi)]. Note that for **11**, *n* value of ≈1 for both $\log K_1$ and $\log K_2$ in salt-free water as well as 0.1 M NaCl is expected for a small monomer molecule (Tables 4.3 and 4.4).

Table 4.3 Details for the First Protonation of Monomer ZDAN ($Z^{\pm =}$) **11** and Polymer PZDAN **8** ($Z^{\pm =}$) at 23 °C in Salt-Free Water and 0.1 M NaCl

run	$ZH_2^{\pm}$ or $Z^{\pm =}$ (mmol)	C_T [a] (mol dm^{-3})	α–range	pH–range	Points[b]	Log K_1^{o} [c]	n_1 [c]	R^2, [d]
Polymer 6 in Salt-Free water								
1	0.2361 ($ZH_2^{\pm}$)	–0.1016	0.88–0.20	8.25–10.11	20	9.33	1.29	0.9986
2	0.2944 ($ZH_2^{\pm}$)	–0.1016	0.90–0.26	8.04–9.93	18	9.29	1.36	0.9976
3	0.3826 (**6:** $ZH_2^{\pm}$)	–0.1016	0.83–0.29	8.42–9.87	22	9.33	1.34	0.9989
Average						9.32 (2)	1.33 (4)	
Log K_1 [e] = 9.32 + 0.33 log [(1-α)/α] For the reaction: $Z^{\pm =} + H^+ \overset{K_1}{\rightleftharpoons} ZH^{\pm -}$								
Polymer 6 in 0.1 M NaCl								
1	0.2323 ($ZH_2^{\pm}$)	–0.1016	0.86–0.18	7.03–9.25	16	8.17	1.49	0.9935
2	0.2637 ($ZH_2^{\pm}$)	–0.1016	0.85–0.17	7.10–9.30	18	8.23	1.58	0.9920
3	0.2950 (**6:** $ZH_2^{\pm}$)	–0.1016	0.83–0.28	7.18–8.88	20	8.18	1.52	0.9910
Average						8.19	1.53 (5)	
Log K_1 [e] = 8.19 + 0.53 log [(1-α)/α] For the reaction: $Z^{\pm =} + H^+ \overset{K_1}{\rightleftharpoons} ZH^{\pm -}$								
Monomer 11 in Salt-Free water								
1	0.1845 (**11**:$Z^{\pm =}$)	+0.1222	0.20–0.86	8.18–6.70	15	7.50	1.04	0.9908
2	0.2577 ($Z^{\pm =}$)	+0.1222	0.24–0.90	8.04–6.61	17	7.54	1.04	0.9875
3	0.3361 ($Z^{\pm =}$)	+0.1222	0.22–0.87	8.04–6.72	18	7.55	1.05	0.9845
Average						7.53	1.04 (1)	
Log K_1 [e] = 7.53 For the reaction: $Z^{\pm =} + H^+ \overset{K_1}{\rightleftharpoons} ZH^{\pm -}$								
Monomer 11 in 0.1 M NaCl								
1	0.2206 (**11:** $Z^{\pm =}$)	+0.1222	0.22–0.89	7.70–6.17	16	7.12	1.03	0.9927
2	0.2621 ($Z^{\pm =}$)	+0.1222	0.19–0.89	7.85–6.20	18	7.11	1.03	0.9880
3	0.3062 ($Z^{\pm =}$)	+0.1222	0.16–0.88	8.01–6.29	20	7.13	1.04	0.9920
Average						7.12 (1)	1.03 (1)	
Log K_1 [e] = 7.12 For the reaction: $Z^{\pm =} + H^+ \overset{K_1}{\rightleftharpoons} ZH^{\pm -}$								

[a] (-)ve and (+)ve values describe respective titrations with NaOH and HCl). [b] Number of data points.
[c] Standard deviations in the last digit are given under the parentheses . [d] R = Correlation coefficient.
[e] $\log K_1 = \log K_1^{o} + (n_1 - 1) \log [(1 - \alpha)/\alpha]$.

Table 4.4 Details for the Second Protonation of Monomer ZDAN ($Z^{\pm =}$) **11** and Polymer PZDAN **8** ($Z^{\pm =}$) at 23 ^{o}C in Salt-Free Water and 0.1 M NaCl

run	$ZH_2^{\pm}$ or $Z^{\pm =}$ (mmol)	C_T [a] (mol dm^{-3})	α–range	pH–range	Points[b]	Log K_2^{o} [c]	n_2 [c]	R^2, [d]
Polymer 6 in Salt-Free water								
1	0.2361 ($ZH_2^{\pm}$)	–0.1016	0.52–0.17	3.29–4.86	20	3.29	2.21	0.9942
2	0.2944 ($ZH_2^{\pm}$)	–0.1016	0.51–0.19	3.17–4.56	22	3.21	2.11	0.9962
3	0.3826 (**6:** $ZH_2^{\pm}$)	–0.1016	0.56– 0.15	3.10–5.02	24	3.28	2.16	0.9925
Average						3.26 (4)	2.16 (5)	

Log K_2 [e] = 3.26 + 1.16 log [(1-α)/α] For the reaction: $ZH^{\pm -} + H^{+} \rightleftharpoons ZH_2^{\pm}$ (K_2)

Polymer 6 in 0.1 M NaCl								
1	0.2323 ($ZH_2^{\pm}$) [f]	–0.1016	0.47–0.27	2.87–3.47	16	2.79	1.52	0.9975
2	0.2637 ($ZH_2^{\pm}$) [f]	–0.1016	0.51–0.31	2.82–3.40	18	2.84	1.65	0.9906
3	0.2950 (**6**: $ZH_2^{\pm}$)	–0.1016	0.41–0.23	3.09–3.76	15	2.85	1.63	0.9869
Average						2.83(3)	1.60(7)	

Log K_2 [e] = 2.83 + 0.60 log [(1-α)/α] For the reaction: $ZH^{\pm -} + H^{+} \rightleftharpoons ZH_2^{\pm}$ (K_2)

Monomer 11 in Salt-Free water								
1	0.1845 (**11:**$Z^{\pm =}$)	+0.1222	0.15–0.52	3.55–2.73	19	2.75	1.02	0.9849
2	0.2577 ($Z^{\pm =}$)	+0.1222	0.16–0.58	3.47–2.61	18	2.72	0.984	0.9926
3	0.3361 ($Z^{\pm =}$)	+0.1222	0.17–0.62	3.50–2.57	20	2.75	1.05	0.9896
Average						2.74 (2)	1.02 (3)	

Log K_2 [e] = 2.74 For the reaction: $ZH^{\pm -} + H^{+} \rightleftharpoons ZH_2^{\pm}$ (K_2)

Monomer 11 in 0.1 M NaCl								
1	0.2206 (**11:**$Z^{\pm =}$)	+0.1222	0.15–0.52	3.71–2.91	16	2.91	0.993	0.9929
2	0.2621 ($Z^{\pm =}$)	+0.1222	0.18–0.52	3.55–2.79	17	2.84	1.06	0.9918
3	0.3062 ($Z^{\pm =}$)	+0.1222	0.17–0.64	3.65–2.70	19	2.94	0.990	0.9936
Average						2.90 (5)	1.01 (4)	

Log K_2 [e] = 2.90 For the reaction: $ZH^{\pm -} + H^{+} \rightleftharpoons ZH_2^{\pm}$ (K_2)

[a] (-)ve and (+)ve values describe respective titrations with NaOH and HCl,. [b] data points from titration curve.
[c] Standard deviations in the last digit are given under the parentheses . [d] R = Correlation coefficient.
[e] log K_i = log K_i^{o} + (n – 1) log [(1 - α)/α].
[f] titration was carried out in the presence of 1.5 mL of 0.1222 M HCl to attain the required values of the α.

4.3.5 Viscometric Titrations

A viscometric titration of a 0.0293-M (i.e., 1 g dL^{-1}) solution of the polymer PZA **6** in 0.1 M NaCl solutions with NaOH at 23 °C is reported in Figure 4.5 (c). The figure also shows the distribution curves of the specie $ZH_2^{\pm}$ (PZA **6**), $ZH^{\pm\ -}$ (PZAN **7**), and $Z^{\pm\ =}$ (PZDAN **9**). The distribution of ionic specie were calculated from the basicity constants (*vide supra*) and pH values. With the increased addition of NaOH, the reduced viscosity increases as a result of increasing repulsions among the excess negative charges. Minimum viscosity is attributed to the presence of fully zwitterionic species **6**. Increasing participation of zwitterionic/anionic and zwitterionic/dianionic species leads to gradual increase in the viscosity values.

4.3.6 Effectiveness of PZA 6 as an Antiscalant

Mineral scales of $CaCO_3$, $CaSO_4$, $Mg(OH)_2$, and so forth, polymeric silica, corrosion products, and suspended matter are hindrance to smooth functioning of desalination process. The ability of antiscalants to sequestrate polyvalent cations and alter the crystal morphology at the time of nucleation, inhibit growth rate of crystal formation.[131,135] Poly(phosphate)s, organophosphates, and polyelectrolytes[136,137] are the commonly used anionic antiscalants.

The feed water in the RO process is split into product water and reject brine streams. Precipitation or scaling occurs as a result of supersaturation of dissolved salts and exceeding their solubility limits. For the current work, antiscalant behavior in the presence and absence of 20 ppm of PZA **6** was investigated by conductivity measurements of a supersaturated solution of $CaSO_4$ containing 2600 ppm of Ca^{2+} and 6300 ppm of SO_4^{2-}. A drop in conductivity is an indication of precipitation of $CaSO_4$. To

our great satisfaction, conductivity did not decrease for about 2700 min (45 h) thus registering an amazing ≈100% scale inhibition in the presence of a meager 20 ppm of PZA **6** **[**Figure 4.5 (d-ii)]. Note that precipitation started immediately in the absence of antiscalant [Figure 4.5 (d-i): Blank]. The optimistic result thus certifies that the new additive is very much suitable for use in inhibiting calcium sulfate precipitation in RO plants. The beneficial combined effect of both sulfonate and phosphonate motifs in the same repeating unit in PZA **6** was confirmed since screening experiments based on visual inspection revealed that under the same conditions polymers having only sulfonate[66] and phosphonate group (**16**)[138] did not give effective inhibition. The system becomes cloudy within 1 h in the presence of **16**, while polyphosphonate **15** performed better as $CaSO_4$ precipitate appeared after 35 h. It is worth mentioning that neither monomers **4** and **9** nor polymer **5** gave any effective inhibition; since screening experiments based on visual inspection revealed that under the same conditions the system becomes cloudy within 1 h.

4.4 CONCLUSIONS

The work describes the synthesis and polymerization of zwitterionic monomer **4**. The PZ 5 represents the first example of a Butler's cyclopolymer containing the dual functionality of phosphonate and sulfonate in the same repeating unit. The hydrolysis of the phosphonate ester groups resulted in the pH-responsive (±) PZA **6** which permitted to study the interesting solution properties (including solubility behavior) that involved its conversion to (± −) PZAN **7** and (± =) PZDAN **8** all having identical degree of polymerization. The solution properties were correlated to the type of charges and their densities on the polymer chain. The apparent basicity constants of the —PO_3H^- and —PO_3^{2-} groups in (± −) PZAN **7** and (± =) PZDAN **8** have been determined. PZA **6** at a

meager concentration 20 ppm imparted excellent inhibition of the formation of calcium sulfate scale and as such it can be used effectively as an antiscalant additive in RO plant.

CHAPTER 5

Synthesis, solution properties and scale inhibiting behavior of a diallylammonium/sulfur dioxide cyclocopolymer bearing Phospho- and Sulfopropyl Pendents

Taken from Shaikh A. Ali and Shamsuddeen A. Haladu, Synthesis, solution properties and scale inhibiting behavior of a diallylammonium/sulfur dioxide cyclocopolymer bearing Phospho- and Sulfopropyl Pendents, *Polymer international (2013)*, DOI: 10.1002/pi.4691.

Abstract

Zwitterion (Z) monomer 3-[diallyl{3-(diethoxyphosphoryl)propyl}ammonio]propane-1-sulfonate underwent cyclocopolymerization with sulfur dioxide to give a new alternating copolymer poly(Z-*alt*-SO_2) in excellent yields (≈90%). The polyzwitterion (±) (PZ) (i.e. poly(Z-*alt*-SO_2), bearing a diethylphosphonate as well as a sulfonate functionality in each repeating unit, upon ester hydrolysis gave its corresponding pH-responsive polyzwitterionic acid (±) (PZA). The pH-induced equilibrations: (+) cationic polyelectrolyte (CPE) ⇌ (±) PZA ⇌ polyzwitterion/anion (± −) (PZAN) ⇌ polyzwitterion/dianion (± =) (PZDAN) have permitted us to examine the effects of charge types and their densities on the interesting solubility and viscosity behaviors. The apparent protonation constants (K_1 and K_2) of the basic functionalities $\equiv N^{\pm}PO_3^{2-}$ in (± =) (PZDAN) and $\equiv N^{\pm}PO_3H^{1-}$ in (± -) (PZAN) in salt-free water and 0.1 M NaCl have been determined using potentiometric titrations. (±) PZA at a meager concentration of 20 ppm was found to be an effective antiscalant to inhibit the precipitation $CaSO_4$ from its

supersaturated solution: After 500 and 800 min, the respective scale inhibitions of 86 and 98%, asserted its potential use as an effective antiscalant in reverse osmosis plant.

KEYWORDS: pH responsive polymers; basicity constant; cyclopolymerization; water-soluble polymers; calcium sulfate scale; antiscalant.

5.1 INTRODUCTION

The architecture of Butler's cyclopolymers from diallylammonium salts[5-8] has been recognized as the eighth major structural type of synthetic polymers having pyrrolidinium moieties embedded in the chains.[4,139] Use of inexpensive sulfur dioxide in the polymerization process has also led to the value added diallyl ammonium salts/SO_2 copolymers.[99,100] The cyclopolymerization protocol has also been an attractive avenue to obtain polyzwitterions (PZs) (±)[6-8] or polyampholytes (+ −).[10] Strong intragroup, intra- and interchain electrostatic dipole-dipole attractions among the dipolar motifs in PZs lead to a collapsed or globular conformation which can undergo a globule-to-coil transition ("antipolyelectrolyte" effect) in the salt (e.g. NaCl)-added solutions owing to the disruption of the network of ionic cross-links.[6,17-20,105]

These cationic cyclopolymers have found manifold applications in industrial processes. There are over 1000 patents and publications involving poly(diallyldimethylammonium chloride) alone; over 35 million pounds of the pioneering cyclopolymer are sold annually for water treatment and personal care formulations.[140] The pH-responsive biomimetic PZs have also been utilized in various fields[6,109,112-116,120-122] including medical,[112] pharmaceuticals,[114-116] etc.

We describe herein, the copolymerization of a zwitterionic monomer **4** with SO_2 to obtain (±) PZ **5**, a precursor to pH-responsive polyzwitterion acid (±) (PZA) **6** leading to type **1**

polymers: polyzwitterion/anion (PZAN) (± −) **7** and polyzwitterion/dianion (PZDAN) (± =) **8** (Scheme 5.1).

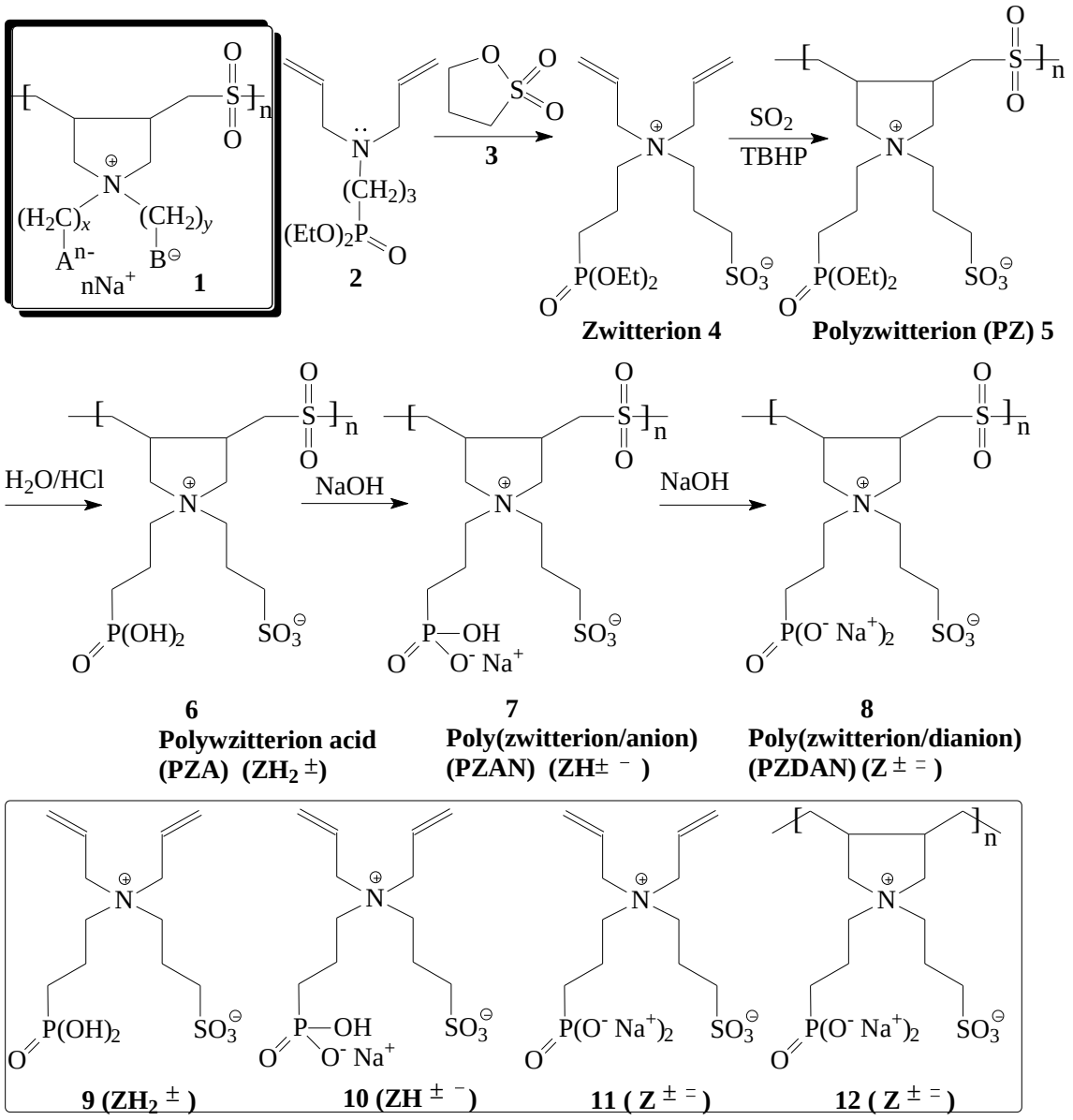

$$Z^{\pm =} + H^{+} \underset{}{\overset{K_1}{\rightleftharpoons}} ZH^{\pm -}$$

8 (or 11) **7 (or 10)**

$$ZH^{\pm -} + H^{+} \overset{K_2}{\rightleftharpoons} ZH_2^{\pm}$$

7 (or 10) **6 (or 9)**

$$\log K_i = \text{pH} - \log[(1-\alpha)/\alpha] \quad \text{Eq 1}$$

$$\text{pH} = \log K_i^{o} + n \log[(1-\alpha)/\alpha] \quad \text{Eq 2}$$

$$\log K_i = \log K_i^{o} + (n-1) \log[(1-\alpha)/\alpha] \quad \text{Eq 3}$$

Scheme 5.1 Cyclopolymers via Butler's cyclopolymerization protocol.

The cyclopolymerization protocol has, so far, documented a very few copolymers of the type **1** bearing (± −) or (± =) ionic traits on the repeating units.[16,75,141] To our knowledge, cyclopolymers **5-8** having phophonate, sulfonate as well as a SO_2 spacer in the same repeating unit will be introduced to the literature for the first time. The synthesis would permit to study the interesting equilibria: (+) cationic polyelectrolyte (CPE) **13** ⇌ **(±) 6** ⇌ **(± -) 7** ⇌ **(± =) 8** involving polymers having identical degree of polymerization (Schemes 5.1 and 5.2). The solution behaviors as well as antiscalant properties of the copolymers will be examined and compared with those of the corresponding homocyclopolymers (e.g. **12**) (Scheme 5.1).[142]

5.2 EXPERIMENTAL

5.2.1 Physical Methods

Elemental analyses were carried out in a Perkin Elmer instrument (Elemental Analyzer Series II Model 2400). IR spectra were measured in a Perkin Elmer instrument (16F PC FTIR). The ^{13}C, ^{1}H and ^{31}P NMR spectra have been measured in D_2O on a JEOL LA 500 MHz spectrometer. The signals at δ 4.65 (^{1}H HOD) and δ 67.4 (^{13}C peak of dioxane) were used as internal standards. ^{31}P was referenced with 85% H_3PO_4 in dimethyl sulfoxide (DMSO). To prevent absorption of CO_2, viscosity measurements were carried out in an Ubbelohde viscometer using CO_2-free water under N_2. A Sartorius pH Meter PB 11 was used for the measurements of pH. The thermogravimetric analysis (TGA) was carried out in a thermal analyzer (STA 449F3) in the range 25–800 °C (at a rate of 15

°C/min) using air (at a flowing rate of 100 mL/min). An Agilent 1200 series instrument with a RI detector and PL aquagel-OH MIXED column having a MW range 100-10,000,000 g/mol was used to determine the molecular weights. An injection volume of 20 μL of an aqueous solution of the polymer (0.5 wt%) with water flowing at a rate of 1.0 mL/min at 25 ^{o}C and three different standards of polyethylene oxide/glycol were used for the GPC measurements.

5.2.2 Materials

2,2′-Azobisobutyronitrile (AIBN) from Fluka AG (Buchs, Switzerland) was crystallized (ethanol-chloroform). DMSO, dried overnight over calcium hydride, was distilled (bp 64-65 °C at 4 mmHg). A Spectra/Por membrane (MWCO of 6000-8000 from Spectrum Laboratories, Inc) was used for dialysis. Zwitterionic monomer **4** was prepared as described.[142]

5.2.3 Monomer 4/SO_2 copolymerization

In a typical experiment (Table 5.1, entry 3), adsorption of SO_2 (20 mmol) in a solution of monomer **4** (7.95 g, 20 mmol) in DMSO (7.2 g) was followed by the addition of initiator AIBN (80 mg). The reaction mixture under N_2 in a closed flask was stirred at 60 ^{o}C for 20 h. Within 30 min, the stir-bar stopped stirring with the appearance of a thick gel. At the end, the hard polymeric mass was crushed to powder and washed with hot (50 ^{o}C) acetone to obtain (±) PZ **5** (8.0 g, 87%).

Table 5.1 Copolymerization[a] of monomer **4** with sulfur dioxide

Entry No.	Monomer (mmol)	DMSO (g)	Initiator[b] (mg)	Yield (%)	Intrinsic[c] viscosity (dL g^{-1})	$\overline{M}_w$	(PDI)[d]
1	10	3.6	30	93	0.517	ND[e]	ND[e]
2	10	3.6	50	92	0.578	1.37×10^5	2.1
3	20	7.2	80	87	0.901	2.44×10^5	2.2

[a] An equimolar mixture of monomer **4** and SO_2 was polymerized at 60°C for 20 h.
[b] Azobisisobutyronitrile.
[c] Viscosity of 1-0.0625 % polymer solution in 0.1 N NaCl at 30°C was measured with Ubbelohde Viscometer (K=0.005718).
[d] Polydispersity index. [e]Not determined.

The thermal decomposition: brown color at 270 °C and black at 290 °C. (Found: C, 41.3; H, 7.2; N, 2.9; S, 13.6 %. $C_{16}H_{32}NO_8PS_2$ requires C, 41.64; H, 6.99; N, 3.03; S, 13.89 %); ν_{max} (KBr): 3447, 2985, 1651, 1486, 1370, 1316, 1217, 1100, 1043, 966, 788, 732 cm^{-1}. δ_P (202 MHz, D_2O): 30.81 (s). ^1H and ^{13}C NMR spectra of PZ **5** are shown in respective Figures 5.1 and 5.2.

5.2.4 Conversion of PZ 5 to poly(zwitterion acid) (PZA) 6

PZ **5** (5.0 g, 10.8 mmol) (entry 3, Table 5.1) was hydrolyzed in water (30 mL) and concentrated HCl (40 mL) at 90 °C for 24 h. During dialysis of the homogeneous mixture (24 h), the polymer separated within 1 h as a gel which redissolved after 3 h. The resulting polymer solution was freeze-dried to obtain (±) PZA **6** as a white solid (4.2 g,

96%). The thermal decomposition: the color changed to dark brown and black at 275 ^{o}C and 285 ^{o}C, respectively; (Found: C, 35.2; H, 6.2; N, 3.3; S, 15.5 %. $C_{12}H_{24}NO_8PS_2$ requires C, 35.55; H, 5.97; N, 3.45; S, 15.82 %); ν_{max} (KBr): 3445 (br), 2971, 2928, 1643, 1471, 1411, 1311, 1215, 1132, 1042, 982, 932, 789, 733 cm^{-1}. δ_P (202 MHz, D_2O): 25.52 (s). The NMR spectra are shown in Figures 5.1 and 5.2.

5.2.5 Solubility measurements

A 2% (w/w) mixture of PZ **5** or PZA **6** in a solvent was stirred at 70 °C for 1 h and the solubility behavior was then checked at 23 °C. The solvent used, with the dielectric constant (ε) and solubility (+) or insolubility (–) written in parentheses, for **5** and **6,** respectively, are as follows: formamide (111, +, +), water (78.4, +, +), formic acid (58.5, +, +), DMSO (47.0, +, –), ethylene glycol (37.3, +, –), DMF (37.0, –, –), methanol (32.3, –, –), triethylene glycol (23.7, –, –), and acetic acid (6.15, +, –).

5.2.6 Solubility measurements in salt-free water and in the presence of HCl

Polymer PZA **6** (25 mg, 5 wt %) is insoluble in water (0.5 mL) but soluble in excess water (1.0 mL). A solution of PZA **6** (30 mg, 0.0617 mmol) in 1.04 M HCl (2.30 mL) was titrated with salt-free water until cloudiness that required the addition of 1.35 mL water. At this point, the concentrations of the polymer and HCl were calculated to be 0.0169 and 0.655 M HCl, respectively. Continued addition of water (50.5 mL) led to disappearance of the cloudiness to a colorless solution, thereby revealing the solubility of 0.00114 M polymer in 0.0442 M HCl.

5.2.7 Potentiometric Titrations

The first and second step protonation constants, K_1 and K_2, of polymer **8** [$ZH_2^{\pm\ =}$] were determined by potentiometric titrations under N_2 in CO_2-free water as described elsewhere using PZA **6** [$ZH_2^{\pm}$] in salt-free water or 0.1 M NaCl (200 mL) (Tables 5.2 and 5.3).[80] The Log K_1 of $–PO_3^{2-}$ (in **8**) and Log K_2 of $–PO_3H^-$ (in **7**) are calculated at each pH value by the Henderson-Hasselbalch eq 2 (Scheme 5.1) where the ratios $[ZH^{\pm\ -}]_{eq}/[Z]_o$ and $[ZH_2^{\pm}]_{eq}/[Z]_o$ represent the respective degree of protonation (α). The $[ZH^{\pm\ -}]_{eq}$ and $[ZH_2^{\pm}]_{eq}$ are the equilibrium concentrations of the first (**7**) and second (**6**) protonated species and $[Z]_o$ is the initial concentration of the repeating units.

For the determination of log K_2 of $–PO_3H^-$ (i.e. $[ZH^{\pm\ -}]$) using titration of polymer **6** $[ZH_2^{\pm}]$ with NaOH, $[Z]_o$ and $[ZH_2^{\pm}]_{eq}$ are related by $[ZH_2^{\pm}]_{eq} = [Z]_o - C_{OH^-} - [H^+] + [OH^-]$, where C_{OH^-}, $[H^+]$ and $[OH^-]$ represent the added concentration of NaOH, and $[H^+]$ and $[OH^-]$ describe the equilibrium concentrations as calculated from the pH values.[77,78] The log K_1 for the first step protonation of $–PO_3^{2-}$ (i.e. $[Z^{\pm\ =}]$) was calculated using volume of the titrant after deducting the equivalent volume from the total volume. In this case, α represents the ratio $[ZH^{\pm\ -}]_{eq}/[Z]_o$ whereby $[ZH^{\pm\ -}]_{eq}$ equals $[Z]_o - C_{OH^-} - [H^+] + [OH^-]$.

The linear regression fit of pH *vs*. log $[(1-\alpha)/\alpha)]$ (eq 2, Scheme 5.1) gave '*n*' and log K^o, the respective slope and intercept. The apparent basicity constants K_i is described by eq 3 (Scheme 5.1) where log K^o = pH at α = 0.5 and n = 1 in the case of sharp basicity constants. Simultaneous protonation of the three basic sites: $-PO_3^{=}$ (log $K_1 \approx +8$), $-PO_3H^-$ (log K_2: $\approx +3$) and $-SO_3^-$ (log K_3: ≈ -2.1)[79] is least likely due to differences of their

basicity constants by about 5 orders of magnitude. Note that basicity constant log *K* of any base B is the pK_a of its conjugate acid BH^+.

5.2.8 Evaluation of antiscalant behavior

The concentration of a reject brine (i.e., concentrated brine (CB)), denoted as 1CB, at 70 % recovery from a reverse osmosis (RO) plant revealed the presence of 866.7 mg/L and 2100 mg/L Ca^{2+} and SO_4^{2-}, respectively.[133] Inhibition of calcium sulfate (gypsum) scaling by PZA **6** was carried out in 3 CB solutions of supersaturated $CaSO_4$ containing Ca^{2+} **(**3×866.7 mg/L i.e., 2600 mg/L) and SO_4^{2-} (3×2100 mg/L i.e. 6300 mg/L). To a solution of 6 CB calcium chloride (60 mL) containing PZA **6** (40 ppm i.e. 40 mg/L) at 40ºC ± 1ºC was added quickly a preheated (40 ºC) solution of 6 CB sodium sulfate (60 mL). The resultant 3 CB solution containing 20 ppm of PZA **6** was stirred at 300 rpm using a magnetic stir-bar, and conductivity measurements were made at an interval of every 10 min initially. Similar experiment was carried out simultaneously using the same heating bath in the absence of the antiscalant PZA **6**. The drop in conductivity (as well as visual inspection) indicated the precipitation of $CaSO_4$.

5.3 RESULTS AND DISCUSSION

5.3.1 Synthesis and Characterization of the ionic polymers

Copolymerization of zwitterion monomer **4** and SO_2 afforded alternate polyzwitterion (PZ) **5** in excellent yields (Scheme 5.1). PZ (±) **5** was hydrolyzed in HCl/H_2O to give PZA (±) **6** which on neutralization with 1 and 2 equivalents of NaOH is expected to generate polyzwitterion/anion (PZAN) (± -) **7** and polyzwitterion/dianion (PZDAN) (± =) **8**.

PZ **5** was observed to be stable up to around 266 ^{o}C as evident from the TGA curve (Figure 5.3). The first steep weight loss in the temperature range 266-320 °C range was due to the losses of sulfopropyl moiety (26%) and SO_2 (14%). The second gradual loss of 36% in the 320-800 °C range was the result of decomposition of the phosphonate ester functionality.[134]

The PZ **5** and PZA **6** were found to be soluble in protic solvents having higher dielectric constants (see Experimental). Even though PZs are usually insoluble in salt-free water,[120,121] the water-solubility of the current PZs is attributed to the steric crowding[20,100,141] which makes it difficult for the sulfonates to move closer to nitrogens to impart zwitterionic interactions.[17,86,123]

A 5 wt% (±) PZA **6** in salt-free water remained heterogeneous while it became soluble when diluted to 2.5 wt%. For the pK_a value of 3.61 of $–PO_3H_2$ in salt-free water (*vide infra*) it is calculated that (±) PZA **6** will be dissociated to (± −) PZAN **7** to the extent of 4.4 mol% and 6.1 mol% in the respective 5 wt% and 2.5 wt% solutions in salt-free water. Greater participation of the zwitterionic/anionic (±−) motifs thus makes the polymer soluble in 2.5 wt% solution. The heterogeneous mixture containing 5 wt% (±) PZA **6** became homogeneous in the presence of 0.1 M NaCl. For a lower pK_a value of 2.98 (*vide infra*) in 0.1 M NaCl, the increased dissociation as well as breaking up zwitterionic interactions[6,17,18,20,105] by the salt increases its solubility.

Interestingly, it was observed that during the dialysis of PZA **6** in 6.9 M HCl, precipitation of the polymer occurred within 1 h and its dissolution after 3 h. On further investigation, it was revealed that while PZA **6** (30 mg, 0.0617 mmol) remained soluble

in 1.04 M HCl (2.30 mL), titration with water (1.35 mL) led to cloudiness. The polymer (0.0169 M) thus became insoluble in the presence of 0.655 M HCl. Continued addition of water (50.5 mL) to the cloudy mixture leads to a colorless solution at a polymer and HCl concentrations of 0.00114 M and 0.0442 M, respectively. The equilibria presented in Scheme 5.2 could explain the interesting solubility behavior. While the undissociated (±) PZA **6** by virtue of being zwitterionic is insoluble in neutral water, the presence of HCl pushes the equilibrium towards water-soluble cationic polyelectrolyte (CPE) (+) **13** which upon extended dialysis is transformed to water-insoluble undissociated (±) PZA **6** with the depletion of HCl.

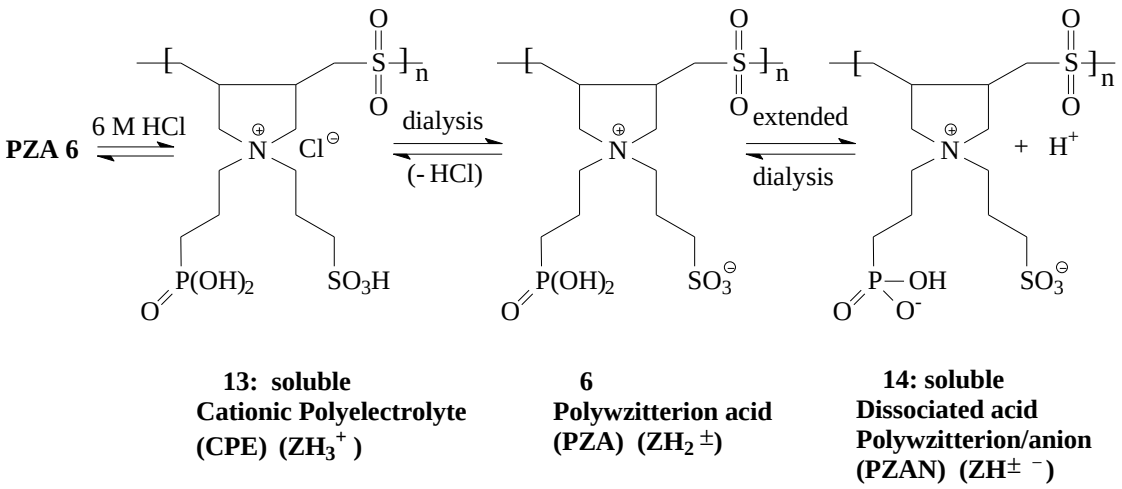

Scheme 5.2 PZA **6** under pH-induced equilibration.

Continued dialysis in the absence of HCl establishes the equilibrium: **6⇋14** in which the increased dilution pushes the equilibrium towards water-soluble (±−) PZAN **14**.

5.3.2 IR and NMR spectra

The strong IR absorptions around ≈ 1216 cm^{-1} and ≈ 1042 cm^{-1} indicate the presence of sulfonate and phosphonate groups in PZ **5** and PZA **6**. The two strong bands at ≈ 1315 cm^{-1} and ~1100 cm^{-1} were assigned to the asymmetric and symmetric vibrations of SO_2 unit. The P=O absorption peaks appeared at 985 (in PZ **5**) and 982 cm^{-1} (in PZA **6**). Figures 5.1 and 5.2 show the respective ^{1}H and ^{13}C NMR spectra of **4**-**6**.

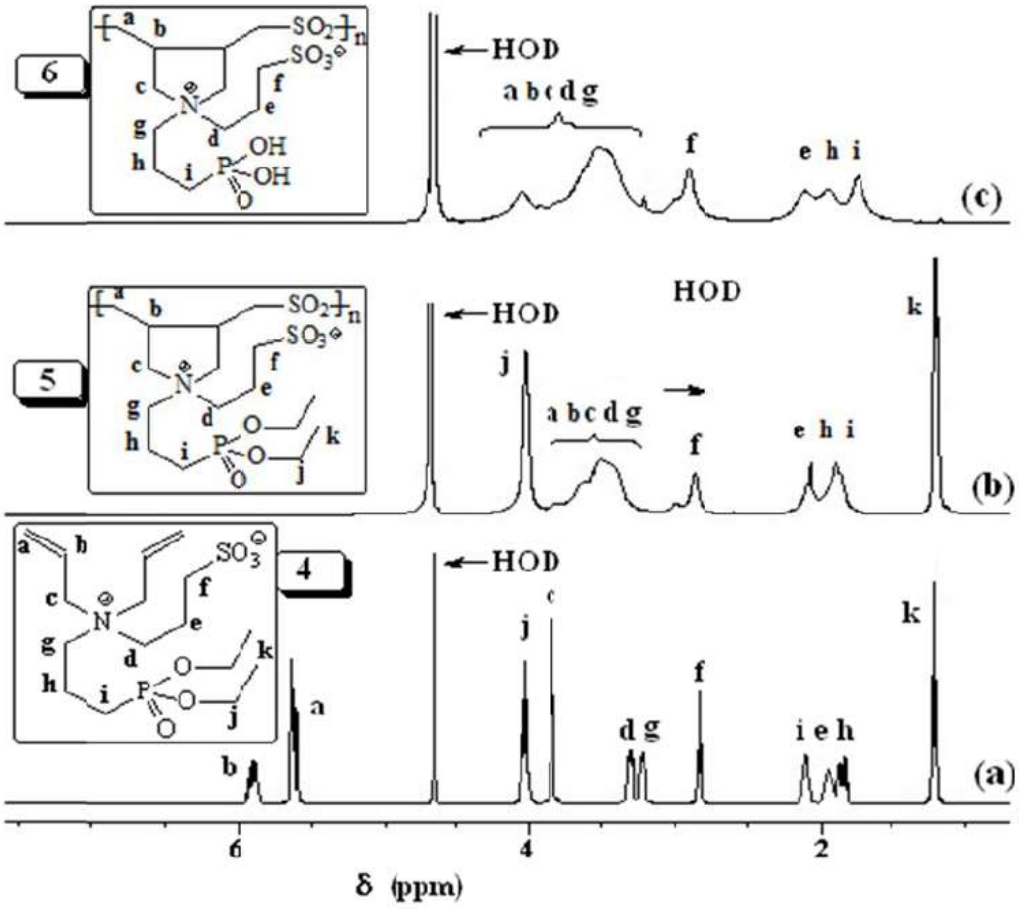

Figure 5.1 ^{1}H NMR spectrum of (**a**) **4**, (**b**) **5**, and (**c**) **6** (+NaCl) in D_2O.

The complete disappearance of any alkene proton or carbon signals ascertains that the termination happens *via* chain transfer and/or coupling process.[88,124] The absence of the ester group (OCH_2CH_3) indicate its removal by hydrolysis as shown in the spectra of **6** Figure 5.1 (c) and 5.2 (c). The stereochemistry of the substituents at $C_{b,b}$ in the polymers as *cis* and *trans* in a 75/25 ratio is similar to earlier findings.[7]

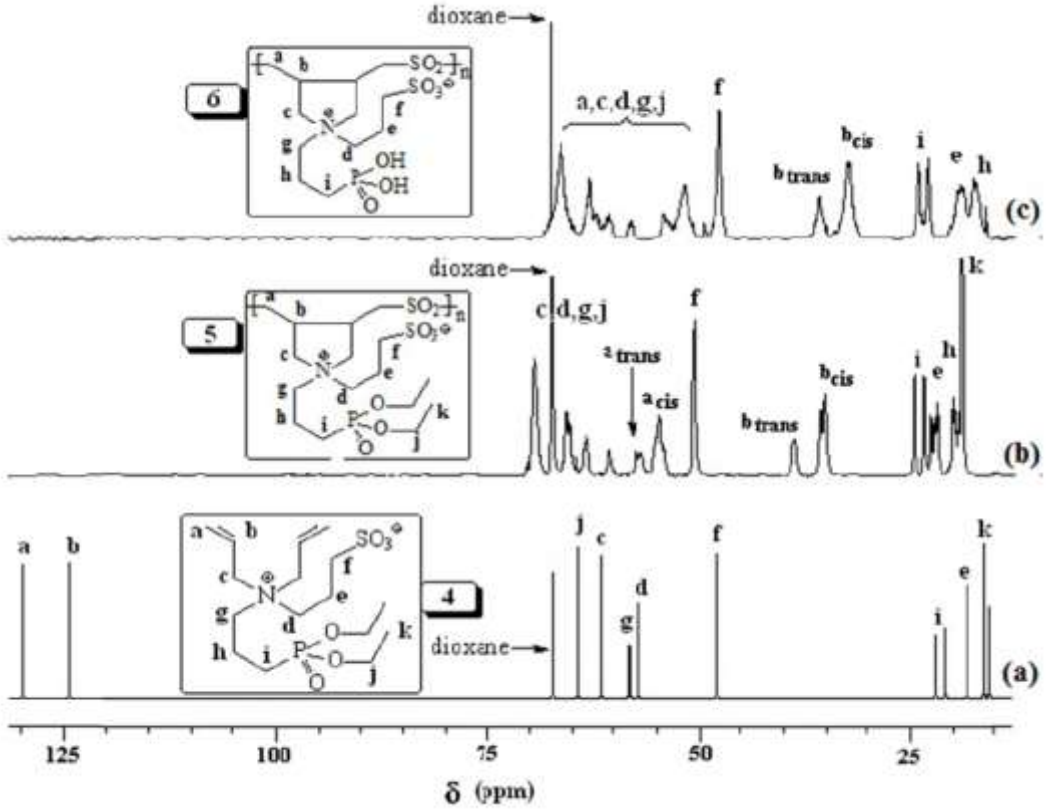

Figure 5.2 [13] NMR spectrum of (**a**) **4**, (**b**) **5**, and (**c**) **6** (+NaCl) **in** D_2O.

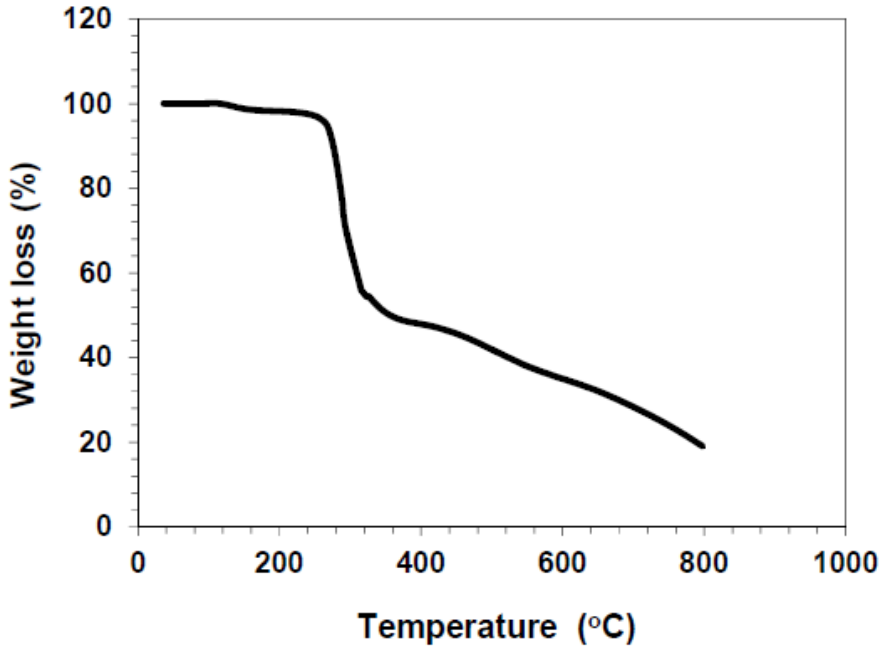

Figure 5.3 TGA curve of PZ **5**.

5.3.3 Viscosity measurements

Eq 4 was developed to give a mathematical expression to rationalize the solution behavior of symmetrically or asymmetrically charged ionic polymers.[20,92-94]

$$v^* = -\frac{\pi(fI_B)^2}{\kappa_S} + \frac{4\pi I_B \Delta f^2}{\kappa_S^2} \qquad (4)$$

where f is the total fraction of charged monomers, Δf is the charge imbalance, I_B is the Bjerrum length, and κ_S is the Debye-Huckel screening parameter. For symmetrically charged polymers i.e. polymers having equal number of charges of both algebraic signs, the second term in eq. 4 is eliminated by virtue of $\Delta f = 0$. In this case the negative excluded volume (v^*) indicates contraction to a collapsed coil. The second term in eq 4

describes the shielding of the Coulombic repulsive interactions as a result of $\Delta f \neq 0$. In the event of charge imbalance as well as domination of second term over the first, the positive electrostatic excluded volume (v*) leads to expansion to a semicoil.

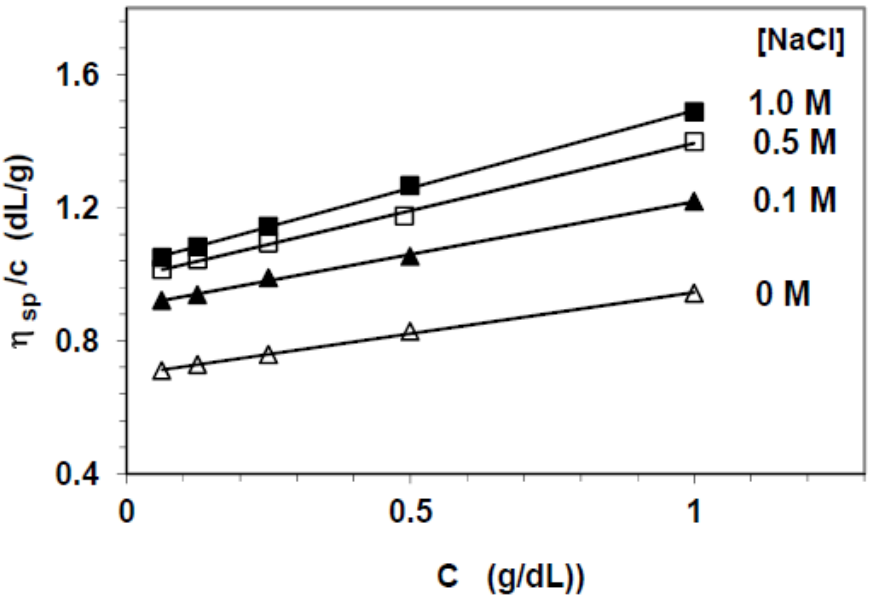

Figure 5.4 Using an Ubbelohde Viscometer at 30 ^{o}C, the viscosity behavior of (±) PZ **5** in ■ 1 M NaCl, □ 0.5 M NaCl, ▲ 0.1 M NaCl, and Δ salt-free water. (Polymer used from entry 3, Table 5.1).

The dependence of viscosity of behavior of (±) PZ **5** on the concentration of NaCl is shown in Figure 5.4. For the electroneutral (±) PZ **5** with $\Delta f = 0$, the viscosity values increases with the increase in salt concentrations. The Cl^- ions effectively shield or bind the positive nitrogens whereas Na^+ with its large hydration shell cannot reach close enough to shield the anionic charges.[18] A net negative charge on (±) **5** thus brings the first as well as second terms in eq 4 to prominence thereby making the Δf lesser negative

with the increase of NaCl concentrations. This leads to the increase in the viscosity values in compare to viscosity in salt-free water.

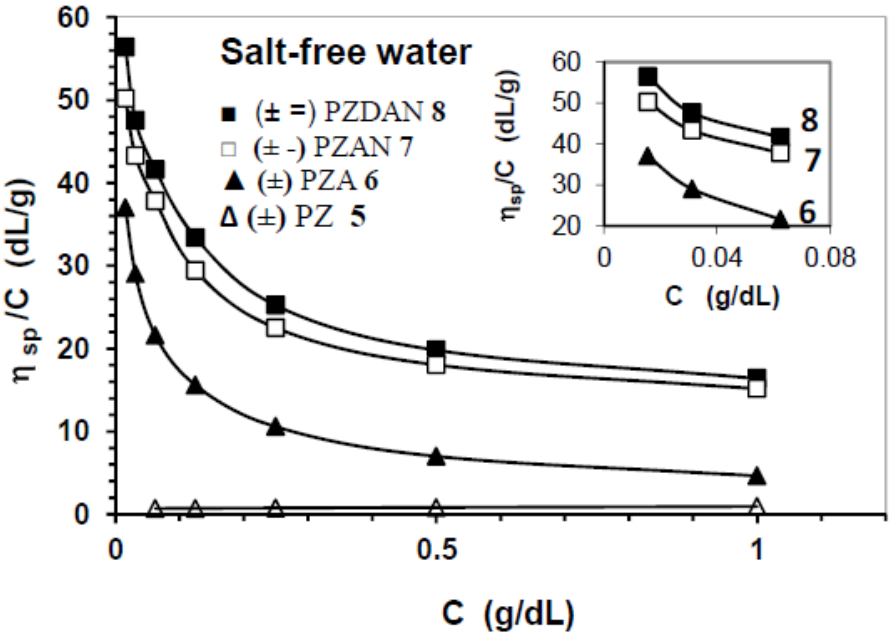

Figure 5.5 Using an Ubbelohde Viscometer at 30 ^{o}C, the viscosity behavior in salt-free water of: (**a**) ■ (± =) PZDAN **8**, (**b**) □ (± -) PZAN **7**, (**c**) ▲ (±) PZ **6** and (**d**) Δ (±) PZ **5**. (All polymers are derived from entry 3, Table 5.1) [Inset describes the viscosity plot in the dilution range 0.0625-0.0156 g/dL].

Figure 5.5 shows the viscosity behavior of **5-8** in salt-free water. Unlike polyzwitterion **5**, the viscosity plots of **6-8** resemble that of a polyelectrolyte i.e. concave upwards. Note that (±) PZA **6** has much higher viscosity values than that of (±) PZ **5** as a result of the dissociation of the former to (± −) PZAN **7** where the net negative charge leads to expansion of the polymer coil (Figure 5.5). For a pK_a value of 3.61 in salt-free water (*vide infra*), the extent of dissociation of PO_3H_2 of (±) **6** to PO_3H^- of (± −) **7** in solutions having polymer concentration of 1, 0.5, 0.25 and 0.125 g/dL is determined as 9.5, 13, 18, and 25 mol%, respectively.

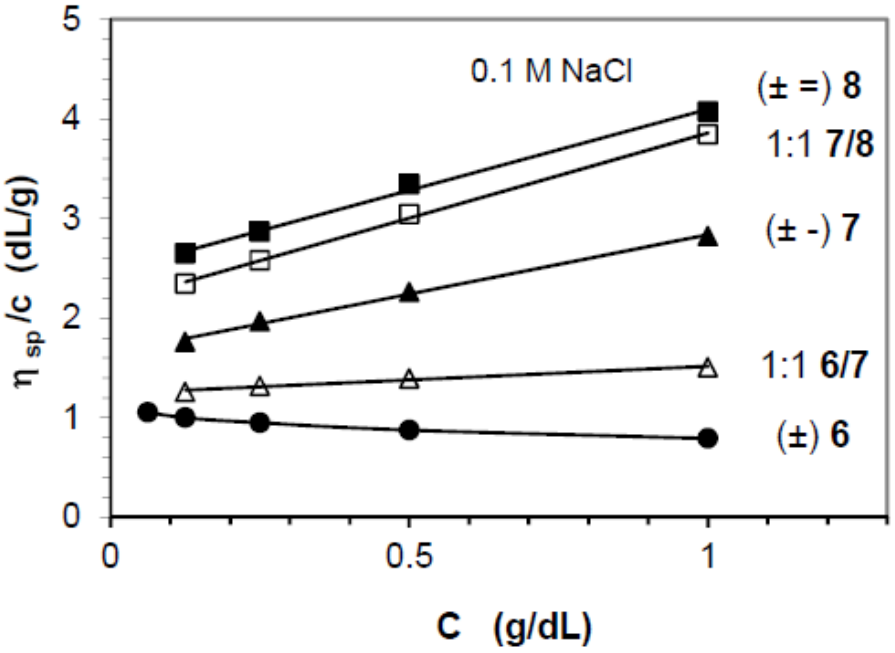

Figure 5.6 Using an Ubbelohde Viscometer at 30 ^{o}C, the viscosity behavior in 0.1 M NaCl of: ■ (± =) PZDAN **8,** □ 1:1 (± -) PZAN **7**/(± =) PZDAN **8;** ▲(± -) PZAN **7**, Δ 1:1 (±) PZA **6**/(± -) PZAN **7**, and ● (±) PZA **6** (all polymers are derived from entry 3, Table 5.1).

Note that the viscosity plot (Figure 5.6) of **6** remains concave upwards while that of **7** remains linear since the weak acidity of -PO_3H^- (pK_a: 7.9) in **7** leads to insignificant level of dissociation to -PO_3^{2-} of **8**. Inspection of Figures 5.5 and 5.6 reveal that the polelectrolyte effect in **6-8** is more pronounced in salt-free water than in 0.1 M NaCl, as a result of the greater contraction of the polymer chain by shielding of the (±)−PO_3H^- and

(±)−PO_3^{2-} anions by Na^+ ions (polyelectrolyte effect) than the expansion caused by disruption of zwitterionic interactions. Conversion of (±) PZA **6** by addition of 0.5, 1.0, 1.5, and 2 equivalents of NaOH to 1:1 (±) **6**/(± -) **7,** (± -) **7,** 1:1 (± -) **7**/(± =) **8,** and (± =) **8,** respectively, results in the increase in viscosity values as a result of increasing concentration of the anionic portions (Figure 5.6)**.**

5.3.4 Basicity constants

The basicity constant log K_1 for the protonation of the $–PO_3^{2-}$ (in **8**)) in salt-free water and 0.1 M NaCl were determined to be 9.51 and 7.90, respectively (Table 5.2), while log K_2 for the respective protonation of the $–PO_3H^-$ (in **7**) were found to be 3.61 and 2.98 (Table 5.3). The log *K* values are thus found to be higher than those of the corresponding monomers **10** and **11** (Scheme 5.1).

Table 5.2 . Details for the First Protonation of Monomer ZDA ($Z^{\pm =}$) **11** and Polymer PZDAN **8** ($Z^{\pm =}$) at 23 ^{o}C in Salt-Free Water

run	$ZH_2^{\pm}$ or Z^- (mmol)	C_T [a] (mol L^{-1})	α–range	pH–range	Points[b]	Log K_i^{o} [c]	n_i [c]	R^2, [d]
			For the protonation of $-PO_3^{2-}$: $Z^{\pm =} + H^+ \overset{K_1}{\rightleftharpoons} ZH^{\pm -}$					
Polymer in Salt-Free water								
1	0.1759 ($ZH_2^{\pm}$)	−0.1016	0.79–0.14	8.77–10.42	14	9.47	1.18	0.9992
2	0.2467 ($ZH_2^{\pm}$)	−0.1016	0.89–0.13	8.57–10.51	15	9.54	1.15	0.9974
3	0.3244 ($ZH_2^{\pm}$)	−0.1016	0.87–0.14	8.58–10.45	17	9.52	1.16	0.9970
Average						9.51 (4)	1.16 (2)	
			Log K_1 [e] = 9.51 + 0.16 log [(1-α)/α]					
Monomer in Salt-Free water: Log K_1 [e] = 7.53								
Polymer in 0.1 M NaCl								
1	0.1995 ($ZH_2^{\pm}$)	−0.1016	0.78−0.13	7.20−9.14	14	7.90	1.54	0.9904
2	0.2486 ($ZH_2^{\pm}$)	−0.1016	0.80−0.13	7.15−9.17	17	7.91	1.42	0.9917
3	0.3034 ($ZH_2^{\pm}$)	−0.1016	0.86−0.15	6.80−8.92	18	7.88	1.39	0.9980
Average						7.90 (2)	1.45 (8)	
			Log K_1 [e] = 7.90 + 0.45 log [(1-α)/α]					
Monomer in 0.1 M NaCl: Log K_1 [e] = 7.12								

[a] (-)ve values describe titrations with NaOH.
[b] data points from titration curve.
[c] Standard deviations in the last digit are given under the parentheses .
[d] R = Correlation coefficient.
[e] log K_i = log K_i^{o} + (n – 1) log [(1 - α)/α].

Table 5.3 Details for the Second Protonation of Monomer ZDAN ($Z^{\pm -}$) **11** and Polymer PZDAN **8** ($Z^{\pm -}$) at 23 ^{o}C in Salt-Free Water

run	$ZH_2^{\pm}$ or Z^- (mmol)	C_T [a] (mol L^{-1})	α–range	pH–range	Points[b]	Log K_i^{o} [c]	n_i [c]	R^2, [d]
	For the protonation of $-PO_3H^-$:		$ZH^{\pm -} + H^+ \overset{K_2}{\rightleftharpoons} ZH_2^{\pm}$					
Polymer in Salt-Free water								
1	0.1759 ($ZH_2^{\pm}$)	−0.1016	0.53–0.23	3.44–4.70	15	3.55	2.13	0.9986
2	0.2467($ZH_2^{\pm}$)	−0.1016	0.53–0.21	3.56–4.97	16	3.64	2.25	0.9980
3	0.3244 ($ZH_2^{\pm}$)	−0.1016	0.59–0.18	3.25–5.10	18	3.63	2.17	0.9970
Average						3.61 (5)	2.18 (6)	
Log K_2 [e] = 3.61 + 1.18 log [(1-α)/α]								
Monomer in Salt-Free water: Log K_2 [e] = 2.74								
Polymer in 0.1 M NaCl								
1	0.1995 ($ZH_2^{\pm}$)[f]	−0.1016	0.54-0.20	2.90-3.73	15	2.97	1.24	0.9929
2	0.2486 ($ZH_2^{\pm}$)[f]	−0.1016	0.56-0.18	2.92-3.88	18	3.02	1.22	0.9906
3	0.3034 ($ZH_2^{\pm}$)[f]	−0.1016	0.58-0.16	2.81-3.95	19	2.94	1.29	0.9925
Average						2.98 (4)	1.25 (4)	
Log K_2 [e] = 2.98 + 0.25 log [(1-α)/α]								
Monomer 11 in 0.1 M NaCl: : Log K_2 [e] = 2.90								

[a] (-)ve values describe titrations with NaOH.
[b] data points from titration curve.
[c] Standard deviations in the last digit are given under the parentheses .
[d] R = Correlation coefficient.
[e] log K_i = log K_i^{o} + (n – 1) log [(1 - α)/α].
[f] titration was carried out in the presence of 1.5-2 mL of 0.1222 M HCl to attain the required values of the α.

Unlike the monomers, all the n_i values of greater than 1 ascertain the "apparent"[97] nature of the basicity constants of the polymers (Tables 5.2 and 5.3) as demonstrated in Figure 5.7, which reveals a decrease in log K with the increase in α as a direct consequence of a decrease in the electrostatic field force that encourages protonation.

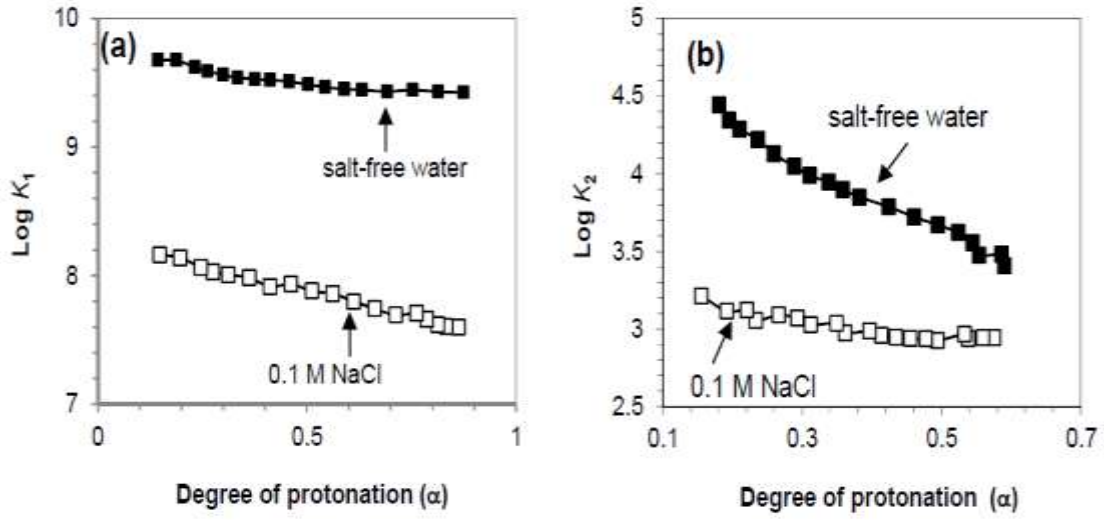

Figure 5.7 Plot for the apparent (**a**) log K_1 versus degree of protonation (α) (entry 3, Table 5.2) for (± =) PZDAN **8** and (**b**) log K_2 versus α for (± -) PZAN **7** in salt-free water and 0.1 M NaCl (entry 3, Table 5.3).

The higher basicity constants in salt-free water compared to values in 0.1 M NaCl could be attributed to the entropy effects associated with the greater release of water molecules from the hydration shell of the repeating unit that is being protonated in the former medium.[98] The higher viscosity values in salt-free water (Figure 5.5, inset) than in 0.1 M NaCl (Figure 5.6) ascertains the polymer backbone is highly extended and as such more hydrated in the former medium. The higher degree of contraction in going from **8** to **7** to **6** in salt-free water reflects greater changes in the hydration number which results in entropy-driven greater basicity constants.

5.3.5 Viscometric titration

Figure 5.8 displays a viscometric titration of a 0.0247 M (i.e. 1 g/dL) solution of the polymer PZA **6** in 0.1 M NaCl with NaOH. The Figure also include the distribution curves of various ionic specie $ZH_2^{\pm}$ (**6**), $ZH^{\pm -}$ (**7**) and $Z^{\pm =}$ (**8**) as calculated from the basicity constants (*vide supra*) and pH values.

Table 5.4 Comparative properties of monomer (± =) **11**, homo- (± =) **12** and cyclopolymer (± =) **8**

Sample	Log K^o_1 (n_1)[a]		Log K^o_2 (n_2)[a]		IE[b] (h)	Polymer yield	[η] (dL g^{-1})[c]	$\overline{M}_W$
	Salt-free H_2O	0.1 M NaCl	Salt-free H_2O	0.1 M NaCl				
Mono-11[d]	7.53 (1)	7.12 (1)	2.74 (1)	2.90 (1)	–	–	–	–
Homo-12[d]	9.32 (1.33)	8.19 (1.53)	3.26 (2.16)	2.83 (1.60)	98% (8.3 h)	76%	0.186	4.37×10^4
Co-8	9.51 (1.16)	7.90 (1.45)	3.61 (2.18)	2.98 (1.25)	≈100% (45 h)	87%	2.47	2.44×10^5

[a] *n* values are written in parentheses.
[b] IE referes to $CaSO_4$ scale inhibition efficiency with time written in parentheses using copolymer PZA **6** and its corresponding homopolymer.[30]
[c] Viscosity of 1-0.0625% polymer solution in 0.1 M NaCl was measured with Ubbelohde Viscometer (K=0.005718) at 30°C. [d]Reference 30.

The reduced viscosity increases with the increase in concentration of added NaOH owing to increasing repulsions among the excess negative charges as a result of

transformation of zwitterionic species (±) to progressively increasing zwitterionic/anionic (± −) or zwitterionic/dianionic (± =) species.

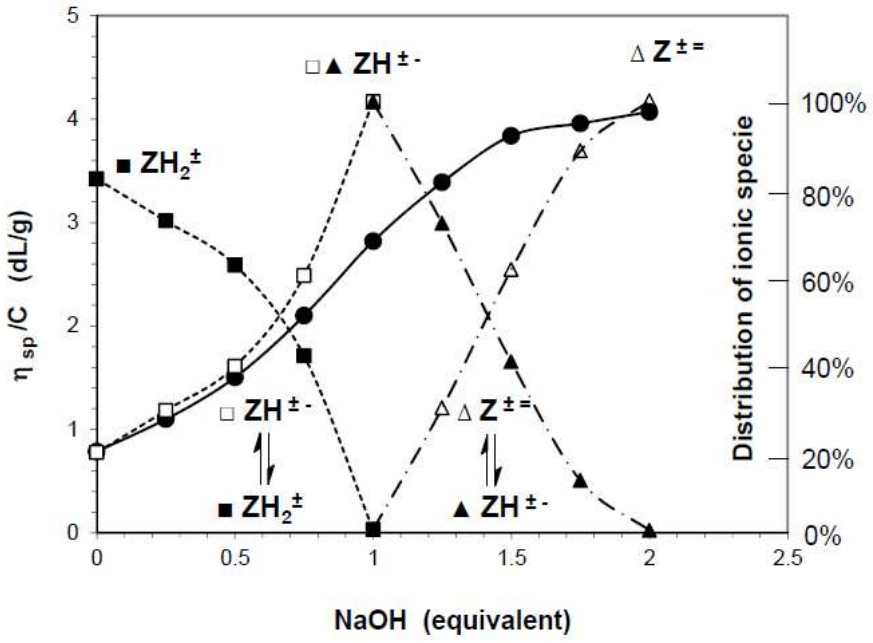

Figure 5.8 Reduced viscosity (η_{sp}/C) at 30°C of a 0.0247 M (i.e. 1 g/dL) solution of polymer PZA **6** in 0.1 N NaCl (•) versus equivalent of added NaOH at 23°C. Distribution curves (dashed lines) of the various ionized species calculated using eq 2 and pH of the solutions in 0.1 N NaCl at 23°C.

5.3.6 Effectiveness of PZA 6 as an antiscalant

Operation of desalination plants is often plagued by precipitation (scale formation) of $CaCO_3$, $CaSO_4$, $Mg(OH)_2$, etc. Inhibition of growth rate of crystal formation by commonly used anionic antiscalants[136,137] is attributed to their ability to sequestrate polyvalent cations and alter the crystal morphology at the time of nucleation.[131,135] Antiscalant behavior of a supersaturated solution of $CaSO_4$ was investigated using conductivity measurements in the absence and presence of in the presence of 20 ppm of PZA **6**. The results are shown in Figure 5.9; a drop in conductivity is indicative of

precipitation of $CaSO_4$. At the time of 0, 500 and 800 min, while the blank solution registered the conductance of 19.97, 16.71 and 16.48 mS/cm, respectively, the corresponding values in the presence of the antiscalant were found to be 19.97, 19.90 and 19.48 mS/cm.

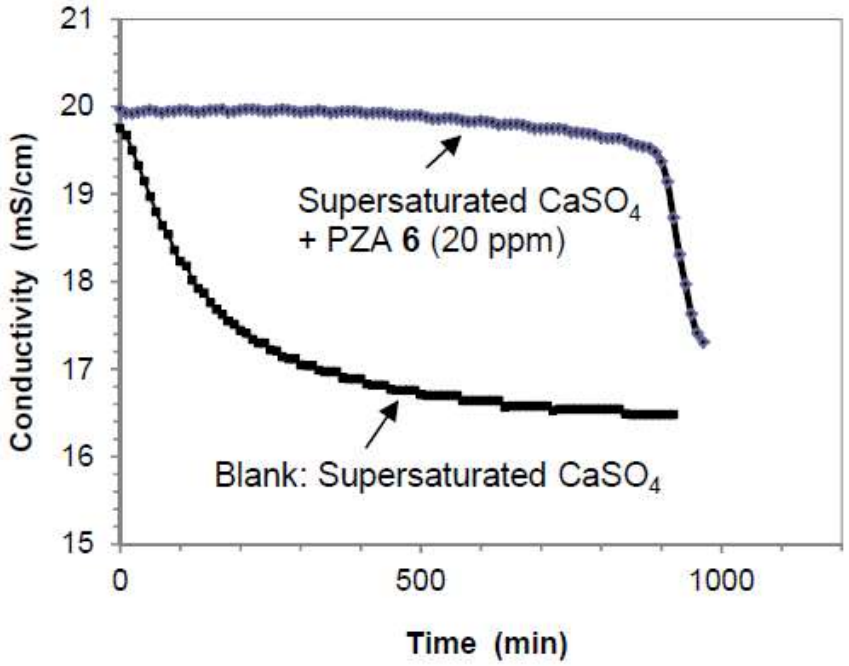

Figure 5.9 Precipitation behavior of a supersaturated solution of $CaSO_4$ in the presence (20 ppm) and absence of PZA **6** at 40°C.

It is assumed that the conductance is proportional to the concentration of the ions. Note that precipitation started immediately in the absence of Figure 5.9 (a): Blank). To our satisfaction, there was no considerable change in conductivity for about 500 min, registering a 98 % scale inhibition as calculated using eq 5:

$$\%\ Scale\ Inhibition = \frac{[Ca^{2+}]_{inhibited(t)} - [Ca^{2+}]_{blank(t)}}{[Ca^{2+}]_{inhibited(t_0)} - [Ca^{2+}]_{blank(t)}} \times 100$$

where $[Ca^{2+}]_{inhibited(t_0)}$ is the initial concentration at time zero, $[Ca^{2+}]_{inhibited\ (t)}$ and $[Ca^{2+}]_{blank\ (t)}$ are the concentration in the inhibited and blank solutions at time t. At the time of 800 min, the scale inhibition was calculated to be 86 %. Usually, a residence time of ≈ 30 min for the brine in osmosis chamber is required. It is worth mentioning that neither monomers **4** and **9** nor polymer **5** gave any effective inhibition; screening experiments based on visual inspection revealed that under the same conditions the system becomes cloudy within 1 h.

5.3.7 Comparative properties of monomer (± =) 11, homo- (± =) 12 and cyclopolymer (± =) 8

Some properties of monomer **11**, homopolymer **12** and copolymer **8** are given in Table 5.4 for the sake of comparison. Copolymer **8** has much higher intrinsic viscosity and molar mass as compared to homopolymer **12**. Both the polymers have similar values for the basicity constants (log *K*) and polyelectrolyte index (*n*). One notable exception is the antiscalant behavior of the polymers; the homopolymer with low molar mass performed better than the copolymer having much higher molar mass.

5.4 CONCLUSIONS

The PZ **5** represents the first example of a poy(zwitterions **4**-*alt*-SO_2) (*via* Butler's cyclopolymerization protocol) containing phosphonate and sulfonate groups in the same repeating unit. The pH-responsive (±) PZA **6** derived from (±) PZ **5** was used to investigate pH-dependent solution properties that involved its conversion to (± -) **7** and (±

=) **8** all having identical degree of polymerization. The apparent basicity constants of the $–PO_3^{2-}$ and $–PO_3H^-$ group in (± -) **7** and (± =) **8** have been determined. PZA **6** at a concentration of 20 ppm was found to be an effective antiscalant in the inhibition of the formation of calcium sulfate scale.

CHAPTER 6

Bis[3-(diethoxyphosphoryl)propyl]diallylammonium Chloride: Synthesis and Use of its Cyclopolymer as an Antiscalant

Taken from Shaikh A. Ali, Shamsuddeen A. Haladu and Hasan A. Al-Muallem, Bis[3-(diethoxyphosphoryl)propyl]diallylammonium Chloride: Synthesis and Use of its Cyclopolymer as an Antiscalant, *Journal of Applied Polymer Science, 2014*

Abstract

A new symmetrically substituted cationic monomer bis[3-(diethoxyphosphoryl)propyl]diallylammonium chloride has been synthesized and cyclopolymerized to give the corresponding cationic polyelectrolyte (CPE) (+) bearing two identical (diethoxyphosphoryl)propyl penedents on the pyrrolidinium repeating units. The hydrolysis of the phosphonate ester in (CPE) (+) gave a pH-responsive cationic polyacid (CPA) (+) bearing the motifs of a tetrabasic acid. The (CPA) (+) under pH-induced transformation was converted into a water-insoluble polyzwitterion acid **(±)** (PZA) or water-soluble polyzwitterion/anion **(± −)** (PZAN) or polyzwitterion/dianion **(± =)** (PZDAN) or polyzwitterion/trianion **(± ≡)** (PZTAN), all having identical degree of polymerization. The interesting solubility and viscosity behaviors of the polymers have been investigated in some detail. The apparent protonation constants of the anioinic centers in **(± ≡)** (PZTAN) and its corresponding monomer **(± ≡)** (ZTAN) have been determined. Evaluation of antiscaling properties of the PZA using supersaturated solutions of $CaSO_4$ revealed ≈100% scale inhibition efficiency at a meager concentration

of 10 ppm for a duration over 71 h at 40ºC. The PZA has the potential to be used effectively as an antiscalant in reverse osmosis plant.

6.1 Introduction

Butler's cyclopolymerization protocol[5-8] using pH-responsive diallylamine salts bearing aminoalkylphosphonate motifs has been utilized in the synthesis of linear[34,67,130] cyclopolymers as well as cross-linked resins.[143] Aminophosphonic acids are structural analogues of amino acids, and as such are suitable for various biological applications.[144] Phosphonates have found application in chelating divalent cations such as $Ca^{2+}$and Ba^{2+} ions in detergents and inhibiting the deposition of scale.[145,146] Polymers having phosphonate functionality have been explored for proton conducting membranes.[147] Some phosphonates are used as medicines: Antiretroviral drug Tenofovir is used in the treatment of viral diseases such as HIV and hepatitis B.[148] Phosphonates are utilized as adhesion promoters to dental tissue[149,150] and bone.[151-153] Two recent reports describe the polymerizations of phosphonated-bis(methacrylamide)s for dental applications[154,155] While some linear polyaminophosphonates, prepared by Butler's cyclopolymerization technique,[5-8] have been used as antiscalants[138,156] and as polymer components in the construction of aqueous two-phase systems,[157] the aminophosphonate resins are found to be very effective in the removal of toxic metal ions.[8,143,158-160]

pH-Responsive bisphosphonates $R^1R^2C(PO_3H)_2$, analogues of pyrophosphates $O(PO_3H)_2$, have also significant industrial importance: They are used as corrosion inhibitors[161] in concrete, complexing agents in oil industries,[162] and inhibitors of boneresorption[163] in bone-related diseases. To date, only a single report describes the

cylopolymerization of a diallyl amine salt [$(CH_2=CH\text{-}CH_2)_2NH^+CH(PO_3H)(PO_3^-)$] bearing bisphosphonate functionality having both the phosphorous attached to the same carbon.[34] To our knowledge, cyclopolymerization of a symmetric bisphosphonate diallyl quaternary ammonium salt (like **4**, Scheme 6.1) having phosphorous atoms attached to two different carbons is yet to be reported.

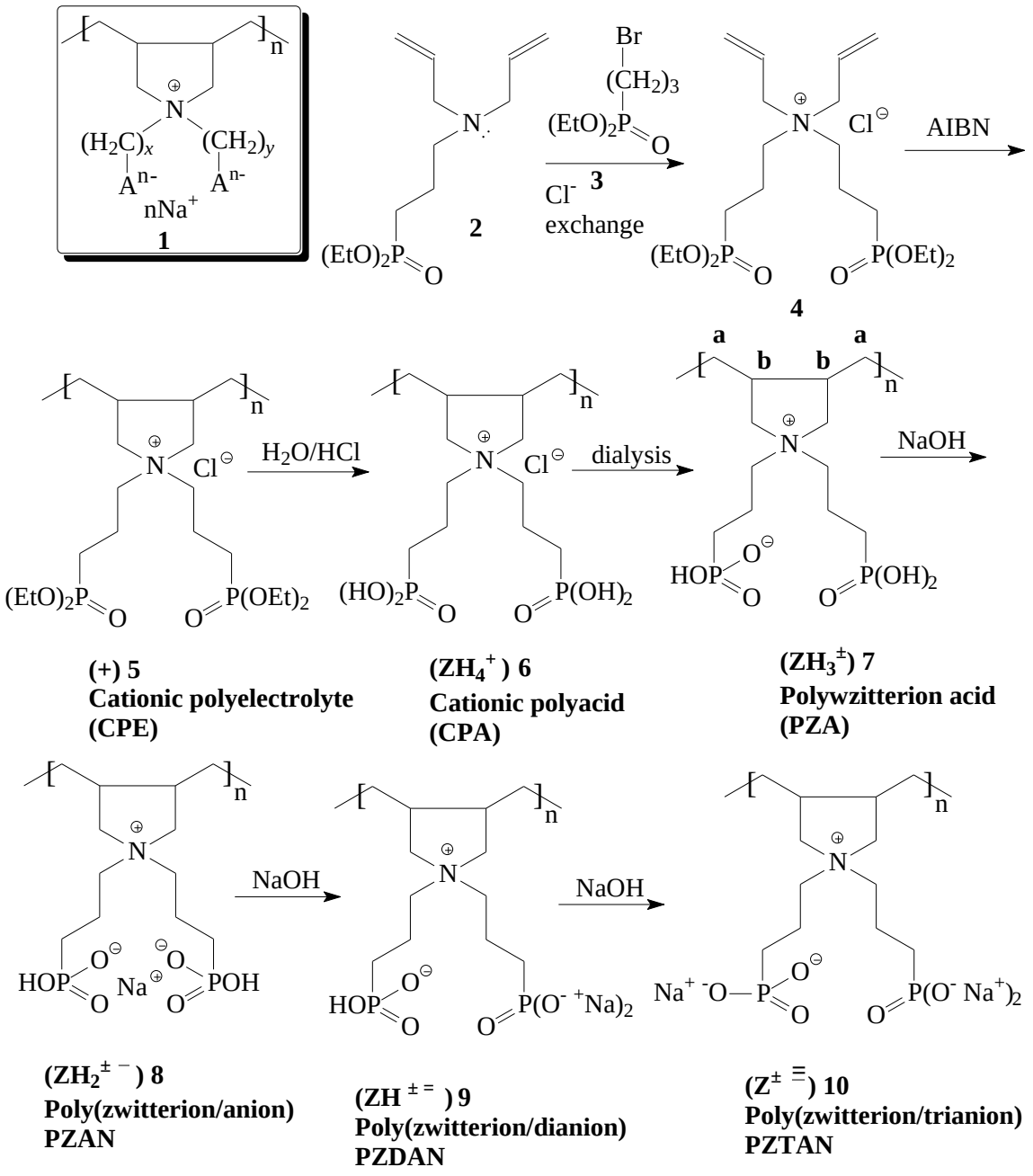

Scheme 6.1 Cyclopolymerization of diallylbisphosphonate monomer.

Keeping in view the importance of the phosphonates and in our continuing studies of aminophosphonate polymers, herein we report the synthesis and cyclopolymerization of new bisphosphonate monomer **4** bearing bis-3-phosphorylpropyl substituents (Scheme

6.1). Ester hydrolysis of cyclopolymer cationic polyelectrolyte (CPE) **5** to pH-responsive **6** would give us the opportunity to examine its solution properties, determine acid dissociation constants and test its efficiency as an antiscalant to inhibit $CaSO_4$ scale formation in desalination plants. The cyclopolymer having bis-phosphonate motifs with multiple adsorption sites is expected to sequester Ca^{2+} ions effectively to inhibit scale formation.

6.2 EXPERIMENTAL

6.2.1 Physical Methods

A Perkin Elmer Elemental Analyzer Series II Model 2400 and a Perkin Elmer 16F PC FTIR spectrometer were used to carry out Elemental analyses and record IR spectra, respectively. The ^{13}C, ^{1}H and ^{31}P NMR spectra have been measured in D_2O (using HOD signal at δ 4.65 and dioxane ^{13}C peak at δ 67.4 as internal standards) on a JEOL LA 500 MHz spectrometer. ^{31}P was referenced with 85% H_3PO_4 in DMSO. Viscosity measurements have been made by Ubbelohde viscometer using CO_2-free water under N_2. A Sartorius pH Meter PB 11 was used to measure pH of the solutions. Conductivity measurements were recorded by a Conductivity meter (Thermo Scientific Model: ORION STAR A212). Molecular weights were determined by the GPC measurement performed on an Agilent 1200 series apparatus having a RI detector and PL aquagel-OH MIXED column using polyethylene oxide/glycol as a standard and water as eluent at a flow rate of 1.0 mL/ min at 25 ^{o}C.

6.2.2 Materials

Ammonium persulfate (APS) and tertiary butylhydroperoxide (TBHP) (70 w/w % in water) from Fluka AG (Buchs, Switzerland) were used as received. A Spectra/Por membrane with a molecular weight cut off (MWCO) value of 6000-8000 (Spectrum Laboratories, Inc) was purchased for dialysis. Tertiary amine **2** was prepared by reacting diallylamine and 1-bromo-3-(diethylphosphonato)propane (**3**).[67]

6.2.3 *N*-Allyl-*N*,*N*-bis[3-(diethoxyphosphoryl)propyl]prop-2-en-1-aminium Chloride (4)

A mixture of **2** (20.2 g, 73.4 mmol) and **3** (31.0 g, 119.7 mmol), K_2CO_3 (10.57 g, 76.6 mmol) in acetonitrile (120 mL) was stirred under N_2 at an oil-bath temperature of 95°C for 96 h. After concentration, the residual liquid was taken up in water (40 mL) and washed with ether (3×50 mL). After saturating the aqueous layer with NaCl and adding concentrated HCl (15 mL), the mixture was stirred for 10 min. The aqueous layer was extracted with $CHCl_3$ (3×50 mL). After removal of $CHCl_3$, the residual liquid in saturated NaCl solution (30 mL) was stirred for 30 min. The aqueous layer was then washed with a 2:1 ether/CH_2Cl_2 mixture (3×50 mL) and finally, extracted with CH_2Cl_2 (3×100 mL). The CH_2Cl_2-extract was dried (Na_2SO_4) and concentrated to obtain **4** as a pale yellow liquid 25.4 g, 71%). (Found: C, 48.6; H, 8.8; N, 2.7%. $C_{20}H_{42}ClNO_6P_2$ requires C, 49.03; H, 8.64; N, 2.86%); ν_{max} (KBr): 3422, 3081, 2984, 2909, 1644, 1471, 1444, 1242, 1163, 1026, 964, 875, 792, 752 and 661 cm^{-1}; δ_H (D_2O) 1.21 (12 H, t, J = 7 Hz), 1.80-2.00 (8H, m), 3.20 (4H, m), 3.83 (4H, d, J = 7.0 Hz), 4.03 (8H, m), 5.61 (4H, m), 5.88 (2H, m), (HOD: 4.65); δ_C (D_2O) 15.52 (s, $PCH_2\underline{C}H_2$), 16.10 (d, 2C, <u>Me</u>, ^3J (PC) 6.2 Hz), 21.10 (d, $P\underline{C}H_2$, ^1J (PC) 142 Hz), 57.92 (d, PCH2CH2$\underline{C}H_2$, ^3J (PC) 16.5 Hz), 61.44 (2C, =CH-

$\underline{C}H_2$, s), 63.99 (d, 2C, $O\underline{C}H_2CH_3$, ^2J (PC) 6.2 Hz), 124.10 (2C, s, $CH_2{=}\underline{C}H$), 129.42 (2C, s, $\underline{C}H_2{=}CH$) (dioxane: 67.40 ppm); δ_P (202 MHz, D_2O): 30.94 (s). The ^1H and ^{13}C NMR spectra are shown in Figures 6.1 and 6.2, respectively. ^{13}C DEPT 135 analysis supported the spectral assignments.

6.2.4 Acid Hydrolysis of 4 to Cationic Acid (CA) 11

A mixture of **4** (15 g, 30.6 mmol), water (25 mL) and concentrated HCl (22 mL) was heated in a flask under N_2 at 95 ^oC for 48 h. The residual liquid after removal of the solvent was dissolved in methanol and poured into acetone to give **11** as a thick liquid (11.0 g, 95%) which crystallized in a freezer as a hygroscopic white solid. Mp. 75-80°C (methanol/acetone); (Found: C, 37.8; H, 7.2; N, 3.6%. $C_{12}H_{26}ClNO_6P_2$ requires C, 38.16; H, 6.94; N, 3.71%); ν_{max} (neat) 3500-2500 (very broad), 2959, 1702, 1642, 1475, 1418, 1368, 1230, 1169, 995, 874, and 714 cm^{-1}. δ_H (D_2O) 1.51 (4H, dt, J = 18.3 and 7.4 Hz), 1.75 (4H, m), 3.04 (4H, m), 3.64 (4H, d, J = 7.3 Hz), 5.42 (4H, m), 5.72 (2H, m), (HOD: 4.65); δ_C (D_2O) 15.87 (2C, s, $PCH_2\underline{C}H_2$), 23.32 2C, (d, $P\underline{C}H_2$, ^1J (PC) 140 Hz), 58.28 (2C, d, $PCH_2CH_2\underline{C}H_2$, ^3J (PC) 18.6 Hz), 61.37 (2C, =CH-$\underline{C}H_2$, s), 124.10 (2C, s, $CH_2{=}\underline{C}H$), 129.20 (2C, s, $\underline{C}H_2{=}CH$) (dioxane: 67.40 ppm); δ_P (202 MHz, D_2O): 26.00 (m). The DEPT 135 NMR analysis supported the ^{13}C spectral assignments.

6.2.5 Procedure for the Cyclopolymerization of 4 or 11

A solution of monomer **4** (7.35 g, 15 mmol, entry 5, Table 6.1), water (3.15 g) and initiator APS (200 mg) in a 25-mL closed vessel under N_2 was stirred at 90°C for 4 h. The reaction mixture after dialysis against deionized water for 24 h was freeze-dried to obtain CPE **5** as a light brown hygroscopic polymer. The thermal decomposition: the color changed to dark brown and black at respective temperatures of 260^{o}C at 320^{o}C. (Found:

C, 48.7; H, 8.8; N, 2.8%. $C_{20}H_{42}ClNO_6P_2$ requires C, 49.03; H, 8.64; N, 2.86%); $\nu_{max.}$(KBr) 3420 (br), 2984, 2933, 2905, 1650, 1460, 1394, 1369, 1221, 1160, 1123, 1050, 1017, 968, 786, 698, 620 and 544 cm^{-1}. δ_P (202 MHz, D_2O): 32.89 (4%), 30.96 (72%), and 22.96 (24%). ^1H NMR and ^{13}C NMR spectra are shown in respective Figure 6.1 and 6.2. Cyclopolymerization of **11** (entry 6, Table 6.1) followed by dialysis afforded PZA **7**.

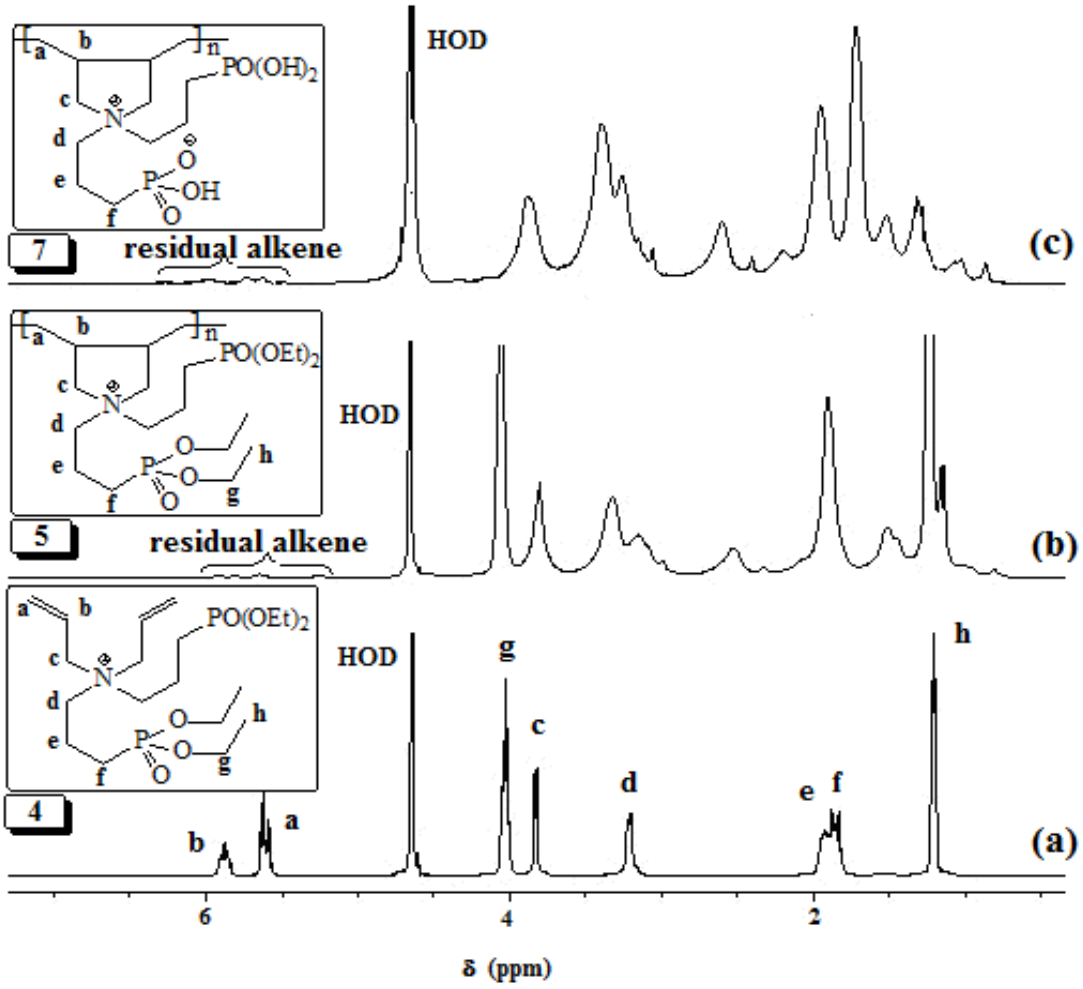

Figure 6.1 ^1H NMR spectrum of (**a**) **4**, (**b**) **5**, and (**c**) **7** (+NaCl) in D_2O.

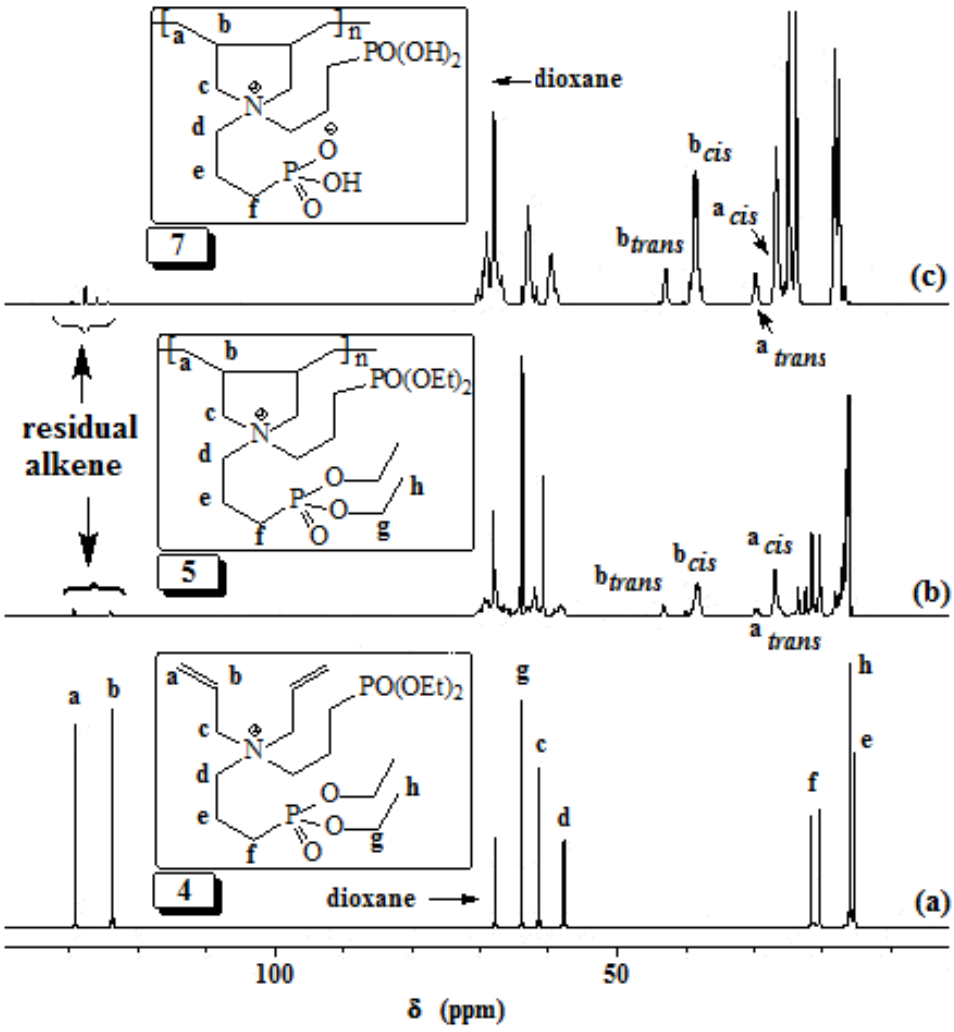

Figure 6.2 ^{13}C NMR spectrum of (**a**) **4**, (**b**) **5**, and (**c**) **7** (+NaCl) in D_2O.

Table 6.1 Cyclopolymerization[a] of Monomers **4** and **11**.

Entry No.	Monomer (mmol)	Water (% w/w)	Initiator[a] (mg)	Temp (°C)	Time (h)	Yield (%) NMR	Yield (%) isolated	$[\eta]^b$ (dL g^{-1})
1	**4** (7.5)	30	APS (100)	90	48	65	37	0.0545
2	**4** (7.5)	30	APS (140)	90	4	70	51	0.0475
3	**4** (7.5)	25	APS (380)	95	3	72	45	0.0417
4	**4** (7.5)	20	TBHP (200)	105	48	75	44	0.0496
5	**4** (15)	30	APS (200)	90	4	76	63	0.0484
6	**11** (7.5)	30	APS (300)	95	5	77	61	0.0632

[a]Polymerization reactions were carried out in aqueous solution of monomer **4** or **11** in the presence of ammonium persulfate (APS) or tertbutylhydroperoxide (TBHP) at specified temperatures to give respective polymers of **5** and **7**, [b]Viscosity of 1-0.25 % solution of **5** in 0.1 M NaCl and **7** in 1.0 M NaCl at 30.0 ± 0.1°C was measured with Ubbelohde Viscometer (K=0.005718).

6.2.6 Acid Hydrolysis of CPE 5 to Poly(zwitterion acid) (PZA) 7

A solution of CPE **5** (3.5 g, 7.14 mmol) (from entry 5, Table 6.1) in water (20 mL) and concentrated HCl (25 mL) was heated at 95°C for 24 h. The homogeneous mixture was dialyzed against deionized water for 24 h. During dialysis, the polymer started to precipitate out as an oily material within 1 h. The resulting mixture was freeze-dried to obtain PZA **7** as a white solid (2.3 g, 94%). The thermal decomposition: the color changed to brown and black at respective temperatures of 260 °C and 310-320 °C. (Found: C, 41.9; H, 7.5; N, 3.9%. $C_{12}H_{25}NO_6P_2$ requires C, 42.23; H, 7.38; N, 4.10%); ν_{max} (KBr) 3425 (br), 2952, 1651, 1463, 1416, 1234, 1146, 1058, 936, 756,710 and 531

cm^{-1}. δ_P (202 MHz, D_2O): 23.78. ^1H NMR and ^{13}C NMR spectra are shown in Figure 6.1 and 6.2, respectively.

6.2.7 Solubility Measurements

After stirring a mixture of CPE **5** or PZA **7** (2 w/w %) in a solvent at 70°C (1 h), the solubility behavior was checked at 23°C. The results are given in Table 6.2. To a stirred mixture of PZA **7** (10 mg, 1 wt%) in deionized water (1 mL) was added NaCl in portions until it became soluble in the presence of 0.71 M NaCl.

Table 6.2 Solubility[a,b] of CPE (+) **5** and PZA (±) **7**

Solvent	ε	**5**	**7**
Formamide	111	+	±
Water	78.4	+	−
Formic acid	58.5	+	+
DMSO	47.0	+	−
Ethylene glycol	37.3	+	−
DMF	37.0	+	−
Methanol	32.3	+	−
Triethylene glycol	23.7	+	−
Acetic acid	6.15	+	−

[a] 2% (w/w) of polymer-water mixture (solution) was made after heating the mixture at 70 °C for 1 h and then cooling to 23°C, [b] '+' indicates soluble, '−' indicates insoluble, and '±' indicates partially soluble.

6.2.8 Potentiometric Titrations

Procedure for the determination of the protonation constants by potentiometric titrations under N_2 in CO_2-free water is described elsewhere.[67,80] A certain mmol of PZA **7** ($ZH_3^{\pm}$) or **11** (ZH_4^{+}) in 0.0175 M NaCl (200 mL) was used in each trial (Tables 6.3 and Table 6.4). The water-insoluble zwitterionic polymer **7** (≈100 mg) was dissolved in 1 M NaCl (3.5 mL), diluted to 200 mL to make the solution in 0.0175 M NaCl. The log K_1, log K_2 and log K_3 of the respective protonation of $^{2-}O_3P-X^{+}-PO_3^{2-}$ [in **10**], $^{2-}O_3P-X^{+}-PO_3H^{-}$ [in **9**] and $^{-}HO_3P-X^{+}-PO_3H^{-}$ [in **8]** were calculated at each pH value by the Henderson-Hasselbalch eq 2 (Scheme 6.2). The degree of protonation (α) of **10**, **9** and **8** is the ratio $[ZH^{\pm\,=}]_{eq}/[Z]_o$, $[ZH_2^{\pm\,-}]_{eq}/[Z]_o$ and $[ZH_3^{\pm}]_{eq}/[Z]_o$, respectively, where $[ZH^{\pm\,=}]_{eq}$, $[ZH_2^{\pm\,-}]_{eq}$ and $[ZH_3^{\pm}]_{eq}$ represent the respective equilibrium concentrations of the first (**9**), second (**8**) and third protonated species (**7**), and $[Z]_o$ describes the initial concentration of repeating units.

For the determination of the third step [**8** ($ZH_2^{\pm\,-}$) + H^{+} ⇋ **7** ($ZH_3^{\pm}$)] protonation constant (log K_3) using the titration of PZA **7** [$ZH_3^{\pm}$] with NaOH, $[Z]_o$ and $[ZH_3^{\pm}]_{eq}$ are related by $[ZH_3^{\pm}]_{eq} = [Z]_o - C_{OH^-} - [H^{+}] + [OH^{-}]$, where C_{OH^-} represents the added NaOH concentration. The equilibrium $[H^{+}]$ and $[OH^{-}]$ values were calculated from the pH value.[80, 133] Continuing the titration, the second step [**9** ($ZH^{\pm\,=}$) + H^{+} ⇋ **8** ($ZH_2^{\pm\,-}$)] protonation constant (log K_2) was determined using volume of the titrant after deducting the equivalent volume from the total volume. Finally, the titration is ended by determination of the first step [**10** ($Z^{\pm\,\equiv}$) + H^{+} ⇋ **9** ($ZH^{\pm\,=}$)] protonation constant (log K_1) using volume of the titrant after deducting the two-equivalent volume from the total volume. The fourth step [**7** ($ZH_3^{\pm}$ + H^{+} ⇋ **6** (ZH_4^{+})] protonation constant (log K_4) using

the titration of PZA **7** [$ZH_3^{\pm}$] with HCl was not carried out since PZA **7** [$ZH_3^{\pm}$] is simultaneously involved in two equilibria: [**8** ($ZH_2^{\pm -}$) + $H^+ \leftrightharpoons$ **7** ($ZH_3^{\pm}$)] for log K_3 and [**7** ($ZH_3^{\pm}$) + $H^+ \leftrightharpoons$ **6** (ZH_4^+)] for log K_4. Simultaneous protonation and deprotonation of PZA **7** owing to the proximity of the log K_3 and log K_4 values made it difficult to determine the later.

For the monomeric unit, log K_4 for the fourth step protonation [**12** ($ZH_3^{\pm}$) + $H^+ \leftrightharpoons$ **11** (ZH_4^+)] was determined in a small window of α using $2[Z]_o$ instead of $[Z]_o$ as the initial concentration of the monomer since both the PO_3H_2 in **11** ($H_2O_3P{-}X^+{-}PO_3H_2$) Cl^- are involved in deprotonation to an extent to make the initial combined H^+ concentration higher than that of $[Z]_o$. Log K_3 for the monomer could not be determined.

Table 6.3 Experimental Details for the Determination of Basicity Constants Using Polymer PZA **7** ($ZH_3^{\pm}$) in 0.0175 M NaCl at 23°C

run	$ZH_3^{\pm}$ (mmol)	C_T [a] (mol dm^{-3})	α–range	pH–range	Points[b]	Log K_1^{o} [c]	n_1 [c]	R^2, [d]
Polymer 7								
1	0.2959 (**7:** $ZH_3^{\pm}$)	–0.09690	0.88–0.34	9.15–11.25	16	10.78	1.88	0.9981
2	0.2652 ($ZH_3^{\pm}$)	–0.09690	0.84–0.39	9.36–11.12	18	10.69	1.90	0.9946
3	0.2324 ($ZH_3^{\pm}$)	–0.09690	0.79–0.39	9.66–11.14	18	10.75	1.98	0.9963
Average						10.74 (5)	1.92 (5)	
Log K_1 [e] = 10.74 + 0.92 log [(1-α)/α] For the reaction: $Z^{\pm\equiv} + H^+ \overset{K_1}{\rightleftharpoons} ZH^{\pm=}$								
Polymer 7								
1	0.2959 (**7:** $ZH_3^{\pm}$)	–0.09690	0.87–0.20	7.38-8.64	12	8.10	0.91	0.9975
2	0.2652 ($ZH_3^{\pm}$)	–0.09690	0.92-0.14	7.30-8.78	15	8.14	0.85	0.9941
3	0.2324 ($ZH_3^{\pm}$)	–0.09690	0.92-0.19	7.31-8.67	13	8.11	0.87	0.9877
Average						8.12 (2)	0.88 (3)	
Log K_2 [e] = 8.12 - 0.12 log [(1-α)/α] For the reaction: $ZH^{\pm=} + H^+ \overset{K_2}{\rightleftharpoons} ZH_2^{\pm-}$								
Polymer **7**								
1	0.2959 (**7:** $ZH_3^{\pm}$)	–0.09690	0.58–0.31	3.21–4.65	17	3.56	3.06	0.9914
2	0.2652 ($ZH_3^{\pm}$)	–0.09690	0.56–0.32	3.23–4.55	16	3.51	3.07	0.9959
3	0.2324 ($ZH_3^{\pm}$)	–0.09690	0.55–0.31	3.28–4.55	14	3.45	3.05	0.9924
Average						3.51 (6)	3.06 (1)	
Log K_3 [e] = 3.51 + 2.06 log [(1-α)/α] For the reaction: $ZH_2^{\pm-} + H^+ \overset{K_3}{\rightleftharpoons} ZH_3^{\pm}$								

[a] Titrant concentration (negative values indicate titrations with NaOH), [b] Number of data points from titration curve, [c] Values in the parentheses are standard deviations in the last digit, [d] R = Correlation coefficient. [e] $\log K_i = \log K_i^{o} + (n_i - 1) \log [(1 - \alpha)/\alpha]$.

Table 6.4 Experimental Details for the for the Determination of Basicity Constants Using Monomer ZDA (ZH_4^+) **11** in 0.0175 M NaCl at 23 °C

run	ZH_4^+ (mmol)	C_T [a] (mol dm^{-3})	α–range	pH–range	Points[b]	Log K_1^{o} [c]	n_1 [c]	R^2, [d]
Monomer 11								
1	0.2912 (**6:** ZH_4^+)	–0.09690	0.91-0.17	8.70-10.65	18	9.84	1.07	0.9937
2	0.2507 (ZH_4^+)	–0.09690	0.84-0.12	9.00-10.6	16	9.76	1.04	0.9903
3	0.2102 (ZH_4^+)	–0.09690	0.90-0.17	8.85-10.5	14	9.80	1.05	0.9956
Average						9.80 (4)	1.05 (2)	
Log K_1 [e] = 9.78			For the reaction: $Z^{\pm\equiv} + H^+ \overset{K_1}{\rightleftharpoons} ZH^{\pm=}$					
Monomer 11								
1	0.2912 (**11:** ZH_4^+)	–0.09690	0.84-0.16	6.75-8.30	17	7.48	1.03	0.9935
3	0.2507 (ZH_4^+)	–0.09690	0.91-0.14	6.50-8.20	16	7.42	0.97	0.9934
2	0.2102 (ZH_4^+)	–0.09690	0.93-0.23	6.40-7.95	14	7.41	0.94	0.9960
Average						7.44 (4)	0.98 (5)	
Log K_2 [e] = 7.43			For the reaction: $ZH^{\pm=} + H^+ \overset{K_2}{\rightleftharpoons} ZH_2^{\pm-}$					
Monomer 11								
1	0.2912 (**11:** ZH_4^+)	–0.09690	0.31-0.21	2.70-2.93	14	2.38	0.95	0.9917
2	0.2507 (ZH_4^+)	–0.09690	0.27-0.19	2.74-2.94	10	2.34	0.96	0.9941
3	0.2102 (ZH_4^+)	–0.09690	0.25-0.16	2.80-3.04	8	2.27	1.06	0.9795
Average						2.33 (6)	0.99 (6)	
Log K_4 [e] = 2.30			For the reaction: $ZH_3^{\pm} + H^+ \overset{K_4}{\rightleftharpoons} ZH_4^+$					

[a]Titrant concentration (negative values indicate titrations with NaOH), [b]Number of data points from titration curve, [c]Values in the parentheses are standard deviations in the last digit, [d]R = Correlation coefficient. [e]log K_1 = log K_i^{o}.

6.2.9 Evaluation of Antiscalant Behavior

Antiscalant behavior of PZA **7** and a commercial antiscalant (PERMATREAT® PC-191 Nalco Company, Illinois, USA) used in our University desalination plant were evaluated in supersaturated $CaSO_4$ solution containing 2,600 and 6,300 ppm of Ca^{2+} (from $CaCl_2$) and SO_4^{2-} (from Na_2SO_4), respectively. This is 3 times the concentration in 1 CB (one concentrated brine) of reject brine procured from a reverse osmosis plant.[133] A

preheated (40 ºC) solution of sodium sulfate (6 CB, 60 mL) was added quickly to a solution of calcium chloride (6 CB, 60 mL) containing PZA **7** (20 ppm) at 40ºC ± 1ºC stirred at 300 rpm using a magnetic stir-bar. Conductivity measurements of the resultant solution containing 10 ppm of PZA **7** were made at an initial interval of every 10 min. A drop in conductivity indicated the precipitation of $CaSO_4$. Any turbidity from precipitation was inspected visually.

6.3 Results and Discussion

Synthesis and Characterization of the Ionic Polymers

The substitution reaction between tertiary amine **2** and bromide **3** gave the salt $R^1{}_2R^2{}_2N^+Br^-$ (i.e. Br^- counterpart of salt **4**) which was treated with large excess of HCl and NaCl in aqueous solution (twice) to replace the Br^- with Cl^-. The exchange is necessary since the Br^- salts are known to give polymers in low yields owing to oxidation of Br^- to Br_2.[5] Cationic monomer **4** underwent cyclopolymerization to afford cationic polyelectrolyte (CPE) **5** in reasonable yields bearing in mind the difficulty in putting four rather bulky substituents on a five-membered ring (Scheme 6.1, Table 6.1). Note that the isolated yields are lower than the yields determined by the NMR analysis of the crude reaction mixture. A considerable portion of the polymer chains escapes the dialysis bag having a MWCO of 6000-8000. The involvement of the ethoxy groups in the chain transfer is one of the causes that lead to the lower yields and intrinsic viscosity [η] values (Table 6.1).[88] The average molar mass $\overline{M}_W$ and polydispersity index of the polymer sample from entry 5, Table 6.1 were determined to be 26,500 g mol^{-1} and 2.1, respectively.

The CPE (+) **5** was hydrolyzed in 6.7 M HCl to give water-soluble cationic polyacid (CPA) (+) **6**, which on extended dialysis gave water-insoluble PZA (±) **7**. Note that cationic acid monomer (+) **11**, obtained *via* hydrolysis of **4**, upon polymerization also afforded (±) PZA **7** (entry 6, Table 6.1, Scheme 6.2). Neutralization of **7** with 1 or 2 or 3 equivalents of NaOH is expected to generate polyzwitterion-monoanion (PZMAN) (± −) **8**, polyzwitterion-dianion (PZDAN) (± =) **9** and polyzwitterion-trianion (PZTAN) (± ≡) **10,** respectively. Likewise, neutralization of **11** would lead to zwitterion acid (±) **12**, zwitterion-anion (± −) **13**, zwitterion-dianion (± =) **14** and zwitterion-trianion (± ≡) **15**.

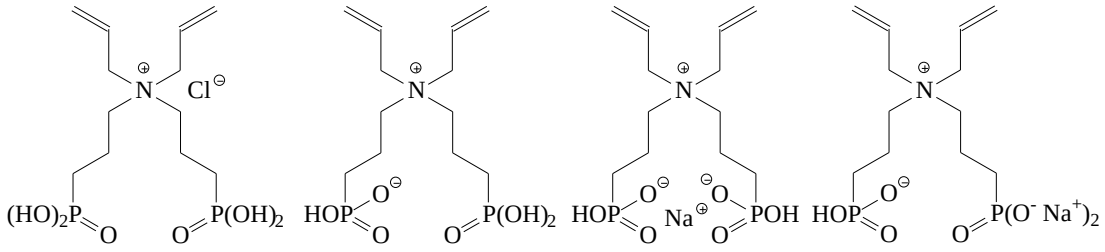

11 (ZH_4^+) **Cationic acid** | **12 ($ZH_3^{\pm}$)** **ZA** | **13 ($ZH_2^{\pm -}$)** **ZAN** | **14 ($ZH^{\pm =}$)** **ZDAN**

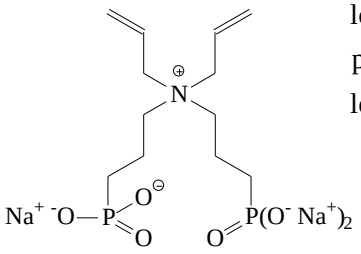

15 ($Z^{\pm =}$) **ZTAN**

$$\log K_i = \text{pH} - \log[(1-\alpha)/\alpha] \quad \text{Eq 1}$$

$$\text{pH} = \log K_i^{o} + n_i \log[(1-\alpha)/\alpha] \quad \text{Eq 2}$$

$$\log K_i = \log K_i^{o} + (n_i - 1)\log[(1-\alpha)/\alpha] \quad \text{Eq 3}$$

$Z^{\pm =} + H^+ \overset{K_1}{\rightleftharpoons} ZH^{\pm =}$

15 (or **10)** **14 (or 9)**

$ZH^{\pm =} + H^+ \overset{K_2}{\rightleftharpoons} ZH_2^{\pm -}$

14 (or **9)** **13 (**or **8)**

$ZH_2^{\pm -} + H^+ \overset{K_3}{\rightleftharpoons} ZH_3^{\pm}$

13 (or **8)** **12 (**or **7)**

$ZH_3^{\pm} + H^+ \overset{K_4}{\rightleftharpoons} ZH_4^+$

12 (or **7)** **11 (**or **6)**

Scheme 6.2 The monomer in different forms and protonation constants.

While CPE (+) **5** was soluble in all the tested solvents, PZA (±) **7** was partially soluble in formamide, and soluble in formic acid, but notably insoluble in water (Table 6.2). This is expected since (±) polyzwitterions are usually insoluble in salt-free water due to the strong electrostatic attractive interactions between the charges of opposite algebraic signs as well as intragroup, intra- and interchain associations promoted by dipolar interactions.[6] Water-insoluble PZA (±) **7** has been shown to be water-soluble in the presence of NaCl with a minimum critical salt concentration (CSC) of 0.71 M, which screens the zwitterionic charges thus permitting expansion of the polymer backbone and globule-to-coil transition.[18,19] However, upon addition of deionized water into the polymer solution in 0.71 M NaCl, it remained soluble below CSC as a result of its progressive dissociation to PZMAN (± −) **8** in which the anionic portion encourages the water-solubility. Solubility of PZA (±) **7** in formic acid could be attributed to its protonation to water-soluble CPA (+) **6**. This was supported by an observation during the dialysis: the polymer remained soluble in 6.7 M HCl owing to the presence of protonated form CPA (+) **6** while after 1 h of dialysis PZA (±) **7** started to precipitate as a result of the depletion of HCl (Scheme 6.1).

6.3.1 NMR Spectra

The ^{1}H and ^{13}C NMR spectra of **4**, **5** and **7** are displayed in Figures 6.1 and 6.2, respectively. The absence of the OCH_2CH_3 signals in the spectra of **7** indicates its removal by hydrolysis (Figures 6.1c and 6.2c). Polymer **5** or **7** even after extended dialysis contains ≈ 4% residual alkene presumably as a result of some chain propagation without cyclization.[6] The integration of the ^{13}C (Figures 6.2b and 6.2c) as well as ^{31}P peaks of CPE **5** (see experimental) revealed a 75/25 *cis-trans* ratio of the configurational

isomers of pyrrolidinium ring at $C_{b,b}$ which is similar to the earlier findings (Scheme 6.1).[67,130]

6.3.2 Viscosity Measurements

Eq. 4 was developed to give a mathematical expression to rationalize the solution behavior of symmetrically or asymmetrically charged ionic polymers.[20,92-94]

$$v^* = -\frac{\pi(fI_B)^2}{\kappa_S} + \frac{4\pi I_B \Delta f^2}{\kappa_S^2} \qquad (4)$$

where f is the total fraction of charged monomers, Δf is the charge imbalance, I_B is the Bjerrum length, and κ_S is the Debye-Huckel screening parameter, and v* is the excluded volume: a negative or a positive value of which indicates chain contraction or expansion, respectively. For symmetrically charged polymers i.e. polymers having equal number of charges of both algebraic signs, the second term in eq. 4 is eliminated by virtue of $\Delta f = 0$; hence a negative excluded volume (v*) indicates contraction to a collapsed coil. In the event of charge imbalance (i.e. $\Delta f \neq 0$), the second term in eq. 4, which describes the shielding of the Coulombic repulsive interactions, would play a role and in case of its domination over the first term may lead to the expansion of the polymer chain to a semicoil owing to a positive v* value.

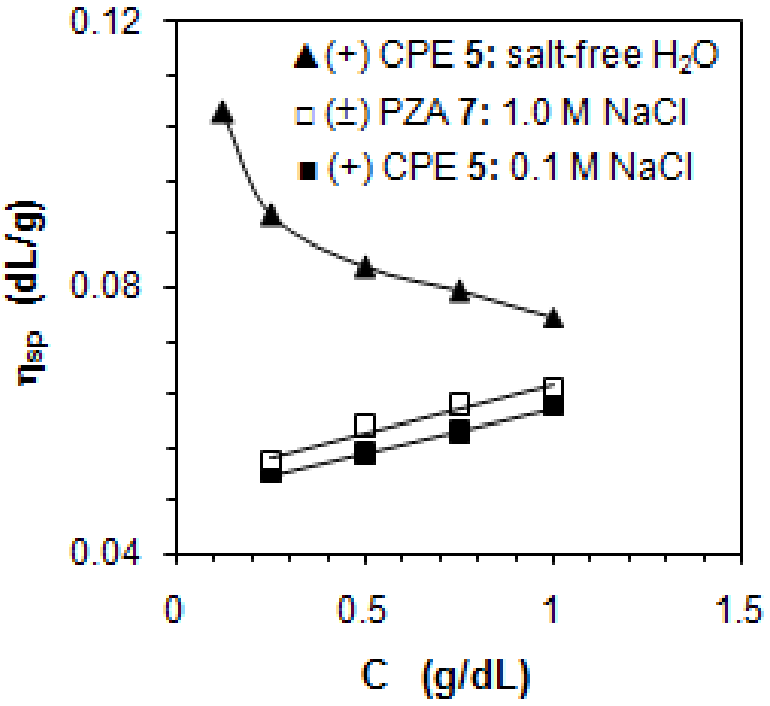

Figure 6.3 The viscosity behavior of (+) CPE **5** in ▲ salt-free water, □ (±) PZA**7** in 1 M NaCl.

Figure 6.3 shows the viscosity behavior of **5** and **7** in salt-free and salt-added water. The viscosity plot of CPE (+) **5** resembles that of a polyelectrolyte i.e. concave upwards in salt-free water and linear in 0.1 M NaCl. The viscosity plot of PZA (±) **7** in 1 M NaCl remains linear and it has higher viscosity values than the CPE (+) **5** in 0.1 M NaCl.

Figures 6.4 and 6.5 demonstrate the pH-responsiveness of the polymers **7-10**. The pHs are increased upon addition of NaOH as a result of the following transformations: (±) **7** $(PO_3H_2)(\ (PO_3H^{1-})\ \rightarrow$ (± −) **8** $(PO_3H^{1-})(\ (PO_3H^{1-})\ \rightarrow$ (± =) **9** $(PO_3H^{1-})(\ (PO_3^{2-}) \rightarrow$ (± ≡) **10** $(PO_3^{2-})(\ (PO_3^{2-})$. The pH of a ≈ 0.0015 M polymer solutions of **7, 8**, **9**, and **10** were found to be 3.21, 7.10, 9.04, and 10.88, respectively. With the successive increase in the

pH values, the increase in size, as demonstrated by the increased viscosities, is caused by the repulsion among the excess negative charges in the polymer chain (Figure 6.4). A meaningful comparison of the viscosity values is made since all the polymers are derived from the same polymer sample (entry 5, Table 6.1). Note that (±) **7** collapses into a water-insoluble polymer which is soluble only in the presence of added salt (NaCl) (*vide supra*).

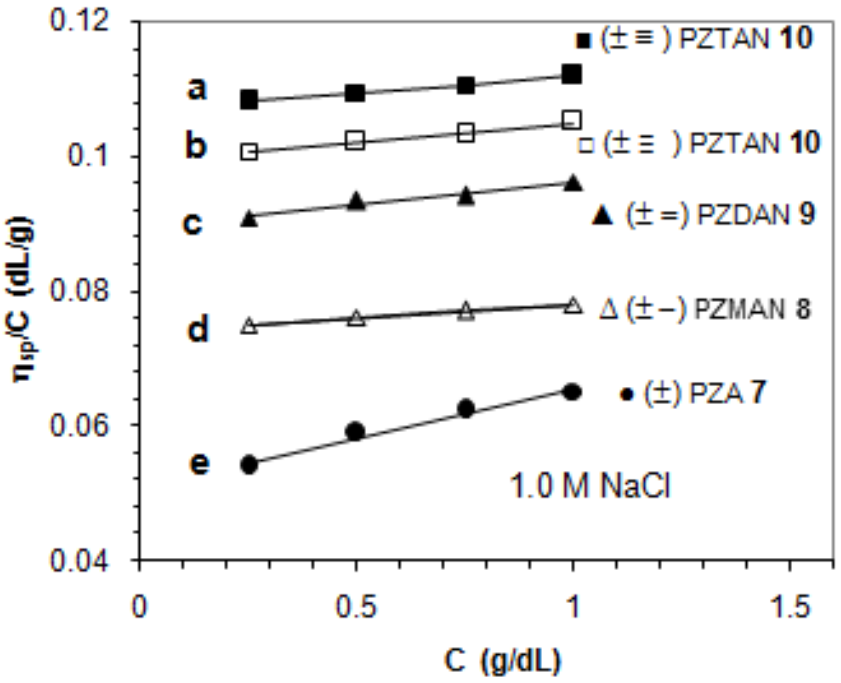

Figure 6.4 The viscosity behavior in 1 M NaCl of: (**a**) ■ (± ≡) PZTAN **10** (PZA **7** + 4 equivalents NaOH), (**b**) □ (± ≡) PZTAN **10** (PZA **7** + 3 equivalents NaOH), (**c**) ▲ (± =) PZDAN **9**, (**d**) Δ (± −) PZMAN **8** and (e) ● (±) PZA **7**, using an Ubbelohde Viscometer at 30°C. (All polymers are derived from entry 5, Table 6.1).

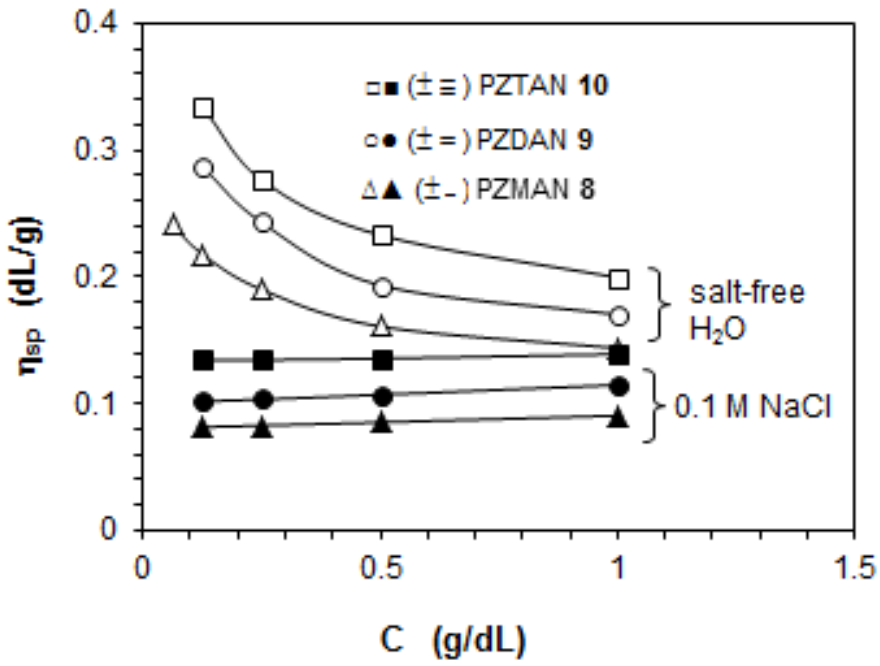

Figure 6.5 The viscosity behavior in salt-free water and 0.1 M NaCl of: □■ (± ≡) PZTAN **10**, ○● (± =) PZDAN **9**, and Δ▲ (± −) PZMAN **8** (**e**) ● (±) PZA**7**, using an Ubbelohde Viscometer at 30°C. (All polymers are derived from entry 5, Table 6.1).

The viscosity values increase in the order: (±) **7** < (± −) **8** < (± =) **9** < (± ≡) **10**. This is in line with the increase in charge imbalance in going from **7** to **10** which in turn makes v* progressively less negative (or more positive) owing to the contribution of the second term in eq. 4 resulting in the expansion of the polymer chains. The higher viscosity values for (± ≡) PZTAN **10** in the presence of 1 equivalent NaOH (Figure 6.4a) than in its absence (Figure 6.4b) can be rationalized in terms of the equilibrium: [**10** ($Z^{\pm\equiv}$) + H_2O ⇋ **9** ($ZH^{\pm\ =}$) + OH^-]; in the presence of OH^- the equilibrium is shifted towards left thereby increasing the proportion of (± ≡) **10**, overall charge imbalance, v* value, and viscosity.

For pure electroneutral zwitterions (±), the viscosity plots are known to be linear either in salt-free or salt-added solutions. Unlike (±) PZs, the viscosity plots of (± −) **8**, (± =) **9** and (± ≡) **10**, like cationic or anionic polyelectrolytes, remain concave upwards in salt-free water and linear in 0.1 M NaCl (Figure 6.5). The viscosity behaviors of these polymers are thus controlled by the anionic portions of the polymers; with the increase in the charge imbalance, the viscosity values increase in the order: **8** < **9** < **10**.

6.3.3 Basicity Constants

Eq 3 (Scheme 6.2) describes the apparent basicity constants of anionic centers where log K_i^o = pH at $\alpha = 0.5$ and $n_i = 1$ in the case of sharp basicity constants. The 'n_i' and log K_i^o as the respective slope and intercept were determined from the linear regression fit of pH *vs*. log $[(1-\alpha)/\alpha)]$. We were able to determine the basicity constants log K_1 (10.74), log K_2 (8.12) and log K_3 (3.51) for the respective protonation of $^{2-}O_3P-X^+-PO_3^{2-}$ in (± ≡) (**10**), $^{2-}O_3P-X^+-PO_3H^-$ in (± =) **9** and $^-HO_3P-X^+-PO_3H^-$ in (± −) **8** (Table 6.3). The log K_4 for the protonation of $H_2O_3P-X^+-PO_3H^-$ in (±) PZA **7** could not be determined owing to its proximity to the value of log K_3 (see experimental). Note that basicity constant log K of any base B is the pK_a of its conjugate acid BH^+.

The log K_1, log K_2 and log K_4 for the monomer (± ≡) **15** were determined to be 9.78, 7.43 and 2.30, respectively (Table 6.4). Log K_3 of the monomer cannot be determined for the reason given in the experimental. The polymer's basicity constants are found to be higher than those of the monomer; the influence of the negative charges on the neighboring units increases the overall electrostatic force that encourages protonation in polymer. The

basicity constants log K_1 and log K_3 are of "apparent"[97] nature ($n > 1$) as demonstrated in Figure 6.6 which reveals a decrease in log K with the increase in degree of protonation (α) as a direct consequence of a gradual decrease in the electrostatic field force that encourages protonation.

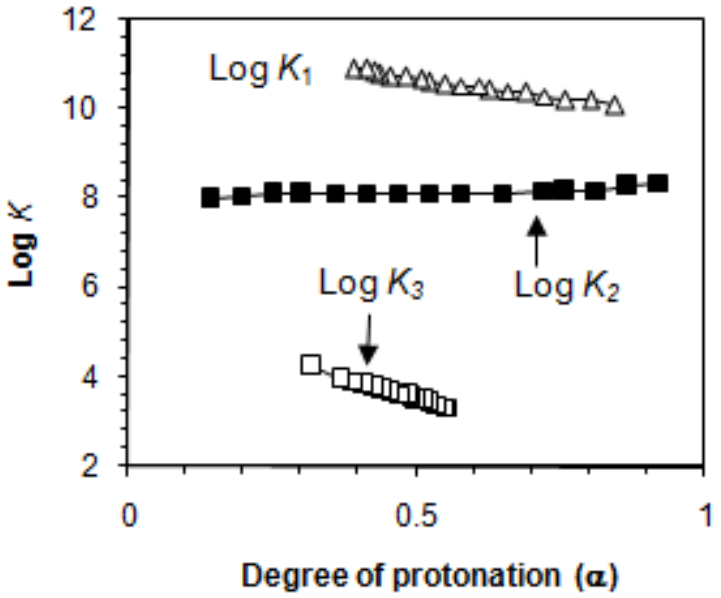

Figure 6.6 Plot for the apparent log K_1, log K_2 and log K_3 versus degree of protonation (α) (entries 3, 3 and 3, Table 6.3) for (±≡) PZTAN **10**.

Note that log K_2 associated with the transformation of $^{2-}O_3P-X^+-PO_3H^-$ [(± =) **9**] to $^{-}HO_3P-X^+-PO_3H^-$ [(± −) **8**] remained almost constant (n = 0.88) with the change in α (Figure 6.6). We cannot, at this stage, offer any rationale for this observation.

Note that the highest polyelectrolyte index i.e. the highest n value of 3.06 belongs to n_3 associated with the transformation of polyzwitterion/anion (± −) **8** to electroneutral polyzwitterions (±) **7** during protonation (Table 6.3). This is a remarkable demonstration

of the beneficial entropy effects[98] associated with the release of a greater number of hydrated water molecules from the repeating unit of more hydrated (± −) **8** to the least hydrated collapsed coil conformation of (±) **7**.

6.3.4 Effectiveness of PZA 7 as an Antiscalant

Smooth functioning of a desalination process is often plagued by precipitation (scale formation) of $CaCO_3$, $CaSO_4$, $Mg(OH)_2$, etc. Inhibition of the growth rate of crystal formation by anionic antiscalants like poly(phosphate)s, organophosphates, and polyelectrolytes[136,137] is associated with their effectiveness in sequestrating cations and altering the crystal morphology at the time of nucleation.[131,135]

The reject brine in the reverse osmosis (RO) process has dissolved salts which precipitate in the event of exceeding their solubility limits. Antiscalant behavior of a supersaturated solution of $CaSO_4$ containing three times the concentration of the Ca^{2+} and SO_4^{2-} ions of a reject brine from a RO plant[133] was investigated in the absence and presence of 10 ppm of PZA **7** and a commercial antiscalant (PERMATREAT® PC-191) (Figure 6.7).

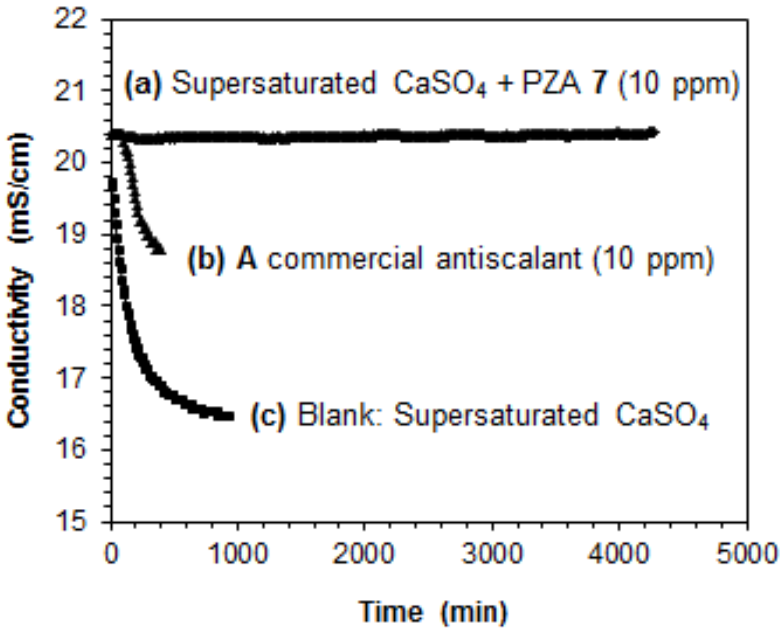

Figure 6.7 Precipitation behavior of supersaturated solution (3 CB) of $CaSO_4$ in the presence (10 ppm) and absence of PZA **7** and a commercial antiscalant**.**

To our great satisfaction, conductivity did not decrease for about 4280 min (71.3 h), thus registering an amazing ≈100 % scale inhibition in the presence of a meager 10 ppm of PZA **7** (Figure 6.7a). The newly developed antiscalant PZA **7** may continue to inhibit precipitation even for longer duration; however the test was abandoned after 71.3 h. Note that precipitation started immediately in the absence of antiscalant (Figure 6.7c: Blank). The commercial antiscalant maintained ≈100 % scale inhibition efficiency up to 100 min, thereafter the conductivity started to decrease gradually (Figure 6.7b). It is worth mentioning that the residence time of reject brine in an osmosis chamber of a desalination plant is for duration of ≈ 30 min only. The optimistic result thus certifies that the additive PZA **7** is very much suitable in inhibiting calcium sulfate scale formation in RO plants. The presence of multi adsorption sites on the bis-phosphonate motifs in PZA **7**

effectively sequestrates the Ca^{2+} ions to inhibit nucleation as well as crystal growth. Note that neither monomers **4** and **11** nor polymer **5** gave any effective inhibition; screening experiments based on visual inspection revealed that under the same conditions the system becomes cloudy within 1 h.

6.4 Conclusions

The work describes the synthesis and polymerization of a new cationic monomer **4**. Polymer CPE **5** represents the first example of a Butler's symmetric cyclopolymer containing two identical phosphopropyl pendents in the same repeating unit. The hydrolysis of the phosphonate ester groups resulted in the pH-responsive CPA (+) **6** which permitted to study the interesting solution properties (including solubility behavior) that involved its conversion to (±) PZA **7**, (± -) PZMAN **8**, (± =) PZDAN **9**, and (± ≡) PZTAN **10** all having identical degree of polymerization. The solution properties were correlated to the type of charges and their densities on the polymer chain. Several apparent basicity constants of (± ≡) PZTAN **10** and monomer (± ≡) ZTAN **15** have been determined. PZA **7** at a meager concentration 10 ppm imparted excellent inhibition of calcium sulfate scale formation, and as such, it can be used as an effective antiscalant in reverse osmosis plants.

CHAPTER 7

A novel Cross-linked Polyzwitterion/anion Having pH-Responsive Carboxylate and Sulfonate Motifs for the Removal of Sr^{2+} from Aqueous Solution at Low Concentrations

Taken from Shaikh A. Ali and Shamsuddeen A. Haladu, A novel cross-linked polyzwitterion/anion having pH-responsive carboxylate and sulfonate motifs for the removal of Sr^{2+} from aqueous solution at low concentrations, *Reactive and Functional Polymers*, 73 (2013) 796–804.

Abstract

A novel cross-linked polyzwitterion (CPZ) was synthesized *via* cycloterpolymerization of *N*,*N*-diallyl-*N*-sulfopropylammonioethanoic acid (92.5 mol%), a cross-linker 1,1,4,4-tetraallylpiperazinium dichloride (7.5 mol%), and sulfur dioxide (100 mol%) in the presence of azoisobutyronitrile in dimethylsulfoxide at 60 °C. CPZ, upon treatment with NaOH, was converted into a cross-linked polyzwitterion/anion (CPZA). The experimental data for the adsorption of Sr^{2+} on CPZA fitted the pseudo-second-order kinetic model and Freundlich as well as Temkin isotherm models. The adsorption process was spontaneous and exothermic in nature with negative values for both ΔG and ΔH. The low activation energy of 7.18 kJ/mol indicated the adsorption as a favorable process. The removal for the initial concentrations of 200 ppb and 1000 ppb (i.e., 1 ppm) of Sr^{2+} ions was observed to be 87% and 92%, respectively. An efficient synthetic access to the resin and excellent adsorption capacity and desorption would enable its use in the treatment of radioactive nuclear waste containing Sr^{2+} ions. The CPZA provided an opportunity to test

the efficacy of a zwiiterionic/anionic group in the removal of Sr^{2+} ions in low concentrations.

7.1 Introduction

Radioactive wastes containing a variety of radionuclides severely pollute the environment. Fission product like ^{89}Sr and ^{90}Sr with half-lives of 51 days and 29 years, respectively,[46] can contaminate underlying layers of soil and groundwater.[47,48] Strontium's resemblance to calcium enables its easy incorporation into bone and by virtue of being a very strong β-emitter, it leads to the development of bone sarcoma and leukemia.[46,49,50] It is thus quite necessary to remove Sr, one of the most hazardous elements, from wastewater. Adsorption with solid adsorbents like polyacrylonitrile/zeolite composite,[51] bentonite,[52] zeolites and clays have been studied for the removal of Sr^{2+} ions,[53,54] and the adsorption capacity is found to be somewhat low. Derivatives of crown ethers,[55,56] cross-linked polymers containing carboxyl motifs[57,58] including gels based on carboxylated polysaccharide derivatives[59] were also used to adsorb Sr^{2+} ions.

A study of $2Na^{+} \rightarrow Sr^{2+}$ exchange equilibria with actual ground water using a synthetic clay revealed high capacity for uptake of ^{90}Sr.[164] A study of adsorption of Sr^{2+} from sulfuric acid solution by different Dowex 50W-X ion exchange resins has been investigated.[165] Among these resins, Dowex 50W-X8 resin showed the maximum sorption of Sr^{2+} from the aqueous solutions. Inorganic cation exchange materials such as niobate molecular sieves,[166] titanate,[167] and synthetic micas[164] have been studied for

the removal of radioactive ions. A few separation processes of Sr^{2+} by liquid–liquid solvent extraction have also been reported.[168-170]

Polyzwitterions synthesized from *N*-vinyl imidazole have been used as sorbents for the removal of Sr^{2+}. The polysulfobetaines (polyzwitterions) carrying both charges on the same repeating unit are good candidate for the water technologies on accounts of its dual role in removing the cationic or anionic effluent and they also can impart anti-microbial properties[60] pH-responsive polyzwitterions are of great academic and industrial interest[6,114,171,172] and useful in water treatment, drag reduction, petroleum recovery, viscosification, coatings, and cosmetics.[100] Recently, the researchers have focused on the syntheses of zwitterionic cross-linked inorganic/organic hybrid materials for the removal of toxic heavy metal ions *via* electrostatic effects.[36,61,62]

The literature presented above describes many sorbent materials to remove larger concentration of Sr^{2+}ions; however, it remains challenging to develop new materials for removing Sr^{2+} ions at ppb-levels. For the removal of metal ions, the materials developed so far include zwitterionic (±) or anionic (−) groups in which the anionic centers are the sites where the metal ions are physically or chemically attached. In the current study, a novel cross-linked polymer containing zwitterionic (±) and anionic (−) groups embedded in the same repeating unit has been synthesized and tested for efficiency as adsorbent for the removal of Sr^{2+} ions at low concentrations from aqueous solutions. To our knowledge, neither the synthesis of cross-linked polymer having zwitterionic/anionic group nor its use has been reported before; as such the study would establish the efficiency of this special functionality for the removal of metal ions.

7.2 Experimental

7.2.1 Physical methods

Elemental analysis was carried out on a Perkin–Elmer Elemental Analyzer Series II Model 2400. IR spectra were recorded on a Perkin–Elmer 16F PC FTIR spectrometer. ^{1}H and ^{13}C spectra were measured on a JEOL LA 500 MHz spectrometer using HOD signal at δ4.65 and dioxane signal at 67.4 ppm as internal standards, respectively. Atomic absorption spectroscopy (AAS) analysis was performed using AAS model iCE 3000 series (Thermo Scientific). The instrumental lower detection limit for Sr^{2+} ions was determined to be 15 ± 3 ppb. Scanning electron microscopy (SEM) images were taken by TESCAN LYRA 3 (Czech Republic) equipped with Oxford, energy-dispersive X-ray spectroscopy (EDX) detector model X-Max. Thermogravimetric analysis (TGA) was performed using a thermal analyzer (STA 429) manufactured by Netzsch (Germany). The polymer sample to be tested (usually ∼5 mg) was placed in a platinum crucible. Aluminum oxide (Al_2O_3; ∼4 mg) was placed in an identical platinum crucible as a reference sample. With the sample carrier system, which had two sets of 10% Pt–Pt/Rh thermocouples, the sample carrier was placed in the middle of the vertical furnace, which was programmed and controlled by a microprocessor temperature controller. The temperature was raised at a uniform rate of 10 °C/min. The analyses were made over a temperature range of 20–800 °C in an air atmosphere flowing at a rate of 100 mL/min.

7.2.2 Materials

Azobisobutyronitrile (AIBN) from Fluka AG was purified by crystallization from a chloroform–ethanol mixture. Diallylamine, from Fluka Chemie AG (Buchs, Switzerland)

were used as received. Dimethylsulfoxide (DMSO) was dried over calcium hydride overnight and then distilled under reduced pressure at a boiling point of 64–65 °C (4 mm Hg). All solvents used were of analytical grade. Considering the high toxicity of radioactive ions, aqueous solutions of non-radioactive Sr^{2+} ions were used in sorption experiments. For this purpose, $Sr(NO_3)_2$ was purchased from Fisher Scientific Company (New Jersey, USA).

7.2.3 Synthesis of zwitterionic ester (1)

Zwitterionic monomer *N*-carboethoxymethyl-3-(*N*,*N*-diallylamino)propanesulfonate (**1**) was prepared in 82% yield by reacting an equimolar mixture of *N*,*N*-diallyl-*N*-carboethoxymethylamine[80] and 1,3-propanesultone in acetonitrile (130 cm^3 for 0.13 mol amine) at 72 °C for 72 h, mp (methanol/acetone/diethyl ether) 162–163 °C.[123]

7.2.4 Acid hydrolysis of zwitterionic ester 1 to zwitterionic acid 2

A solution of zwitterionic ester **1** (16.4 g, 53.7 mmol) in 6 M HCl (60 mL) was heated in a closed vessel at 80 °C for 27 h. The resulting solution was then freeze-dried to obtain **2** as a thick liquid which was crystallized from a mixture of MeOH/CH_3CN/diethylether as white crystals (14.2 g, 95%). (Found: C, 47.4; H, 7.0; N, 4.9; S, 11.3%. $C_{11}H_{19}NO_5S$ requires C, 47.64; H, 6.91; N, 5.05; S, 11.56%); ν_{max} (KBr) 3500–2600 (br), 3015, 2980, 2930, 1728, 1642, 1479, 1400, 1324, 1197, 1166, 1081, 1040, 999, 972, 957, 941, 888, 801, 732, 698, 619, 596, 573, and 521 cm^{-1}; δ_H (D_2O) 2.07 (2H, quint, *J* 7.05 Hz), 2.77 (2H, t, *J* 6.7 Hz), 3.47 (2H, apparent t,*J* 7.95 Hz), 3.98–4.02 (6H, m), 5.56 (4H, m), 5.84 (2H, m), (HOD: 4.65); δ_C (D_2O) 18.36, 47.86, 56.82, 58.32, 62.68 (2C), 124.25 (2C), 130.42 (2C), 167.61 (dioxane: 67.40 ppm).

7.2.5 1,1,4,4-Tetraallylpiperazinium dichloride (3)

Monomer **3**, a cross-linker, was prepared as described.[69]

7.2.6 Terpolymerization of monomers 2, 3 and sulfur dioxide to form cross-linked polyzwitterion (CPZ) 4

Sulfur dioxide (1.28 g, 20 mmol) was absorbed in a mixture of **2** (5.55 g, 20 mmol) and cross-linker **3** (1.62 mmol, 0.52 g) in DMSO (7.0 g). Initiator AIBN (140 mg) was then added, and the mixture stirred at 65 °C for 24 h. At the end of the elapsed time, the hardened solid mass was soaked in water for 24 h, with frequent changing of water, and finally dried under vacuum at 55 °C to a constant weight (5.00 g, 68%). (Found: C, 39.2; H, 5.9; N, 4.2; S, 17.7%. monomer **2**/SO_2 $C_{11}H_{19}NO_7S_2$ (92.5 mol%) and monomer **3**/$SO_2C_{16}H_{28}Cl_2N_2O_2S$ (7.5 mol%) requires C, 39.56; H, 5.74; N, 4.34; S, 18.00%).

7.2.7 Basification of CPZ 4 to cross-linked polyzwitterion/anion (CPZA) 5

A mixture of CPZ **4** (4.6 g, 13.4 mmol) and sodium hydroxide (0.74 g, 18.5 mmol) in water (150 ml) was stirred for 24 h, after which it was poured into excess methanol. The resin **5** was filtered and dried under vacuum at 55 °C to a constant weight (4.7 g, 97%) TGA analysis show initial decomposition around 250 °C). (Found: C, 37.5; H, 5.4; N, 4.1; S, 16.7%. monomer **2**/SO_2 $C_{11}H_{18}NNaO_7S_2$ (92.5 mol%) and monomer **3**(dihydroxide)/SO_2 $C_{16}H_{30}N_2O_4S$ (7.5 mol%) requires C, 37.79; H, 5.27; N, 4.17; S, 17.02%).

7.2.8 Adsorption experiments

The procedure for the adsorption experiments of the cross-linked polymer CPZA **5** for Sr^{2+} ions can be described briefly as follows: a mixture of CPZA **5** (50 mg) in an aqueous $Sr(NO_3)_2$ (1 mg L^{-1}) solution (20 mL) was stirred using a magnetic stir-bar at different pH for 24 h. The filtrate was analyzed by atomic absorption spectroscopy to determine the amount of Sr^{2+} remained. The adsorption capacity ($q_{Sr^{2+}}$) in mg g^{-1} can be calculated using the following equation:

$$q_{Sr^{2+}} = \frac{(C_0 - C_f)V}{W} \qquad (1)$$

where C_0 and C_f are the initial and final concentration of Sr^{2+} ions in mg L^{-1}, respectively, W is the weight of the polymer in g, and V is the volume of the solution in L. Data presented are average of triplicate runs and varied by less than 4% in all the cases studied. The values of adsorption capacity (q) at various times and equilibrium are denoted as q_t and q_e, respectively, whereas C_e is used to refer to the equilibrium metal concentration in the solution.

For adsorption kinetic studies, the resin sample was stirred in a 1 mg L^{-1} $Sr(NO_3)_2$ solution for different adsorption times at pH 3 at 296, 308 and 323 K. Based on the adsorption data from experiments carried out at different temperatures (296, 308 and 323 K), the pseudo-second-order rate constant (k_2) at various temperatures and the activation energy (E_a) for the adsorption process were determined (section 7.3.7). Thermodynamic parameters ΔG, ΔH and ΔS for Sr^{2+} removal were calculated using q_e and C_e values for the adsorption experiments carried out as described above using 1 mg L^{-1} $Sr(NO_3)_2$ solution. The adsorption isotherms were constructed by

changing the concentration of $Sr(NO_3)_2$ solution from 200 μg L^{-1} (i.e. ppb) to 1000 μg L^{-1} at 296 K for 24 h.

7.2.9 Desorption experiment

Adsorption of Sr^{2+} ions was performed by stirring 50 mg resin in aqueous $Sr(NO_3)_2$ (1 mg L^{-1}) solution (20 mL) for 24 h. The amount of Sr^{2+}adsorbed (i.e., $q_{Sr}^{2+)}$ was determined as described in the above section. The loaded resin was then filtered, dried and quantitatively transferred to a stirring 0.1 M HNO_3 (20 mL) for 24 h for the desorption experiment. After filtration, the amount of Sr^{2+} ions desorbed in the filtrate (~19 mL) was determined; the efficiency of the desorption process was calculated by the ratio of desorbed amount of Sr^{2+} ions to the amount of adsorbed Sr^{2+} ions (i.e., $q_{Sr}^{2+)}$ in the resin.

7.2.10 FTIR spectroscopy

Unloaded and loaded resins were investigated by FTIR spectroscopy. Unloaded resins (30 mg) were immersed in 0.1 M $Sr(NO_3)_2$ solution (10 mL) for 4 h at a pH of 3, filtered, and dried under vacuum until constant weight was achieved.

7.3 Results and discussion

7.3.1 Synthesis of cross-linked polyzwitterion/anion (CPZA 5)

Butler's cyclopolymerization protocol has been utilized to synthesize the current resin **5** (Scheme 7.1). Butler's pioneering discovery of the cyclopolymerization involving a variety of *N*,*N*-diallylammonium monomers has led to the synthesis of an array of scientifically and technologically important water-soluble cationic polyelectrolytes.[1,4,5] The polymer-architecture, having the five-membered cyclic units embedded in the

backbone, has been recognized as the eighth major structural type of synthetic polymers.[4] Over 33 million pounds of poly(diallyldimethylammonium chloride) alone are sold annually for water treatment and another 2 million pounds are used for personal care formulation.[5] Recently, a pH-responsive cross-linked polyzwitterion containing phosphonate motifs has been synthesized *via* Butler's cyclopolymerization and tested for the removal of heavy metal ions.[35]

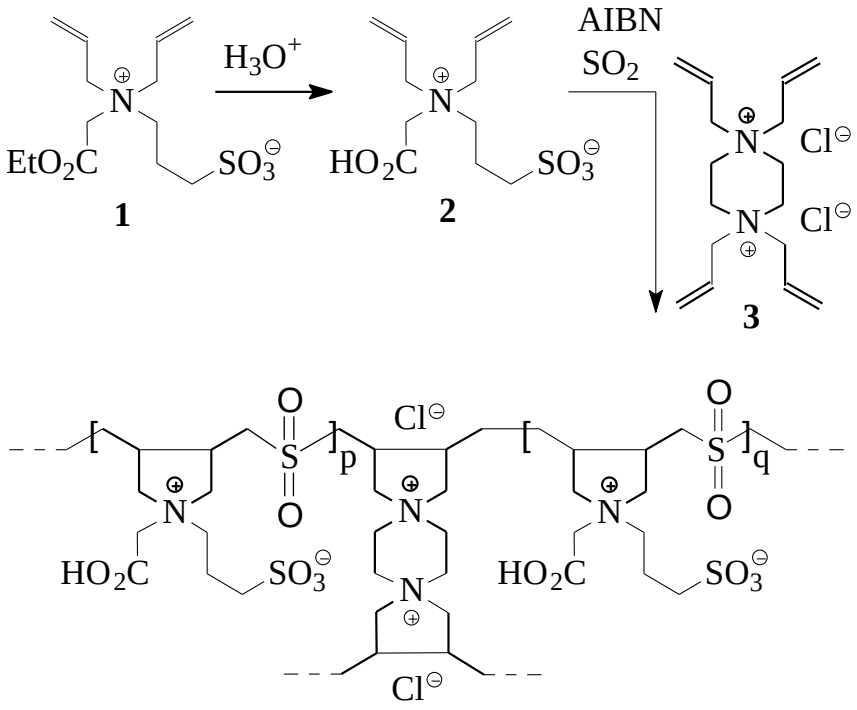

4: Cross-linked polyzwitterion (CPZ)

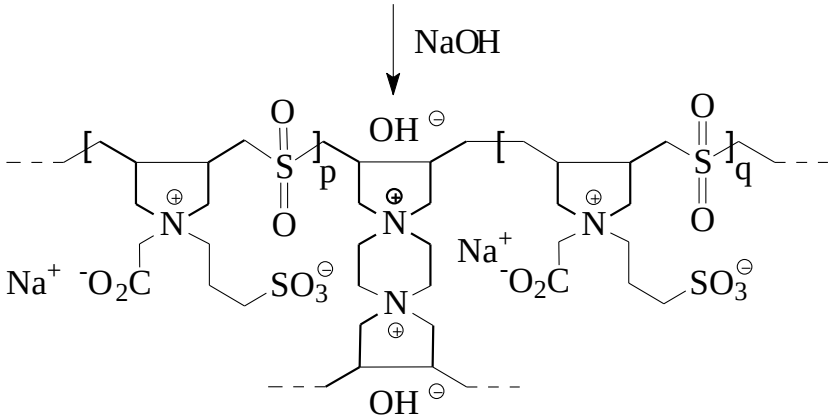

5: Cross-linked polyzwitterion/anion (CPZA)

Scheme 7.1 Synthesis cross-linked polyzwitterion/anion polymers.

Zwitterionic ester **1**,[123] prepared by reacting an equimolar mixture of *N*,*N*-diallyl-*N*-carboethoxymethylamine and 1,3-propanesultone in acetonitrile on acidic hydrolysis afforded the zwitteionic acid **2** in excellent yield (95%) (Scheme 7.1). Ester hydrolysis

was ascertained by NMR spectroscopy and elemental analysis (Experimental). Thus the conversion of the ester moiety $CO_2CH_2CH_3$ in **1** to CO_2H in **2** was confirmed by the absence of ethyl protons and carbons in the NMR spectra of the later. The CH_3 proton and CH_3 carbon of the $CO_2CH_2CH_3$ group in **1** were reported to appear at δ1.28 and 64.46 ppm, respectively.[123]

A mixture of monomer **2** (92.5 mol%), cross-linker **3** (7.5 mol%), and SO_2 (100 mol%) in solvent DMSO underwent cyclocopolymerization in the presence of initiator AIBN to give cross-linked polyzwitterion (CPZ **4**) (Scheme 7.1) as a white solid. CPZ **4** upon treatment with excess NaOH led to the formation of cross-linked polyzwitterion/anion CPZA **5**. To the best of our knowledge this is the first cross-linked polymer *via* Butler's cyclopolymerization protocol that ensured the embedding of the zwitterionic as well as anionic groups in each repeating unit. Elemental analysis of CPZ **4** and CPZA **5** confirmed the incorporation of monomer **2** and cross-linker **3** into the polymer in an approximate mol ratio of 93:7, which is similar to the feed ratio.

Thermogravimetric analysis (TGA) curve of CPZA **5** (Figure 7.1) showed two major loss in weight: first slow weight loss of 4.0% is attributed to loss of water imbedded inside the cross-linked polymer, the second major loss of 28% around 250 °C is attributed to the loss SO_2, and the third major loss of 52% is the result of combustion of nitrogenated organic fraction with the release of CO_2, NO_x and H_2O gases.[134] The residual mass at 800 °C was found to be 16%.

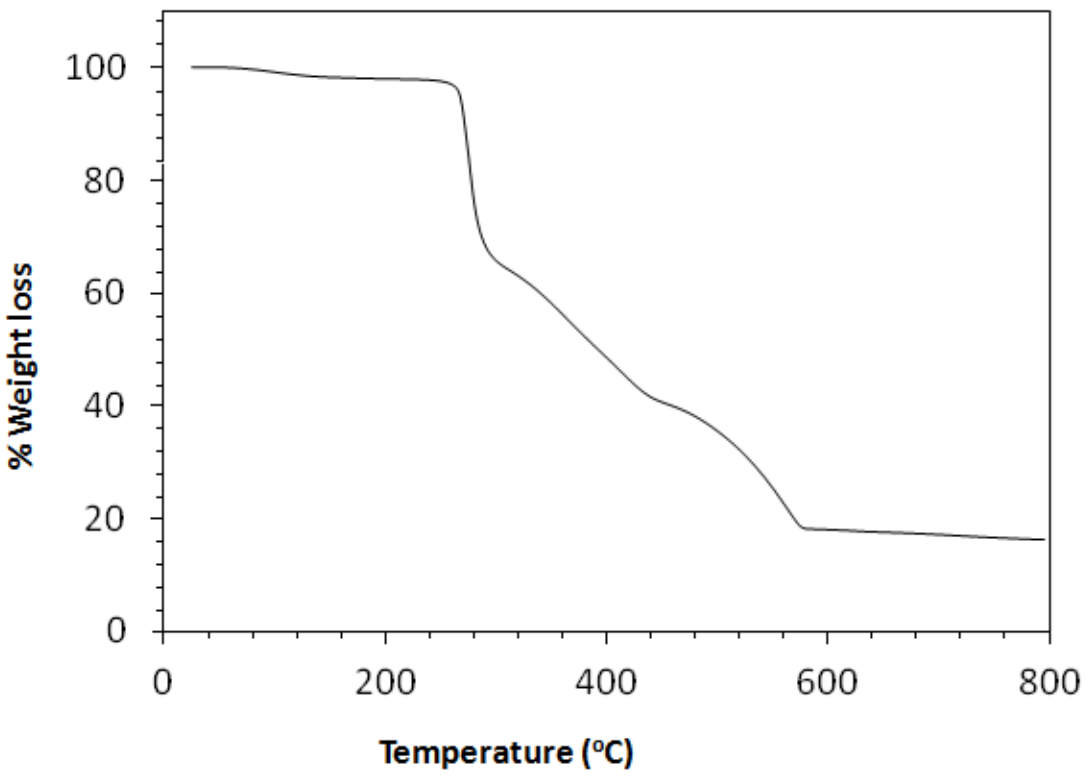

Figure 7.1 TGA curve of CPZA **5.**

7.3.2 FTIR characterization of monomers and polymers

The IR spectrum of zwitterionic monomer **2** indicates the presence of sulfonate group by its strong characteristic bands at 1197 $cm^{-1}$and 1040 cm^{-1},[126] while the absorption at 1728 cm^{-1} is attributed to C=O stretch of COOH.[80] The corresponding absorptions for the CPZ **4** appear at 1212, 1041, and 1741, respectively (Figure 7.2a). The symmetric and antisymmetric stretching of COO^- in the dipolar form[80] of CPZ **4**were observed at 1412 and 1634 cm^{-1}, respectively (Figure 7.2a). The two moderately strong bands at 1313 cm^{-1} and 1131 cm^{-1} were assigned to the asymmetric and symmetric vibrations of SO_2 unit[134] (Figure 7.2a).

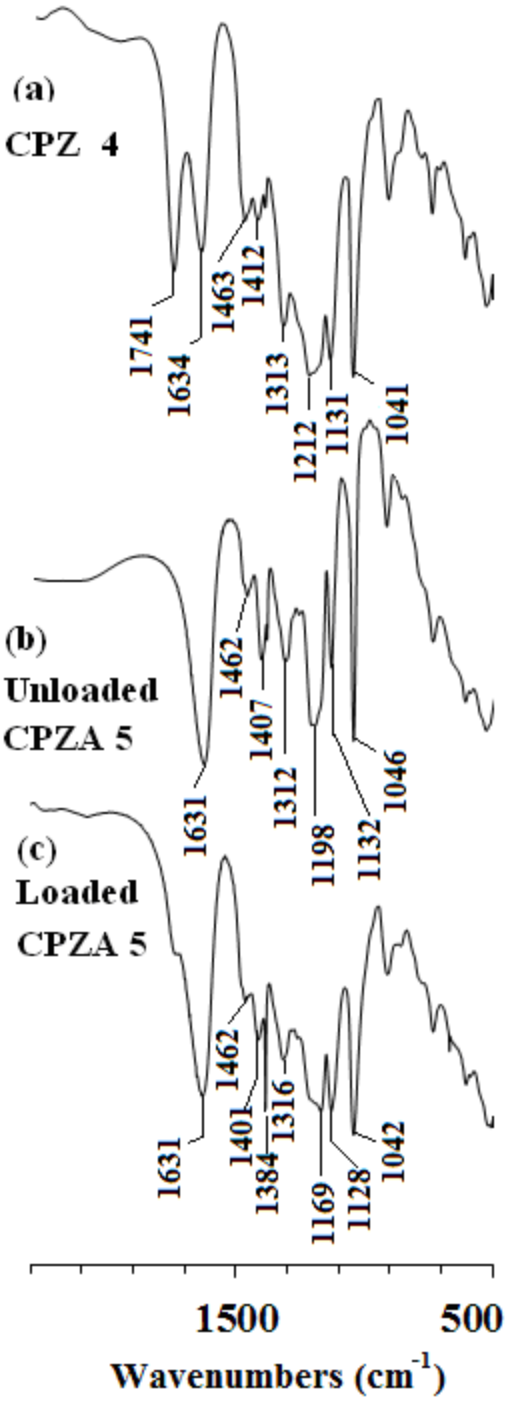

Figure 7.2 IR spectra of (a) cross-linked CPZ **4**, (b) CPZA **5**, and (c) CPZA **5** loaded with Sr^{2+}.

For the unloaded resin CPZA **5**, the absorption due to C=O stretch of COOH was missing, instead the symmetric and antisymmetric stretching of COO^- appeared at 1407 and 1631 cm^{-1} (Figure 7.2b). The appearance of a new band at 1384 cm^{-1} (Figure 7.2c) was attributed to the presence of ionic nitrate group since the adsorption process was carried out in the presence of $Sr(NO_3)_2$.[173] Interestingly, the presence of this band implies the ability of the resin to act also as an anion exchanger. Note that the absorption band attributed to the nitrate ion is absent in the IR spectrum of the unloaded resin **5** (Figure 7.2b). The IR spectra of the resin loaded with Sr^{2+} (Figure 7.2c) revealed the increase in the intensity and broadness of the C=O vibrations as a result of the adsorption of the metal ions.[174]

7.3.3 Effect of pH and temperature on adsorption

The effect pH (in the range 2.5–9) on the uptake of Sr^{2+} was investigated at a fixed concentration (1 mg L^{-1}) and time of 24 h at 23 °C. The pH of the media was controlled by acetic acid/sodium acetate buffer in the lower pH range while ammonia/ammonium chloride buffer was used in the higher pH range. To attain a pH of 2.5, additional amount of HCl was added to the buffer solution. Results of metal uptake at different pH are shown in Figure 7.3a. Optimum pH was found to be 3; after reaching the minimum at pH 6, the adsorption capacity increases on further increasing the pH. Sr^{2+} ions may be captured by carboxyl and sulfonate groups by chelation as depicted in Scheme 7.2. It is worth mentioning that pK_a of CO_2H and SO_3H groups in this resin are expected to be +2.5 and −2.1, respectively.[80] At pH 3 or even at 2, a sizable proportion of CO_2^- will exist in the acid–base equilibrium and almost the entire SO_3H will remain in the dissociated form of SO_3^-.

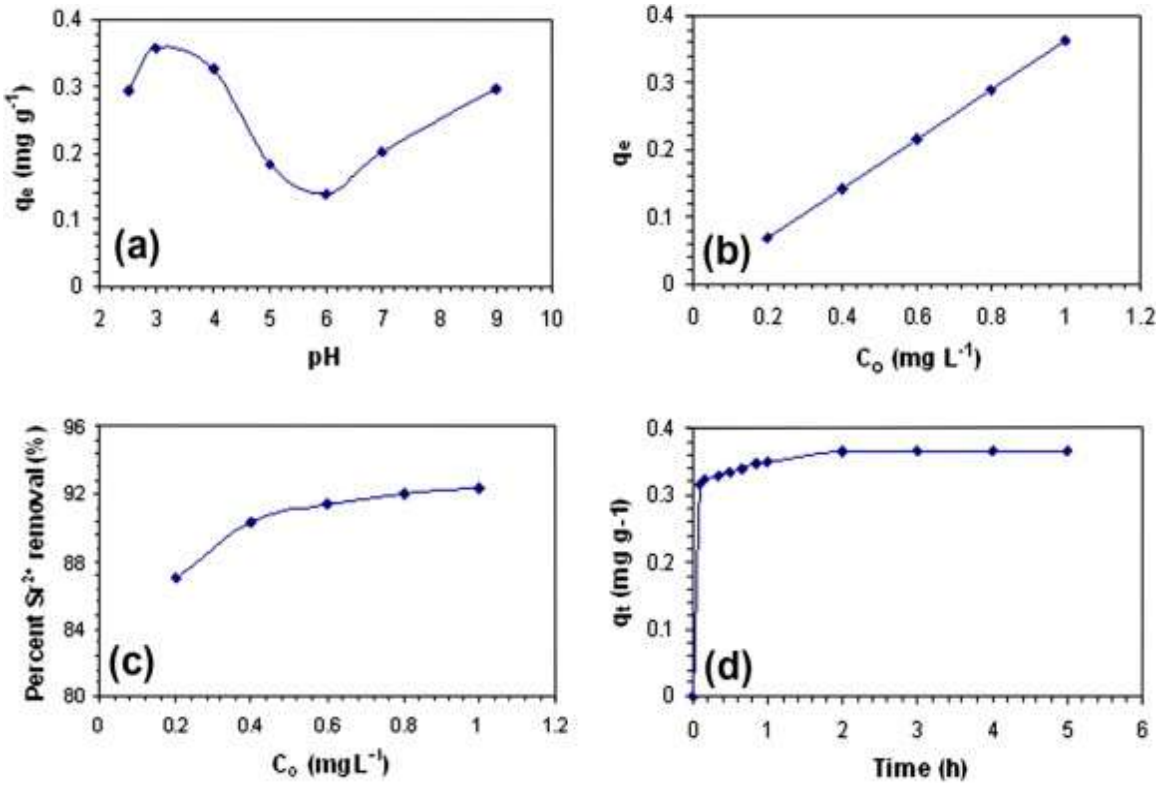

Figure 7.3 (a) The effect of pH on the adsorption capacity of CPZA **5** at Sr^{2+} initial concentration of 1.00 ppm for 24 h at 23°C; (b) The effect of initial concentration of Sr^{2+} on the adsorption capacity of CPZA **5** at pH 3 for 24 h at 23°C; (c) The percent removal of Sr^{2+} at its various initial concentrations at pH 3 for 24 h at 23°C; (d) Absorption kinetic curve of Sr^{2+} in 1.00 ppm Sr^{2+} solution at pH 3 at 23°C.

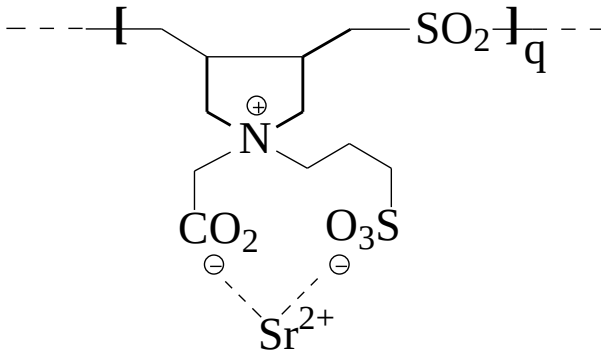

Scheme 7.2 Adsorption of Sr^{2+} on CPZA **5**.

The adsorption of Sr^{2+} reaches a maximum at a pH of 3. At pH values <3, the abundant H^+ ions in the solution will compete with Sr^{2+} ions to combine with CO_2^- or SO_3^- groups, while plentiful Cl^- ions will shield the positive nitrogens of the sulfobetaine zwitterionic groups. The decrease of adsorption with the increase of pH in the range 3–6 and reaching a minimum at pH 6 is somewhat baffling even though there are some literature precedences. Thus, the adsorption of Sr^{2+} on a hybrid gel prepared from bis(trimethoxysilylpropyl)amine is reported to reach a maximum at a pH of 4.7, minimum at 7.3 and further increase at higher pH values.[175] A polyacrylonitrile/zeolite composite adsorbent has been shown to have maximum adsorption of Sr^{2+} at a pH of 5.2 and at higher pHs the percent adsorption capacity decreases.[51] The percent removal for Sr^{2+} by a zwitterionic polysulfobetaine has been shown to have a minimum at pH 5.8.[60] It is to be noted that Sr^{2+} could form mono-valent ionic pairs such as $SrCl^+$ and $SrOH^+$ before being adsorbed.[175,176] Sr in the pH range 1–11 can be present in the form of Sr^{2+} and a very negligible $Sr(OH)^+$ which increases in concentration above 10.[51] There are many factors that may affect the adsorption behavior. The pH of the media may affect the network characteristics such as pore size, the water uptake as well as the ion uptake behavior of the resin. The adsorption in the form monovalent ion pair like $SrCl^+$ requires one exchange site while a divalent Sr^{2+} is expected to demand two exchange sites. Neither the reported articles nor our current work are able to provide an effective rationale for the observed minimum around pH 6. The rest of the adsorption studies were carried out at the optimal pH of 3.

7.3.4 Effect of initial concentration on the adsorption of Sr^{2+} ions

As shown in Figure 7.3b, the adsorption capacity of CPZA **5** increased with increasing concentrations of Sr^{2+}ions. The percent removal for the initial concentrations of 200 ppb and 1000 ppb (i.e. 1 ppm) was determined to be 87 and 92, respectively (Figure 7.3c).

7.3.5 Adsorption kinetics

The adsorption kinetics, which describes the relationship between adsorption capacity and adsorption time, is presented in Figure 7.3d. The adsorption process was found to be fast and it reached the equilibrium within 2 h indicating the strong ability of this resin to remove Sr^{2+} ions from aqueous solutions.

7.3.6 Lagergren first-order and pseudo-second-order kinetics

Lagergren first-order kinetics describes the adsorption process in a solid–liquid system based on the adsorption capacity of the solid, where it assumes that one metal ion is adsorbed onto one adsorption site on the surface of the adsorbent.[177] The linear form of the model can be described in the following equation:

$$\log(q_e - q_t) = \log q_e - \frac{k_1 t}{2.303} \qquad (2)$$

where q_e and q_t (mg g^{-1}) (are the adsorption capacities at equilibrium and at time t (h), respectively, and k_1 is the first-order rate constant. The k_1 and q_e were evaluated experimentally using the slope and intercept of the plots of $\log(q_e - q_t)$ versus t (Table 7.1 and Figure 7.4a). The fitness of the data was found to be excellent having square of regression coefficient (R^2) of 0.9934; only the low time zone linear fit, not the longer time fit, was considered. However, agreement between experimentally observed equilibrium adsorption ($q_{e,\exp}$ = 0.365 mg g^{-1}) and that derived using 1st order equation is

very poor ($q_{e,cal}$ = 0.0760 mg g^{-1}) thereby indicating that the adsorption process does not fit with Lagergren first-order kinetic model (Table 7.1).[178]

Table 7.1 Lagergren kinetic model parameters for Sr^{2+} Adsorption.

Pseudo second–order						
Temp (K)	$q_{e,exp}$ (mg g^{-1})	k_2 ($h^{-1}g\ mg^{-1}$)	h^a ($h^{-1}g^{-1}$ mg)	$q_{e,cal}$ (mg g^{-1})	R^2	E_a (kJ mol^{-1})
296	0.365	72.2	9.80	0.369	0.9998	
308	0.352	82.3	10.3	0.354	0.9991	7.18
323	0.336	92.2	10.5	0.338	0.9995	
Pseudo first–order						
Temp (K)	$q_{e,exp}$ (mg g^{-1})	k_1 (h^{-1})	$q_{e,cal}$ (mg g^{-1})	R^2		
296	0.365	0.651	0.0760	0.9934		

[a]Initial adsorption rate $h = k_2 q_e^2$.

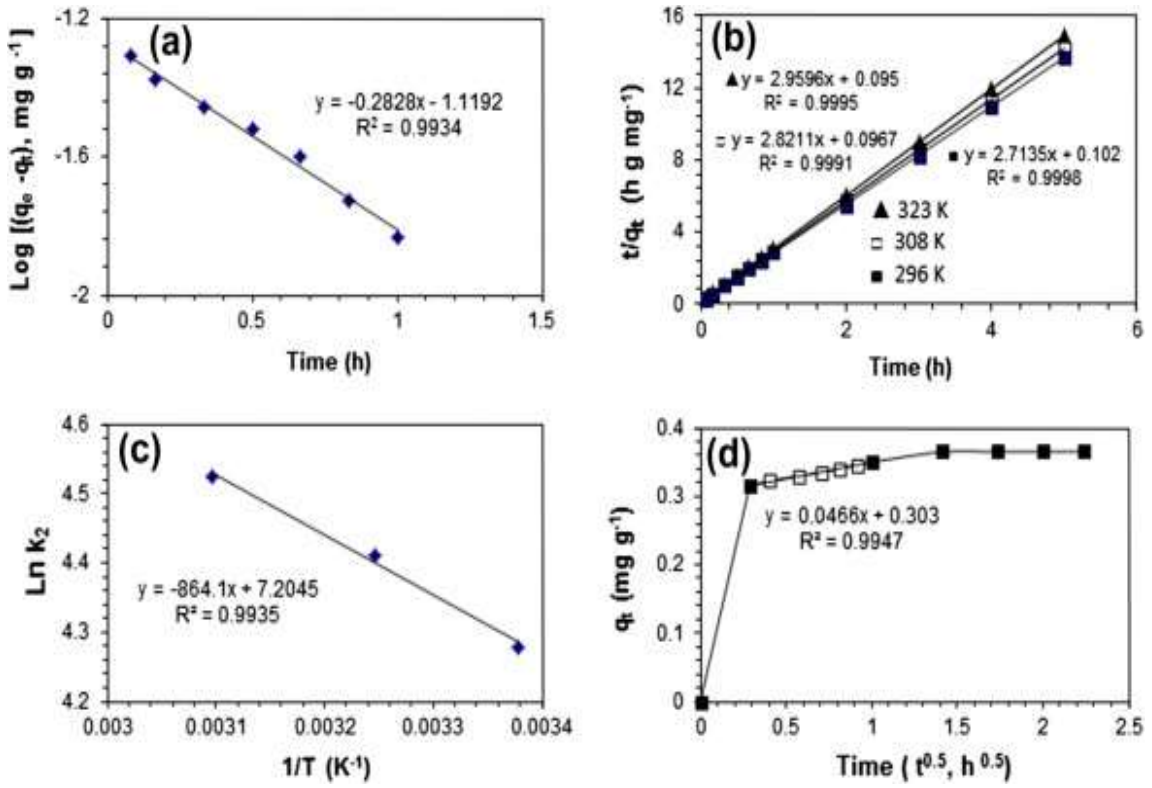

Figure 7.4 (a) Lagergren first-order kinetic model for adsorption of Sr^{2+} (1.00 ppm) on CPZA **5** at pH 3 at 23°C; (b) Pseudo-second-order kinetic model for adsorption of Sr^{2+} (1.00 ppm) on CPZA **5** at pH 3 at 23°C; (c) Determination of the activation energy for Sr^{2+} adsorption on CPZA **5**; (d) Intraparticle diffusion plot for of Sr^{2+} adsorption on CPZA **5** at pH 3 at 23°C.

The linear pseudo-second-order kinetic model[179] can be expressed by the following equation:

$$\frac{t}{q_t} = \frac{1}{k_2 q_e^{\,2}} + \frac{t}{q_e} \qquad (3)$$

where k_2 is pseudo-second-order rate constant, q_t and q_e are the respective adsorption capacity of the metal ions at a time t and at equilibrium.

It is evident from Figure 7.4b and Table 7.1 that the pseudo-second-order kinetic model fitted well with the adsorption of Sr^{2+} indicating that the adsorption process might be a chemical adsorption.[180] Also the equilibrium adsorption capacities ($q_{e,cal}$: 0.369 mg g^{-1}) derived from Eq. (3) are in close agreement with those observed experimentally ($q_{e,exp}$: 0.365 mg g^{-1}) at 23 °C. The experimental data so far revealed that the resin is an efficient adsorbent for the removal of Sr^{2+} ions from aqueous solutions.

7.3.7 Adsorption activation energy

The adsorption activation energy can be deduced from the rate constants (k_2) obtained from the pseudo-second-order kinetic model (Table 7.1) using the Arrhenius equation (Eq. (4)) expressed as:

$$\ln k_2 = -\frac{E_a}{2.303RT} + \text{constant} \qquad (4)$$

where k_2 is the second order rate constant (g mg^{-1} h), E_a is the activation energy (kJ mol^{-1}), R is the universal gas constant (8.314 J mol^{-1} K^{-1}) and T is the solution temperature (K). A plot of ln k_2 versus 1/T gives a linear plot, with slope $-E_a/R$ (Figure 7.4c and Table 7.1). The low activation energy value of 7.18 kJ mol^{-1} is an indication of the feasibility of the adsorption process.[178, 181]

7.3.8 Intraparticle diffusion model

The mechanism of adsorption can be understood by determining the rate-limiting step, and this can be determined by using some adsorption diffusion models which are always constructed on the basis of three consecutive steps: (1) film diffusion (i.e., diffusion across the liquid film surrounding the adsorbent particles); (2) intraparticle diffusion (i.e., diffusion in the liquid contained in the pores and/or along the pore walls); and (3) mass

action (i.e., fast physical adsorption and desorption between the adsorbate and active sites). The intraparticle diffusion model assumes that the metal ions are transported from the solution through an interface between the solution and the adsorbent (i.e., film diffusion) followed by a rate-limiting intraparticle diffusion step which bring them into the pores of the particles in the adsorbent. Following equation expresses the relation of the adsorption capacity and time[182-184]:

$$q_t = x_i + k_p t^{0.5} \qquad (5)$$

where q_t is the adsorption capacity at time t, k_p is the rate constant of intraparticle diffusion, x_i is related to boundary layer thickness. According to the Weber–Morris model,[177,179] a straight line fit for the plot of q_t versus $t^{0.5}$ passing through the origin implies the intraparticle diffusion as the rate-limiting step.[185] Since the initial linear plot did not pass through the origin, that is, there is an intercept which indicates that rapid adsorption occurs within a short period of time (Figure 7.4d).

The intercept x_i of the linearized line was used to define the initial adsorption factor (R_i) as:

$$R_i = 1 - \frac{x_i}{q_e} \qquad (6)$$

where x_i is the initial adsorption amount and q_e the final adsorption amount at the longer time. The x_i andq_e values of 0.303 and 0.365 mg g^{-1}, respectively, gave an R_i value of 0.17 which means that the relatively strong rapid initial adsorption has already reached 83% before the first adsorption data was collected at a time of 5 min. The other 17% of adsorption is governed by intraparticle diffusion as indicated by the linear relation with an excellent square of correlation coefficient (R^2) of 0.9947 (Figure 7.4d). In this case,

the intraparticle diffusion within the pores of the resins was the rate-limiting step. Note that the last linear section represents the final equilibrium stage.

7.3.9 Adsorption isotherms

As shown in Figure 7.3b, the adsorption capacity of CPZA **5** increases with the increase in the initial concentration of Sr^{2+} ions. To further explore the adsorption mechanism, Langmuir, Freundlich and Temkin isotherm models were used to analyze the adsorption data. The Langmuir isotherm model,[186,187] which assumes the mechanism of the adsorption process as a monolayer adsorption on completely homogeneous surfaces where interactions between adsorbed molecules are negligible, can be expressed by the following equation:

$$\frac{C_e}{q_e} = \frac{C_e}{Q_m} + \frac{1}{Q_m b} \qquad (7)$$

where C_e and q_e are the concentrations of metal ion in the solution and resin, respectively, Q_m and b are the Langmuir constants. The Langmuir plot of C_e/q_e versus C_e enables the calculation of Langmuir constants from the intercept and slope of the linear plot. The adsorption of Sr^{2+} by the resin did not fit the Langmuir isotherm model, so the relevant graph has not been displayed.

Freundlich isotherm model, which describes the non-ideal adsorption occurring on a heterogeneous surface with uniform energy as well as multilayer adsorption, are expressed by the following equations:

$$q_e = k_f C_e^{1/n} \qquad (8)$$

$$\log\ q_e = \log k_f + \frac{1}{n}\log C_e \qquad (9)$$

where k_f and n represent the Freundlich constants, which can be calculated from the slope and intercept of the linear plot of log q_e versus log C_e as presented in Figure 7.5a. The value of n was determined to be 0.652. A $1/n$ value above unity implies cooperative adsorption.[188]

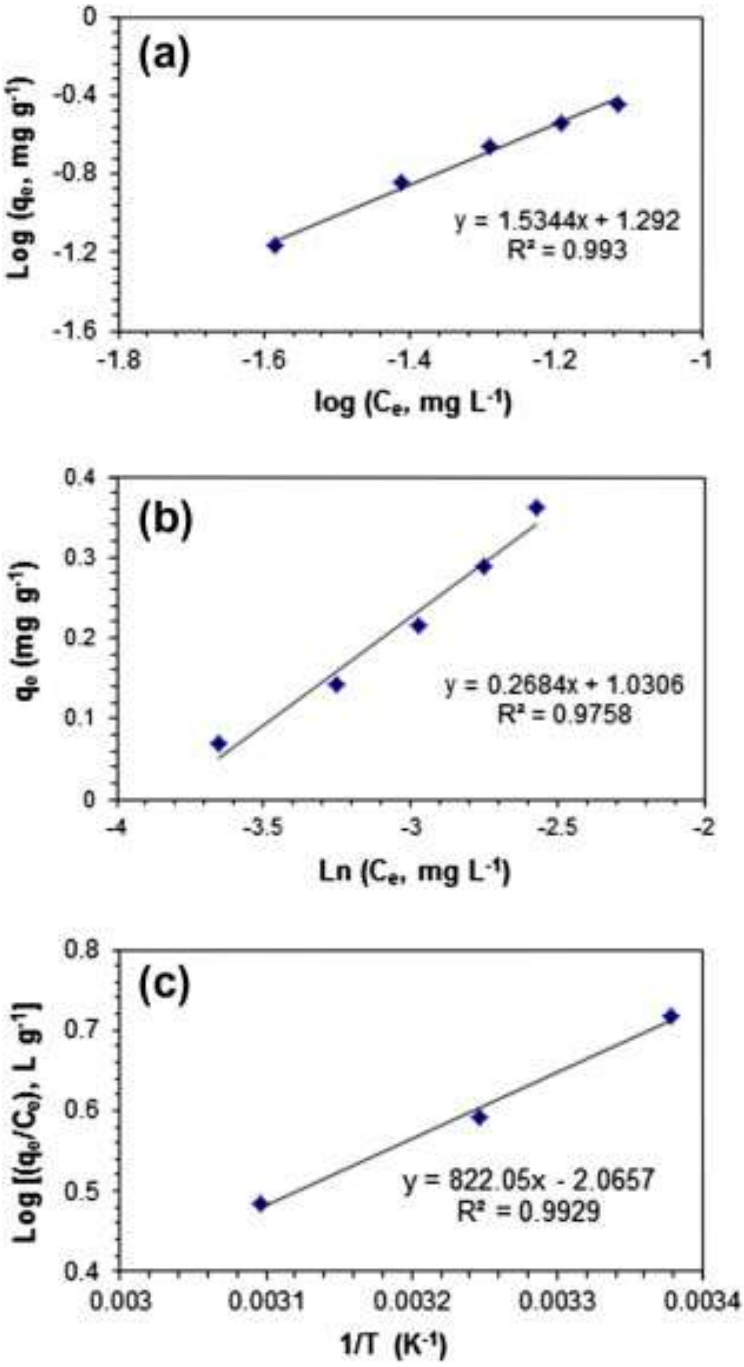

Figure 7.5 (a) Freundlich isotherm for Sr^{2+} adsorption on CPZA **5**; (b) Temkin isotherm for Sr^{2+} adsorption on CPZA **5**; (c) plot of $\log(q_e/C_e)$ versus (1/T).

The Temkin isotherm equation assumes that the heat of adsorption of all the molecules in layer decreases linearly with coverage due to adsorbent-adsorbate interactions, and that

the adsorption is characterized by a uniform distribution of the bonding energies up to some maximum binding energy. The Temkin isotherm[189,190] has been used in the following form:

$$q_e = \frac{RT}{b} \ln(aC_e) \qquad (10)$$

A linear form of the Temkin isotherm can be expressed as:

$$q_e = \frac{RT}{b} \ln A + \frac{RT}{b} \ln C_e \qquad (11)$$

$$q_e = B \ln A + B \ln C_e \qquad (12)$$

where R is gas constant (8.314 J mol^{-1} K^{-1}), T is temperature (K), A is the equilibrium binding constant (L/g) corresponding to the maximum binding energy, and constant $B = RT/b$ is related to the heat of adsorption. A plot of q_e versus ln C_e (Figure 7.5b) is used to calculate the Temkin isotherm constants A and B. Figure 7.5a and b illustrates that the adsorption of Sr^{2+} ions fitted well the Freundlich and Temkin isotherm models, thereby implying that the adsorption may occur as a heterogeneous surface adsorption. The Freundlich and Temkin isotherm model constants are given in Table 7.2.

Table 7.2 Freundlich and Temkin isotherm model constants for Sr^{2+} adsorption.

Freundlich isotherm model		
k_f ($mg^{1-1/n}$ g^{-1} $L^{1/n}$)	n	R^2
19.6	0.652	0.9930
Temkin isotherm model		
A (L g^{-1})	B (J/mol)	R^2
46.5	0.268	0.9758

7.3.10 Adsorption thermodynamics

Adsorption experiments were also performed to obtain the thermodynamic parameters. The adsorption capacity decreases with the increase of temperature, thus suggesting the exothermic nature of the adsorption process and the weakening of bonds between Sr^{2+} and active sites of adsorbents at high temperatures (Table 7.1). A plot of log (q_e/C_e) versus $1/T$ is displayed in Figure 7.5c. The thermodynamic parameters ΔG, ΔH and ΔS were calculated using vant-Hoff equation (Eq. (13)), and are tabulated in Table 7.3. The negative ΔG values ascertain the spontaneity of the adsorption process.

$$\log\left(\frac{q_e}{C_e}\right) = -\frac{\Delta H}{2.303RT} + \frac{\Delta S}{2.303R} \qquad (13)$$

Table 7.3 Thermodynamic Data for Sr^{2+} adsorption.

Temperature (K)	ΔG (kJ/mol)	ΔH (kJ/mol)	ΔS (J/mol K)	R^2
296	-4.03	-15.7	-39.5	0.9929
308	-3.56			
323	-2.97			

As the temperature increases, the ΔG values become less negative, indicating that the adsorption process is less favorable at the higher temperatures. The negative ΔH of -15.7 kJ mol^{-1} indicates the exothermic nature of the adsorption process; similar exothermic behavior ($\Delta H = -5.9$ and -5.2 kJ mol^{-1}) has been noted in two different reports describing the adsorption of Sr^{2+} on polyacrylonitrile/zeolite composite adsorbent[51] and Dowex 50W-X Resins.[165] The negative value of ΔS (-39.5 J mol^{-1} K^{-1}) is quite unexpected, however it suggests the decrease in randomness at the solid/solution interface during the adsorption process as a result of replacement of Na^+ with Sr^{2+}.

7.3.11 Desorption experiment

Desorption experiment was conducted to study the sorbent regeneration options. Sr^{2+} ions in the loaded resin were desorbed by stirring in a 0.1 M HNO_3 medium. The results indicated that the percentage efficiency of the desorption process to be 88%.

7.3.12 SEM and EDX images for CPZ 4 and CPZE 5 unloaded and loaded with Sr^{2+} ions

Unloaded CPZ **4** and CPZA **5** as well as loaded resin **5** were investigated by scanning electron microscopy (SEM). Unloaded resin (60 mg) were immersed in $Sr(NO_3)_2$ solution (500 ppm in Sr^{2+}, 20 mL) for 24 h at a pH of 3, filtered, and dried under vacuum until constant weight was achieved. Loaded and unloaded polymers were then sputter-coated for 2 min with a thin film of gold.

SEM and EDX images (Figure 7.6) show that the morphology has been altered by the adsorption of Sr^{2+} ions (cracked morphology to smooth); the EDX analysis (Figure 7.6a and b) shows that composition of unloaded CPZ**4** and CPZA **5** was similar to the proposed in Scheme 7.1, while the former has more tight surface morphology as a result of H-bonding involving COOH, the later confirms the presence of Na^+ with an open morphology as a result of repulsion between the negative charges of the CO_2^-. Figure 7.6c shows that the Sr^{2+} ions have displaced the sodium ions in CPZA **5** thus confirming the adsorption of the metal ions. The SEM and EDX confirmed that CPZA **5** could be used as an efficient adsorbent of Sr^{2+} in aqueous solutions at low concentrations.

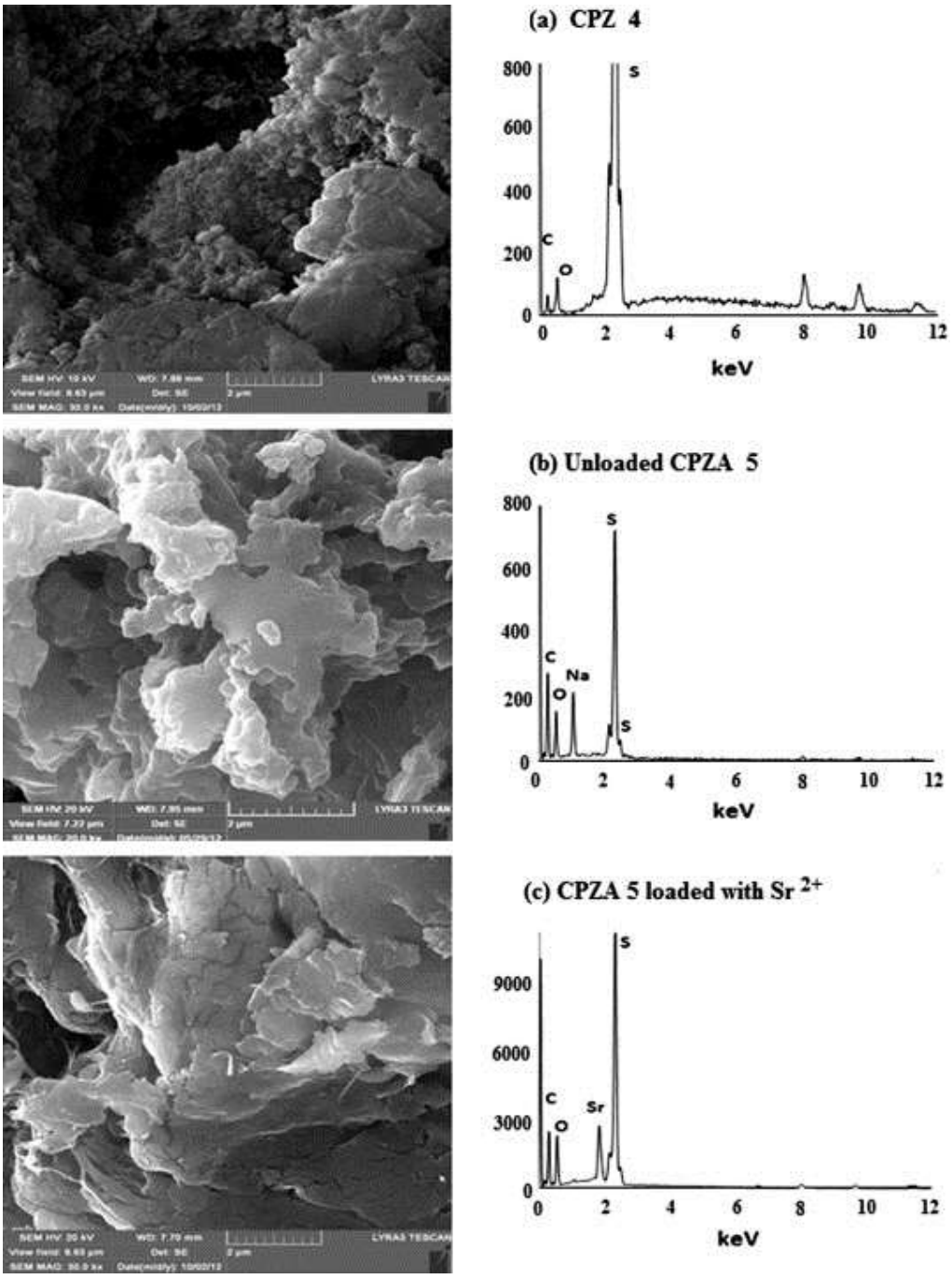

Figure 7.6 SEM images for (**a**) unloaded CPZ 4, (**b**) unloaded CPZA **5** and loaded **5** with Sr^{2+}.

7.4 Conclusion

A novel cross-linked polyzwitterion/anion (CPZA) was prepared using Butler's cyclopolymerization protocol. The CPZA provided an opportunity to test the efficacy of a zwitterionic/anionic group in the removal of a model metal ion in low concentrations. The resin was found to have a very good adsorption capacity for Sr^{2+}ions at low concentrations. The relatively strong rapid initial adsorption of 83% Sr^{2+} ions was followed by slower adsorption of the remaining 17% which was described by intraparticle diffusion model. The adsorption followed pseudo-second-order kinetic model and Temkin as well as Freundlich isotherm models. The negative ΔGs and ΔH ensured the spontaneity and the exothermic nature of the adsorption process. The excellent adsorption and desorption efficiencies implied the efficacy of the resin in removing as well as recovering the metal ions from aqueous solution. Given that the efficiencies of many investigated materials towards Sr^{2+} were low at low pH, the current CPZA seems to be promising for the removal of Sr^{2+} from acidic media.

CHAPTER 8

Adsorption of Cd^{2+} and Cu^{2+} ions from aqueous solutions by a cross-linked polysulfonate-carboxylate resin

Taken from Shamsuddeen A. Haladu, Othman Charles S. Al Hamouz and Shaikh A. Ali, Novel cross-linked polysulfonate-carboxylate resin for the removal of Cu^{2+} and Cd^{2+} from wastewater, *Arabian Journal of Chemistry*, 2013, (submitted)

Abstract

A new cross-linked polyzwitterion (CPZ) was synthesized through cyclocopolymerization of 3-[diallyl(carboxymethyl)ammonio]propane-1-sulfonate (92.5 mol %), and a cross-linker 1,1,4,4-tetraallylpiperazine-1,4-diium chloride (7.5 mol %) in the presence of tert-butylhydroperoxide. The cross-linked polyzwitterion/anion (CPZA) was obtained by the basification of CPZ with NaOH. The adsorption data fits both Temkin and Freundlich isotherm models. The adsorption trend on CPZA is as Cu^{2+} > Cd^{2+} and both followed pseudo-second-order kinetic model. The negative ΔG and positive ΔH values ascertained the spontaneous and endothermic nature of the adsorption process. The efficacy of a zwitterionic-anionic motif consisting of quaternary nitrogen, sulfonate and carboxylate groups has been tested for the first time for capturing Cd^{2+} and Cu^{2+} ions at low concentrations.

8.1 Introduction

Heavy metal ions existence in the environment poses formidable health problems to various living organisms due to their inherent toxicity which can even lead to death.[35,191] The contamination of water by cadmium occurs majorly *via* metal plating, cadmium–nickel batteries, mining, smelting and phosphate fertilizers among others. The toxicity of cadmium in human body leads to emphysema, hypertension, renal damage and testicular atrophy[192] and also enlisted by USEPA as an endocrine disruptor and priority control pollutant.[193] However, copper pollution emanates from brass manufacture, copper mining, electroplating industries, smelting, Cu-based agri-chemicals,[192] paint manufacturing and copper polishing. The intake of copper can cause diseases such as vomiting, diarrhea, nausea, liver and kidney damage.[194]

The threshold level stipulated by WHO for cadmium in drinking water is 0.003 mg/L[44] and that of copper is 0.2 mg/L.[42] In view of the above, the treatment of cadmium and copper contaminated waters is of utmost importance before discharge.

Several methods have been employed in the treatment of metal contaminated waters. Among them are; reverse osmosis, precipitation, dialysis, extraction, adsorption and ion exchange, of which adsorption has received a remarkable attention likely by virtue of the existence of a variety of inexpensive green adsorbents.[195,196] Polyzwitterions bearing pH-responsive groups have experienced increased attention academically and industrially[6,171] and found applications in water treatment, petroleum recovery, coatings, drag reduction, cosmetics and viscosification. Recently, several zwitterionic hybrid materials have been used effectively to remove toxic metal ions.[36,62]

In this study, the synthesis of a cross-linked polymer from a monomer having dual functionalities of anionic and zwitterionic groups has permitted us to test its efficiency for capturing Cd^{2+} and Cu^{2+} from aqueous solutions at low concentrations. This study, to our knowledge, would reveal for the first time the employment of a zwitterionic-anionic framework for Cd^{2+} and Cu^{2+} ions removal.

8.2 Experimental

8.2.1 Physical Methods

An Elemental Analyzer Series II (Perkin Elmer: Model 2400) was used to carry out elemental analysis. IR spectra were obtained using a Perkin Elmer 16F PC FTIR spectrometer. ^{1}H and ^{13}C spectra were measured in a JEOL LA 500 MHz spectrometer with the residual proton resonance of the D_2O (at δ 4.65 ppm) and dioxane carbon resonance (at δ 67.4 ppm) as internal standards, respectively. An Atomic absorption spectroscopy (AAS) model iCE 3000 series (Thermo Scientific) was used to carry out the metal analysis. A TESCAN LYRA 3 (Czech Republic) instrument having an energy-dispersive X-ray spectroscopy (EDX) detector (model: X-Max, Oxford) was used to obtain the scanning electron microscopy (SEM) images. A thermal analyzer (STA 429, Netzsch, Germany) was employed to carry out thermogravimetric analysis (TGA) using a temperature range 20–800 °C (10 °C/min) and air flowing at a rate of 100 mL/min.

8.2.2 Materials

t-Butylhydroperoxide (TBHP) (70% in water), diallylamine and 1,3-propanesultone from Fluka Chemie AG (Buchs, Switzerland) were utilized.

8.2.3 Zwitterionic ester 1 and acid 2

The monomer (**1**) and the corresponding acid (**2**) were synthesized as reported in. [123]

8.2.4 1,1,4,4-tetraallylpiperazine-1,4-diium chloride (4)

Monomer **4**, a cross-linker, was prepared as described.[69]

8.2.5 Copolymerization of 2 and 4

The monomer **2** (13.9 g, 50 mmol) and cross-linker **4** (1.3 g, 4.05 mmol) were dissolved in deionized water followed by the addition of TBHP (375 mg). The mixture in a closed flask was stirred for 24 h at 85 °C. After several hours, the magnetic stir-bar became static. The gel-like polymer was transferred to water and allowed to soak with repeated change of water. The resin **5** was soaked in hot acetone, filtered and then dried *in vacuo* at 70 ^{o}C (8.75 g, 62.2%).

8.2.6 Transformation of CPZ 5 to cross-linked polyzwitterion/anion (CPZA) 6

CPZ **5** (7.35 g, 26.1 mmol) mixed with sodium hydroxide (1.36 g, 34 mmol) in water (33 ml) were stirred for 24 h. After adding excess methanol, resin **6** was filtered and then dried *in vacuo* at 65 ^{o}C (6.8 g, 87 %). At 280^{o}C initial decomposition of the resin was shown by TGA analysis.

8.2.7 Adsorption experiments

CPZA **6** (50 mg) was mixed with aqueous $Cd(NO_3)_2$ (1 mg L^{-1}) solution (20 mL) at different pH and stirred for 24 h. The amount of Cd^{2+} remained in the filtrate was measured by AAS. Using Eq. 1, the adsorption capacity ($q_{Cd^{2+}}$) in mg g^{-1} was calculated:

$$q_{Cd^{2+}} = \frac{(C_0 - C_f)V}{W} \qquad (1)$$

where C_f and C_o represent the respective final and initial concentration (mg L^{-1}) of Cd^{2+}, V and W are the respective volume (L) of the solution and the weight (g) of the polymer. The data from the triplicate experiments varied within 4%. The adsorption capacity (q) at equilibrium and various times are designated as q_e and q_t, respectively, while C_e denotes the equilibrium concentration of the metal ions.

Evaluation of the adsorption isotherm was accomplished in the Cd^{2+} concentration range 200 µg L^{-1} (i.e. ppb) to 1000 µg L^{-1} for 24 h at 294 K. The adsorption kinetic experiments were carried out using 1 mg L^{-1} $Cd(NO_3)_2$ solution at different times at a pH of 3 at 294, 308 and 328 K. The data obtained was used to calculate k_2 (the pseudo-second-order rate constant) of the adsorption process and its energy of activation (E_a). The thermodynamic parameters, ΔG, ΔH and ΔS were determined using the q_e and C_e values. In the same way, the adsorption of Cu^{2+} ions using $Cu(NO_3)_2$ solution were conducted.

8.2.8 FT IR spectroscopy

FTIR spectra of the loaded and unloaded resins have been recorded. About 30 mg of the unloaded resin in 0.1 M $Cd(NO_3)_2$ solution (20 mL) at pH of 3 was stirred for 4 h, filtered, and dried under reduced pressure to a constant weight.

8.3 Results and discussion

8.3.1 Synthesis of CPZA 6.

The present resin **6** (Scheme 8.1) has been prepared by cyclopolymerization reaction. The cyclopolymerization involving various *N*,*N*-diallylammonium monomers has generated

various water-soluble cationic polyelectrolytes.[5] Recently, a resin having aminophosphonate groups has been synthesized *via* cyclopolymerization and evaluated for its efficacy in the removal of toxic metal ions.[35]

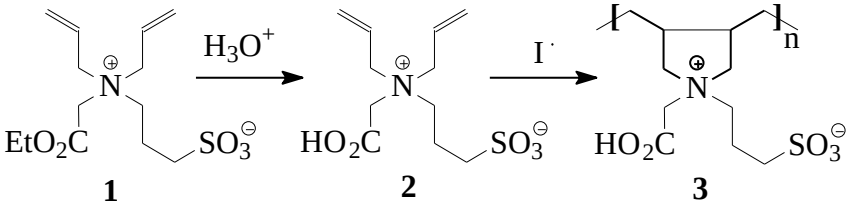

1 **2** **3**

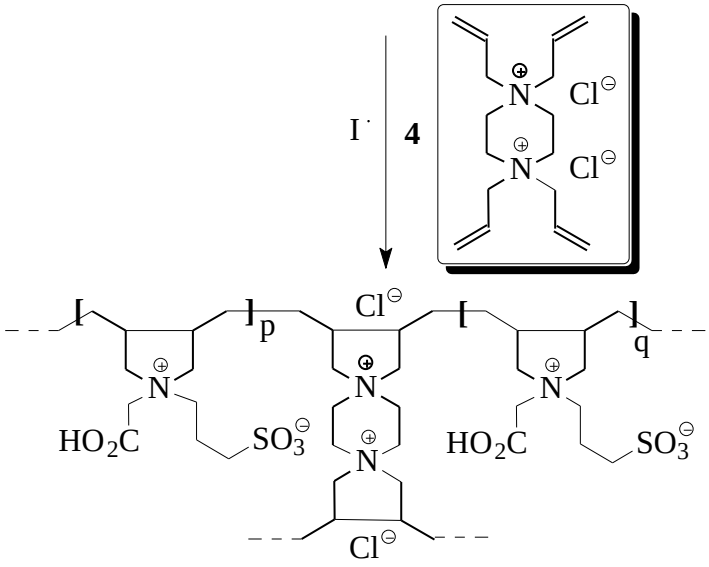

5: Cross-linked polyzwitterion (CPZ)

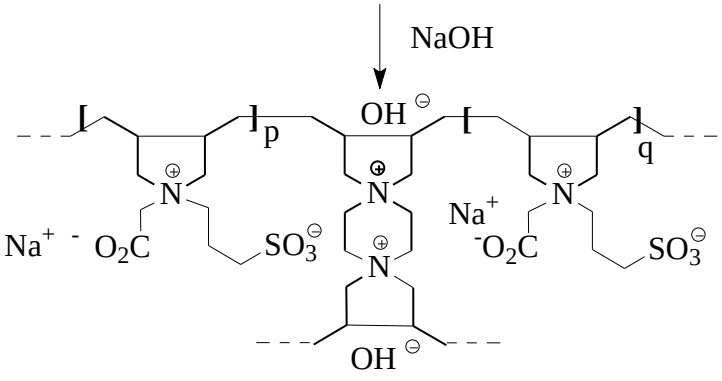

6: Cross-linked polyzwitterion/anion (CPZA)

Scheme 8.1 Synthesis of monomer and cross-linked polymers.

A mixture of monomer **2** (92.5 mol %), cross-linker **4** (7.5 mol %) in water were cyclocopolymerized using TBHP as an initiator giving CPZ **5** (Scheme 8.1). Upon treatment of the CPZ **5** with excess NaOH, CPZA **6** was formed. A mol ratio of ≈93:7 for monomer **2** /cross-linker **4** as determined by elemental analysis of CPZ **5** was similar to the feed ratio.

Three major weight losses were revealed in the TGA curve of CPZA **6** (Figure 8.1). The first slow weight loss of 3.0 % resulted from the release of water trapped in the cross-linked polymer. The first sharp loss of 22.4% resulted from the release of SO_2, the second loss of 28.9% and the third loss of 7.7% were associated with the respective decarboxylation of the carboxylates and the degradation of the nitrogenated organic fraction.[134] At 800 ^{o}C, the residual mass was found to be 38%.

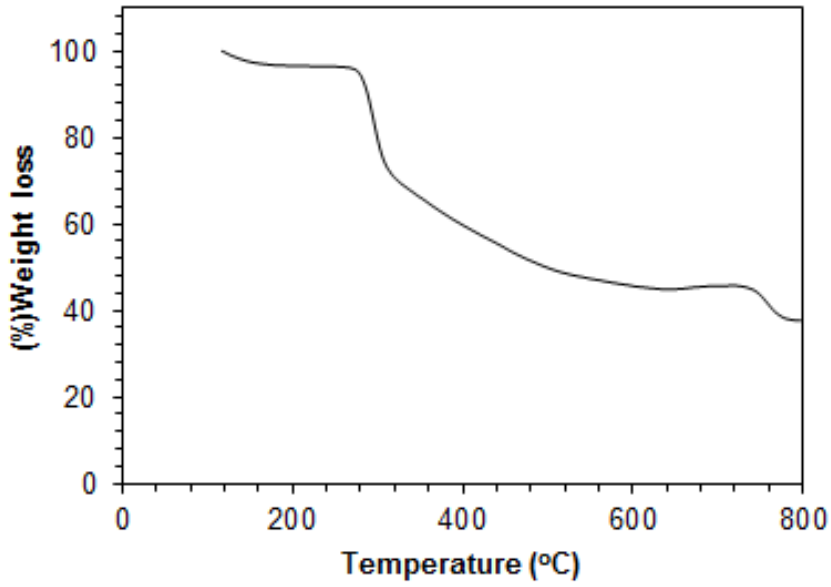

Figure 8.1 TGA curve of CPZA **6**.

8.3.2 Characterization of synthesized materials using FTIR

The IR spectrum of CPZ **5** shows strong absorption bands at 1197 and 1041, which are attributed to the sulfonate groups.[126] The absorption at 1734 cm^{-1} indicates the presence C=O stretch of COOH[80] (Figure 8.2a).

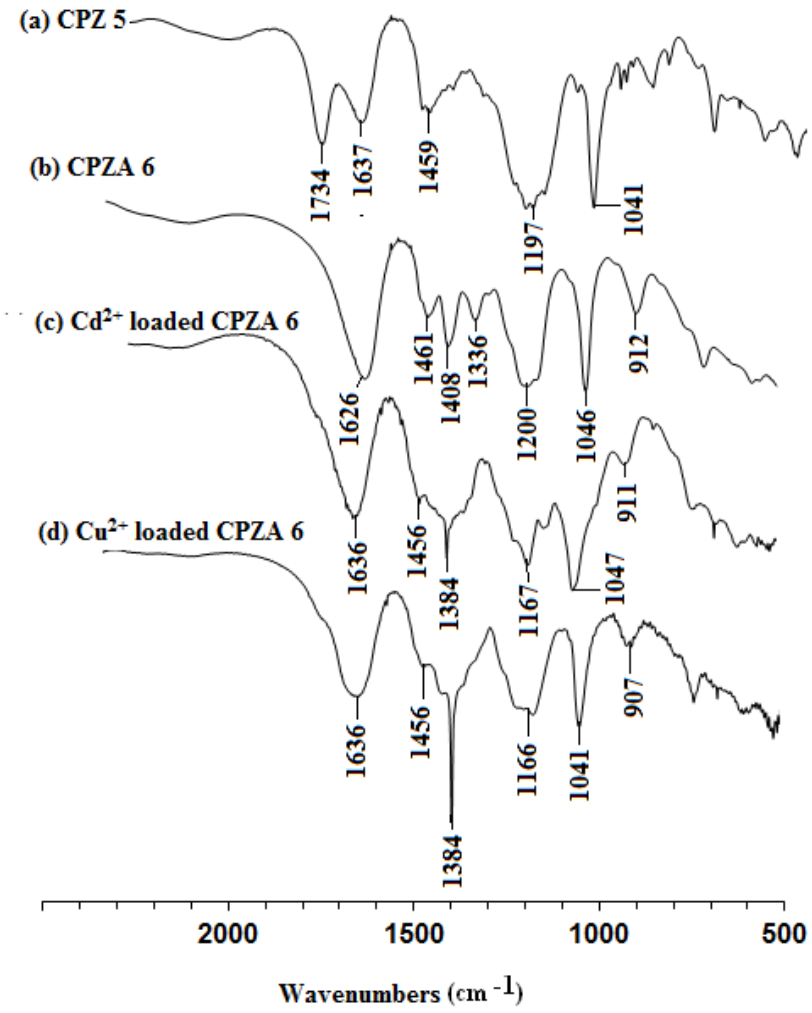

Figure 8.2 IR spectra of (a) cross-linked CPZ **5** (b) CPZA **6** (c) Cd^{2+} loaded CPZA **6** (d) Cu^{2+} loaded CPZA **6**.

The C=O (of COOH) stretching absorption was missing in the unloaded resin CPZA **6**; however, the absorptions at 1408 and 1626 cm^{-1} were attributed to the symmetric and

antisymmetric stretching of COO^- (Figure 8.2b). The new band that appears at 1384 cm^{-1} (Figure 8.2c and 8.2d) was assigned to the NO_3^- group due to the adsorption process being carried out using copper and cadmium nitrates.[173] Thus, the resin can also act as an anion exchanger due to the presence of this new band. The increased intensity and broadness of the SO_3^- and C=O peaks of the resin loaded with Cu^{2+} and Cd^{2+} (Figure 8.2c and 8.2d) indicated the adsorption of the metal ions.[174]

8.3.3 Adsorption kinetics.

The kinetics for the removal of Cu^{2+} and Cd^{2+}on CPZA **6** is presented in Figures 8.3d and 8.4d, which depict the changes in adsorption capacity with adsorption time at different temperatures. The adsorption process was relatively fast as it reached the equilibrium within 40 min. At higher temperatures, the adsorption capacities increased indicating larger swelling allowing more ions to be diffused and adsorbed on CPZA **6**.

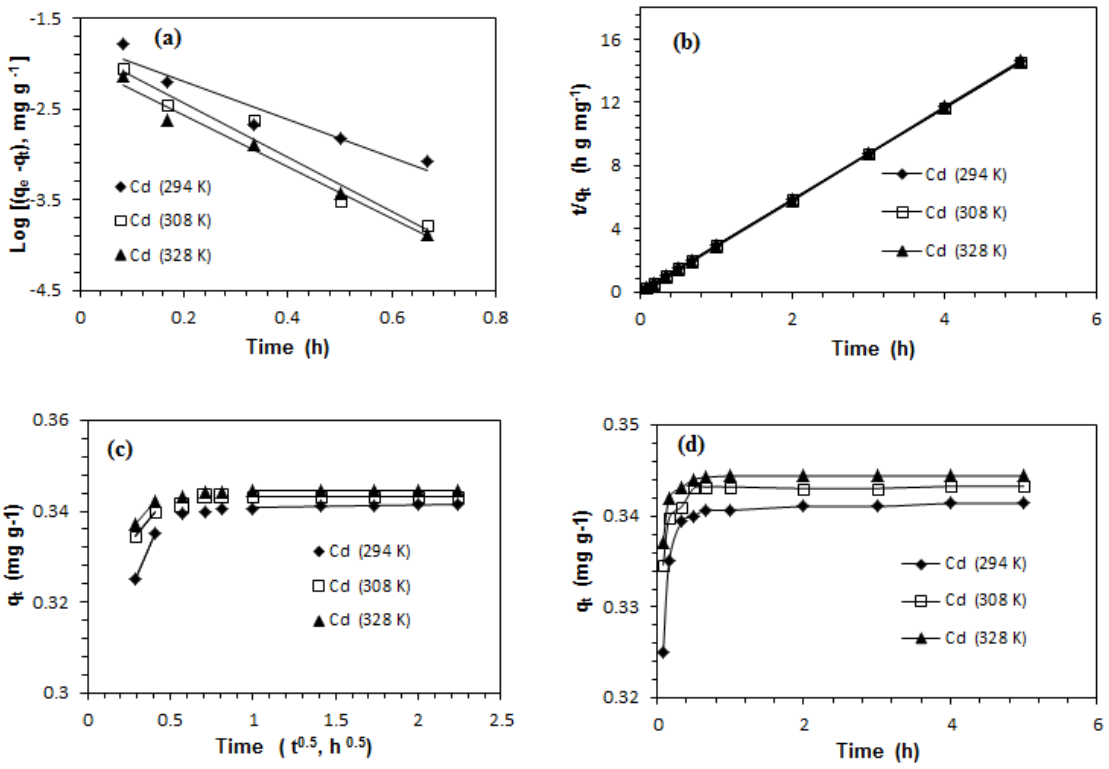

Figure 8.3 The adsorption of Cd^{2+} (1.00 ppm) on CPZA **6** at pH 3 fitted to (a) Lagergren first-order kinetic model; (b) Lagergren second-order kinetic model; (c) Intraparticle diffusion model; and (d) Adsorption kinetic curve.

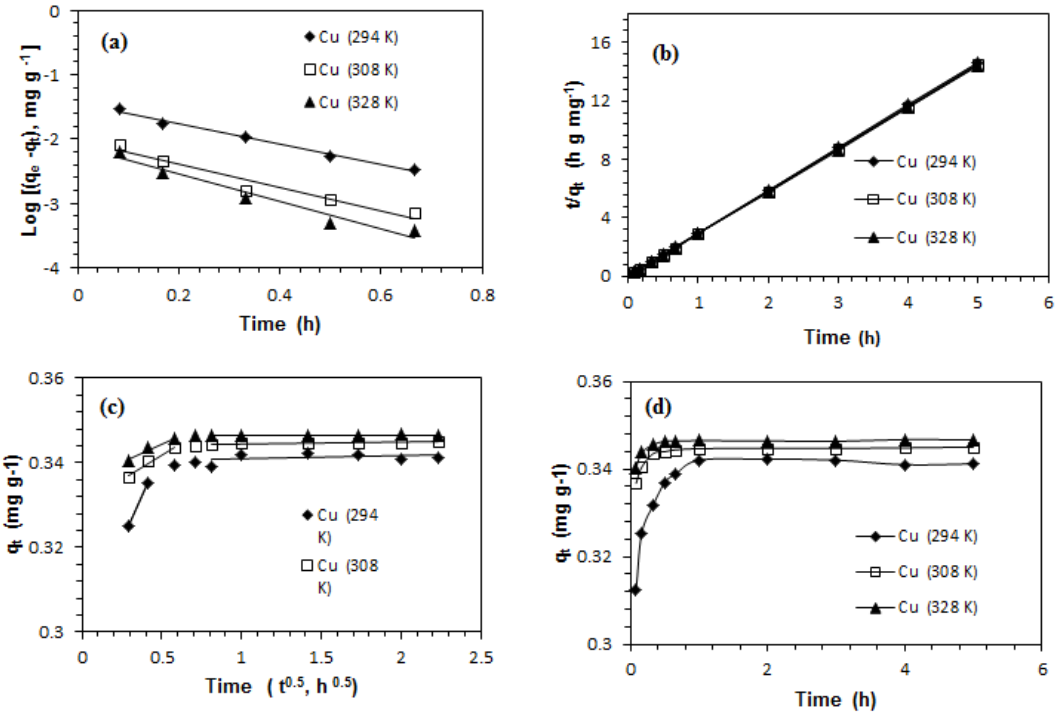

Figure 8.4 The adsorption of Cu^{2+} (1.00 ppm) on CPZA **6** at pH 3 fitted to (a) Lagergren first-order kinetic model for; (b) Lagergren second-order kinetic model; (c) Intraparticle diffusion model; and (d) Adsorption kinetic curve.

8.3.4 Lagergren first-order kinetics

Lagergren first-order kinetics assumes that each metal ion occupies one adsorption site. The following equation describes the model:

$$\log(q_e - q_t) = \log q_e - \frac{k_1 t}{2.303} \qquad (2)$$

where q_t and q_e (mg g^{-1}) are the adsorption capacities at time t (h), and at equilibrium respectively, and k_1 is the first-order rate constant. The intercept and slope of the plots of $\log(q_e-q_t)$ versus t (Table 8.1, Figure 8.3a and 8.4a) were used to evaluate q_e and k_1 experimentally. Only the data of the low time region was found to fit the model; hence the longer time region was neglected.

Table 8.1 Kinetic parameters for Cd^{2+} and Cu^{2+} ions[a] adsorption.

			Lagergren first- order			*Lagergren second-order*				
Metal ion	Temp (K)	$q_{e,\,exp}$ (mg g^{-1})	k_1 (h^{-1})	$q_{e,\,cal}$ (mg g^{-1})	R^2	k_2 ($h^{-1}g\ mg^{-1}$)	h[b] ($h^{-1}g^{-1}$ mg)	$q_{e,\,cal}$ (mg g^{-1})	R^2	E_a (kJ mol^{-1})
Cd^{2+}	294	0.341	4.81	0.016	0.9285	1008.19	23.4	0.3416	1	25.5
	308	0.343	6.94	0.014	0.9573	2068.37	30.4	0.3434	0.999	
	328	0.344	6.52	0.009	0.9813	3008.75	48.5	0.3445	1	
Cu^{2+}	294	0.341	3.66	0.035	0.986	538.16	9.43	0.3419	1	37.3
	308	0.345	4.16	0.009	0.9387	538.16	13.3	0.3451	1	
	328	0.349	-4.91	0.007	0.9516	1584.49	16.1	0.345	1	

[a]Initial metal ion concentration 1 mg/L. [b]Initial adsorption rate $h = k_2\, q_e^{\,2}$.

However, there is a wide disagreement between the equilibrium adsorption capacities using first-order equation ($q_{e,\,cal}$ = 0.016 mg g^{-1} for Cd and 0.035 for Cu at 294 K) and the ones observed experimentally ($q_{e,\,exp}$ = 0.341 mg g^{-1} for both Cd and Cu at 294 K). The Lagergren first-order kinetic equation thus cannot describe the exchange process (Table 8.1).[178]

8.3.5 Pseudo-second-order kinetics

The second-order kinetic equation for the adsorption of the metal ions can be expressed in linear form by the equation below:

$$\frac{t}{q_t} = \frac{1}{k_2 q_e^{\,2}} + \frac{t}{q_e} \qquad (3)$$

where adsorption capacities are described by q_t and q_e at the respective time of t and at equilibrium, and k_2 represents the second-order rate constant.

Figure 8.3b, 8.4b and Table 8.1 proved that the adsorption of Cd^{2+} and Cu^{2+} fits with the second-order kinetic equation implying that the exchange of metal ions was likely to be a chemical.[180] Likewise, the experimentally observed equilibrium adsorption capacities were in conformity with those derived from Eq. (3)

8.3.6 Adsorption activation energy

The kinetic rate constants (k_2) model was used to calculate the adsorption energy of activation (Table 8.1) using the Arrhenius equation (Eq. 4):

$$\ln k_2 = -\frac{E_a}{2.303RT} + \text{constant} \qquad (4)$$

where k_2 is the rate constant (g mg^{-1} h), R, E_a and T represent the gas constant (8.314 J mol^{-1} K), energy of activation (kJ mol^{-1}) and temperature (K), respectively. A straight line plot of ln k_2 versus $1/T$ gives a slope of $-E_a/R$ (Figure 8.5 and Table 8.1). The energy of activation for the adsorption of Cd^{2+} and Cu^{2+} were found to be 25.5 kJ mol^{-1} and 37.3 kJ mol^{-1} respectively.

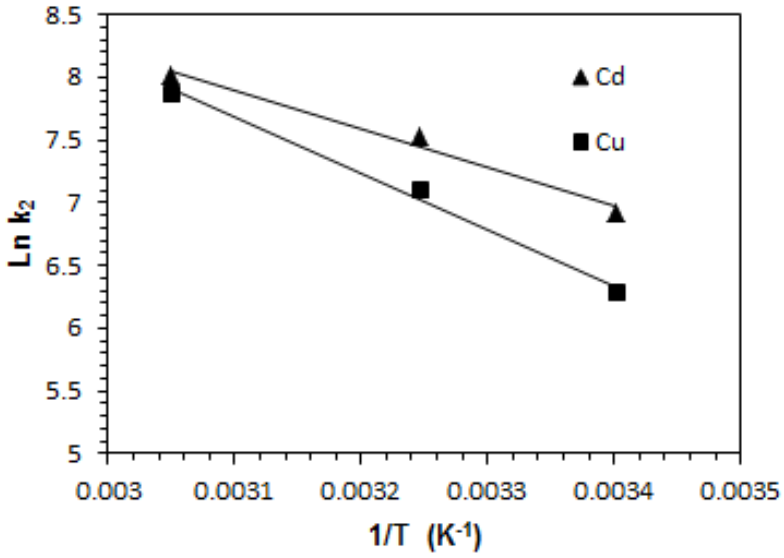

Figure 8.5 The Arrhenius plot for the metal adsorptions.

8.3.7 Intraparticle diffusion model

The determination of the rate-limiting step paves the way to understand the adsorption mechanism. Different adsorption diffusion models are constructed based on three steps: first, film diffusion; second, intraparticle diffusion and third, mass action. According to intraparticle diffusion model, there exist interfacial movements (i.e., film diffusion) of the metal ions between the adsorbent and the solution, then a subsequent intraparticle diffusion rate-limiting step which deliver the ions into the adsorbent pores. The relation of the adsorption capacity and time[182,184] is expressed as:

$$q_t = x_i + k_p t^{0.5} \qquad (5)$$

where k_p is the intraparticle diffusion rate constant, q_t is the adsorption capacity at time t and x_i is related to the thickness of the boundary layer. In accordance with the Weber–

Morris model,[181,182] intraparticle diffusion is the rate-limiting step if a linear fit for the q_t versus $t^{0.5}$ plot passes through the origin.

Table 8.2 Intraparticle Diffusion constants and intercept values for the adsorption of Cd^{2+} and Cu^{2+}ions at different temperatures.

Metal ion	Temp (K)	k_p (mg g^{-1} $h^{0.5}$)	Intercept values (x_i)	R^2
Cd^{2+}	294	0.0843	0.3007	1
	308	0.0436	0.3221	1
	328	0.0406	0.3255	1
Cu^{2+}	294	0.0843	0.3007	1
	308	0.0233	0.3304	0.9757
	328	0.0177	0.3357	0.93

The values of the intercept x_i in the initial linear plots for Cd^{2+} were found to be 0.3007, 0.3221, and 0.3255 mg g^{-1} at 21, 35, and 55°C, respectively (Figure 8.3c). The corresponding values of 0.3007, 0.3304, and 0.3357 mg g^{-1} for Cu^{2+} confirms the similar trend of increasing x_i with the increase in temperature (Figure 8.4c). An intercept exists in the initial linear plot indicating the occurrence of rapid adsorption. The initial adsorption factor (R_i) was defined in terms of the x_i as:

$$R_i = 1 - \frac{x_i}{q_e} \qquad (6)$$

where x_i and q_e are the respective initial adsorption and the final adsorption at the longer time. For Cd^{2+} and Cu^{2+} ions, the x_i *and* q_e values of 0.3007 (Figure 8.3c) and 0.341 mg g^{-1}, respectively, at 21 °C gave an R_i value of 0.12 which means about 88% of the intial adsorption has taken place before 5 min. The other 12% of adsorption is controlled by

intraparticle diffusion. Hence, the intraparticle diffusion within the pores of the resins became the rate-limiting step. Note that the horizontal line depicts the equilibrium stage.

8.3.8 Effect of pH on the adsorption

The pH effect (in the range 3-6) on the adsorption of Cd^{2+} and Cu^{2+} on CPZA **6** was studied at 21 ^{o}C and a fixed concentration (1 mg L^{-1}) for 24 h. The solutions pH was maintained using a buffer of acetic acid/sodium acetate. The adsorption of metal ions with the variation of pH is displayed in Figure 8.6a. The best pH was observed to be 3; the adsorption capacity was found to increase with further increase in the pH, after the minimum observed at pH 5. Carboxyl and sulfonate groups may capture Cd^{2+} and Cu^{2+} ions by chelation. The respective pK_a values of SO_3H and CO_2H functionalities in CPZA **6** are known to be –2.1 and +2.5.[80]

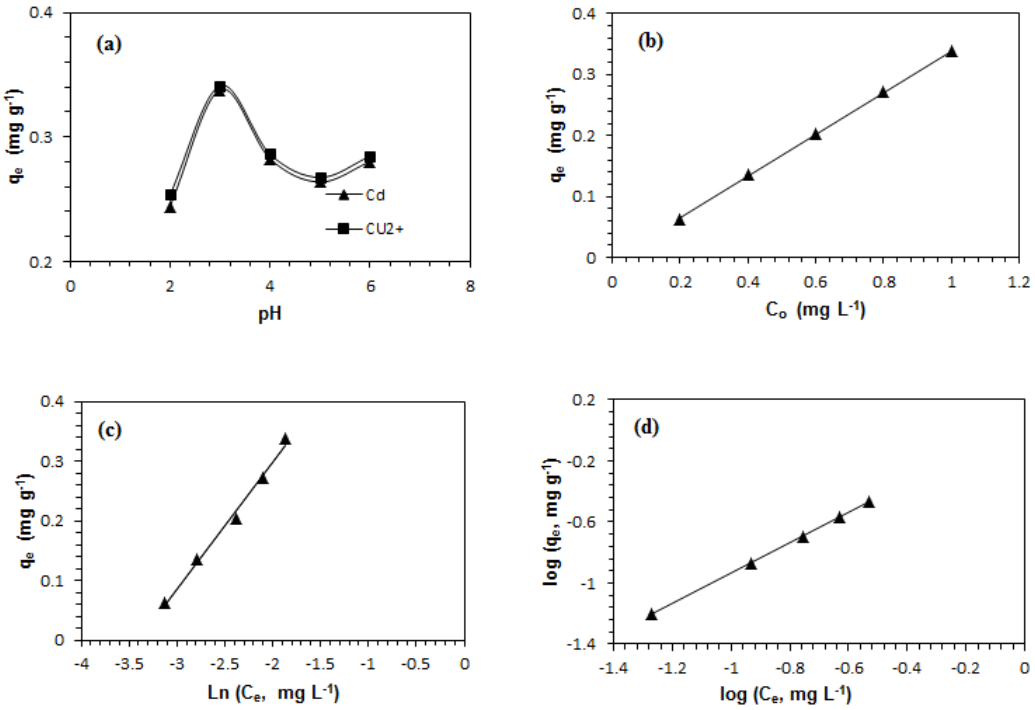

Figure 8.6 (a) The pH versus adsorption capacity of CPZA for1.00 ppm Cd^{2+} solution for 24 h; (b) The initial concentration of Cd^{2+} versus adsorption capacity of CPZA **6** at pH 3 for 24 h at 21°C; (c) Temkin isotherm for Cd^{2+} adsorption on CPZA **6**; (d) Freundlich isotherm for Cd^{2+} adsorption on CPZA **6**.

At pH 3 or even at 2, the acid-base equilibria will involve a certain portion of CO_2^- while most of the SO_3H will exist in the conjugate base form of SO_3^-. Low adsorption of Cd^{2+} and Cu^{2+} at pH < 3 could be attributed to competition of H^+ ions with Cd^{2+} and Cu^{2+} ions for the exchange sites in the adsorbent. The metal hydroxides, which are formed owing to the hydrolysis of the metal ions at higher pH values, can compete with the resin for the uptake of the metal ion.[188] The optimal pH of 3 was chosen for the adsorption studies.

8.3.9 Adsorption isotherms

The adsorption capacity of CPZA **6** increases as the initial concentration of Cu^{2+} and Cd^{2+} ions increases, Figures 8.6b and 8.7a. The mechanism of the adsorption was

investigated by analysis of the data using Freundlich, Langmuir and Temkin isotherm models. The Langmuir isotherm model,[186] based on a monolayer adsorption process on homogeneous surfaces where a negligible interaction occurs between the adsorbed molecules, can be expressed by Eq. (7):

$$\frac{C_e}{q_e} = \frac{C_e}{Q_m} + \frac{1}{Q_m b} \qquad (7)$$

where C_e and q_e are the respective metal ion concentrations in the solution and adsorption capacity of resin, Q_m and b are the Langmuir constants. The constants Q_m and b are obtained from the slope and intercept of C_e/q_e versus C_e plot. The Langmuir isotherm model plots for the adsorption of Cu^{2+} and Cd^{2+} on the resin have not been presented due to the non-fitting of the data.

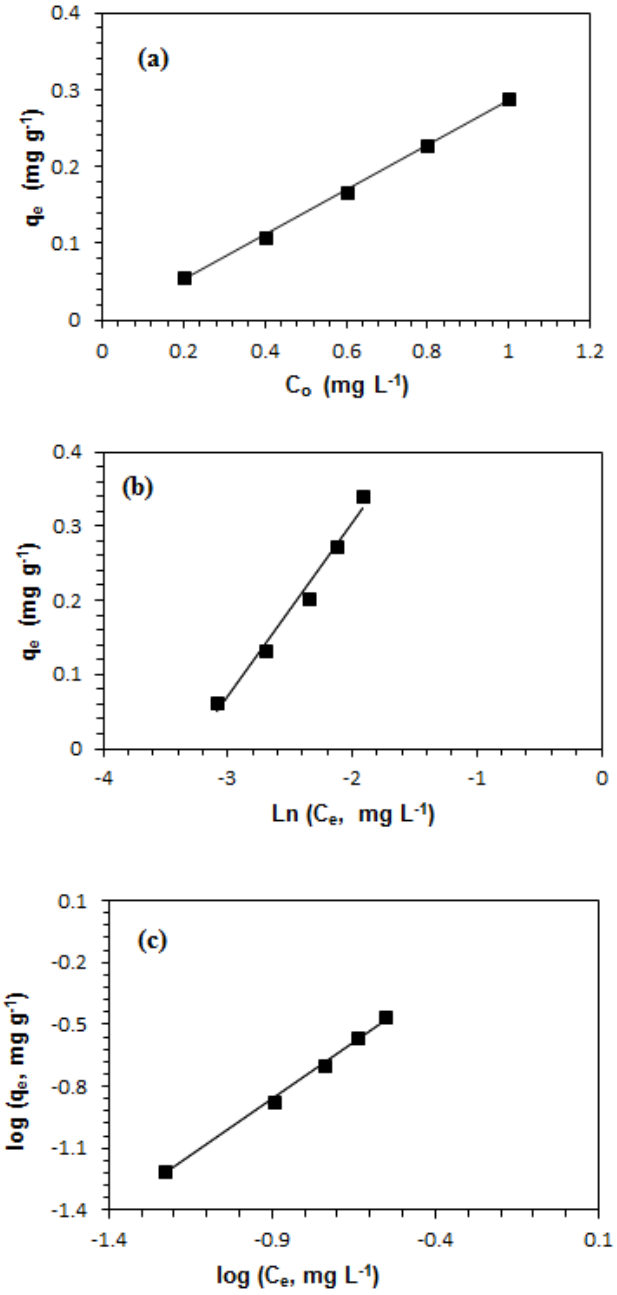

Figure 8.7 (a) The initial concentration of Cu^{2+} versus adsorption capacity of CPZA **6** at pH 3 for 24 h at 21°C; (b) Temkin isotherm for Cu^{2+} adsorption on CPZA **6**; (c) Freundlich isotherm for Cu^{2+} adsorption on CPZA **6**.

However, Freundlich isotherm model (as expressed by Eqs. (8) and (9) assumes that a heterogeneous surface with uniform energy is involved with a multilayer non-ideal adsorption:

$$q_e = k_f\, C_e^{\,1/n} \qquad (8)$$

$$\log\, q_e = \log k_f + \frac{1}{n}\log C_e \qquad (9)$$

where q_e and C_e represent the respective equilibrium absorption capacity of the resin and concentration of metal ion in the liquid phase, k_f and n denote the Freundlich constants (Table 8.1), obtainable from the slope and intercept of the log q_e versus log C_e in Figure 8.6d and 8.7c. An adsorption is considered favorable if the values fall within the range of 1 to 10. The slope (1/n) range of 0 - 1 is described as a surface heterogeneity or a measure of adsorption intensity, which become more heterogeneous when its value approaches zero. A chemisorption process occurs for *1/n* value below unity, while *1/n* above one implies cooperative adsorption (Table 8.3).[188]

Table 8.3 Isotherm model constants for Cd^{2+} and Cu^{2+} ions adsorption.

	Freundlich isotherm model		
Metal ion	k_f ($mg^{1-1/n}$ g^{-1} $L^{1/n}$)	n	R^2
Cd^{2+}	1.13	1.0115	0.9999
Cu^{2+}	1.35	0.9074	0.997
	Temkin isotherm model		
	A (L g^{-1})	B (J/mol)	R^2
Cd^{2+}	30.1	0.2116	0.9991
Cu^{2+}	26.9	0.2356	0.9814

The Temkin isotherm equation assumes a linear decrease in the heat of adsorption of all the molecules in a layer with the increase in the surface coverage owing to the adsorbent-adsorbate interactions. The Temkin isotherm[189] can be expressed as Eqs (10)-(12):

$$q_e = \frac{RT}{b}\ln(aC_e) \qquad (10)$$

$$q_e = \frac{RT}{b}\ln A + \frac{RT}{b}\ln C_e \qquad (11)$$

$$q_e = B\ln A + B\ln C_e \qquad (12)$$

where R, T, and A represent gas constant (8.314 J mol^{-1} K^{-1}), temperature (K), and equilibrium binding constant (L/g) corresponding to the maximum binding energy, respectively. Constant B (i.e. RT/b) is related to the heat of adsorption. Temkin isotherm constants A and B, calculated from the plot of q_e versus lnC_e (Figure 8.6c and 8.7b), are given in Table 8.3. The adsorption of Cd^{2+} and Cu^{2+} ions fitted well with the Temkin

isotherm model as shown in Figure 8.6c and 8.7b. This ascertains that the adsorption encounters a heterogeneous surface.

8.3.10 Adsorption thermodynamics

The thermodynamic parameters of the adsorption were also determined. The endothermic nature of the adsorption was ascertained by the increase in the adsorption capacity as the temperature increases. A log (q_e/C_e) versus 1/T plot is shown in Figure 8.8.

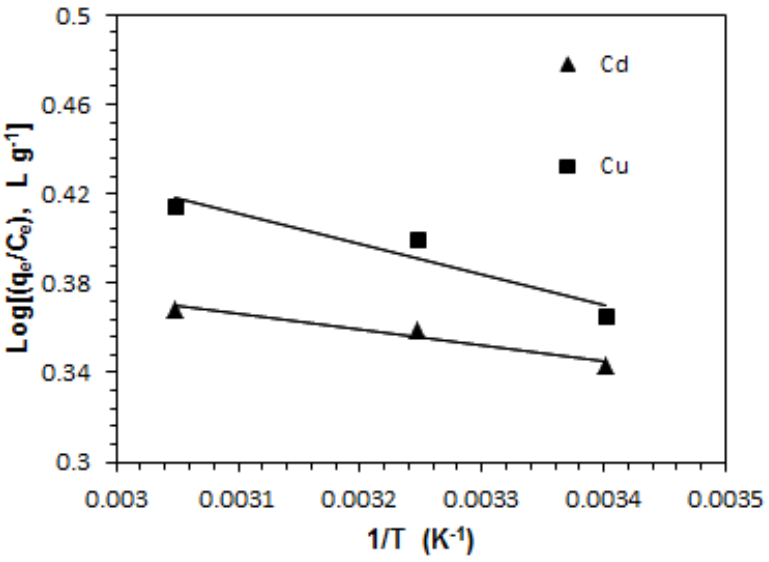

Figure 8.8 Vant-Hoff plot.

Vant-Hoff equation (Eq.12) was employed to calculate the thermodynamic parameters ΔS, ΔH and ΔG and tabulated in Table 8.4.[178] The negative values of ΔG confirmed the spontaneity of the exchange process.

$$\log\left(\frac{q_e}{C_e}\right) = -\frac{\Delta H}{2.303RT} + \frac{\Delta S}{2.303R} \qquad (12)$$

The ΔG values become more negative with the increase in temperatures, thereby indicating more favorable adsorption process at the higher temperatures because of greater swelling and increased diffusion of the metal ions into the resin. The positive values of ΔH is an indication of endothermic adsorption process. The ΔS values for the adsorption process were positive (Table 8.4) owing to the release of water molecules from the metal ions' large hydration shells.

Table 8.4 Thermodynamic parameters for Cd^{2+} and Cu^{2+} adsorptions.

Metal ion	Temperature (K)	ΔG (kJ/mol)	ΔH (kJ/mol)	ΔS (J/mol K)	R^2
Cd^{2+}	294	-1.94	1.36	11.2	0.9563
	308	-2.1			
	328	-2.32			
Cu^{2+}	294	-2.08	2.61	16	0.9155
	308	-2.31			
	328	-2.63			

8.3.11 SEM and EDX images for CPZA 6 unloaded and loaded with Copper and Cadmium ions

SEM has been used to examine both the unloaded and loaded resins. For this purpose, the unloaded resins were stirred in 0.1 M $Cu(NO_3)_2$ and 0.1 M $Cd(NO_3)_2$ at a pH of 3 for 24 h. The resins were filtered, and dried *in vacuo* to constant weights. Both resins were then sputter-coated for 4 min with a thin film of carbon.

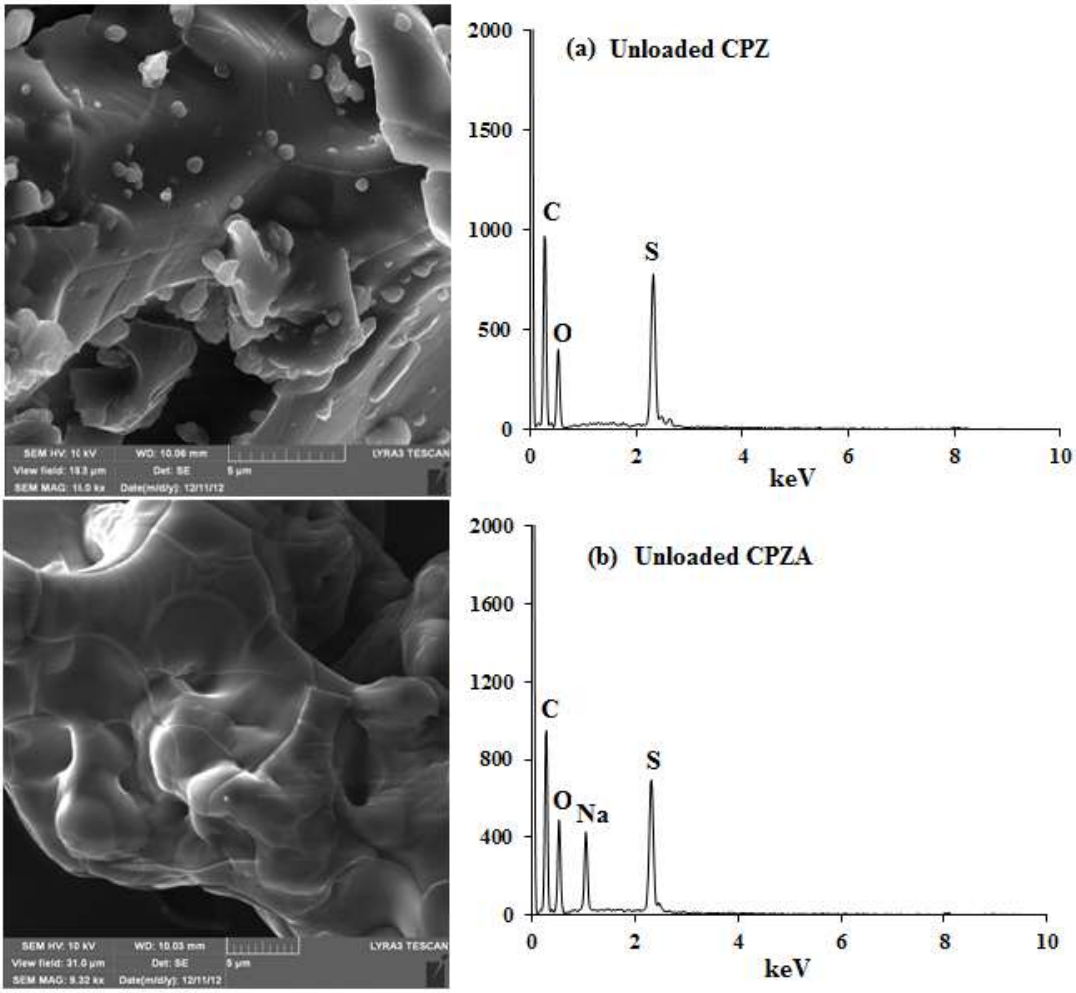

Figure 8.9 SEM and EDX images for (a) Unloaded CPZ **5** (b) Unloaded CPZA **6**.

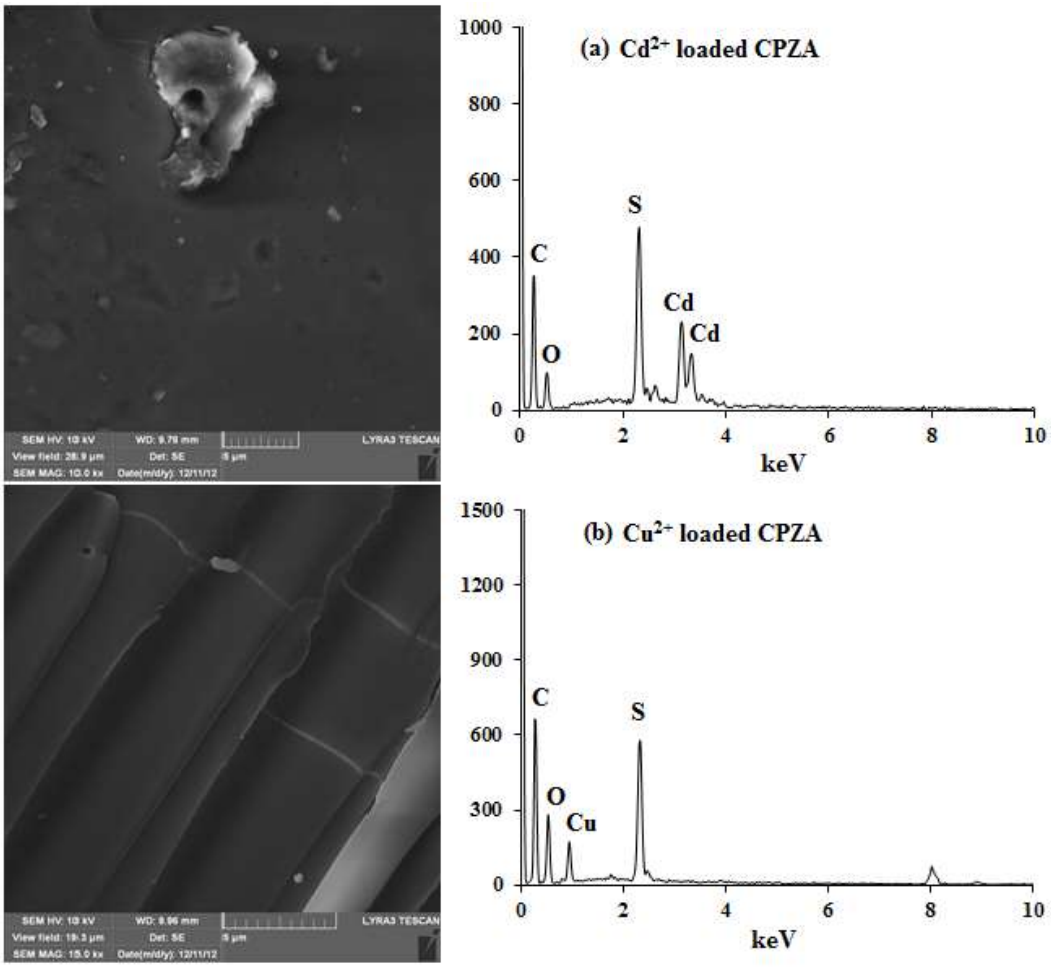

Figure 8.10 SEM and EDX images for (a) Cd^{2+} loaded CPZA **6** (b) Cu^{2+} loaded CPZA **6**.

The SEM image of the unloaded CPZ **5** and CPZA **6** (Figure 8.9a and b) reveals that the surface morphology of CPZ **5** is tighter due to the H-bonding among the COOH groups, while the open morphology of CPZA **6** confirms the presence of Na^{+} due to the repulsion between the negative charges of the CO_2^{-}. The corresponding EDX analysis shows that the composition of was similar to the proposed in scheme 8.1.

Due to the change in morphology of the SEM images (Figure 8.9 and 8.10) from cracked to smooth, it indicates that the adsorption of cadmium and copper ions had occurred on

the resin. Likewise, the displacement of the sodium ions in CPZA **6** by cadmium and copper ions, Figure 8.10a and b confirmed the adsorption of the metal ions.

8.4 Conclusion

Cyclopolymerization technique provided entry into a novel CPZA which was used to examine the efficiency of a zwitterionic/anionic motif in capturing Cd^{2+} and Cu^{2+} ions in low concentrations. At an initial concentration of 1 ppm, the respective removal of Cd^{2+} and Cu^{2+} were found to be 84.5 and 85.3%. The spontaneity and the endothermic nature of the adsorption process were ensured by the negative ΔGs and positive ΔHs.

CHAPTER 9

Evaluation of selected monomers and polymers as corrosion inhibitors

A selected number of polymers and monomers containing various functionalities as shown in Figure 9.1 have been evaluated as corrosion inhibitors of mild steel in HCl environment using both gravimetric and electrochemical methods. Concentrated HCl solutions are used in the stimulation treatment of oil and gas wells. The acids act by enhancing the permeability of the reservoir rock and remove formation damage.[197] Hydrochloric acid is a good choice for such treatments because the main reaction products (calcium chloride) are soluble in water.[198] Without the use of corrosion inhibitors, the acid would ultimately destroy the steel it contacts. Industrial acid cleaning also subjects mild steel to severe corrosive attack.

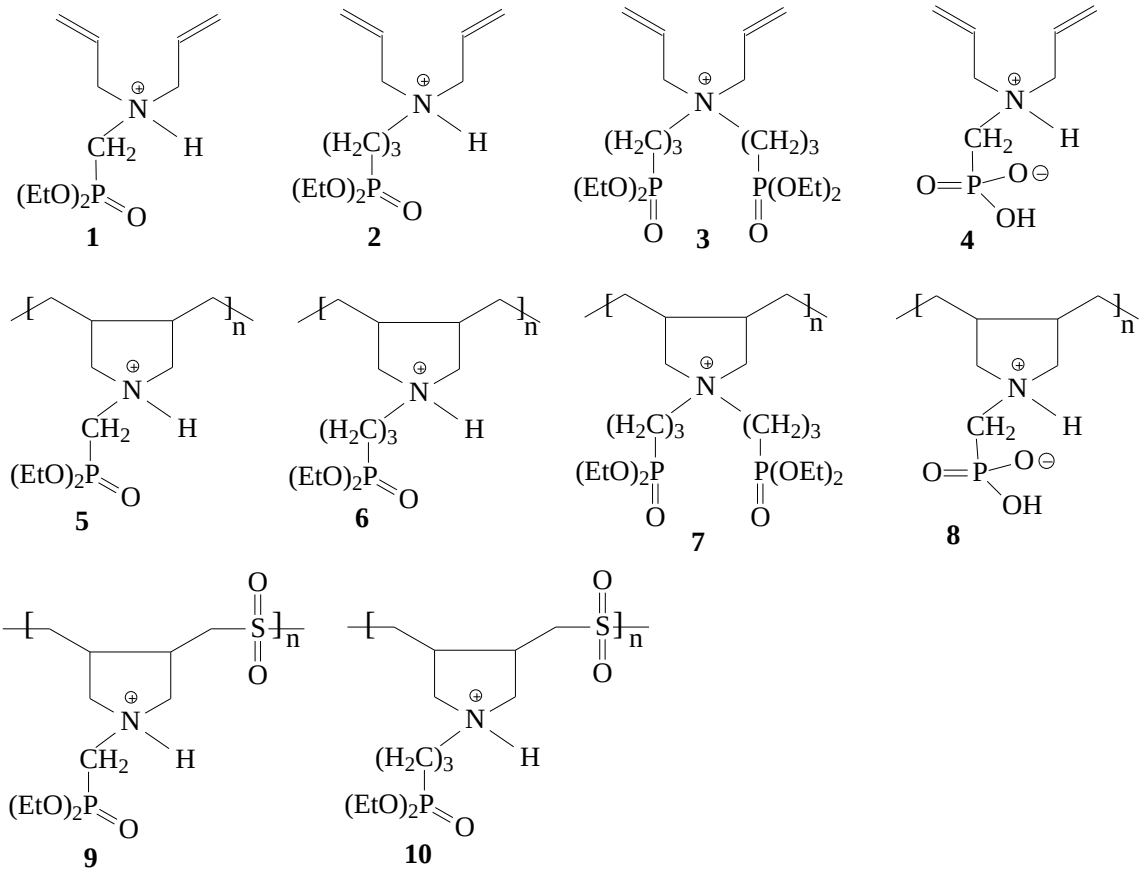

Figure 9.1 Corrosion inhibitor molecules screened

The mechanisms through which the corrosion inhibitors function have been ascribed to adsorption processes on the anodic or cathodic sites on the steel surfaces. Organic compounds bearing high electron density heteroatoms as well as hydrophobes of long alkyl chains are known to be efficient corrosion inhibitors. The heteroatom nucleophilicity leads to chemisorption via coordination with the iron ions of the metal surface, while the hydrophobes inhibit corrosion by the virtue of its ability to form a barrier film that shields the surface thereby reducing the corrosion through acid/steel reaction.[199] The essential requirements for a good protective film are: (1) Polar groups

with high affinity to the metal surface, (2) Long chain hydrocarbon tails, attached to the polar groups and hydrophobic in character and (3) Polymeric compound formed in secondary reaction between the adsorbed inhibitor molecules.

The mechanism of corrosive attack in the HCl medium is given in the reactions below (1) to (5) in anode and (6) to (8) in cathode:[200,201]

Anodic dissolution of Fe:

$$Fe + Cl^- \leftrightharpoons (FeCl^-)_{ads} \quad (1)$$

$$(FeCl^-)_{ads} \leftrightharpoons (FeCl)_{ads} + e^- \quad (2)$$

$$(FeCl)_{ads} \rightarrow FeCl^+ + e^- \quad (3)$$

$$FeCl^+ \leftrightharpoons Fe^{2+} + Cl^- \quad (4)$$

$$(FeCl^-)_{ads} + Inhb^+ \leftrightharpoons (FeCl^-.....Inhb^+)_{ads} \quad (5)$$

Cathodic evolution of H_2:

$$Fe + H^+ \leftrightharpoons (FeH^+)_{ads} \quad (6)$$

$$(FeH^+)_{ads} + e^- \rightarrow (FeH)_{ads} \quad (7)$$

$$(FeH)_{ads} + H^+ + e^- \rightarrow Fe + H_2 \quad (8)$$

$$Fe + Inhb^+ \leftrightharpoons (FeInhb^+)_{ads} \quad (9)$$

The destructive reactions are hampered by consecutive adsorption of a chloride ion and a cationic inhibitor ($Inhb^+$) as described in step (5) which restricts the steps (2)-(4) from happening. The corrosion by cathodic evolution of hydrogen**,** however, can be minimized by effective competition of the $Inhb^+$ with H^+ (step 6 vs. step 9**)**.

The film $(FeCl^{-}\cdots Inh^{+})_{ads}$ formed protects the metal against corrosive HCl media.

9.1 Experimental

9.1.1 Physical methods

Potentiostat (Model 283, EG&G PARC) was used for the electrochemical measurements.

9.1.2 Synthesis

The molecules **1**, **2**, **4**, **5**, **6**, **8**, **9**, **10** as reported and **3** and **7** were synthesized as reported in section 6.2.3 and 6.2.5 respectively.

9.1.3 Specimens

Corrosion study by gravimetric and electrochemical methods were carried out with mild steel coupons of the following composition: 0.089% (C), 0.037 (Cr), 0.34% (Mn), 0.022 (Ni), 0.010 (P), 0.007 (Mo), 0.005 (V), 0.005 (Cu), 99.47% (Fe). For the electrochemical tests, a 1 mm thick mild steel sheet was machined to a flag shape with an approximate stem of 3 cm. Insulating the stem by araldite (affixing material) provided 2 cm^2 exposed area which was abraded with increasing grades of emery papers (100, 400, 600 and 1500 grit size), washed with acetone deionized water. For the gravimetric test, the mild steel coupons were cleaned as described above. The dried specimens were stored in a desiccator. Before their use, the electrode specimens were placed in an ultrasonic bath for 5 min, washed with distilled water and used immediately.

9.1.4 Gravimetric measurements

For gravimetric measurements, the steel coupons measuring 2.5×2.0×0.1 cm^3 were used. Inhibitor efficiency at 63 ºC for 7 h was determined by hanging the steel coupon measuring 2.5×2.0×0.1 cm^3 into a 1 M HCl (250 cm^3) in the absence and presence of the

inhibitors (200 ppm). At the end, the coupons were cleaned with distilled water, abraded lightly with emery paper, followed by washing with distilled water, acetone and drying at 110 ºC.

9.1.5 Electrochemical measurements

9.1.5.1 Tafel extrapolation method

The polarization studies were carried out in a 250 cm^3 of 1 M HCl solution in the absence and presence of 200 ppm inhibitors at 63ºC. The experiments were started only after a stable open circuit potential (OCP) was achieved usually within the exposure time of 30 min. The electrochemical cell, assembled in a 750 cm^3 round-bottomed flask, consisted of a saturated calomel electrode (SCE) as a reference electrode, mild steel working electrode, and the graphite counter electrode (≈ 5 mm diameter). The SCE electrode was connected to the cell using a Luggin-Haber capillary salt bridge, the tip of which was separated from the surface of the working electrode by a distance of ≈ 2 mm. An electrometer was used to connect all three electrodes to a Potentiostat (Model 283, EG&G PARC). A rate of 1.6 mV/s was used to scan a range of ±250 mV with respect to open circuit potential.

9.1.5.2 Linear Polarization resistance (LPR) method

The cell described above was also used for the LPR measurement. The current potential plots (in a range of ±10 mV around E_{corr}) provided the polarization resistance values.

9.2 Results

9.2.1 Gravimetric measurements

The results of weight loss measurements at 63°C after 7 h of immersion of coupons (in 1M HCl) for all the compounds studied are reported in Table 9.1.

Percent inhibition efficiency (η %) was calculated using eq 17:

$$\eta\ \% = \frac{\text{Weight loss (blank)} - \text{Weight loss (inhibitor)}}{\text{Weight loss (blank)}} \times 100 \qquad (17)$$

Table 9.1 The η % for different inhibitors at 200 ppm for the inhibition of corrosion of mild steel exposed at 63 ºC in 1 M HCl (7 h).

Compound	η %
1	71
2	88
3	94
4	91
5	91
6	92
7	93
8	91.2
9	93
10	93

9.2.2 Electrochemical measurements

9.2.2.1 Tafel extrapolation

The results of the Tafel plot extrapolation for mild steel in 1 M HCl (blank) at 63 °C containing the inhibitors are summarized in Table 9.3. The Tafel plots for the inhibition in 1 M HCl are shown in Figure 9.2.

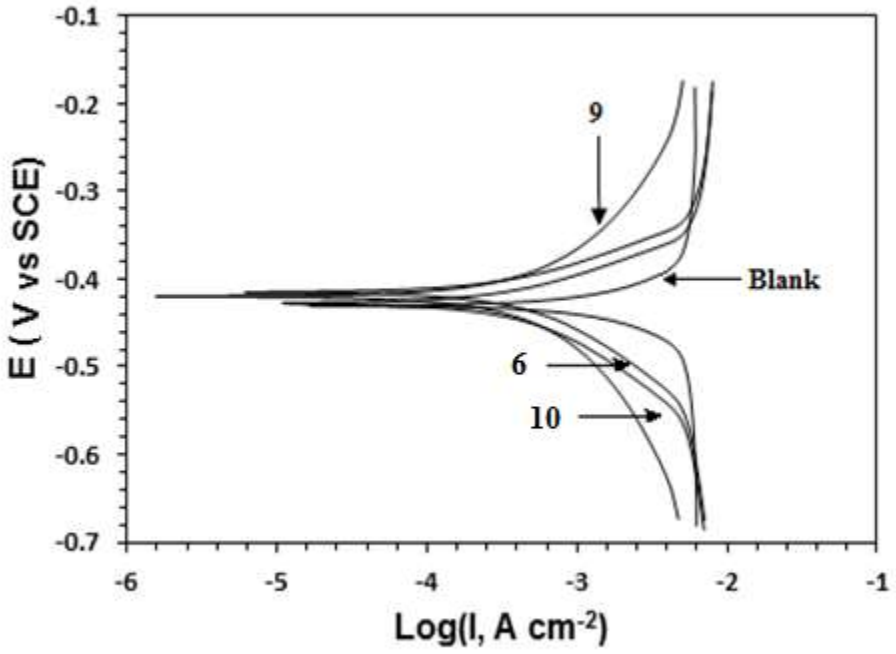

Figure 9.2 Potentiodynamic polarization curves at 63 °C for mild steel in 1 M HCl containing 200 ppm the inhibitor molecules.

9.2.2.2 LPR

The η % from LPR technique was calculated using eq.18:

$$\eta(\%) = \left(\frac{R'_p - R_p}{R'_p}\right) x\ 100 \qquad (18)$$

where R_p and R'_p are the respective polarization resistances in solution without or with the inhibitors in 1 M HCl at 63 ºC (Table 9.3)

9.3 Discussion

The results of corrosion inhibition tests for the molecules in 1 M HCl 63 °C using weight loss method are included in Table 9.1. Most of the inhibitors exhibit high surface activity and demonstrated good η % of more than 90% as determined by gravimetric method except for the monomers **1**, **2** where the η % is relatively lower, 71% and 88% respectively. Due to the similarities in the structure and composition of the inhibitor molecules studied, the η % is virtually the same around 93%. The observed activity of the molecules could be majorly attributed to the donation of their lone pair of electrons to the metal ions.[202,203] It is known that the polymers are adsorbed more stronger on the metal surface due to the presence of multiple adsorption centers which make the desorption process less favorable.[204]

Even though gravimetry is more reliable and simpler, the results for the η % of the inhibitor molecules (200 ppm) in 1 M HCl by Tafel extrapolations (Table 9.2 and Table 9.3) corroborated the findings of the weight loss method (Table 9.1). Significant decrease in the i_{corr} values affirms the inhibitive nature of the inhibitor molecules. The slight positive shift of the E_{corr} values in the presence of the inhibitor molecules suggests

their likelihood of being anodic type inhibitors which mainly suppress the anodic reaction.

Table 9.2 Corrosion inhibition efficiency, η (%) using polarization resistance, Tafel plots and gravimetric method of mild steel samples in various solutions containing 200 ppm of the inhibitors in 1 M HCl at 63 ºC.

Compound	η (%)		
	Polarization method	Tafel method	Gravimetric method
10	87	83	93
9	93	86	93
6	89	88	92

An inhibitor that shifts an OCP by at least 85 mV can be classified as a cathodic or anodic type inhibitor.[205] A slight displacement of 2 to 16 mV (Table 9.3) in the positive direction is insufficient to qualify the molecules as anodic type inhibitors. A pronounced decrease in anodic current densities is an indication of a greater decrease in anodic oxidation rate than the rate of cathodic evolution of hydrogen. The nature of the results suggests that the inhibitors are behaving as mixed-type inhibitors under the major influence of anodic control.

Table 9.3 Results of Tafel plots in solutions containing 200 ppm of the inhibitor in 1 M HCl at 63 ºC.

Sample	Tafel plots					Polarization resistance	
	E_{corr} vs *SCE* (mV)	β_a (mV/dec)	β_C (mV/dec)	i_{corr} ($\mu A/cm^2$)	%IE[b]	R_p ($\Omega\ cm^2$)	η (%)[b]
Blank[a]	−430	54.4	56	754	–	4.5	–
10	−428	34.2	40.5	124.6	83	34	87
9	−420	41.2	45	105.3	86	60	93
6	−414	29	30	89.7	88	41.3	89

[a] The blank was a 1 M HCl solution.
[b] Inhibition Efficiency, IE (i.e., η) = surface coverage θ.

9.4 Conclusions

The evaluated compounds have displayed very good corrosion inhibition activity. At a concentration of 200 ppm virtually all the inhibitor molecules imparted an IE of greater than 90% in 1M HCl. The results of the gravimetry closely match the results obtained by electrochemistry.

References

[1] Butler, G. B., *J. Polym. Sci., Part A: Polym. Chem.*, (1996) **34**, 913.

[2] Butler, G. B.; Ingley, F. L., *J. Am. Chem. Soc.*, (1951) **73**, 1512.

[3] Asrof, A. S.; Zaka, A. S.; Wazeer, M. I. M.; Hamad, E. Z., *Polymer*, (1997) **38**, 3385.

[4] Butler, G. B., *J. Polym. Sci., Part A: Polym. Chem.*, (2000) **38**, 3451.

[5] Butler, G. B., Cyclopolymerization and cyclocopolymerization, In Marcel Dekker: New York, (1992).

[6] Kudaibergenov, S.; Jaeger, W.; Laschewsky, A., *Adv. Polym. Sci.*, (2006) **201**, 157.

[7] Singh, P. K.; Singh, V. K.; Singh, M., *e-Polym.*, (2007) **30**, 1.

[8] Jaeger, W.; Bohrisch, J.; Laschewsky, A., *Prog. Polym. Sci.*, (2010) **35**, 511.

[9] Lowe, A. B.; McCormick, C. L., *Chem. Rev. (Washington, DC, U. S.)*, (2002) **102**, 4177.

[10] Abu-Thabit, N. Y.; Al-Muallem, H. A.; Ali, S. A., *J. Appl. Polym. Sci.*, (2011) **120**, 3662.

[11] Lee, W.-F.; Lee, C.-H., *Polymer*, (1997) **38**, 971.

[12] Anton, P.; Laschewsky, A., *Makromol. Chem.*, (1993) **194**, 601.

[13] Thomas, D. B.; Armentrout, R. S.; McCormick, C. L., *Polym Prepr.* , (1999) **40**, 275.

[14] Ali, S. A.; Rasheed, A.; Wazeer, M. I. M., *Polymer*, (1999) **40**, 2439.

[15] Ali, S. A.; Rasheed, A., *Polymer*, (1999) **40**, 6849.

[16] Ali, M. M.; Perzanowski, H. P.; Ali, S. A., *Polymer*, (2000) **41**, 5591.

[17] Wielema, T. A.; Engberts, J. B. F. N., *Eur. Polym. J.*, (1987) **23**, 947.

[18] Salamone, J. C.; Volksen, W.; Olson, A. P.; Israel, S. C., *Polymer*, (1978) **19**, 1157.

[19] Skouri, M.; Munch, J. P.; Candau, S. J.; Neyret, S.; Candau, F., *Macromolecules*, (1994) **27**, 69.

[20] Higgs, P. G.; Joanny, J. F., *J. Chem. Phys.*, (1991) **94**, 1543.

[21] Hudgins, C. M., Jr., *JPT, J. Pet. Technol.*, (1992) **44**, 604.

[22] Schmitt, G., *Br. Corros. J.*, (1984) **19**, 165.

[23] Chen, Y.; Hong, T.; Gopal, M.; Jepson, W. P., *Corrosion Science*, (2000) **42**, 979.

[24] Martin, J. A.; Valone, F. W., *Corrosion (Houston)*, (1985) **41**, 281.

[25] Durnie, W.; De, M. R.; Jefferson, A.; Kinsella, B., *J. Electrochem. Soc.*, (1999) **146**, 1751.

[26] Dougherty, J. A., Aggressive agents as corrosion inhibitors in gas and oil production, In NACE International: (2004); pp 20/1.

[27] Moiseeva, L. S.; Kuksina, O. V., *Prot. Met.*, (2003) **39**, 490.

[28] Kermani, M. B.; Morshed, A., *Corrosion (Houston, TX, U. S.)*, (2003) **59**, 659.

[29] Zhao, Y.; Wang, J.; Zuo, Y.; Xiong, J., *Shiyou Huagong Fushi Yu Fanghu*, (2010) **27**, 1.

[30] Annand, R. R.; Hurd, R. M.; Hackerman, N., *J. Electrochem. Soc.*, (1965) **112**, 138.

[31] Bacskai, R.; Schroeder, A. H.; Young, D. C., *J. Appl. Polym. Sci.*, (1991) **42**, 2435.

[32] Encyclopaedia of polymer science and technology, In (1964); Vol. 1, p 558.

[33] Kraljic, M.; Mandic, Z.; Duic, L., *Corros. Sci.*, (2002) **45**, 181.

[34] Riedelsberger, K.; Jaeger, W., *Des. Monomers Polym.*, (1998) **1**, 387.

[35] Al Hamouz, O. C. S.; Ali, S. A., *Sep. Purif. Technol.*, (2012) **98**, 94.

[36] Liu, J.; Ma, Y.; Xu, T.; Shao, G., *J. Hazard. Mater.*, (2010) **178**, 1021.

[37] Vinodh, R.; Padmavathi, R.; Sangeetha, D., *Desalination*, (2011) **267**, 267.

[38] Camci-Unal, G.; Pohl, N. L. B., *J. Chem. Eng. Data*, (2010) **55**, 1117.

[39] Kiefer, R.; Hoell, W. H., *Ind. Eng. Chem. Res.*, (2001) **40**, 4570.

[40] Boparai, H. K.; Joseph, M.; O'Carroll, D. M., *J. Hazard. Mater.*, (2011) **186**, 458.

[41] Hasan, S. H.; Talat, M.; Rai, S., *Bioresour. Technol.*, (2006) **98**, 918.

[42] WHO, Copper in drinking-water, guidelines for drinking-water quality, In World Health Organization, Geneva (2003).

[43] Netzer, A.; Hughes, D. E., *Water Res.*, (1984) **18**, 927.

[44] WHO, Guidelines for Drinking Water Quality: Recommendations, In World Health Organization, Geneva, (2008); Vol. 1.

[45] Butter, T. J.; Evison, L. M.; Hancock, I. C.; Holland, F. S.; Matis, K. A.; Philipson, A.; Sheikh, A. I.; Zouboulis, A. I., *Water Res.*, (1998) **32**, 400.

[46] Chakraborty, D.; Maji, S.; Bandyopadhyay, A.; Basu, S., *Bioresour. Technol.*, (2007) **98**, 2949.

[47] Chegrouche, S.; Mellah, A.; Barkat, M., *Desalination*, (2009) **235**, 306.

[48] Ongley, L. K., *Ground Water*, (1999) **37**, 5.

[49] Zhang, A.; Wei, Y.; Kumagai, M., *React. Funct. Polym.*, (2004) **61**, 191.

[50] Chang, R.; Editor, *Chemistry, Seventh Edition*, McGraw-Hill: (2005); p p328.

[51] Yusan, S.; Erenturk, S., *World J. Nucl. Sci. Technol.*, (2011) **1**, 6.

[52] Khan, S. A.; Riaz ur, R.; Khan, M. A., *Waste Manage. (N. Y.)*, (1995) **15**, 641.

[53] Smiciklas, I.; Dimovic, S.; Plecas, I., *Appl. Clay Sci.*, (2007) **35**, 139.

[54] Missana, T.; Garcia-Gutierrez, M., *Phys. Chem. Earth*, (2007) **32**, 559.

[55] Zhang, A.; Wei, Y. Z.; Kumagai, M.; Koyama, T., *J. Radioanal. Nucl. Chem.*, (2004) **262**, 739.

[56] Zhang, A.; Wang, W.; Chai, Z.; Kumagai, M., *J. Sep. Sci.*, (2008) **31**, 3148.

[57] Rifi, E. H.; Rastegar, F.; Brunette, J. P., *Talanta*, (1995) **42**, 811.

[58] Oezeroglu, C.; Keceli, G., *J. Radioanal. Nucl. Chem.*, (2006) **268**, 211.

[59] Wang, M.; Xu, L.; Peng, J.; Zhai, M.; Li, J.; Wei, G., *J. Hazard. Mater.*, (2009) **171**, 820.

[60] Garg, G.; Chauhan, G. S.; Ahn, J.-H., *Polym. Adv. Technol.*, (2011) **22**, 1794.

[61] Liu, J.; Ma, Y.; Zhang, Y.; Shao, G., *J. Hazard. Mater.*, (2010) **173**, 438.

[62] Liang, W.-J.; Wu, C.-P.; Hsu, C.-Y.; Kuo, P.-L., *J. Polym. Sci., Part A: Polym. Chem.*, (2006) **44**, 3444.

[63] Rajan, K. S.; Murase, I.; Martell, A. E., *J. Amer. Chem. Soc.*, (1969) **91**, 4408.

[64] Westerback, S. J.; Martell, A. E., *Nature (London, U. K.)*, (1956) **178**, 321.

[65] Yamashoji, Y.; Matsushita, T.; Shono, T., *Technol. Rep. Osaka Univ.*, (1985) **35**, 331.

[66] Ali, S. A.; Mazumder, M. A. J.; Al-Muallem, H. A., *J. Polym. Sci., Part A: Polym. Chem.*, (2002) **41**, 172.

[67] Ali, S. A.; Abu-Thabit, N. Y.; Al-Muallem, H. A., *J. Polym. Sci., Part A: Polym. Chem.*, (2010) **48**, 5693.

[68] Baber, A.; de Vries, J. G.; Orpen, A. G.; Pringle, P. G.; von der Luehe, K., *Dalton Trans.*, (2006), 4821.

[69] Ali, S. A.; Ahmed, S. Z.; Hamad, E. Z., *J. Appl. Polym. Sci.*, (1996) **61**, 1077.

[70] Gueclue, G.; Guerdag, G.; Oezguemues, S., *J. Appl. Polym. Sci.*, (2003) **90**, 2034.

[71] Abu-Thabit, N. Y.; Kazi, I. W.; Al-Muallem, H. A.; Ali, S. A., *Eur. Polym. J.*, (2011) **47**, 1113.

[72] Ali, S. A.; Umar, Y.; Abu-Sharkh, B. F.; Al-Muallem, H. A., *J. Polym. Sci., Part A: Polym. Chem.*, (2006) **44**, 5480.

[73] Kathmann, E. E.; White, L. A.; McCormick, C. L., *Polymer*, (1997) **38**, 871.

[74] Ali, S. A.; Al-Muallem, H. A.; Wazeer, M. I. M., *J. Polym. Sci., Part A: Polym. Chem.*, (2002) **40**, 2464.

[75] Mazumder, M. A. J.; Umar, Y.; Ali, S. A., *Polymer*, (2004) **45**, 125.

[76] Al-Muallem, H. A.; Wazeer, M. I. M.; Ali, S. A., *Polymer*, (2001) **43**, 1041.

[77] Felty, W. L., *J. Chem. Educ.*, (1978) **55**, 576.

[78] Barbucci, R.; Casolaro, M.; Ferruti, P.; Barone, V.; Leli, F.; Oliva, L., *Macromolecules*, (1981) **14**, 1203.

[79] Guthrie, J. P., *Can. J. Chem.*, (1978) **56**, 2342.

[80] Al-Muallem, H. A.; Wazeer, M. I. M.; Ali, S. A., *Polymer*, (2002) **43**, 4285.

[81] Ali, S. A.; Ali, A., *Polymer*, (2001) **42**, 7961.

[82] Walsh, D. J.; Cheng, G. L., *Polymer*, (1984) **25**, 499.

[83] Thomas, D. B.; Vasilieva, Y. A.; Armentrout, R. S.; McCormick, C. L., *Macromolecules*, (2003) **36**, 9710.

[84] Armentrout, R. S.; McCormick, C. L., *Macromolecules*, (2000) **33**, 419.

[85] Shao, Q.; He, Y.; White, A. D.; Jiang, S., *J. Phys. Chem. B*, (2010) **114**, 16625.

[86] Soto, V. M. M.; Galin, J. C., *Polymer*, (1984) **25**, 254.

[87] Pearson, J. F.; Slifkin, M. A., *Spectrochim. Acta, Part A*, (1972) **28**, 2403.

[88] Pike, R. M.; Cohen, R. A., *J. Polym. Sci.*, (1960) **44**, 531.

[89] De, V. V.; Goethals, E. J., *Macromol. Rapid Commun.*, (1997) **18**, 149.

[90] Lancaster, J. E.; Baccei, L.; Panzer, H. P., *J. Polym. Sci., Polym. Lett. Ed.*, (1976) **14**, 549.

[91] Liaw, D. J.; Shiau, S. J.; Lee, K. R., *J. Appl. Polym. Sci.*, (1992) **45**, 61.

[92] Candau, F. J., J. F. Ed. *Polymeric Materials Encyclopedia*, CRC Press: Boca Raton, FL, (1996); Vol. 7.

[93] Wittmer, J.; Johner, A.; Joanny, J. F., *Europhys. Lett.*, (1993) **24**, 263.

[94] Everaers, R.; Johner, A.; Joanny, J. F., *Europhys. Lett.*, (1997) **37**, 275.

[95] Nishida, K.; Kaji, K.; Kanaya, T.; Fanjat, N., *Polymer*, (2001) **43**, 1295.

[96] Salamone, J. C.; Rice, W. C.; Watterson, A. C., *J. Macromol. Sci., Chem.*, (1991) **A28**, 885.

[97] Barbucci, R.; Casolaro, M.; Danzo, N.; Barone, V.; Ferruti, P.; Angeloni, A., *Macromolecules*, (1983) **16**, 456.

[98] Barbucci, R.; Casolaro, M.; Ferruti, P.; Nocentini, M., *Macromolecules,* (1986) **19**, 1856.

[99] Ali, S. A.; Al-Hamouz, O. C. S., *Polymer*, (2012) **53**, 3368.

[100] Umar, Y.; Abu-Sharkh, B. F.; Asrof, A. S., *Polymer*, (2005) **46**, 10709.

[101] Tripathy, S. K.; Kumar, J.; Nalwa, H. S.; Editors, *Handbook of Polyelectrolytes and Their Applications*, American Scientific Publ: (2002); Vol. 1-3.

[102] Dautzenberg, H.; Jaeger, W.; Koetz, J.; Phillip, B.; Seidel, C.; Stscherbina, D., *Polyelectrolytes: Formation, Characterization and Application*, Hanser: (1994); p 343 pp.

[103] Lowe, A. B.; Billingham, N. C.; Armes, S. P., *Chem. Commun. (Cambridge)*, (1996), 1555.

[104] Lowe, A. B.; Vamvakaki, M.; Wassall, M. A.; Wong, L.; Billingham, N. C.; Armes, S. P.; Lloyd, A. W., *J. Biomed. Mater. Res.*, (2000) **52**, 88.

[105] Dobrynin, A. V.; Rubinstein, M., *J. Phys. II*, (1995) **5**, 677.

[106] Salamone, J. C.; Volksen, W.; Israel, S. C.; Olson, A. P.; Raia, D. C., *Polymer*, (1977) **18**, 1058.

[107] Corpart, J. M.; Candau, F., *Macromolecules*, (1993) **26**, 1333.

[108] Ohno, H.; Ito, K., *Chem. Lett.*, (1998), 751.

[109] Yoshizawa, M.; Ohno, H., *Chem. Lett.*, (1999), 889.

[110] Yoshizawa, M.; Hirao, M.; Ito-Akita, K.; Ohno, H., *J. Mater. Chem.*, (2001) **11**, 1057.

[111] Ravi, P.; Dai, S.; Tam, K. C., *J. Phys. Chem. B*, (2005) **109**, 22791.

[112] Chan, G. Y. N.; Hughes, T. C.; McLean, K. M.; McFarland, G. A.; Nguyen, X.; Wilkie, J. S.; Johnson, G., *Biomaterials*, (2006) **27**, 1287.

[113] You, Y.-Z.; Hong, C.-Y.; Pan, C.-Y., *Nanotechnology*, (2006) **17**, 2350.

[114] Kudaibergenov, S. E.; Editor, *Polyampholytes: Synthesis, Characterization and Application*, Kluwer Academic/Plenum Publishers: (2002); p 220 pp.

[115] Salamone, J. C.; Rice, W. C., *Encyclopedia of Polymer Science and Engineering, Vol. 11*, Mark, H. F.; Bikales, N. M.; Overberger, C. G.; Menges, G.; Kroschwitz, J. I. Eds.; John Wiley & Sons: (1987); Vol. 11.

[116] Mumick, P. S.; Welch, P. M.; Salazar, L. C.; McCormick, C. L., *Macromolecules*, (1994) **27**, 323.

[117] Ernst, R.; Miller, E. L., *Amphoteric Surfactants*, Bluestein, B. L.; Wilton, C. L. Eds.; Marcel Dekker: New York, (1982).

[118] Lloyd, A. W.; Baker, J. A.; Smith, G.; Olliff, C. J.; Rutt, K. J., *J. Pharm. Pharmacol.*, (1992) **44**, 507.

[119] Lloyd, A. W.; Olliff, C. J.; Rutt, K. J., *Int. J. Pharm.*, (1996) **131**, 257.

[120] Filippini, D.; Aasberg, P.; Nilsson, P.; Inganaes, O.; Lundstroem, I., *Sens. Actuators, B*, (2006) **113**, 410.

[121] Zhang, L. M.; Tan, Y. B.; Li, Z. M., *Carbohydr. Polym.*, (2000) **44**, 255.

[122] Didukh, A. G.; Sigitov, V. B.; Kudaibergenov, S. E., *Oil Gas*, (2004) **4**, 64.

[123] Haladu, S. A.; Ali, S. A., *Eur. Polym. J.*, (2013) **49**, 1591.

[124] Butler, G. B.; Angelo, R. J., *J. Am. Chem. Soc.*, (1957) **79**, 3128.

[125] Timofeeva, L. M.; Vasilieva, Y. A.; Kleshcheva, N. A.; Topchiev, D. A., *Russ. Chem. Bull.*, (1999) **48**, 856.

[126] Ali, S. A.; Al-Muallem, H. A.; Mazumder, M. A. J., *Polymer*, (2003) **44**, 1671.

[127] Galin, M.; Chapoton, A.; Galin, J. C., *J. Chem. Soc., Perkin Trans. 2*, (1993), 545.

[128] Wyman, J., Jr.; McMeekin, T. L., *J. Am. Chem. Soc.*, (1933) **55**, 908.

[129] Barbucci, R.; Casolaro, M.; Di, T. A.; Magnani, A., *Macromolecules*, (1989) **22**, 3138.

[130] Al-Hamouz, O. C. S.; Ali, S. A., *J. Polym. Sci., Part A: Polym. Chem.*, (2012) **50**, 3580.

[131] Davey, R. J., The role of additives in precipitation processes, In North-Holland: (1982); pp 123.

[132] Fong, D. W.; Marth, C. F.; Davis, R. V., Sulfobetaine-containing polymers and their utility as calcium carbonate scale inhibitors, US 6,225,430 B1, (2001).

[133] Butt, F. H.; Rahman, F.; Baduruthamal, U., *Desalination*, (1995) **103**, 189.

[134] Silvia, M.-T. H.; Cabeza, A.; Bruque, S.; Pertierra, P.; Garcia-Granda, S.; Aranda, M. A. G., *J. Solid State Chem.*, (2000) **151**, 122.

[135] Spiegler, K. S.; Laird, A. D. K.; Editors, *Principles of Desalination, Pt. A. 2nd Ed*, Academic Press: (1980); p 357 pp.

[136] Gill, J. S., *Desalination*, (1999) **124**, 43.

[137] Hasson, D.; Shemer, H.; Sher, A., *Ind. Eng. Chem. Res.*, (2011) **50**, 7601.

[138] Kazi, I. W.; Rahman, F.; Ali, S. A., *Polym. Eng. Sci.*, (2014) **54**, 166.

[139] McGrew, F. C., *J. Chem. Educ.*, (1958) **35**, 178.

[140] McCormick, C. L., *J. Polym. Sci., Part A: Polym. Chem.*, (1996) **34**, 911.

[141] Ali, S. A.; Haladu, S. A., *J. Appl. Polym. Sci.*, (2013) **129**, 1394.

[142] Haladu, S. A.; Ali, S. A., *J. Polym. Sci., Part A: Polym. Chem.*, (2013) **51**, 5130.

[143] Al, H. O. C. S.; Ali, S. A., *Ind. Eng. Chem. Res.*, (2012) **51**, 14178.

[144] Kafarski, P.; Lejczak, B., *Phosphorus, Sulfur Silicon Relat. Elem.*, (1991) **63**, 193.

[145] Nowack, B., *Water Res.*, (2003) **37**, 2533.

[146] Thatcher, G. R. J.; Campbell, A. S., *J. Org. Chem.*, (1993) **58**, 2272.

[147] Abu-Thabit, N. Y.; Ali, S. A.; Zaidi, S. M. J.; Mezghani, K., *J. Mater. Res.*, (2012) **27**, 1958.

[148] De, C. E., *Annu. Rev. Pharmacol. Toxicol.*, (2011) **51**, 1.

[149] Moszner, N.; Salz, U.; Zimmermann, J., *Dent. Mater.*, (2005) **21**, 895.

[150] Xu, X.; Wang, R.; Ling, L.; Burgess, J. O., *J. Polym. Sci., Part A: Polym. Chem.*, (2006) **45**, 99.

[151] Erez, R.; Ebner, S.; Attali, B.; Shabat, D., *Bioorg. Med. Chem. Lett.*, (2008) **18**, 816.

[152] Alferiev, I.; Vyavahare, N.; Song, C.; Connolly, J.; Travis, H. J.; Lu, Z.; Tallapragada, S.; Bianco, R.; Levy, R., *Biomaterials*, (2001) **22**, 2683.

[153] Wang, L.; Zhang, M.; Yang, Z.; Xu, B., *Chem. Commun. (Cambridge, U. K.)*, (2006), 2795.

[154] Akgun, B.; Savci, E.; Avci, D., *J. Polym. Sci., Part A: Polym. Chem.*, (2012) **50**, 801.

[155] Bilgici, Z. S.; Ordu, O. D.; Isik, M.; Avci, D., *J. Polym. Sci., Part A: Polym. Chem.*, (2011) **49**, 5042.

[156] Ali, S. A.; Kazi, I. W.; Rahman, F., *Polym. Int.*, (2013), Ahead of Print.

[157] Al-Hamouz, O. C. S.; Ali, S. A., *J. Chem. Eng. Data*, (2013) **58**, 1407.

[158] Al, H. O. C. S.; Ali, S. A., *Sep. Purif. Technol.*, (2012) **98**, 94.

[159] Alexandratos, S. D.; Hong, M.-J., *Sep. Sci. Technol.*, (2002) **37**, 2587.

[160] Alfano, N. J.; Shenberger, D. M., Scale control in metal mining circuits using polyether polyamino methylene phosphonates, US5454954A, (1995).

[161] Gunasekaran, G.; Natarajan, R.; Muralidharan, V. S.; Palaniswamy, N.; Rao, B. V. A., *Anti-Corros. Methods Mater.*, (1997) **44**, 248.

[162] Russell, R. G. G., *Bone (Amsterdam, Neth.)*, (2011) **49**, 2.

[163] Fleisch, H.; Neuman, W. F., *Am. J. Physiol.*, (1961) **200**, 1296.

[164] Komarneni, S.; Kodama, T.; Paulus, W. J.; Carlson, C., *J. Mater. Res.*, (2000) **15**, 1254.

[165] Hafizi, M.; Abolghasemi, H.; Moradi, M.; Milani, S. A., *Chin. J. Chem. Eng.*, (2011) **19**, 267.

[166] Nyman, M.; Tripathi, A.; Parise, J. B.; Maxwell, R. S.; Nenoff, T. M., *J. Am. Chem. Soc.*, (2002) **124**, 1704.

[167] Behrens, E. A.; Sylvester, P.; Clearfield, A., *Environ. Sci. Technol.*, (1998) **32**, 101.

[168] Chiarizia, R.; McAlister, D. R.; Herlinger, A. W., *Solvent Extr. Ion Exch.*, (2003) **21**, 171.

[169] Herbst, R. S.; Law, J. D.; Todd, T. A.; Romanovskiy, V. N.; Babain, V. A.; Esimantovskiy, V. M.; Smirnov, I. V.; Zaitsev, B. N., *Solvent Extr. Ion Exch.*, (2002) **20**, 429.

[170] Luo, H.; Dai, S.; Bonnesen, P. V., *Anal. Chem.*, (2004) **76**, 2773.

[171] Dobrynin, A. V.; Colby, R. H.; Rubinstein, M., *J. Polym. Sci., Part B: Polym. Phys.*, (2004) **42**, 3513.

[172] Lowe, A. B.; Billingham, N. C.; Armes, S. P., *Macromolecules*, (1999) **32**, 2141.

[173] Sahni, S. K.; Van, B. R.; Reedijk, J., *Polyhedron*, (1985) **4**, 1643.

[174] Kolodynska, D.; Hubicki, Z.; Pasieczna-Patkowska, S., *Acta Phys. Pol., A*, (2009) **116**, 340.

[175] Li, Q.; Liu, H.; Liu, T.; Guo, M.; Qing, B.; Ye, X.; Wu, Z., *Chem. Eng. J. (Amsterdam, Neth.)*, (2010) **157**, 401.

[176] Duong, T. D.; Nguyen, K. L.; Hoang, M., *J. Colloid Interface Sci.*, (2006) **301**, 446.

[177] Lagergren, S., *Vetenskapsakad. Handl.*, (1898) **2462**, 1.

[178] Ramesh, A.; Hasegawa, H.; Maki, T.; Ueda, K., *Sep. Purif. Technol.*, (2007) **56**, 90.

[179] Ho, Y. S.; McKay, G., *Process Biochem. (Oxford)*, (1999) **34**, 451.

[180] Minceva, M.; Markovska, L.; Meshko, V., *Maced. J. Chem. Chem. Eng.*, (2007) **26**, 125.

[181] Lin, Y.; Chen, H.; Lin, K.; Chen, B.; Chyowsan, C., *J. Environ. Sci. (Beijing, China)*, (2011) **23**, 44.

[182] Weber, W. J.; Morris, J. C., *J. Sanit. Eng. Div., Am. Soc. Civil Engrs.*, (1963) **89**, 31.

[183] Wu, F.-C.; Tseng, R.-L.; Juang, R.-S., *Chem. Eng. J. (Amsterdam, Neth.)*, (2009) **153**, 1.

[184] Liu, J.; Si, J.; Zhang, Q.; Zheng, J.; Han, C.; Shao, G., *Ind. Eng. Chem. Res.*, (2011) **50**, 8645.

[185] Ozcan, A.; Ozcan, A. S.; Gok, O., Adsorption kinetics and isotherms of anionic dye of Reactive Blue 19 from aqueous solutions onto DTMA-sepiolite, In Nova Science Publishers, Inc.: (2007); pp 225.

[186] Vijayaraghavan, K.; Padmesh, T. V. N.; Palanivelu, K.; Velan, M., *J. Hazard. Mater.*, (2006) **133**, 304.

[187] Kundu, S.; Gupta, A. K., *Chem. Eng. J. (Amsterdam, Neth.)*, (2006) **122**, 93.

[188] Haghseresht, F.; Lu, G. Q., *Energy Fuels*, (1998) **12**, 1100.

[189] Liu, J.; Song, L.; Shao, G., *J. Chem. Eng. Data*, (2011) **56**, 2119.

[190] Alyuez, B.; Veli, S., *J. Hazard. Mater.*, (2009) **167**, 482.

[191] Srivastava, V.; Weng, C. H.; Singh, V. K.; Sharma, Y. C., *J. Chem. Eng. Data*, (2011) **56**, 1414.

[192] Madhava, R. M.; Ramesh, A.; Chandra, R. G. P.; Seshaiah, K., *J. Hazard. Mater.*, (2006) **129**, 123.

[193] Huang, X.; Gao, N.-y.; Zhang, Q.-l., *J. Environ. Sci. (Beijing, China)*, (2007) **19**, 1287.

[194] Pandey, P. K.; Sambi, S. S.; Sharma, S. K.; Singh, S., *Proceedings of the World Congress on Engineering and Computer Science*, (2009) **1**,

[195] Wu, H.; Jin, Y.; Luo, M.; Bi, S., *Anal. Sci.*, (2007) **23**, 1109.

[196] Shahtaheri, S. J.; Khadem, M.; Golbabaei, F.; Rahimi-Froushan, A.; Ganjali, M. R.; Norouzi, P., *Int. J. Occup. Saf. Ergon.*, (2007) **13**, 137.

[197] Frenier, W.; Hill, D.; Jasinki, R., In *Oilfield Rev.*, Schlumberger: Tulsa, Oklahoma, USA, Vol. 1, pp 15.

[198] Al-Taq, A. A.; Aramco, S.; Nasr-El-Din, H. A.; Ali, S. A., Inhibition Performance of a New Series of Mono/Diamine-based Corrosion Inhibitors for HCl Acid Solutions, In Society of Petroleum Engineers: (2008).

[199] Ali, S. A.; Zaidi, S. M. J.; El-Sharif, A. M. Z.; Al-Taq, A. A., *Polym. Bull. (Heidelberg, Ger.)*, (2012) **69**, 491.

[200] Morad, M.; Morvan, J.; Pagetti, J., *Proceedings of the 8th European Symposium on Corrosion Inhibitors (8 SEIC), Ann. Univ. Ferrara, N. S., Sez V, Suppl: N. 10:159, 1995.* , Elsevier: (1995).

[201] Aramaki, K.; Hagiwara, M.; Nishihara, H., *Corrosion Science*, (1987) **27**, 487.

[202] Behpour, M.; Ghoreishi, S. M.; Mohammadi, N.; Salavati-Niasari, M., *Corros. Sci.*, (2011) **53**, 3380.

[203] Cao, P. G.; Yao, J. L.; Zheng, J. W.; Gu, R. A.; Tian, Z. Q., *Langmuir*, (2002) **18**, 100.

[204] Ali, S. A.; Saeed, M. T.; El-Sharif, A. M. Z., *Polym. Eng. Sci.*, (2012) **52**, 2588.

[205] Riggs, O. L., Jr., Corrosion Inhibitors 2nd Edition, In Nathan, C. C. Ed. Houston, TX: (1973).

Vitae

Name :Shamsuddeen Abdullahi Haladu

Nationality :Nigerian

Date of Birth :9/26/1980

Email :shamsuhd2@yahoo.com

Address :KFUPM, P.O.Box: 7392, Dhahran, 31261, Saudi Arabia

Academic Background :

PhD. Chemistry, King Fahd University of Petroleum and Minerals, 2014 (Dissertation title: Synthesis of a New Class of Linear and Cross-linked Polyzwitterion-anions and Their Applications as Corrosion Inhibitors and Adsorbents).

M.Sc. Chemistry, King Fahd University of Petroleum and Minerals, 2010 (Thesis title: Total synthesis of bioactive natural products).

B.Sc. Chemistry, Bayero University Kano, 2005

Publications:

1. Nisar Ullah and **Shamsuddeen A Haladu**, "The first total synthesis of aspergillusol A, an alpha-glucosidase inhibitor," *Natural Product Communications*, 2010, 5, 993-1160.
2. Nisar Ullah, **Shamsuddeen A. Haladu** and Basem A. Mosa, "An improved total synthesis of spermatinamine, an inhibitor of isoprenylcysteine carboxyl methyltransferase" *Tetrahedron Letters*, 2011, 52, 212-214.

3. **Shamsuddeen A. Haladu** and Shaikh A. Ali, Cyclopolymerization protocol for the synthesis of a new poly(electrolyte-zwitterion) containing quaternary nitrogen, carboxylate, and sulfonate functionalities, *European Polymer Journal* 49 (2013) 1591–1600.

4. Shaikh A. Ali and **Shamsuddeen A. Haladu**, Cyclopolymerization Protocol for the Synthesis of a Poly(zwitterion-alt-sulfur dioxide) to Investigate the Polyzwitterion-to-Poly(anion-zwitterion) Transition, *Journal of Applied Polymer Science,* 129: 1394–1404, 2013

5. Shaikh A. Ali and **Shamsuddeen A. Haladu**, A novel cross-linked polyzwitterion/anion having pH-responsive carboxylate and sulfonate motifs for the removal of Sr^{2+} from aqueous solution at low concentrations, *Reactive and Functional Polymers,* 73 (2013) 796–804.

6. **Shamsuddeen A. Haladu,** Shaikh A. Ali A, pH-Responsive Cyclopolymer Having Phospho- and Sulfopropyl Pendents in the Same Repeating Unit: Synthesis, Characterization and its Application as an Antiscalant, *Journal of Polymer Science Part A: Polymer Chemistry* 2013, 51, 5130–5142.

7. Shaikh A. Ali and **Shamsuddeen A. Haladu**, Synthesis, solution properties and scale inhibiting behavior of a diallylammonium/sulfur dioxide cyclocopolymer bearing Phospho- and Sulfopropyl Pendents, *Polymer international (2013)*, DOI: 10.1002/pi.4691.

8. Shaikh A. Ali, **Shamsuddeen A. Haladu** and Hasan A. Al-Muallem, Bis[3-(diethoxyphosphoryl)propyl]diallylammonium Chloride: Synthesis and Use of its Cyclopolymer as an Antiscalant , *Journal of Applied Polymer Science,2014,* DOI: 10.1002/app.40615

9. **Shamsuddeen A. Haladu,** Othman Charles S. Al Hamouz and Shaikh A. Ali, Novel cross-linked polysulfonate-carboxylate resin for the removal of Cu^{2+} and Cd^{2+} from wastewater, *Arabian Journal of Chemistry* (submitted).

Conferences:

1. Nisar Ullah and **Shamsuddeen A Haladu**, "The first total synthesis of aspergillusol A, an alpha-glucosidase inhibitor," 93rd Canadian Chemistry Conference and Exhibition, Canada; May 2010.

2. Shaikh A. Ali, Othman Charles S. Al Hamouz and **Shamsuddeen A. Haladu**, Butler's cyclopolymerization protocol in the synthesis of novel cross-linked resins for removal of toxic metal ions, at University Town, National University of Singapore, Singapore (December 2012).